Novel concepts of microtubule regulation during axon growth and maintenance

A thesis submitted to the University of Manchester for the degree of Doctor of Philosophy (PhD) in Neuroscience in the Faculty of Life Sciences

2015

Yue Qu

Table of Content

Final word count: 52042

Index of Figures

Index of Tables

Abstract

University: The University of Manchester **Name:** Yue Qu
Degree title: Doctor of Philosophy (PhD) **Date:** 11/02/2015
Thesis title: Novel concepts of microtubule regulation during axon growth and maintenance

Axons are up-to-a-meter-long cable-like cellular processes of neurons. The proper function of nervous systems requires that axons grow and wire up correctly during development or regeneration. The uniquely challenging architecture of axons has to be sustained for an organism's lifetime, and renders them key lesion sites during healthy ageing, in injury and neurodegenerative diseases. Notably, axon degeneration is considered as the cause rather than consequence for neuron decay in the context of various neurodegenerative diseases. The structural backbones of axons are formed by parallel bundles of microtubules (MTs) which also provide the highways for life-sustaining long-distance transport between cell bodies and the growth cones or synaptic endings.

To better understand axon development, regeneration, maintenance and degeneration during ageing, my PhD project has focused on mechanisms underpinning the regulation of MT bundles in axons. For this, I have capitalised on fast and genetically and experimentally amenable research possible in *Drosophila* neurons, both in primary culture and *in vivo*. I have used systematic combinatorial genetics and pharmacological approaches to unravel mechanisms and roles of actin as well as the cortical collapse factor Efa6 in MT regulation during axon formation and maintenance. I was able to gain a number of novel mechanisms contributing to the *de novo* alignment and maintenance of ordered MT bundles.

First, it has been proposed that Spectraplakins (large actin-microtubule linkers) guide the extension of polymerising MTs along cortical F-actin, thus directly laying axonal MTs out into parallel bundles. Here, I have used manipulations of actin networks as well as hybrid constructs of Shot where the actin binding domain was replaced by actin associating domains of other molecules. My data strongly suggest that Shot's ABD domain has unique properties that can sense specific properties of F-actin networks, and this is important for its ability to appropriately regulate MT behaviours. Second, using combinations of actin and Shot manipulations, I found that Shot displays not only these actin-dependent guidance functions, but it displays novel actin-independent function in MT bundle maintenance for which I present a working hypothesis. Third, I found a novel and Shot-independent role of axonal actin in maintaining MTs and promoting axon growth, and my results suggest that these functions involve promotion of MT polymerisation. MT maintenance is therefore mediated through two complementary mechanisms involving Shot on the one hand and actin on the other, and simultaneous removal of Shot and actin leads to entire loss of axons. Finally, I have unravelled novel axonal functions of the cortical collapse factor Efa6 which serves as a check point in MT bundle maintenance by eliminating "off track" MTs that have escaped the axonal bundle organisation. In the absence of this factor, a gradual increase of disorganised, criss-crossed MTs occurs as a matter of days.

These new mechanisms strongly suggest that different MT-regulatory mechanisms act in parallel in axons and complement each other in one common mechanism of MT bundle formation and maintenance. I propose here a local homeostasis model of axonal MT bundle maintenance which provides new ways to think about problems of ageing as well as a range of different neurodegenerative diseases.

Declaration

No portion of the work referred to in the thesis has been submitted in support of an application for another degree or qualification of this or any other university or other institute of learning.

Copyright Statement

i. The author of this thesis (including any appendices and/or schedules to this thesis) owns certain copyright or related rights in it (the “Copyright”) and s/he has given The University of Manchester certain rights to use such Copyright, including for administrative purposes.

ii. Copies of this thesis, either in full or in extracts and whether in hard or electronic copy, may be made **only** in accordance with the Copyright, Designs and Patents Act 1988 (as amended) and regulations issued under it or, where appropriate, in accordance with licensing agreements which the University has from time to time. This page must form part of any such copies made.

iii. The ownership of certain Copyright, patents, designs, trade marks and other intellectual property (the “Intellectual Property”) and any reproductions of copyright works in the thesis, for example graphs and tables (“Reproductions”), which may be described in this thesis, may not be owned by the author and may be owned by third parties. Such Intellectual Property and Reproductions cannot and must not be made available for use without the prior written permission of the owner(s) of the relevant Intellectual Property and/or Reproductions.

iv. Further information on the conditions under which disclosure, publication and commercialisation of this thesis, the Copyright and any Intellectual Property and/or Reproductions described in it may take place is available in the University IP Policy (see http://documents.manchester.ac.uk/DocuInfo.aspx?DocID=487), in any relevant Thesis restriction declarations deposited in the University Library, The University Library’s regulations (see http://www.manchester.ac.uk/library/aboutus/regulations) and in The University’s policy on Presentation of Theses.

Acknowledgements

I would like to express my deepest and sincere gratitude to my supervisor Professor Andreas Prokop, who offered me the remarkable opportunity to carry out this PhD project. Without his invaluable guidance, wondrous patience and encouragement both in science and in life, I will have not been able to conclude this PhD.

I would also like to thank all the members of the Prokop lab (past and present), who feels like a family for me: particularly to Dr. Natalia Sánchez-Soriano for frequent help and discussion, Dr. Ines Hahn for bring great advice to my project and thesis, Dr. Robin Beaven for training and support, and Jill Parkin and Meredith Lees for their help. I would also like to thank Sanjai Patel, for all of the assistance with fly work.

I am grateful to my advisers Dr. Karel Dorey and Dr. Martin Baron for their help and advice. I would like to thank Dr. Tom Millard and his lab members for the help he has given through our shared lab meetings. I would also like to thank Dr. Christoph Ballestrem and his lab members for discussions and advice on mammalian cell culture and FRAP technique. I am also grateful to the collaborative opportunity providing by STFC facility.

My deepest grateful will give to my parents and family for their constant financial and emotional support throughout my PhD. I would also deeply thanks to my boyfriend Alessandro for his help, support and understanding over the last three years. I am also deeply grateful to my precious friends Siyao Wang, Ulrike Klemstein, Man Zhao and Jia Jia, who motivated me and made my life much easier, fun and colourful during my PhD. I would also like to thank my friend and roommate Yue Han and Xinyu Wang, who provided me with a comfortable living environment during my thesis writing.

Finally, I would like to thank my parents and the Faculty of Life Sciences for funding my PhD.

Abbreviations

+TIPs	MT plus end-binding proteins
ABD	Shot actin-binding domain
Abl	Abelson
ABPs	Actin binding proteins
ACF7/MACF1	Actin cross linking family 7/ microtubule and actin cross linking factor 1
AD	Alzheimer's disease
AIS	axon initiation segment
Ank	Ankyrin
Arf6	ADP-ribosylation factor 6
BPAG1e	Bullous pemphigoid antigen 1e
C domain	Central domain
CB	Cytoskeleton buffer
C-ERMAD	C-terminal ERM association domain
CFP	Cyan Fluorescent Protein
CG	Growth cone
CHD	Calponin homozygote domain
Chic	Chickadee
CLASP	CLIP-associated protein
CLF	Central Laser Facility
CLIPs	Cytoplasmic linker proteins
CNS	Central nervous system
CoIP	Co-Immunoprecipitation
ConA	concanavalin A
CP	Capping proteins
CytoD	Cytochalasin D
DIV	Day *in vitro*
DMEM	Dulbecco’s Modified Eagle's medium
DRG	Dorsal root ganglion
Dvl1	Dishevelled-1
EB proteins	End binding proteins
ECM	Extracellular matrix
Efa6	Exchange factor for ARF6

Ena	Enabled
ERM	Ezrin–Radixin–Moesin
F-actin	Filamentous actin
FCS	Foetal Calf Serum
FERM	4.1 protein-Ezrin–Radixin–Moesin
FRAP	Fluorescence recovery after photobleaching
FRET	Fluorescence resonance energy transfer
G-actin	Globular actins
GAPs	GTPase-activating proteins
GAS	Growth arrest-specific
GEFs	Guanine nucleotide exchange factors
GFP	Green fluorescent protein
GOF	Gain-of-function
GPI	glycosylphosphatidylinositol
GRD	Gas2-related domain
HBSS	Hank's Balanced Salt Solution
HIV	Hour *in vivo*
hts	hu li tai shao
IF	Intermediate Filaments
IFD	IF-like repeat domains
Ig CAMs	Immunoglobulin cell-adhesion molecules
IPC	Inter-ommatidial precursor cells
IQGAP1	*IQ* motif-containing GTPase-activating protein 1
Jag	Jaguar
Kra	Krasavietz/eIF5C
L2000	Lipofecatmine 2000
LatA	latrunculin A
Lifeact	Lifeactin
Lis1	Lissencephaly 1
LOF	Loss-of-function
MAG	Myelin-associated glycoprotein
MAPs	Microtubule associate proteins
MCAK	Mitotic centromere-associated kinesin

MCS	Multiple cloning site
MICAL	Molecule interacting with CasL
MLCK	Myosin light chain kinase
Moe	Moesin
MT	Microtubule
MTBPs	MT-binding proteins
NGF	Nerve grow factor
NgR	Nogo-66 receptor
noco	nocodazole
OMgp	Oligodendrocyte-myelin glycoprotein
OTK	Off track
P domain	Peripheral domain
$p75^{NTR}$	p75 neurotrophin receptor
PALM	Photo-activated localization microscopy
PBS	Phosphate buffered saline
PBT	Phosphate buffered saline with 0.3% TritonX-100
PFA	Paraformaldehyde in 0.05M phosphate buffer
PH domain	Pleckstrin homology domain
PI(4,5)P2	Phosphatidylinositol-4,5-bisphosphate
PNS	Peripheral nervous system
PP1	Protein phosphatase 1
PRR	plakin-repeat region
PSD	Plekstrin-Sec7 domains gene
RE	Restriction enzyme
SEM	Standard error of the mean
Sema	Semaphorins
Shot	Short stop
SIM	Structured illumination microscopy
Ssp4	Short spindle 4
Ssp4	Short spindle 4
STED	Stimulated emission depletion
STFC	Science & Technology Facilities Council's
STORM	Stochastic optical reconstruction microscopy

T zone	Transition zone
T-E	Trypsin-EDTA
VASP	Vasodialator-stimulated protein
WASP	Wiskott - Aldrich syndrome Protein
wt	Wildtype
YFP	Yellow Fluorescent Protein

Chapter 1

Introduction

1.1. The importance of axons during nervous system development, function and maintenance

The nervous system of most animals is composed of two parts, central nervous system (CNS) and peripheral nervous system (PNS). The most important function of the PNS is to perceive stimuli from the environment and of the CNS to process that information and generate behaviour, in particular control the movement of muscles and the activity of glands (Jessell et al., 2000).

One organisational principle of the nervous system is that specified neurons, which are positioned in characteristic locations of the body and nervous system, connect to other neurons, muscles and glands through their long and thin neuritic processes, called axons and dendrites. Of these, axons are unique structures in that they can be up to meters long and act as the essential cables that electrically wire the brain and the brain to the body. For this, they conduct electrical messages primarily in form of action potentials which can be passed on to other cells at specialised cell contacts called synapses (Fig. 1.1) (Jessell et al., 2000).

In order to achieve this organisation during development (and regeneration), axons grow at motile structures at their tips, called growth cones (GCs), which are guided by spatiotemporal cues in tissues towards their precise target areas and cells. Therefore, understanding axon growth and maintenance will not only help us to better understand how the nervous system develops, it will also aid in our understanding of neurodevelopmental diseases, such as forms of mental retardation, lissencephalies or autism where neuronal circuits are not well established (Nugent et al., 2012), or in neuroregeneration where the failed re-growth of axons is one important reason for incomplete recovery, (e.g. paralysis as a consequence of spinal cord injury) (Bichenback, 2013).

Once axons are formed, they have to be maintained for decades. Given their delicate structure, it is therefore no surprise that about 50% of axons are gradually lost towards high age even in the healthy brain (Marner et al., 2003). Notably, axons are key lesion sites in neurodegeneration, and axon deterioration is considered the cause rather than consequence for neuron decay in the context of various neurodegenerative diseases (Prokop, 2013, Adalbert and Coleman, 2012).

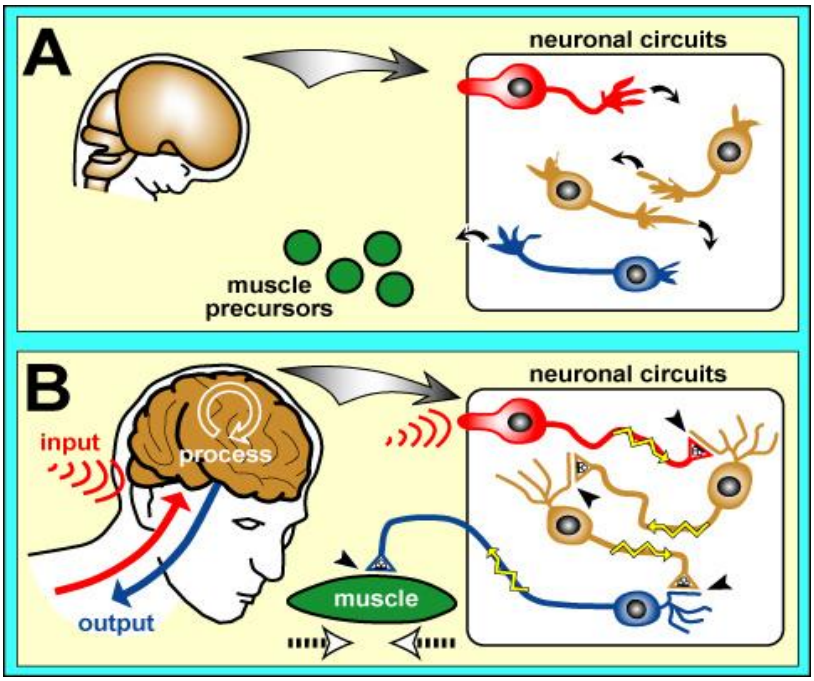

Figure 1.1. *Neuronal growth plays a crucial role in neural circuit formation.*

A. *During nervous system development, neuronal axons, dendrites and synaptic terminals grow out through GCs at their tips along reproducible paths (curved arrows).* ***B.*** *The resulting neuronal circuits allow directed conduction of signals as a key property of nervous system function: "input" signals are received by sensory neurons (red), passed on to interneurons (beige) for processing and finally to motorneurons (blue) which innervate peripheral targets, such as muscles (green), to generate an "output" signal (dashed arrows indicating muscle contraction). Signals primarily consist in fast propagating action potentials (yellow zigzag arrows) which travel along axons and dendrites and get passed on from cell to cell through the process of synaptic transmission at synaptic contacts (black arrow heads). Taken from www.prokop.co.uk.*

1.2. Principal mechanism of axon growth

The growth of axons during development or regeneration as well as their maintenance for a lifetime essentially depends on the cytoskeleton. Bundles of filamentous microtubules (MT) form the structural backbones of axons and also provide the highways for life-sustaining long-distance transport (Prokop, 2013), and networks of actin filaments generate filopodial and lamellipodial protrusions at GCs or points of collateral branching (Letourneau, 2009) and they assemble into ring-like structures in axon shafts (Xu et al., 2013).

During early development, GCs play a crucial role in the regulation of axonal growth. GCs are motile structures at the tips of axons, vaguely reminiscent of the leading edges of migrating cells (Dent et al., 2011). They are able to respond to chemical

guidance cues in their environment with predictable morphogenetic changes, such as turning, collapse, acceleration or pausing (Dent et al., 2011, Lowery and Van Vactor, 2009, Geraldo and Gordon-Weeks, 2009). To understand these responses, I will first explain the principal signalling mechanisms underpinning GC guidance, and then explain the organisation of GCs and the role of the cytoskeleton within.

1.2.1. Principals of signalling during axonal growth

The directionality of axon elongation is regulated through a key-in-lock principal involving spatiotemporal patterns of extracellular signals and neuron-specific receptive machinery (Fig. 1.2) (Tessier-Lavigne and Goodman, 1996). Extracellular signals can be of different nature. They can be short distance, i.e. firmly anchored to cell surfaces or forming sharp borders anchored to extracellular matrix. Alternatively, they can be long distance, i.e. forming diffusible gradients or gradients anchored to extracellular matrix. But what will determine how individual GCs respond to these guidance cues? GCs carry receptors on their surfaces, often at the tips of filopodia. The nature of membrane receptors and downstream signalling pathway components displayed by any particular neuron is specific and a function of their respective developmental history. Different neurons displaying distinct receptive machineries can therefore respond differently to the same set of extracellular signals (Fig. 1.2) (Huber et al., 2003, Bashaw and Klein, 2010). Notably, a chemical signal is not attractive or repulsive *per se*. The same chemical signal can be either ignored, elicit attraction or cause repulsion. If a GC is blind to a signal, i.e. does not display any appropriate receptors, it will not respond. If receptors are present, the molecular nature of this receptor and the available pathway components downstream of it will determine the kind of response that is elicited. For example, netrin tends to elicit attractive responses when binding to DCC receptor, but induces repulsion through unc-5 receptor (Huber et al., 2003, Bashaw and Klein, 2010). Other examples involve different concentrations of signals, such as semaphorin-3A which triggers different signalling responses through the same receptor when present at higher or lower concentrations (Manns et al., 2012).

Notably, any responses triggered by signal/receptor pairings will have to effect on the cytoskeleton in order to induce any morphogenetic changes in GC behaviour (Fig. 1.2).

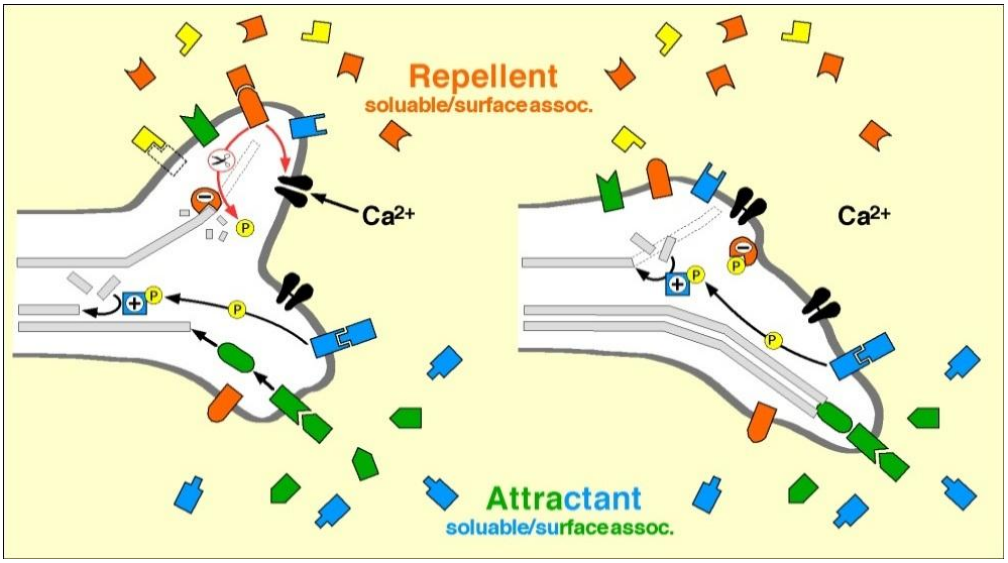

Figure 1.2. *A model for GC steering via extracellular cues.*

A GC (outlined in grey) is exposed to attractive (green or blue) and repulsive (red or yellow) signals in a spatial pattern. Signals for which they have no receptor (dashed empty symbol) are ignored, those that bind to receptors trigger signalling pathways that will eventually target the GC's cytoskeleton, either directly (symbolised as adding or removing phosho-groups) or indirectly (symbolised as regulating calcium influx locally). The ultimate event is the advance and stabilisation of MTs (blue square with a "+") away from repulsive and towards attractive signals and the destabilisation and retraction of MTs on the other side (red oval with a "-"). Image provided by A. Prokop.

1.2.1.1. Slits

Slits are evolutionarily well conserved extracellular signalling molecules. During neuronal development, Slits show a wide range of functions, such as guiding axonal growth, regulating dendrite branching, and guiding neuronal cell migration (Bashaw and Klein, 2010, Chedotal, 2007). Slits, were originally found in *Drosophila*, where they were shown to interact with Robo receptors. Thus, Slits are localised in the midline of the brain where they provide a strong repulsive cue for GCs displaying Robo receptors (Ypsilanti et al., 2010). This role of Slit and Robo in midline guidance is conserved in mammals (Dickinson and Duncan, 2010). Furthermore, the Slit-Robo receptor complex has been shown in *Drosophila* to contain Syndecan and Neurexin-IV as co-receptors which together form a quaternary complex (Broadie et al., 2011). Signalling components downstream of Slit/Robo include the tyrosine kinase Abelson (Abl), the actin regulator Ena (Bashaw et al., 2000) and the small GTPase Rac (Fan et al., 2003, Wong et al., 2001, Sanchez-Soriano et al., 2007).

1.2.1.2. Netrins

Netrins are a highly conserved family of secreted proteins that play an important role in GC guidance. They can induce attractive and repulsive responses in GC guidance depending on which membrane receptors they bind to (Round and Stein, 2007, Moore et al., 2007). The DCC protein, also known as UNC-40 in *C.elegans* and Frazzled in *Drosophila*, is a typical receptor on the membrane of GCs. Binding of Netrin to DCC changes P3 region conformation of DCC, which creates a ligand-gated multimerisation, to mediate the attractive function of Netrin (Stein et al., 2001). The attractive function of Netrin induced by DCC requires downstream functions of scaffold proteins like Nck or regulation of Rho GTPase family members (Li et al., 2002, Ziel and Sherwood, 2010). DCC can cooperate with the UNC-5 transmembrane receptor for Netrin to mediate the repellent function of Netrin. The UNC-5 receptor has quite a distinct structure to DCC protein (Keleman and Dickson, 2001, Hong et al., 1999). Repulsive Netrin-dependent guidance through UNC-5 has been reported to involve the *C.elegans* multidomain cytoplasmic protein MAX-1(Huang et al., 2002). It has been suggested that changes in cAMP levels are important for Netrin function (Huber et al., 2003, Bashaw and Klein, 2010). However, precise signaling networks downstream of Netrins are still unclear. Netrin not only associates with the developing CNS midline, but also functions in guide axons and effect tissue morphogenesis (Moore et al., 2007).

1.2.1.3. Semaphorins

Semaphorins (Sema) belong to a big protein family of transmembrane proteins with key functions in the regulation of nervous system development, such as cell migration and axonal GC guidance (Roth et al., 2008). In axonal growth, Semaphorins show both repulsive and attractive functions via different receptors and downstream signalling pathways. Plexins and neuropilins are the main Semaphorin receptors which signal via downstream proteins, such as the transmembrane protein OTK (off track), or the *Drosophila* multidomain protein MICAL (molecule interacting with CasL). There is also evidence that Semaphorin receptors affect the actin cytoskeleton via the regulation of Rho family GTPases (Yazdani and Terman, 2006). Semaphorins function is not limited to the regulation of neuron system, it also perform a crucial in various biological processes, such as angiogenesis, osteogenesis, immune regulation, vasculogenesis, tumor progression and cardiogenesis (Nkyimbeng-Takwi and Chapoval, 2011).

1.2.1.4. Ephrins

Ephrins and Eph form bi-directional ligand/receptor complexes which function in cell- cell communication during axon guidance and cell migration (Xu and Henkemeyer, 2012). Ephrins and Ephs are both membrane associated proteins, so the signaling between them has two opposite ways to work: “forward” or “reverse”; this bidirectional signal transduction works through two classes of Ephrin/Eph complexes: glycosylphosphatidylinositol (GPI)-linked Ephrin-As/EphA receptors work in the “forward” way and a hydrophobic transmembrane domain containing Ephrin-Bs/EphB receptors function in the “reverse” way (Huot, 2004). In the “forward” way, the signalling transfers from the Ephrin-A presenting cell to the EphA receptor expressing cell. Events downstream of EphA receptors involve Ras GAP, the tyrosine kinase Abl, or the GEF Ephexin (Eph interacting exchange factor) which controls the activity of RhoA, Rac and Cdc42 (Huot, 2004, Xu and Henkemeyer, 2012). In contrast, in the “reverse” way, the signaling transfers from the EphB expressing cell to the Ephrin-B presenting cell. The downstream signaling pathway components in Ephrin-B binding cells include PDZ-RGS, the cytoplasmic adaptor protein Grb4 and the scaffolding protein and kinase FAK (Xu and Henkemeyer, 2012).

1.2.1.5. Myelin-associated inhibitors

Three myelin-associated inhibitors, myelin-associated glycoprotein (MAG), Nogo A and Oligodendrocyte-myelin glycoprotein (OMgp), have been identified which are repulsive to growing axons, all binding and acting through the Nogo-66 receptor (NgR) which binds to p75 neurotrophin receptor ($p75^{NTR}$) and activates GTPase RhoA (Domeniconi and Filbin, 2005). First, MAG which is found in both CNS and PNS is likely to inhibit axon outgrowth through binding to NgR and gangliosides (GT1b and GD1a) (Schnaar and Lopez, 2009). Nogo A inhibits axonal sprouting/growth and regulates axon guidance in neurons by transfer signalling to downstream receptor NgR (Schmandke and Schwab, 2014). OMgp is expressed by mature oligodendrocytes and is likely inhibitory to axon extension (Domeniconi and Filbin, 2005). These factors are particularly important during processes of nervous system regeneration, especially in the CNS where they are not removed by glial cells after injury, thus forming a barrier for re-growing axons (Schwab, 2010).

1.2.1.6. Cell adhesion molecules

Immunoglobulin (Ig) cell-adhesion molecules (CAMs), cadherins and integrins are all cell-adhesion receptors that are abundant in the developing and functioning nervous

system (Shapiro et al., 2007). They can interact with ligands which exist in the extracellular matrix or on adjacent cells. Through these interactions CAMs can guide axon growth. Ig CAM family members and cadherins (calcium-dependent adherent proteins) primarily support intercellular adhesions mostly through homophilic interactions. In contrast, the integrins, are heterodimeric cell-surface receptors that normally link to extracellular matrix (ECM). All these cell-adhesion receptors perform important functions during axon growth and guidance (Huber et al., 2003, Myers and Gomez, 2011). On the one hand, they form physical links from the extracellular adhesion to the underlying cytoskeleton within the cell thus providing a means to transmit and sense forces across the membrane, on the other they act as signalling receptors activating downstream signalling pathways which often involve Rho family GTPases.(Huber et al., 2003). Notably, physical linkage between cell-adhesion receptors and CAMs is often required to generate tension as an important prerequisite for the induction of signalling events (clutch mechanism, see 1.2.2.2) (Giannone et al., 2009).

1.2.2. The organisation of the cytoskeleton in growth cones

In ideal cases, GCs can be divided roughly into three areas: a peripheral domain (P domain), a transition zone (T zone) and a central domain (C domain; Fig. 1.3) (Bouquet and Nothias, 2007). The P domain is composed of membrane protrusions rich in filamentous actin (F-actin), called filopodia and lamellipodia; filopodia are “finger-like” protrusions containing F-actin bundles, lamellipodia are “veil-like” protrusions containing lattice-like actin filament networks (Dent et al., 2011). F-actin networks in the GC periphery perform constant retrograde flow that can translate into protrusion of membranes. Through the activity of myosin II linking into these networks, they mediate force-producing contractility. The C domain is rich in MTs which form the distal end of the MT bundles of the axon shaft (Dent et al., 2011), From this pool of MTs, single MTs emanate and splay out to invade the GC periphery where they frequently enter lamellipodia and filopodia often advancing along F-actin bundles (Dent et al., 2011, Sanchez-Soriano et al., 2010). Furthermore, the C domain displays a high degree of molecular movement, such as the transport of organelles and vesicles (Dent et al., 2011). Finally, the T domain is located between the P domain and C domain; in this region, actin arcs form a semi-circle arranged perpendicular to F-actin bundles (Lowery and Van Vactor, 2009). In the T zone, F-actin bundles are often buckled by the Myosin II-driven compression and that way disassembled (Lowery and Van Vactor, 2009, Blanchoin et al., 2014).

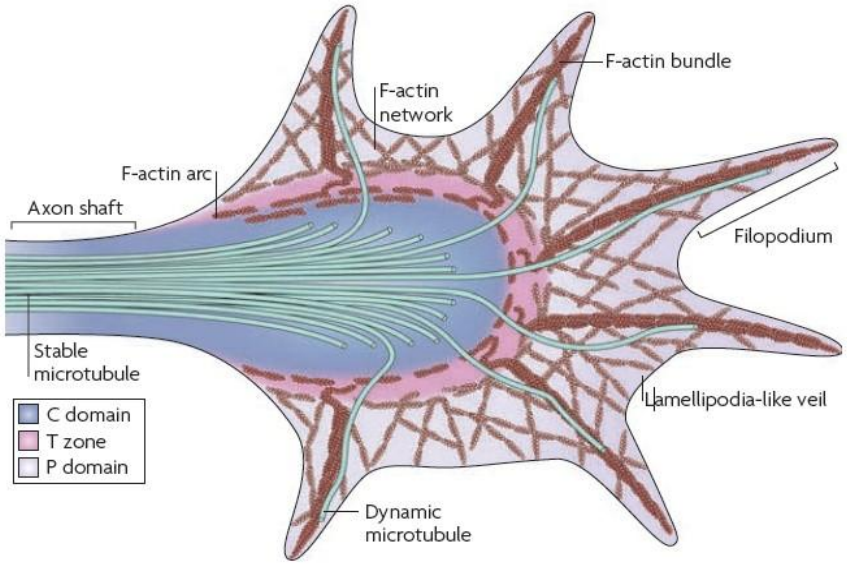

Figure 1.3. *The structure of GCs.*

Cytoskeleton distribution in the C, T and P domains in GCs. The turquoise lines represent MTs, and the red-brown lines actin. In the P domain, filopodia are containing F-actin bundles and single dynamic MTs, whereas lamellipodia are veil-like structures formed by F-actin network. In the T zone, F-actin arcs are arranged perpendicular to MTs. In the C domain, MTs from the axon shaft splay out and invade into the leading edge of the GC. Figure taken from (Lowery and Van Vactor, 2009).

1.2.2.1. The principal mechanisms of axonal growth

Axonal growth which is implemented at GCs during axonal pathfinding can be separated into three main steps: protrusion, engorgement and consolidation, and both actin filaments and MTs play crucial roles during these processes (Figs. 1.4 and 1.5) (Dent and Gertler, 2003, Lowery and Van Vactor, 2009, Suter and Miller, 2011, Prokop et al., 2013), as explained in the following.

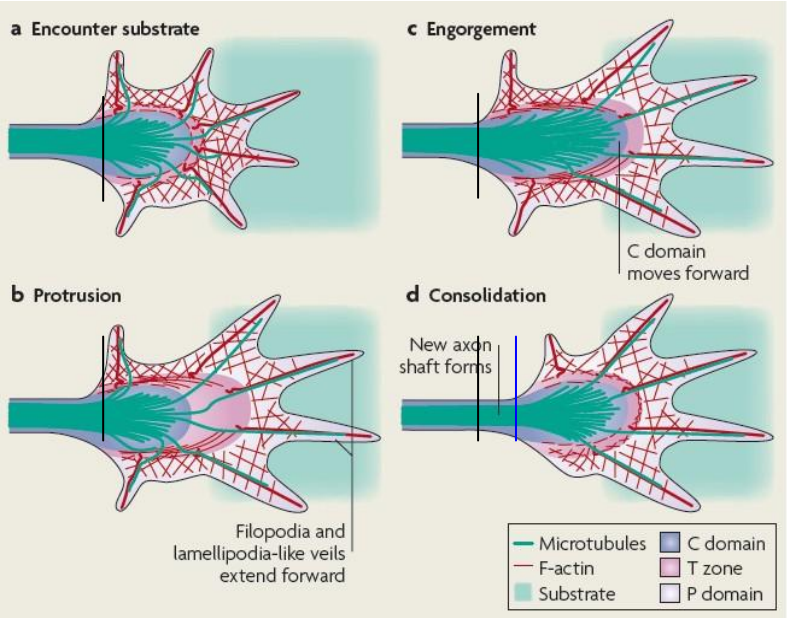

Figure 1.4. *The stages of axonal growth.*

A. *Resting GCs: F-actin networks remain primarily in a steady-state treadmilling condition, i.e. they undergo continuous back flow from the leading edge to the central domain through well balanced barbed end-polymerisation and pointed end-disassembly (see Chapter 1.3) (Suter and Miller, 2011).* ***B.*** *Upon encounter with extracellular guidance signals, GCs become polarised and protrusions are formed in a certain direction.* ***C.*** *During engorgement, F-actin structures give way for bulk extension of MTs into this area.* ***D.*** *During consolidation, the neck constriction moves anterogradely restricting actin protrusions to the newly established tip, i.e. shifting the GC forward. Figure taken from (Lowery and Van Vactor, 2009).*

1.2.2.2. The role of actin and MT networks in growth cones

F-actin is an important factor for the directionality of GC guidance, whereas MTs are key factors both in axon elongation and directionality. For example, cytochalasin B and D inhibit the addition of actin monomers to actin filaments (i.e. significantly reduce levels of F-actin in cells). Application of these drugs to growing neurons in culture does not inhibit axon growth, but it suppresses their ability to turn, and GCs no longer respond to guidance cues (Fig. 1.5) (Challacombe et al., 1996, Dent et al., 2011, Prokop et al., 2013). When confronted with borders of repellent signals, control GCs normally turn away when reaching these borders. However, on treatment with cytochalasins, this GC turning is prevented and growth is stalled instead (Challacombe et al., 1996). Such experiments suggest a crucial role for F-actin in the directionality of axon growth.

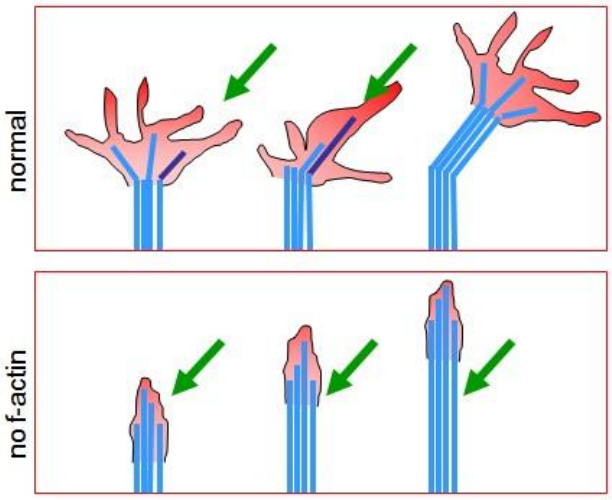

Figure 1.5. *The F-actin regulates the directionality of axonal growth.*

Top: *During the stage of protrusion (left), extracellular signals (green arrow) can induce regional stabilisation of single splayed MTs. During the stage of engorgement (middle), these single directionally stabilised MTs serve as pioneers for the bulk elongation of further MTs invading this region. During the stage of consolidation (right), the actin protrusions shift further distal, thus establishing a directionally elongated axon.* ***Bottom:*** *Without F-actin, the GC cannot respond to the attractive signalling, but the axon still extends. Therefore, MTs implement axon elongation, but F-actin is crucially required to guide this event. Image kindly provided by A. Prokop.*

The importance of actin networks during axonal guidance can be explained through a number of mechanisms. First of all, actomyosin-driven protrusions help to explore the environment and open up space for single MTs to change direction of the extending axon. Second, subcellular organisation of actin networks can provide guidance to MTs through pushing them into a certain direction (Lee and Suter, 2008) or by linking them through specialised proteins (see Chapter 1.4). Third, contractile actomyosin networks contribute to signalling processes, as best illustrated by the clutch model. The clutch model proposes that back flowing F-actin couples to extracellularly engaged adhesion complexes (see Chapter 1.2.1.6), so that myosin II-dependent tension can build up. This tension is required for the signalling processes of the adhesion receptors which essentially influence actin dynamics and MT stabilisation (Giannone et al., 2009). However, although the clutch mechanism is a well-established phenomenon, not all signalling events require tensile forces (Davenport et al., 1993).

The stabilisation of MTs is a key factor both in axon elongation and directionality. F-actin networks generate membrane protrusions on all sides of GCs that can be invaded by MTs in any direction. This facilitates lateral extension and stabilisation of MTs as an important prerequisite for GC turning.

Importantly, the lack of GC turning was observed when MTs were pharmacologically stabilised (Challacombe et al., 1997), suggesting that MTs are important players in this context. Also another set of further pharmacological experiments has nicely illustrated the role of MTs in GC turning (Buck and Zheng, 2002). Thus, when the MT stabilising drug taxol was directionally applied from one side to a GC (i.e. stabilising MTs in this direction), the axon was growing into that direction, thus mimicking attraction behaviour. On the contrary, when the MT destabilising drug nocodazole was applied in the same manner, the GC was repelled in the opposite direction. Therefore, directionality of MT polymerisation and stabilisation is an essential feature implementing directionality of axon growth (Fig. 1.6) (Buck and Zheng, 2002). Notably, co-application of cytochalasin D abolished this directionality (Fig. 1.6D) (Buck and Zheng, 2002).

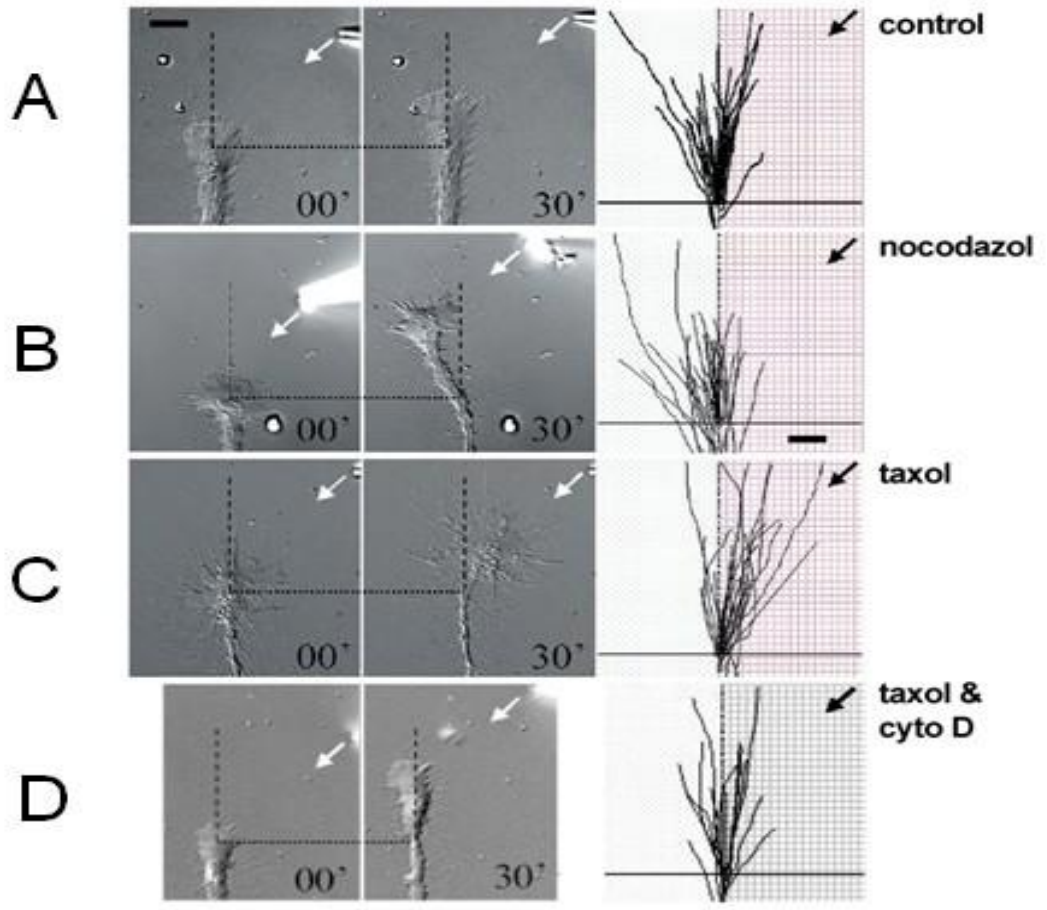

Figure 1.6. *MT and actin dynamic required for axon turning responses.*

A. *Directional application of vehicle from a capillary (white arrow) does not induce GC turning.* ***B.*** *When using the MT-destabilising drug nocodazole, the axon is repelled.* ***C.*** *The MT-stabilising drug taxol attracts GCs.* ***D.*** *When actin-destabilising cytochalasin drugs are applied together with taxol, GC attraction is suppressed. Image taken from (Buck and Zheng, 2002).*

These data lead to the following current models of axon growth. Actin-driven protrusions of GCs provide exploration space for splayed MTs to extend into all directions. During the protrusion stage, F-actin pushes out membrane protrusions, and extracellular signals can instruct their directionality. Single MTs become directionally stabilised through external signals, and F-actin networks can play an important mediator in this event, for example through the clutch mechanism. Bulk elongation of further MTs into this region causes the engorgement as precursor of the future new axon segment. Finally, engorgement is followed by constriction of F-actin networks around the newly formed MT bundle section, thus elongating the axon shaft and consolidating the new axon segment whilst restricting actin protrusions (hence the GC) to the newly formed tip (Challacombe et al., 1996, Dent and Gertler, 2003, Lowery and Van Vactor, 2009, Buck and Zheng, 2002, Prokop et al., 2013).

1.2.3. The principal mechanisms of axon growth at post-GC stages

However, not all axon growth is GC-dependent. During late embryogenesis and at postnatal stages, many GCs have reached their target cells and transform into synapses. However, during subsequent late embryonic and postembryonic stages where the body continues to grow, fully wired axons still have to keep growing to adapt to the dimensions of expanding tissues. In this situation, axon growth is no longer led by GC, but has to be performed within the axons themselves. It has been suggested that the mechanical tension which comes from the expanding tissue can induces axon growth and, accordingly, mechanical pulling force induced by dragging axons with a microelectrode can enhance the speed of axon growth (Heidemann et al., 1995, Bray, 1984, Franze et al., 2013). Furthermore, axon growth may also be induced by “MT sliding” which can be driven by motor proteins including Dynein/dynacin, kinesin-1 or mitotic kinesins (Ahmad et al., 2006, Baas et al., 2006, Prokop, 2013, Lu et al., 2013, del Castillo et al., 2015). For this, the motor proteins anchor to long MTs or cortical F-actin and walk along shorter MTs, thus moving them in either direction. It has been proposed that “MT sliding” can contribute to axon growth (Prokop, 2013).

As indicated, axonal actin may contribute to processes of MT sliding. Given the enormous influence that F-actin can have on MT dynamics (Prokop et al., 2013), it would not be surprising if actin in the axon shafts may play further roles during the regulation of axonal MT bundles. New opportunities have been provided by more precise descriptions of axonal actin. Thus, the proximal ends of axons were shown to contain dense F-actin networks within the axon initiation segment (AIS) which can act as filters selectively permitting cargo to enter axons and be transported anterogradely (Rasband, 2010,

Grubb and Burrone, 2010). However, most of the axon shaft contains a very different actin cytoskeleton. Thus analyses based on super-resolution microscopy, Stochastic optical reconstruction microscopy (STORM), in mature mouse axons (after 7DIV) revealed that actin filaments in axons are short, adducin-capped and arranged into rings which are evenly spaced with a periodicity of ~180 to 190 nm (Xu et al., 2013) (Fig. 1.7). This even spacing was proposed to be mediated by spectrin which is a long, antiparallel dimer able to bridge two adjacent rings (Xu et al., 2013). Recently, this periodic ring-like pattern of axonal actin has been confirmed using new SiR-actin probes with Stimulated emission depletion (STED) microscopy (Lukinavicius et al., 2014). Although the function of these ring structures is still unclear, it is in an ideal position to play roles in maintaining the elasticity and stability of axons, regulating the organisation of the plasma membrane, the formation of axon branches, or the behaviours of axonal MT (see Discussion 4.2.5) (Xu et al., 2013, Gallo, 2011).

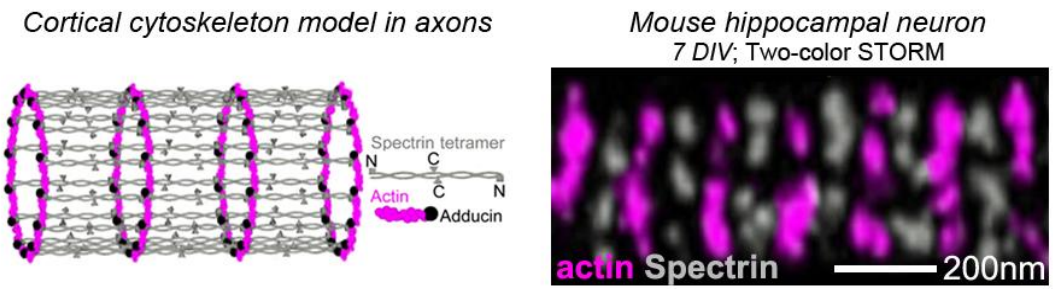

Figure 1.7. *STORM reveals a conserved periodic ring-like pattern of axonal actin.*

A) *A cortical actin model in axons has been proposed (Xu et al., 2013). Short actin filaments (magenta) bundle up into periodic ring-like patterns in axon. Spectrin tetramers (gray) connect between two actin ring structures (C and gray triangles indicate the C terminus of Spectrin; N and gray squares indicate the N terminus). Actin filaments are capped by adducin (black) at one end.* ***B)*** *The periodic patterns of actin and spectrin in axons of mouse hippocampal neurons at 7DIV imaged with two-colour STORM super-resolution microscopy (Xu et al., 2013).*

Given that these actin rings surround the parallel bundles of MTs which form the backbones of axons and provide the transport highway in axons, they may play important roles in their maintenance which is essential for axon longevity (Adalbert and Coleman, 2012, Millecamps and Julien, 2013, Schwarz, 2013). Thus, in ageing or demented brains, an increasing number of axons displays diverticula or blebbings which are areas of axons with severely disorganized MTs. They are considered an indication of putative axon degeneration since disorganised MTs can disturb axonal transport and trap organelles such as mitochondria, thus leading to their senescence and oxidative stress

which eventually can cause axon degeneration (Adalbert and Coleman, 2012, Fiala et al., 2007). Preventing such diverticula and maintaining MTs in a bundled arrangement is therefore a major challenge in ageing axons and the MT regulating mechanisms involved may not only invole MT-binding proteins but also depend on the axonal actin.

1.3. The nature and intracellular regulation of cytoskeleton

As mentioned before, axons are cable-like processes of neurons which electrically wire the nervous system, and they are highly delicate structures that can be up to a meter long in humans (Prokop et al., 2013). The cytoskeleton, including MTs, actin filaments and intermediate filaments (IFs) (Fletcher and Mullins, 2010), plays key roles in forming and maintaining the axonal architecture (Prokop et al., 2013). In axons, parallel bundles of long MT fragments form the structural backbones and transport highways, and they are surrounded by rings of actin bundles. In contrast, GCs form more complex and dynamic actin networks which mediate the formation of lamellipodia and filopodia and regulate axonal growth and guidance (Prokop et al., 2013). So far, I have not mentioned the roles of IFs in neurons which are involved in regulating axon diameters and are linked to neurodegenerative diseases, but the underlying mechanism is still unknown (Lepinoux-Chambaud and Eyer, 2013). Also, IFs seem functionally dispensable as indicated by the fact that there are no IFs in *Drosophlia* (Herrmann and Strelkov, 2011). Therefore, in my thesis, I will not discuss IFs any further, but focus on MTs and actin.

To understand how actin and MTs perform their roles in axons, one needs to understand the nature and intracellular regulation of the cytoskeleton. In the following, I will first introduce the fundamental properties of cytoskeleton and then explain its immediate regulators, first focussing on F-actin then on MT regulation and then on mechanisms linking the two.

1.3.1. The molecular nature of actin

Actin networks are composed of actin filaments polymerised from globular actins (G-actin). G-actins are the products of individual genes. They are polar proteins, and their plus-to-minus end polymerisation results in polarised F-actin with two distinct ends (Pak et al., 2008, Blanchoin et al., 2014). The “barbed” end mainly contains ATP-actin and is the end where polymerisation preferentially occurs in cells (Dent et al., 2011). The “pointed” end mainly contains ADP-actin and is the end where depolymerisation or disassembly generally happens *in vitro* and in cells (Fletcher and Mullins, 2010, Blanchoin et al., 2014). During axonal growth, aspects like F-actin polymerisation,

disassembly and stabilisation are regulated through actin binding proteins (ABPs), and their integrated function equips F-actin networks with the ability to drive membrane protrusions and to perform retrograde flow and contractions (Blanchoin et al., 2014) (Fig. 1.8).

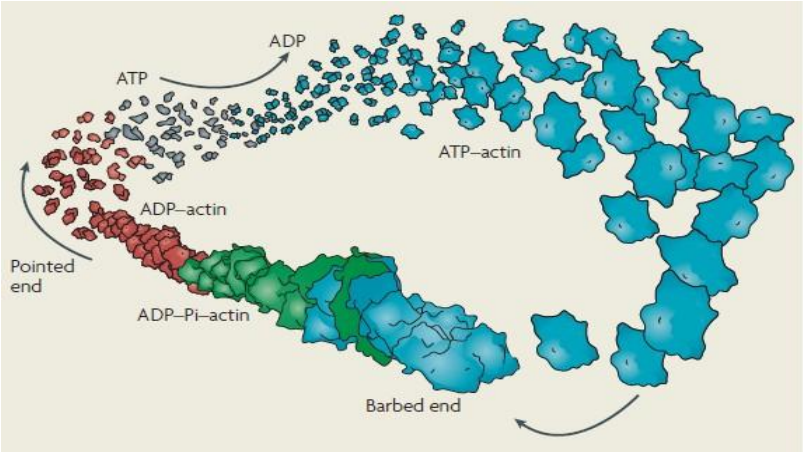

Figure 1.8. *The basic processes of actin assembly and disassembly.*

Globular ATP-actin (turquoise) of the cytosol, is added to the barbed end in an energy-favoured polymerisation step. It degrades to ADP-Pi-actin (green) and eventually to ADP-actin (red) which has a higher tendency to disassociate at the pointed end, at least in vitro. Conversion of ADP-actin to ATP-actin requires enzymatic activity through proteins, such as profilin. Image taken from (Pak et al., 2008).

1.3.2. Actin-binding proteins (ABPs) as immediate regulators

Different classes of ABPs are involved in the regulation of actin dynamics. Grouped by function they include actin nucleators (seeding new filaments; e.g. formins, Arp2/3 complex, Spire), barbed-end binding factors (positively or negatively regulating polymerisation; e.g. Ena/VASP, profilin, capping proteins, adducin), proteins binding along actin filaments (stabilising and cross-linking them; e.g. tropomyosin, fascin, actinin, filamin, fimbrin), pointed end-binding proteins (stabilising them; e.g. patronin; disassembling them; e.g. cofilin, gelsolin) and different classes of actin-based motorproteins moving/binding along them (different classes of myosins; Figs. 1.9) (Pak et al., 2008, Prokop et al., 2013). In GCs, the activity of many of these proteins is regulated through signalling events involved in pathfinding (Huber et al., 2003, Ng and Luo, 2004, Hall and Lalli, 2010). However, how these molecular pathways operate and are integrated at the GC level to implement predictable morphogenetic changes is little understood.

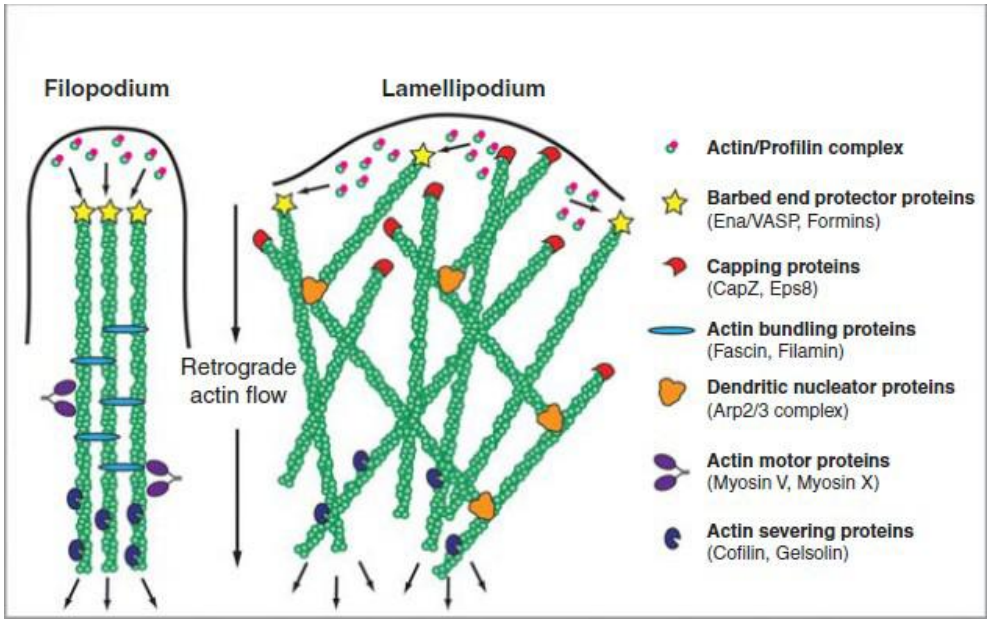

Figure 1.9. *The subcellular distribution of principal ABPs in filopodia and lamellipodia.*

Different classes of ABPs (explained on the right) interact with actin filaments in filopodia (forming parallel cross-inked bundles; left) and lamellipodia (forming lattice-like polarised networks; right). In both structures, F-actin networks have a polarised, barbed end-out configuration, and polymerisation occurs exclusively at the distal end and disassembly at the proximal end, thus mediating a treadmilling effect associated with retrograde actin flow. Further explanations are given in the text. Figure taken from (Dent et al., 2011).

The nuleator proteins include members of very different protein families and comprise the Arp2/3 complex, formins, Spire, Cobl, Lmod, VopL/VopF and TARP (Chesarone and Goode, 2009). Except formins, they all interact with actin through WASP-Homology 2 domains (Dominguez, 2009). The Arp2/3 complex which is highly conserved in all eukaryotes works by serving as substrate for actin monomers and this step is essentially catalysed through the Wiskott-Aldrich syndrome Protein (WASP) or the SCAR/Wave complex (Qualmann and Kessels, 2008). Formins act by stabilising existing actin oligomers, which may be provided through actin binding sites in the C-terminus of APC1 (Okada et al., 2010). The other nucleators tend to work by providing G-actin binding sites arranged in tandem, thus lining them up and catalysing their polymerisation by bringing them in close spatial proximity.

The barbed end-promoting/protecting proteins, such as Ena/VASP, formins and profilin catalyse barbed end polymerisation (Pak et al., 2008). Ena/VASP plays a number of different roles including protecting barbed ends against negative regulators (in particular capping proteins), catalyzing the G-actin transfer onto the barbed end (through interaction with profilin) and also aggregating barbed ends through its ability to oligomerise (Bear and Gertler, 2009). Profilin binds G-actin, catalyses the exchange of

GDP for GTP and can bind Ena/VASP during the polymerisation process (Yarmola and Bubb, 2006). Formin dimers form a ring structure at the barbed end and elongate the filaments through mechanisms described as the "stair-stepping model" (Paul and Pollard, 2009). In contrast to these positive regulators, capping proteins (CP) also bind to the barbed ends of actin filaments, but they prevent the association and dissociation of actin monomers, thus inhibiting actin polymerisation (Kim et al., 2010, Nakano and Mabuchi, 2006). Adducin caps F-actin barbed ends where it prevents actin polymerisation but also recruits other proteins to actin, such as Spectrin (Li et al., 1998, Baines, 2010).

The actin bundling/stabilising proteins normally cross-link and stabilise actin filaments (Aratyn et al., 2007). Fascin is one of the most highly expressed actin bundling proteins (De Arcangelis et al., 2004). It tends to induce linear, parallel actin bundles, for example in filopodia (Cohan et al., 2001). Tropomyosin is another stabiliser of actin filaments by binding on particular points between the surface of actin and itself (Ujfalusi et al., 2009). Filamin cross-links actin filaments into parallel arrays or three-dimensional lattices, but also mediates binding of actin filaments to signalling pathway factors and membrane proteins (Nakamura et al., 2011, Uribe and Jay, 2009). α-actinin, which binds to actin through its two calponin homology (CH) actin binding domains, forms an antiparallel dimer which can crosslink two actin filaments (Broderick and Winder, 2005, Sjoblom et al., 2008). Similar to Filamin, α-actinin also mediates the interaction of actin filaments with signalling pathway factors and membrane proteins, such as integrins (Broderick and Winder, 2005, Sjoblom et al., 2008).

Pointed end-binding factors comprise severing and stabilising proteins. For example, cofilin can sever actin filaments primarily in GDP-rich areas away from the barbed ends by changing the twisting structure of actin filaments (McGough et al., 1997). Cofilin can also enhance the speed of actin depolymerisation at the pointed end by recruiting and binding actin monomers (Carlier et al., 1997), although it is being debated in the field whether depolymerisation occurs *in vivo* or whether disassembly prevails (Blanchoin et al., 2014). Another factor that has been revealed to disassemble lamellipodial F-actin networks at their proximal end is myosin II which appears to overcontract and thus break actin filaments when in high concentration (Blanchoin et al., 2014). In contrast, Tropomodulin also binds to the pointed ends of actin filaments, but it stabilises the actin filaments by building a blocking cap on pointed ends, preventing pointed end polymerisation as well as depolymerisation, and this capping of pointed ends is particularly important for long lived actin filaments (Weber, 1999).

Myosins are actin motor proteins powered by ATP hydrolysis, which impose forces on actin networks and mediate transport of cargo along actin filaments (Nambiar et al., 2010, Hartman et al., 2011). Different myosins have distinct directionality. For example, myosin V moves to the barbed ends and myosin VI to the pointed ends (Kapitein and

Hoogenraad, 2011). Apart from transport functions, myosins have been suggested to establish important actin-membrane linkage (Hartman et al., 2011), and myosin II which harbours two motor domains can intercalate into lattice-like actin networks or antiparallel actin fibres and drive their contraction (Vallenius, 2013, Blanchoin et al., 2014).

1.3.3. The molecular nature of microtubule

MTs are tubular structures composed of 13-15 linear protofilaments formed from tubulin dimers (α- and β-tubulin heterodimers). Depending on the different binding of GTP or GDP at the nucleotide exchange site (E site) on β-tubulin, dimers can be classified as GTP-tubulin and GDP-tubulin (Conde and Caceres, 2009). MTs display dynamic instability, i.e. they cycle between rapid polymerisation (growth) and depolymerisation (shrinkage) (Akhmanova and Steinmetz, 2008, Etienne-Manneville, 2010). During polymerisation, GTP-tubulin is added to the plus ends of MTs providing a GTP cap that stabilises MTs; after or during polymerisation, GTP-tubulin can be hydrolyzed to GDP-tubulin which has a tendency to be disassembled from MT plus ends, thus favouring MT shrinkage (Akhmanova and Steinmetz, 2008, Etienne-Manneville, 2010). The term “catastrophe” is used to describe the transformation from polymerisation to depolymerisation, and “rescue” when depolymerisation turns into polymerisation (Conde and Caceres, 2009). The γ-tubulin, a third tubulin isoform, is located at the minus ends of MTs and connects with capping proteins. γ-tubulin is essential for nucleation processes, i.e. the seeding of new MTs which, in axons, does not depend on centrosomes/centrioles (Fig. 1.10) (Conde and Caceres, 2009, Basto et al., 2006, Stiess et al., 2010).

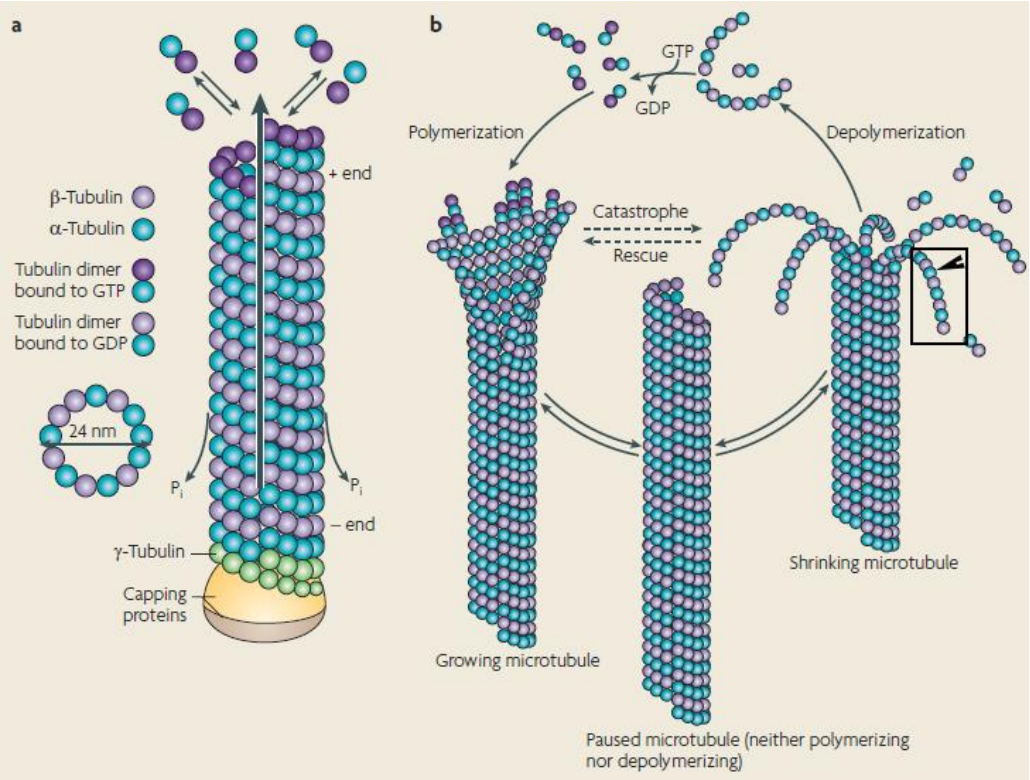

Figure 1.10. *The basic processes of MT assembly and disassembly.*

a) *The basic component and structure of MTs. Tubulin dimers are composed of α-tubulin and β-tubulin. These tubulin dimers can be associated with GTP or GDP. These tubulin dimers are added to the plus end during polymerisation and also disassociate from this end during depolymerisation. MTs have a helical and hollow structure of ~24nm diameter, composed of 13-15 parallel protofilaments (indicated in the black box with arrowhead in b). γ-tubulin is essential for nucleation processes of new MTs at centromeres/centrioles and subsequently stays associated with the minus ends which are often protected by minus end capping proteins.* ***b)*** *Three states of MTs: Growing MT (MT polymerisation), shrinking MT (MT depolymerisation) and paused MT (neither polymerisation nor depolymerisation). The terms "catastrophe" and "rescue" describe the transition between polymerisation and depolymerisation stages. After GDP-tubulin depolymerises from plus ends of MTs, the GDP is replaced by GTP, with the help of GEFs (Guanine nucleotide exchange factors). Picture taken from (Conde and Caceres, 2009).*

1.3.4. Microtubule binding proteins (MTBPs) as immediate regulators

Comparable to roles of ABPs in F-actin regulation, the dynamics of MTs are regulated through different classes of microtubule binding protein (MBPs), many of which are highly expressed in neurons (Fig. 1.11) (Conde and Caceres, 2009). In the following, I will provide a brief overview of the classes of MBPs contributing to MT regulation.

MT plus end-tracking proteins (+TIPs) regulate the polymerisation, depolymerisation and stabilisation of MT plus ends, and they regulate the direction of MT growth as well as their targeting to subcellular structures and organelles (Akhmanova and Steinmetz, 2010, Etienne-Manneville, 2010, Gouveia and Akhmanova, 2010). EB (end binding) proteins are believed to be the essential proteins that can directly bind to MT plus ends through their N-terminal domains, whereas other +TIPs, such as APC, Clip, dynein, CLASPs or spectraplakins, predominantly associate with MT plus ends through binding to EB proteins (Akhmanova and Steinmetz, 2008). Given the very different nature and subcellular localisation of these +TIPs, their competition for limited EB1 binding sites is believed to be an essential mechanism by which MT polymerisation dynamics and directionality can be regulated in space and time.

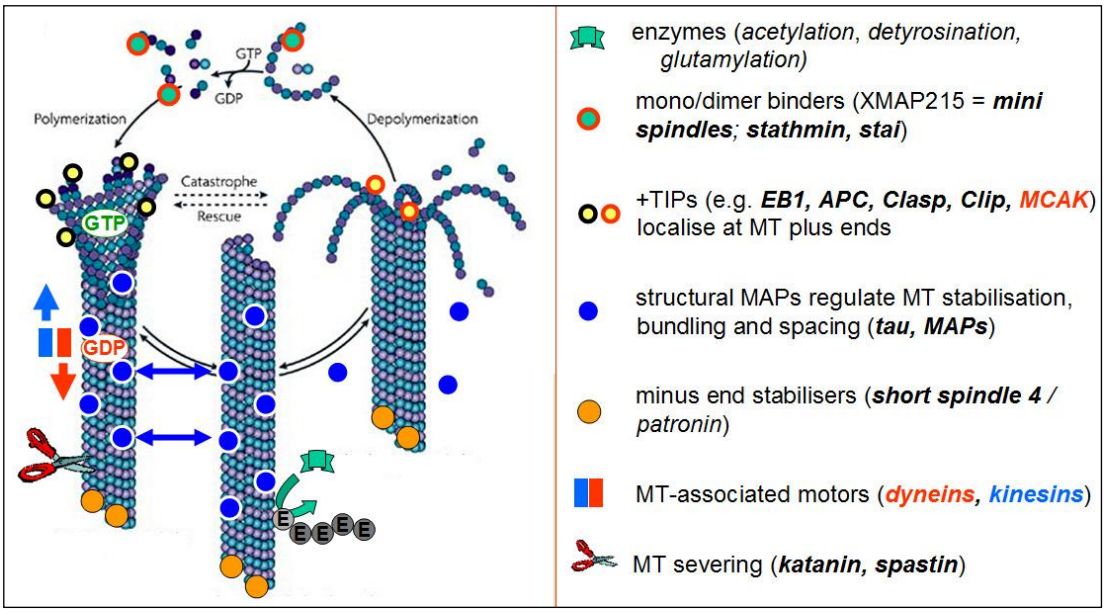

Figure 1.11. *Principal classes of MTBP regulating MT dynamics.*

This picture shows MTs during polymerisation (left), pausing (middle) and depolymerisation (right), with the transition between polymerisation and depolymerisation referred to as catastrophe and rescue (stippled arrows). Different classes of MTBPs (explained on the right) regulate MT dynamics in different states of MTs. Further explanations about these factors are given in the text. For details see text. Image kindly provided by A. Prokop.

MT minus end-binders, such as Patronin/Ssp4 (short spindle 4) can stabilise against minus end polymerisation and depolymerisation (Goodwin and Vale, 2010). Depletion of Patronin in *Drosophila* S2 cells by RNAi causes MTs to undergo

depolymerisation at the minus end; this result suggests that Patronin plays a crucial role in MT minus end capping and stabilisation (Goodwin and Vale, 2010).

Proteins localizing along MT shafts primarily in neuronal axons are known as structural MT-associate proteins (MAPs), which help axon formation and to stabilise MTs by protecting against MT severing or destabilisation (Chilton, 2006). Structural MAPs, such as MAP1A, MAP1B, MAP2 and Tau, are particularly abundant in neurons, and play a key role in neuron development and neurodegenerative disease (Bouquet and Nothias, 2007). For example, Tau can help tubulin nucleation at the beginning of MT assembly, and it can stabilise MTs and avoid MT severing via binding to MTs (Morris et al., 2011); pathological forms of Tau protein tend to be highly phosphorylated and detached from MTs and are seen as being causative in neurodegenerative diseases, such as Alzheimer's disease (AD), Pick's disease or other tauopathies (Wang and Liu, 2008, Morris et al., 2011).

MT motor proteins can transport material along MTs, with kinesins being primarily anterograde and dynein/dynactin retrograde transporters (Terada et al., 2010, Kapitein and Hoogenraad, 2011, Prokop, 2013). The orientation of MT-based transport is heavily dependent on the regionally restricted modifications of MTs and the orientation of MTs, which are oriented with their plus ends facing distal in axons, whereas dendritic MTs form anti-parallel bundles. Kinesin is a plus-end oriented motor protein composed of 2 parts: heavy chains and light chains. Cargoes transported along axons bind to the light chain (often involving linker molecules), whereas their heavy chain propels along MTs in an ATP-dependent manner (Hirokawa et al., 2010). In contrast, dynein/dynactin is a large protein complex acting as a minus-end oriented motor, primarily transporting retrogradely in axons (Akhmanova and Steinmetz, 2008, Kapitein and Hoogenraad, 2011). However, when anchoring to F-actin or to long MTs it can transport short MT fragments anterogradely or slide them, thus producing forces, thus contributing to axonal growth (Myers et al., 2006b). Furthermore, dynein can bind membranes which could explain some MT membrane interactions (Hirokawa et al., 2010).

MT severing proteins, such as Katanin or Spastin, can sever MTs, thus helping to remodel MT networks, for example during axonal branching (Yu et al., 2008). Katanin which is present at higher levels than Spastin in the neuron, is crucial for axon growth because it produces short MT fragments that can be transported into the axon or be used as substrate for new polymerisation events (Qiang et al., 2006, Yu et al., 2008). Spastin tends to accumulate at branch sites along the axon and plays an important role in axonal branch formation (Yu et al., 2008, Kalil and Dent, 2014, Krause and Gautreau, 2014). Tau has been shown to protect MTs against Katanin severing but not against Spastin (Yu et al., 2008).

Finally, there are numerous enzymes that can posttranslationally modify MTs thus inducing their acetylation, (poly)-glycation, (poly)-glutamylation and de-tyrosination; but the regulatory roles of these modifications are only beginning to emerge (Janke and Bulinski, 2011, Janke and Kneussel, 2010)

As explained above, MTs are pivotal for axon extension. Accordingly, MTBP-mediated functions, such as MT polymerisation, severing of MTs, anterograde transport, the stabilisation of MTs or their linkage to actin, have been shown to contribute to axon growth (Fig. 1.12).

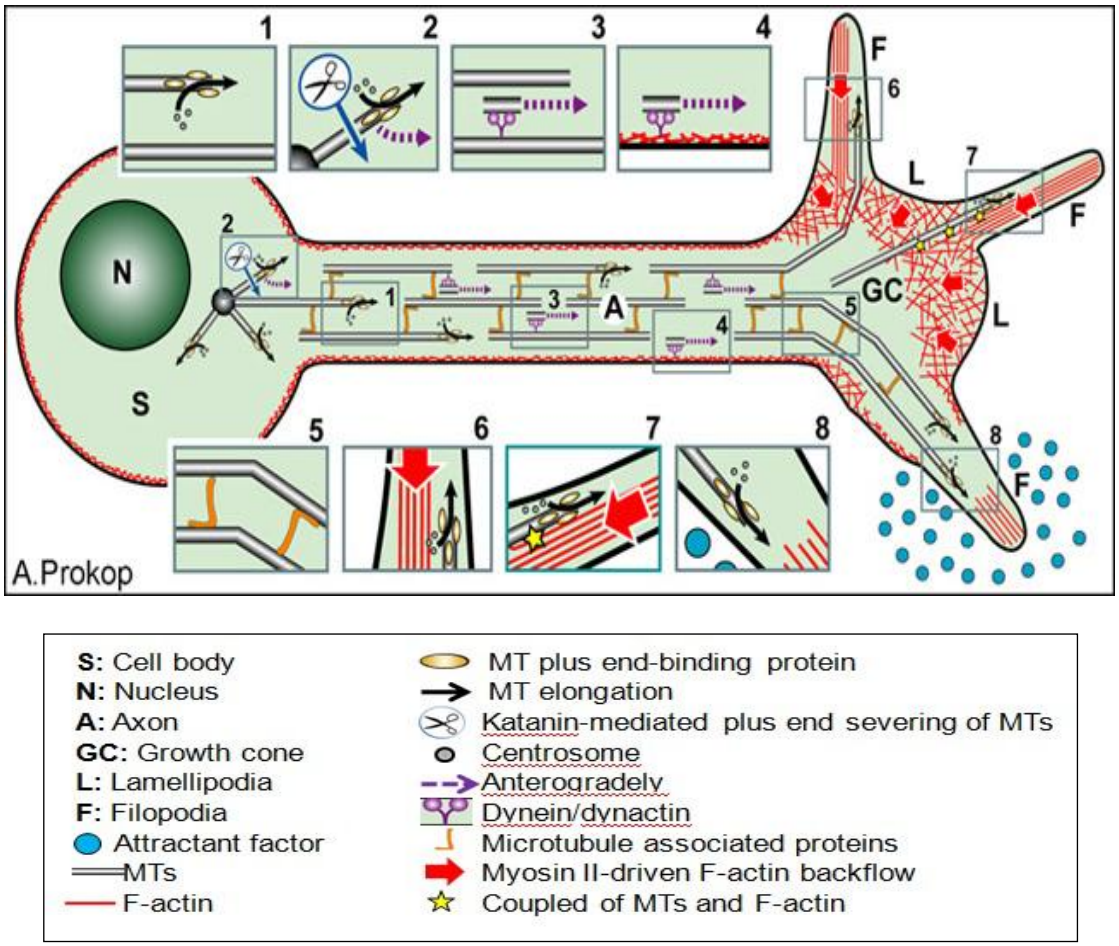

Figure 1.12. *Proposed MT related mechanisms of axon elongation.*

MT plus end-associated proteins (+TIPs) regulate MT polymerisation/depolymerisation, i.e. the dynamics of MT elongation (1). Katanin-mediated plus end severing of MTs produces MT fragments (2) which contribute to axon elongation by being transported anterogradely through MT-associated dynein/dynactin motor complexes (anchored to longer MTs or F-actin network; 3,4). MT bundling and stabilisation primarily through structural MAPs (MT associated protein) can contribute to axon elongation (5). An essential regulatory mechanism of MTs is their interaction with F-actin, by using F-actin structures to guide the direction of their plus end polymerisation processes (6), by

coupling to F-actin backflow as an event that inhibits MT advance (7), or by invading areas that have been cleared from F-actin as a consequence of signalling (e.g. clutch mechanism; see Chapter 1.2.1.6; 8). Image kindly provided by A. Prokop.

1.4. Actin-MT cross-talk

F-actin and MTs are not independent entities in cells, but they cross-talk and mutually regulate their dynamics. For example, actin-MT interactions can regulate F-actin destabilisation or tubulin stabilisation under steady state condition in GCs (Dent and Kalil, 2001). Consequently, actin-MT cross-talk plays an important role in GC steering and axonal growth guidance.

1.4.1. Direct interaction of F-actin and MTs

In large GCs of the sea slug *Aplysia* it was well demonstrated that actin backflow is an important factor in regulating directional MT stabilisation and extension (Forscher and Smith, 1988, Schaefer et al., 2008). Using fluorescent speckle analysis in *Aplysia* GCs, it was shown that F-actin can regulate MTs directly. For example through dynamic constrictions of F-actin networks, MT advance can be pushed into a certain direction. When applying beads functionalised with apCAM (a homophilic Ig CAM present on *Aplysia* GCs) and restraining them so that they induce mechanical forces upon adhesion (see clutch mechanisms described in Chapter 1.2.1.6), these beads can induce GC turning, and actin-MT coupling plays an important role in this process (Suter and Forscher, 2000, Suter et al., 2004).

1.4.2. Mono-molecular actin-MT linkage

The actin-MT cross-talk can be mediated by single linker molecules. Original MT binders have often been shown to also bind F-actin, and examples for this are MAP1B, Tau and Shot. For example, MAP1B is a classical MAP which stabilises and cross-links MTs, and it is also able to bind to F-actin (Halpain and Dehmelt, 2006, Villarroel-Campos and Gonzalez-Billault, 2014). It has been suggested that MAP1B can regulate GC turning by stabilising MTs (Mack et al., 2000), and this function of MAP1B may also require its F-actin binding ability, since actin is crucial for GC turning. Also Tau binds to MTs via it MTBD and stabilises them (Buee et al., 2000, Iqbal et al., 2009). Tau has been also shown to bind to actin through its N-terminus, and it has been proposed that other molecules can be recruitment to actin by binding to tau (Yu and Rasenick, 2006, Buee et al., 2000). Accordingly, tau is involved in the formation of F-actin and cofilin containing Hiromi bodies in Alzheimer's disease (Bamburg and Bloom, 2009).

Prototype proteins acting as dedicated actin-MT linkers are the Gas2-like proteins and the spectraplakins. GAS2 family proteins are well conserved from *C. elegans* to *H. sapiens,* suggesting that they play important biological roles. They all contain an F-actin-binding domain (ABD) composed of a calponin homology domain (Korenbaum and Rivero, 2002) and a MT-binding and -stabilising Gas2-related domain (GRD). All family members but one harbour a carboxy-terminus called Ctail that regulates the interaction with MTs (Stroud et al., 2011). Some of Gas2 family proteins are functionally relevant. For example, Gas2 is involved in signalling pathways controlling cell growth, apoptosis and cancer, and Gas2 overexpression in *Xenopus* embryos inhibited cell cycle progression (Brancolini et al., 1995, Zhang et al., 2011). Also knock-down of GAS2L3 in mammalian epithelial cells affected mitosis leading to multinucleated cells. In agreement with such a role, Gas2L3 localises to the centrosome, mitotic spindle and the midbody (Wolter et al., 2012)

The spectraplakin ACF7/MACF1 (actin cross linking family 7/ MT and actin cross linking factor 1) has been shown to target MTs to focal adhesions, integrin-associated adhesion complexes that anchor stress fibres and are essential for cell migration in culture. In the absence of ACF7, MTs fail to target to focal adhesions, and focal adhesions are enlarged in these cells, suggesting that ACF7-mediated MT targeting is required for focal adhesion disassembly (Kodama et al., 2003, Wu, 2008 #3196). ACF7 binds to F-actin, along the shaft of MTs and EB1 at MT plus ends. A current model suggests that, via ACF7, MTs track along F-actin stress fibres to focal adhesions (Kodama et al., 2004). Work on the fly homologue Short stop (Shot) has shown that guidance of MT plus ends along actin structures and stabilisation of MT by its Ctail is important for proper MT bundle formation and axonal growth, and it requires simultaneous interactions with actin, MTs and EB1 (Alves-Silva et al., 2008, Sanchez-Soriano et al., 2009, Alves-Silva et al., 2012).

1.4.3. Actin-MT links through combinations of MTBPs and ABPs

The actin-MT cross talk can also be regulated by a chain of binding proteins interconnecting MTs and actin. For example, the F-actin-binding protein drebrin anchors to actin networks at the base of filopodia in GCs and binds to EB3 at the tip of polymerising MTs; through this link the entry of MTs into filopodia can be regulated (Geraldo et al., 2008). As a second example, the EB1-independent MT plus end-binding factor Doublecortin has been shown to organise MTs at the GC neck. In this context it is regulated through Protein phosphatase 1 (PP1) which is targeted to the GC neck by the actin-binding protein Spinophilin (Bielas et al., 2007). This example demonstrates how F-actin networks can regulate MTBPs to mediate the formation of specific MT networks.

Also molecular motor proteins can regulate functional links between F-actin networks and MTs. Thus, it has been proposed that MT-associated dynein (usually known for its key role in retrograde axonal transport) counteracts myosin II-driven F-actin backflow. In the absence of dynein, MTs were found to be less effective in invading the P domain correlating with reduced axon growth and GC turning, and these phenotypes could be rescued by co-inhibiting myosin II (Myers et al., 2006b). Another mechanism that may contribute here is the anterograde transport of short MT fragments through dynein which also can contribute to axonal growth (Ahmad et al., 1998). These results indicate that dynein and myosin II can perform opposing but cooperative functions which regulate MTs downstream of F-actin (Myers et al., 2006b).

1.5. Two fundamental functions of cortical interactions of MTs: capture and collapse

1.5.1. Capture as a means of targeted transport and signalling

Cellular roles of MTs often require that their tips are targeted to and captured at organelles or special cortical regions. This process is believed to regulate the directional transport of signals and/or structural components. Targeting and capture of MTs has been shown to be essential for cell migration (Fukata et al., 2002, Kodama et al., 2003, Wu et al., 2008) and can therefore be expected also to regulate axonal growth.

First, capture of MT plus ends at focal adhesion sites seems to play an important role in cell migration in fish fibroblasts (Kaverina et al., 1998, Efimov et al., 2008). After MTs are captured they can either become stabilised (as indicated by resistance to the MT depolymerisation drug nocodazole) or undergo catastrophe and retract (Kaverina et al., 1998, Efimov et al., 2008). After treating cells with nocodazole in fish fibroblasts, most MTs are eliminated, but during their re-growth they immediately target focal adhesion sites indicating clear directionality in this behaviour (Kaverina et al., 1998). Also in neurons, crosstalk of MTs with adhesion sites was shown to play important roles. One good example is the targeting of MTs of cortical neurons to the neural cell adhesion molecule NCAM180 at synapses (i.e. a highly specialised area of the cell cortex). This process requires dynein-NCAM180 interaction and seems to provide a mechanism to direct cargo transport to synapses, thus contributing to synapse maintenance (Perlson et al., 2013).

Another example is CLIP-170-mediated MT capture which leads to prolonged pausing of MTs at the cell cortex of fibroblasts (Fukata et al., 2002). In this context, CLIP-170 (a +TIP binding to EB1 at MT tips; Chapter 1.3.4) forms a tripartite complex with the small GTPases Rac1/Cdc42 and the scaffold protein IQGAP1 which is closely

associated with F-actin networks (Briggs and Sacks, 2003). A similar mechanism involving IQGAP1 and CLIP-170 was reported to play a role also during the growth of neuronal dendrites (Swiech et al., 2011).

Targeting and capture of MTs can be essentially mediated through actin-MT cross-talk, usually mediated by +TIPs (i.e. proteins that are enriched at the polymerising plus ends of MTs). As mentioned above (Chapter 1.4.2), the spectraplakin ACF7 is a +TIP which binds directly and simultaneously to MTs and to actin, and this allows it to guide MT extension along actin stress fibres in cultured visceral endodermal cells (Kodama et al., 2003, Kodama et al., 2004). Since actin stress fibres are anchored to focal adhesions, this actin-MT linkage mechanism provides an easy way to target MT extension to those sites. Also, G2L1 and G2L2, two actin-MT crosslinkers of the Gas2 family of proteins, were described to localise to actin and sense the amount of actin filaments to regulate the MT growth and dynamics by binding to the +Tip protein EB1. This function of Gas2 family proteins is influenced by different extracellular matrix substrates, suggesting that actin acts downstream of extracellular signals to regulate MTs behaviors (Stroud et al., 2014).

1.5.2. MT Collapse: Efa6 as a negative regulator of cortical MT capture

Besides mechanisms of cortical MT capture (e.g. via CAMs), also MTs cortical collapse factor have been proposed, such as Efa6 (Exchange factor for Arf6). The first human cDNA encoding EFA6 (in humans also referred to as pleckstrin and sec7 domains-containing protein / PSD; from now on referred to as hsEfa6) was described to be a specific guanine exchange factor for the small GTPase Arf6 (Franco et al., 1999), although recent research showed that it can also act as a membrane-bound Arf1-GEF (Padovani et al., 2014). For its GEF functions, Efa6 contains a conserved Sec7 domain, which catalyses the guanine nucleotide exchange. Furthermore, Efa6 contains a pleckstrin homology (PH) domain, which can target it to the plasma membrane via binding to PI(4,5)P2 (Macia et al., 2008, Franco et al., 1999), as well as a coiled-coil domain which is essential for the formation of actin filament through mechanisms little understood (Derrien et al., 2002).

However, recent work has shown that *Drosophila* Efa6 (dmEfa6) fails to activate Arf6 in certain contexts and, accordingly, localises outside its expression domain (Huang et al., 2009, Johnson et al., 2011). Furthermore, a study in early embryonic cells of *C. elegans* has shown that EFA6 of the nematode (ceEfa6) can mediate cortical collapse of MTs, limiting their growth at the cell cortex (O'Rourke et al., 2010). This function might be responsible for a role of ceEfa6 in slowing down axon regeneration in the nervous system of the worm (Chen et al., 2011). The functions in both cortical collapse and axon

regeneration only require the N-terminus but not the Sec7 domain and C-terminus; hybrid constructs containing the N-terminus fused to CAAX box, a membrane-associating domain derived from *C. elegans* MIG-2, were fully functional in those two contexts (O'Rourke et al., 2010, Chen et al., 2011). In the mouse the isoforms A, C, D of EFA6 (musEfa6) are mainly expressed in the brain (Perletti et al., 1997, Sakagami et al., 2006), Notably, also *dm*Efa6 has been found to be expressed in the embryonic nervous system (Huang et al., 2009), and might therefore play roles in regulating MT collapse and/or axon regeneration, but it might as well act as an Arf6 GEF in the nervous system.

Many more insights were gained into roles and functions of Efa6 family members. For example, in non-neuronal cells, musEfa6A binds to the N-BAR domain of endophilin via its Sec7 domain, and recruits endophilin to the plasma membrane. This interaction between musEfa6A and endophilin regulates its ability to generate membrane curvature (Boulakirba et al., 2014). During development of the compound eye of *Drosophila*, dmEfa6 associates with junctions of inter-ommatidial precursor cells (IPC) to regulate their positioning during eye patterning (Cagan, 2009). Together with other Arf-class regulators, dmEfa6 helps to pattern and maintain the fly eye, and its deficiency causes a degenerative eye phenotype for which the underlying mechanisms still need to be investigated (Johnson et al., 2011). Also musEfa6 is involved in cell junction regulation, and has been shown to organise the actin cytoskeleton at tight junctions using two cooperating pathways, the activation of Arf6 on the one hand and functions associated with its C-terminus on the other for which the mechanisms still need to be investigated (Klein et al., 2008).

In neuronal cells, musEfa6A has been shown to be associated with plasma membranes and intracellular vesicles of cell bodies, dendritic shafts, dendritic spines and filopodia-like protrusions, but not in axons (Sakagami et al., 2007). Overexpression of musEfa6A in dissociated primary adult dorsal root ganglion (DRG) neurons as well as in α9 integrin-expressing PC12 cells has been shown to inhibit neurite outgrowth. In these experiments, the axons of transfected primary DRG neurons showed abnormally bunched and branched stubs (Eva et al., 2012). In dendritic spines, musEfa6A binds to the first spectrin repeat of actinin, and this interaction was proposed to allow musEfa6A to activate Arf6 in close proximity to the actin cytoskeleton and membrane-associated dendritic proteins (Sakagami et al., 2007). In primary hippocampal neurons, overexpression of a musEfa6A variant carrying a point mutation in the Sec7 domain induced an increase in the number of filopodia and the length of dendritic branches, but a decrease in the diameters of dendritic branches (Sakagami et al., 2004, Choi et al., 2006). Since musEfa6A and Arf6 mRNAs showed different spatiotemporal expression patterns during early postnatal development of the hippocampus (Sakagami et al., 2004),

this suggests that musEfa6A may have an Arf6-independent role in regulating the dendritic development of hippocampal neurons.

Notably, Efa6 is of clinical importance. Thus, it has been reported that Efa6 is involved in the regulation of glioma cell invasion (Li et al., 2006) and teratoma-associated encephalitis (Vitaliani et al., 2005), through mechanisms little understood so far.

1.6. *Drosophila* as a suitable model for the study of axon extension

Due to the complexity of the cytoskeletal machinery, cellular understanding of axonal growth and maintenance regulation still remains poor. A helpful strategy to unravel these complex processes is the use of genetic invertebrate model organisms (Prokop et al., 2013). *Drosophila* was introduced as a model organism over 100 years ago (Kohler, 1994, Ashburner, 1993), and today roughly 10,000 researchers work with *Drosophila*. There are a number of general advantages for the use of *Drosophila* (Roote and Prokop, 2013).

1) *Drosophila* is easy and cheap to keep. Many different fly stocks can be kept in the laboratory, which is highly convenient for high-throughput experiments, such as genetic screens.
2) *Drosophila* has a short generation time which is about 10 days at 25 °C. Therefore, genetic crosses can be used to combine mutations or transgenic constructs in new *Drosophila* stocks as a matter of weeks or a few months. Experiments can thus be planned and carried out rapidly.
3) The genome of *Drosophila* has been fully sequenced (Myers et al., 2000, Adams et al., 2000), genetic tools for almost every gene tend to be readily available from fly stock centres, experimental techniques to discover and manipulate genes are well established (Venken and Bellen, 2005, Johnston et al., 2002), and there is a huge body of knowledge about fly genetics and biology well accessible through data bases (Matthews et al., 2005).

These advantages can be directly applied to studies of the cytoskeleton, and a number of more specific advantages for such research need to be mentioned:

A) Most of the ABPs and MTBPs are well conserved and usually exist as single genes without redundant paralogues in the fly genome (Sanchez-Soriano et al., 2007). In cases where loss-of-function mutant phenotypes of actin and MT regulators have been described for both flies and vertebrates, they are comparable (Sanchez-Soriano et al., 2009, Sanchez-Soriano et al., 2010, Gonçalves-Pimentel et al., Prokop et al., 2013).

B) Nervous system development, the organisation of the nervous system and morphology of neurons have been well described in *Drosophila*. Systematic application of this knowledge in combination with the genetic and experimental repertoire of analysis strategies have led to the discovery of many mechanisms underpinning nervous system development and function, including neuronal pathfinding and signalling pathway (Sanchez-Soriano et al., 2007, Araujo et al., 2003, Reeve, 2001, Pulver et al., 2011, Bellen et al., 2010).

C) Neurons are well conserved in their organisation, and the principles of axonal growth would therefore be expected to be comparable to higher animals (Sanchez-Soriano et al., 2007, Sanchez-Soriano and Prokop, 2005). Indeed, many fundamental mechanisms of the nervous system have turned out to be applicable to higher organisms (Bellen et al., 2010).

D) Work on axonal growth has primarily been executed *in vivo* in a range of different neuronal cellular models providing information about the relevance of genetic functions and mechanisms (Sanchez-Soriano et al., 2007). However, work in the Prokop laboratory has led to the establishment of a primary neuron system for *Drosophila* which ideally complements *in vivo* studies of the neuronal cytoskeleton (Sanchez-Soriano et al., 2007, Sanchez-Soriano et al., 2010, Prokop et al., 2012). During the cell culture process, a mix of different type of cells, include primary neurons, has been obtained from embryo (referrer to material and methods). Stage 11 embryos were selected since at this stage neurons are already differentiatied, but have not yet formed axons. In these primary neurons, cytoskeletal dynamics and experimentally induced phenotypes can be studied with much higher resolution than has ever been achieved in *Drosophila* neurons before. Notably, many of the key properties of the cytoskeleton observed in fly primary neurons, are well conserved with those of vertebrate neurons, including filopodia dynamics, F-actin backflow rates, axon growth rates and MT polymerisation dynamics (Sanchez-Soriano et al., 2010).

1.7. Current problems in the field and project aims

A lot is known about signalling in the context of axon growth (Araujo and Tear, 2003, Huber et al., 2003), and there is a basic understanding of the principal requirements of the cytoskeleton (Lowery and Van Vactor, 2009, Dent et al., 2011). As explained before (Chapter 1.3.2. and 1.3.4.), we know a lot about the individual, biochemical functions of many of the actin- and MT-binding proteins and their impact on cytoskeleton *in vitro*, but any models for their cellular functions in the context of axon growth remain hypothetical and are derived from knowledge obtained in a multitude of

different cellular systems (Pak et al., 2008, Conde and Caceres, 2009). Although many nice examples of molecular mechanisms exist, as explained in my introduction, our understanding of how they work together in cells, or form or maintain MT bundles in axons is little understood. Clearly, the molecular complexity of cytoskeletal machinery poses a major barrier.

Drosophila neurons have been developed as a model over the past years in which the various aspects of cytoskeletal regulators and machinery can be studied in parallel to understanding their cellular functions and integration at the level of growing neurons. A feasible strategy to make use of this model is to focus on certain aspects of cytoskeletal machinery, decipher its mechanisms and then integrate it with the knowledge about other parts of that machinery.

The overarching goal of my project is to focus on actin-MT linkage and crosstalk and cortical capture of MTs during axon growth and unravel underlying genetic and molecular mechanisms. For this, I will build on the role of Shot during axonal growth and use it as a promising molecular platform from which to explore further mechanisms (Prokop et al., 2013). As explained above (Chapter 1.4.2.), Shot links to F-actin with its N-terminus and binds MTs and EB1 through its C-terminus and these interactions are essential for organising MT bundles by guiding extending MTs along axonal actin thus laying them out into parallel bundles (Alves-Silva et al., 2012, Prokop et al., 2013). Through these interactions, Shot lies at the heart of different aspects of cytoskeletal machinery, in particular the regulatory networks of +TIPs centred around EB1, structural MAPs including Tau and MAP1B, and the regulatory machinery of F-actin networks. During my project I have addressed three specific aims:

1) To use structure-function approaches to test how changes in the Shot actin-binding N-terminus affect its function in MT organisation, and complement these studies with genetic manipulations of actin regulators. Through this, I aimed to gain mechanistic understanding of Shot-specific aspects of actin-MT linkage.

2) To use genetic and pharmacological approaches to investigate how actin regulates MT behaviours in general during axon growth and maintenance, thus addressing wider mechanisms and principles of actin-MT crosstalk.

3) To build on findings in *C. elegans* proposing EFA-6 as a cortical collapse factor and test it as a candidate in *Drosophila* neurons, thus opening up new molecular avenues for investigating MT regulation at the cell cortex and their implications for axon growth and maintenance.

Chapter 2

Materials and Methods

2.1. Fly stocks

Table 2.1. *List of fly stocks used*

Mutant name	Location and nature of allele	Source/original reference	Additional info
Df(3R)Exel6273	3R; deficiency covering 94B2--94B11 (LOF for *Efa6*)	Bloomington #7740; (Liao et al., 2006)	
Df(3R)ED6091	3R; deficiency covering 94B5--94C4 (LOF for *Efa6*)	Bloomington #9092; (Ryder et al., 2004)	
$efa6^{KO\#1}$	3R; LOF (genomically engineered)	(Huang et al., 2009)	
$efa6^{GX6[w-]}$	3R; LOF (genomically engineered)	(Huang et al., 2009)	
$efa6^{GX6[w+]}$	3R; LOF (genomically engineered)	(Huang et al., 2009)	
$arf6^{GX16[w-]}$	2R; LOF (genomically engineered)	(Huang et al., 2009)	
$chic^{221}$	2L; amorph – genetic evidence. Deletion of 5' non-coding and some of coding region of chic	From D. Van Vactor (Verheyen and Cooley, 1994)	LOF for *Drosophila* profilin (Gonçalves-Pimentel et al., 2011)
$chic^{05205}$	2L; P-element insertion immediately upstream of the second coding exon	From D. Van Vactor (Wills et al., 1999)	anti-Chic staining is strongly reduced in $chic^{05205}$ mutant CNS and primary neurons(Gonçalves-Pimentel et al., 2011)
$shot^{3}$	2R; LOF, diepoxybutane	(Sanchez-Soriano et al., 2009)	
$shot^{sf20}$	2R; LOF, EMS	(Sanchez-Soriano et al., 2009)	
$sop2^{1}$	2L; EMS allele, 207bp genomic deletion removes last 62 codons of Sop2 (=7th WD40 domain)	Bloomington #3585 (Hudson and Cooley, 2002)	lethal with $Sop2^{Q25sd}$ (Gonçalves-Pimentel et al., 2011)
$SCAR^{\Delta 37}$	2L; LOF allele	Bloomington #8754 (Schenck et al., 2004)	mutant allele of *Drosophila* WAVE
Df(2L)BSC145	2L; deficiency covering 32C1-32C1	Bloomington #9505	LOF for *SCAR*
Hem^{03335}	3L; hypomorphic allele - genetic evidence	Bloomington #11584 (Schenck et al., 2004)	mutant allele of *Drosophila kette*
hts^{1}	2R; Loss of function allele, hypomorphic allele - genetic evidence	K. Röper (Roper, 2007, Yue and Spradling, 1992)	mutant allele of *Drosophila* adducin (*hts*)

Table 2.2. *List of transgenic lines used.*

Name of line	Insertion Site	Source/ original reference	Additional
UAS-Efa6-RNAi	3rd	VDRC# 42321	
UAS-eb1-GFP	2nd	P. Kolodziej (Alves-Silva et al., 2012)	
efa6::GFP-C	3rd	(Huang et al., 2009)	genomically engineered
dArf6::GFP-C	2nd	(Huang et al., 2009)	genomically engineered
scabrous-GAL4	2nd	A. Chiba (Budnik et al., 1996)	the *scabrous* promoter is active in the CNS and PNS from embryonic stage 9 to 14 (Mlodzik et al., 1990)
elav-GAL4	2nd	(Luo et al., 1994)	The pan-neuronal driver
UAS-shot-LA-GFP (shot-FL)	X	(Alves-Silva et al., 2012)	
UAS-shot-LC	2rd	(Lee and Kolodziej, 2002)	
UAS-shot-LA-ΔABD-GFP	3rd	Prokop lab (see 2.2.1)	
UAS-shot-LA-Life-GFP	3rd	Prokop lab (see 2.2.1)	
UAS-shot-LA-Moe-GFP	3rd	Prokop lab (see 2.2.1)	
UAS-shot-LA-ΔPlakin-GFP	3rd	(Bottenberg et al., 2009)	
UAS-shot-EGC	3rd	From Talila Volk	

2.2. Molecular biology

2.2.1. Generation of transgenic flies carrying *shot* constructs with modified ABD

The constructs *UAS-Shot-LA-ΔABD-GFP, UAS-Shot-LA-Life-GFP* and *UAS-shot-Moe-GFP* (detailed in Fig. 3.1) were generated by Jill Parkin in our laboratory. Transgenic lines were generated through PhiC31-mediated site-specific insertion into the third chromosome, using *M-6-attB-UAS-1-3-4*-born constructs and the *PBac{y-attP-3B} CG13800*^{VK00031} transgenic landing line (Bloomington line #9748; transgenic production outsourced to BestGene Inc.). The vector used for site-specific transgenesis was the M-6-attB-UAS-1-3-4 (p[acman]-1-3-4-chloranphenicol), subsequently referred to as p[acman] (Alves-Silva et al., 2012).

2.2.2. Cloning of *eGFP, shot-N-ABD, shot-N-Moe and shot-N-Life*

The constructs *pUASp-eGFP*, *pUASp-shot-N-ABD-eGFP*, *pUASp-shot-N-Moe-eGFP* and *pUASp-shot-N-Life-eGFP* were generated by Jill Parkin and me (I carried out the last cloning steps of pUASp-Shot-N-ABD). Here, I will describe the cloning of *pUASp-shot-N-ABD-eGFP*, which has been partially generated by me. Cloning steps were carried out in a modified version of the pUASp vector (Invitrogen; kindly provided by Tom Millard) which confers ampicillin resistance and contains eGFP, and is subsequently referred to as pUASp-eGFP. The sequence of Shot-N-ABD was cloned from MpET-20b-Nterm constructs (generated by Jill Parkin) using the appropriate primers (pUASP_Nterm_Fw and pUASP_Nterm_Rev; generated by Jill Parkin and me; Table 2.3). The modified vectors contain NotI and XbaI restriction enzyme (RE) sites after the eGFP sequence, therefore the sequence of Shot-N-ABD was inserted into the vector inbetween these two RE sites, thus tagging the construct N-terminally with eGFP. The constructs were sub-sequentially sent for sequencing. pUASP_Nterm_seq_Fw and pUASP_Nterm_seq_Rev were used to sequence from within an eGFP sequence at least 50nt upstream of the NotI site (Table 2.3). The engineered *pUASp-eGFP* plasmids containing *shot-N-ABD* sequence were amplified in chemically competent TOP10 *E. coli*.

Table 2.3. *The list of primer.*

Name	Sequence
pUASP_Nterm_Fw	TTAATCGCGGCCGCAATGGCATCGCATTCCTAC
pUASP_Nterm_Rev	GGCAACTCTAGACTAAAGGATAACCTCGCGATC
pUASP_Nterm_seq_Fw	GACAACCACTACCTGAGC
pUASP_Nterm_seq_Rev	CTTGACCATGGGTTTAGG
pUAST_GFP_Fw	CTGGGTACCGGCGCGCCTTAATTAACGTGAGCAAG GGCGAGGAGCTGTTCACC
pUAST_GFP_Rev	CGATCTAGACTACTTGTACAGCTCGTCCATGCCGA GAGTGATCCCGGCGGCGG
pUAST_seq_Fw	CTGAAATCTGCCAAGAAG
pUAST_seq_Rev	CTCTGTAGGTAGTTTGTC
FL-IP15395_Fw_1a	CTAGGCGCGCCAACATGAGCGAAGAACTGAAAGTG GTGCTGCGGCGCAG
IP15395-Nterm_Rev	GGATTAATTAAGCTACCGCTGCCGCTACCTTTCTGC AGCAGCTTTGCCTC
IP15395-ΔCterm_Rev	GGATTAATTAAGCTACCGCTGCCGCTACCGGTCAT CATGCCCAGCGGCTC

2.2.3. Cloning of *efa6-Nterm* and *efa6-∆Ctail*

The constructs *pUAST-eGFP, pUAST-efa6-Nterm-eGFP* and *pUAST-efa6-∆Ctail-eGFP* were generated by Jill Parkin and me. Cloning steps were carried out in the pUAST vector (Invitrogen; kindly provided by Tom Millard) which confers ampicillin resistance, and subsequently referred to as pUAST. The pUAST vector does not contain a GFP tag, so the eGFP sequence was added into the vector. The pUAST vector contains KpnI and XbaI RE sites, therefore the eGFP sequence was inserted between

these two RE sites. All the other restriction sites in the multiple cloning site (MCS) of pUAST cut the Efa6 sequence. Therefore when cloning in the eGFP gene we used the forward primer to add the RE sites AscI and PacI to the vector. The RE sites AscI and PacI have been used to generate p[acman] vector (Alves-Silva et al., 2012). This will result in the *efa6* sequence being inserted before the eGFP tag. The sequence of the eGFP was cloned from *pUASp-eGFP* vector (as mentioned before) using the appropriate primers (pUAST_GFP_Fw and pUAST_GFP_Rev; generated by Jill Parkin and me; Table 2.3) and inserted into the pUAST vector. Then the pUAST vector containg the eGFP (pUAST-eGFP) was sent for sequencing. pUAST_seq_Fw and pUAST_seq_Rev were used to sequence from upstream to the downstream of MCS of pUAST. The engineered pUAST-eGFP plasmids were amplified in chemically competent TOP10 *E. coli*.

Next, we have inserted the *efa6-Nterm* sequence (containing the first 410 amino acids) and *efa6-*Δ*Ctail* sequence (containing the first 897 amino acids) into the *pUAST-eGFP* vector. The sequences of *efa6-Nterm* and *efa6-*Δ*Ctail* were cloned from the modified version of *efa6* cDNA IP15395 sequence (Ensembl; modified by Jill Parkin) using the appropriate primers (FL-IP15395_Fw_1a, IP15395-Nterm_Rev and IP15395-ΔCterm_Rev; generated by Jill Parkin and me; Table 2.3), and inserted into the *pUAST-eGFP* vector. In order to increase the stability of the construct, a 6 amino acid linker sequence (GSGSGS) was inserted between the *efa6* constructs and *GFP* tag using the reverse primers. Then the *pUAST-eGFP* vectors containing different *efa6* constructs were sent for sequencing. pUAST_seq_Fw and pUAST_seq_Rev were used to sequence from upstream to downstream of MCS of pUAST. The engineered pUAST-eGFP plasmids were amplified in chemically competent TOP10 *E. coli*.

2.3. Cell culture

2.3.1. *Drosophila* primary neuron culture

Neuronal cell cultures were carried out as described in a previous paper (Sanchez-Soriano et al., 2010). After being dechorionated using domestic bleach (diluted 1:1 with water) for 1.5 mins, embryos were moved onto agar plates and correct stages were selected (stage 11) under a fluorescent dissection microscope. 3 slides per genotype were generated, and about 7 embryos were selected per slide. In order to sterilise the surface of the embryos, embryos were put into sterilized centrifuge tubes containing 100µl of 70% ethanol. Further manipulations were performed under the cell culture hood. Ethanol was removed after 30 s and replaced with 100 µl of cell culture medium to wash. The preparation of culture medium was as follows: Schneider's *Drosophila* medium (Schneider, 1964) (Life Technologies) was mixed with fetal bovine serum (20%, sterile-

filtered, suitable for cell culture, Sigma) in a sterilized tube, and was filtered sterile. Then the tubes were covered with foil and kept in an incubator at 26°C for 3 days. After 3 days, 2 µg/ml insulin (Sigma, St Louis, MO; human, stored at 4°C) was added and the pH adjusted to 6.8–6.9. The readily prepared culture medium was aliquoted and stored at -80°C (kept for a maximum of 4 months) and thawed at 37°C for use. Before use, the cell culture medium was filtered sterile under a hood. Then the culture medium was replaced by 100 µl dispersion medium and embryos were crushed with a pestil for cell dispersion. The resulting mechanically dispersed cells were then treated with chemical dispersion medium for 4 mins at 37°C. The preparation of chemical dispersion medium was as follows: 30 ml 10x HBSS (Hank's Balanced Salt Solution, Gibco), 3 ml penicillin/streptomycin-solution (Gibco), 0.01 g phenylthiourea (Sigma) and 167 ml autoclaved distilled water were mixed, incubated for 30 mins at 37°C, then filtered and stored as a stock solution at 4°C (ref as HBSS solution). To 1 ml working solution 0.5 mg collagenase (Worthington, Cellsystems) and 2.5 mg dispase (Roche) were added in 1ml HBSS solution and filtered (can be kept at 4°C for 1 week). After chemical dispersion, 200µl of cell culture medium was added to stop the reaction. The suspension was centrifuged 4 mins at 1500 rpm, the supernatant was removed and the cells were re-suspended in cell culture media by pipetting 20 times up and down. To culture cells, 30 µl of the final suspension were added into the centre of custom chambers (made in the lab; a microscope slide with a 15-mm hole were glued on the top of an intact slide) (Dübendorfer and Eichenberger-Glinz, 1980). The chamber hole was covered with a cover slip made of lead-free glass (VWR international MENZBB024024A123 24 x 24 mm, no. 1; prepared by dipping in acetone, drying, then followed by autoclaving or flaming whilst still wet). To make Concanavalin A (ConA) coated cover slips, 0.5 mg/ml ConA (Sigma) was incubated on freshly opened lead-free cover slips for 1.5 hrs at 37°C, and then the cover slips were washed twice with sterile H_2O and left to dry at room temperature. Vaseline was used to produce a seal between the slide and cover slip. Chambers were flipped upside-down so that cells can settle on the down-facing cover slips. After 1.5 hrs, cells have adhered to the cover slip and the chambers can be flipped back (hanging drop culture), so that any debris can fall off and does not accumulate around cells. For incubation, chambers are placed in a tray protected from light by foil. Standard incubation was for 6-8 hrs at 26°C.

2.3.2. Transfection of *Drosophila* primary neurons

A number of changes were introduced to the procedures for *Drosophila* primary neuron culture to transfect primary neurons: instead of using 7 embryos per slide, 15 embryos were used. After stopping the chemical dispersion by adding cell culture medium, suspension was centrifuged 4 mins at 1500 rpm, supernatant was removed,

and cells were re-suspended in 100 µl of transfection mix media [final media contain 0.5µg DNA and 2µl Lipofecatmine 2000 (L2000)]. To generate this media, dilutions of 0.5 µg DNA in 50 µl Schneider's medium and 2 µl L2000 in 50 µl Schneider's medium were prepared, then mixed together and incubated at room temperature for 5 mins before being added to the cells. Cells in the transfection mix media were kept in centrifuge tubes for 24 hrs at 26°C in an incubator. Cells were then centrifuged 4 mins at 1500 rpm, supernatant was removed and cells were re-suspended into 100 µl of dispersion medium (see Chapter 2.3.1) by pipetting up and down. The suspension was then incubated for 3 mins at 37°C. To stop the reaction, 200 µl cell culture medium was added. Then the suspension was centrifuged 4 mins at 1500 rpm, the supernatant removed and cells were re-suspended in cell culture media by pipetting 20 times up and down: 30 µl per slide were used. Cells were grown in the special chambers at 26°C overnight (as described in Chapter 2.3.1).

2.3.3. Transfection of mammalian cell lines

The mammalian cell line cultures and transfections were carried out by Meredith Lees in our laboratory. The sample fixation, live imaging and data analysis were carried out by me. NIH/3T3 cells were cultured in cell culture media at 37°C in a humidified incubator at 5% CO_2. The cell culture media was prepared as follows: in a fresh opened bottle of DMEM (Dulbecco's Modified Eagle's medium, Sigma Cat No. D5796), 1% glutamine (Invitrogen), 1% penicillin/streptomycin antibiotics (Invitrogen) and 10% foetal calf serum (FCS, Sigma) were added. Cells were diluted every 2-3 days to avoid the confluence of cells over 80%. In order to transfect NIH/3T3 cells, cells were first prepared as follows: (1) cell culture media, phosphate buffered saline (PBS) and trypsin-EDTA (T-E) solution (Sigma) were pre-warmed to 37°C; (2) the cell culture media was removed and cells were washed with 10ml PBS to remove any traces of serum; (3) PBS was replaced with 3-4 ml of T-E solution and incubated at 37°C for 5 mins, dishes were gently shaken a couple of times during the incubation to help the cells detach from the dish; (4) to stop the T-E solution reaction, 7ml of culture media were added and then pipetted 10-20 times up and down to suspend the cells; (5) the number of cells was counted using a haemocytometer. Cells were diluted to ~$1x10^5$ per ml, and 2 ml of cell containing solution was added per well into 6-well plates. Cells were left at 37°C in a humidified incubator at 5% CO_2 overnight to achieve ~ $2×10^5$ cell per ml on the following day. Then the transfection was carried out. The transfection mix media was prepared in a centrifuge tube as follows: 500 µl media with no serum (DMEM media with 1% glutamine) was mixed with 1 µg of DNA and 1µl of Plus reagent (Invitrogen), and was then incubated at room temperature for 10 mins. After the incubation, 3 µl of Lipofectamine (Invitrogen) were added into the mixed media (mentioned before) to make the final transfection mix

media, and incubated at room temperature for 25 mins. Thereafter, the media on the cells was removed to make sure no serum was present. The cell culture media was removed, and then 1ml of media with no serum was added on the cells. The dish was then gently swirled to wash the old cell culture media off. Subsequently the media in the dish was replaced by 1ml of fresh media with no serum. Finally, after 25 mins, 500 µl of media with no serum were removed from the cells, and 500 µl of transfection mix media were added slowly as droplets from the pipette and spread around the whole well. Then the cells were incubated for 3 hrs at 37°C. After the incubation, media was replaced by 1 ml of cell culture media (with serum). In order to observe the transfected NIH/3T3 cells via live imaging or after fixation, cells were prepared as follow: cells were washed with 2 ml of PBS. To re-suspend the cells, they were incubated for 5 mins with 400 µl of trypsin, and 3 ml cell culture media was added to the cells to stop the trypsin reaction. Cells were then re-suspended by pipetting 10-20 times up and down. For live imaging, a fibronectin coated glass-bottom 35mm dish (MatTek) was used. Fibronectin was coated on MatTek by adding 300 µl of 5 µg/ml fibronectin (Sigma-Aldrich) in PBS to the glass-bottom area of a MatTek dish, and incubated for 1 hr at 37°C. 1 ml of the cell culture media with cells with extra 1 ml cell culture media were mixed and added into the MatTek dish. Cells were then grown for 7 hrs at 37°C. During live imaging, cell culture media was replaced with imaging media (2 ml Ham's F-12 media with 4% FCS). For fixation, 1 ml of cells with an extra 2 ml of cell culture media were added to each well of a six well plate containing a cover slip made of lead-free glass (VWR international MENZBB024024A123 24 x 24 mm). The cells were left for 24 hrs at 37°C in a humidified incubator at 5% CO_2, and then fixed (Chapter 2.4).

2.3.4. Inhibitors

For drug treatments, solutions were prepared in a cell culture medium from stock solutions in DMSO. Cells were treated with 200 nM latrunculin A (Biomol International) for 1hr or 6hrs, 0.4 µg/ml cytochalasin D (Sigma) for 4 hrs or 6 hrs, 20 µM nocodazole (Sigma) for 2.5 hrs or 100 nM CK666 (Sigma) for 2 hrs or 4 hrs, respectively. For controls, equivalent concentrations of DMSO were diluted in Schneider's medium.

2.4. Immunocytochemistry

Fixation of *Drosophila* primary neurons in culture: culture medium was carefully removed and cells were fixed for 30 mins with 4% paraformaldehyde (PFA) in 0.05 M phosphate buffer (pH 7-7.2), then washed in phosphate buffered saline with 0.3% TritonX-100 (PBT) 3 times, followed by staining.

For anti-EB1 staining, cells were fixed for 10 mins with a mixed fixative composed of 90% methanol, 3% formaldehyde, 5 mM sodium carbonate (pH 9). The fixative was stored at -80°C and, for use, was transferred from -80°C onto ice and rapidly placed on the cells (Rogers et al., 2002), then washed in PBT 3 times, followed by staining.

Fixation of mammalian cell lines in culture: For anti-tubulin staining or anti-EB1 staining, cells were fixed for 5 mins with -20°C methanol. For phalloidin staining, cells were fixed for 30 mins with 4% PFA. Then cells were washed 3 times in PBT for 10 mins each time, followed by staining (Alves-Silva et al., 2012).

Antibodies were prepared in PBT or PBS without blocking reagents, then directly added to the samples and incubated at room temperature for 2 hrs (primary antibodies) or 1hr (secondary antibodies), or at 4°C overnight. The primary antibodies which have been used are listed in Tab. 2.4. FITC-, Cy3- or Cy5-conjugated secondary antibodies (Jackson Immunoresearch) against the IgG of the primary antibodies were derived from donkey and used at 1:100. F-actin was stained with TRITC-, FITC and Cy5-conjugated Phalloidin (1:100, Sigma). Cover slips with stained neurons were mounted on slides using Vectashield medium (Vector labs).

Table 2.4. *The list of primary antibody.*

Epitope	Species raised in	Concentration	Source	Notes
GFP	goat	1:500	Abcam	
dEB1	rabbit	1:1000	Hiro Ohkura	(Clohisey et al., 2014)
α-tubulin	mouse	1:1000	Sigma	clone DMIA
α-tubulin	rat	1:500	Millipore	MAB1864
Jaguar	mouse	1:20	K. Miller	clone 3C7 (Kellerman and Miller, 1992)
α-Spectrin	mouse	1:20	DHSB	

2.5. Imaging and analysis

2.5.1. Imaging and analysis of fixed samples

For fixed samples, an AxioCam camera mounted on an Olympus BX50WI microscope was used (using a 100×/1.30 oil iris Ph3 ∞/0.17 objective, and a 1.6× Optovar). FITC, Cy3 and Cy5 channels were used by applying different filters. AxioVisionLE Release 4.6.3 software was used to acquire images.

Axon lengths were calculated using α-tubulin staining, and measured from the edge of the cell body to the furthest point of the longest axonal branch using ImageJ (segmented lines tool). Filopodia numbers were also counted per axon, including filopodia along axon shafts and at GCs, but excluding the cell body. MT networks of GCs

and axons were classified as shown in Fig. 2.1. In GCs, the classifications "bundled", "looped" and "splayed" are considered as organized, whereas "spread" is considered disorganized (Sanchez-Soriano et al., 2010).

GraphPad Prism 5 was used to calculate the mean and standard errors of the mean (SEM), and to perform statistical tests. The data of axon length or filopodia number was generally non-parametric and therefore the Mann-Whitney U test was applied. When data fell into categories, the Chi^2 test was used. For each experiment, the statistical test methods have been indicated individually in the Result chapter.

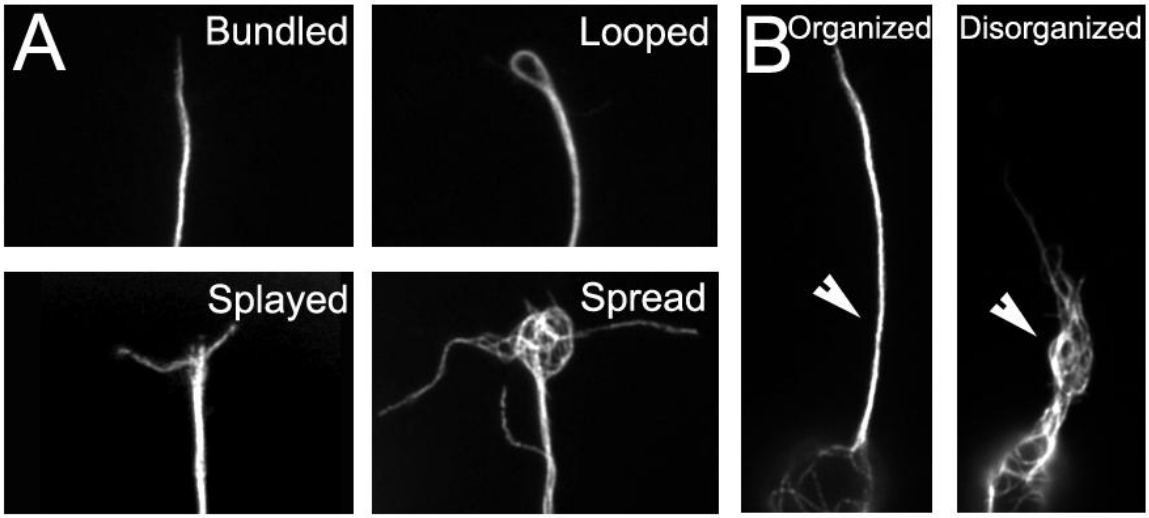

Figure 2.1. *The classification of MT networks within GCs and axons.*

A) *Classification of MT networks in growth cones: bundled (upper left, pointed extension of the axonal MT bundle), looped (upper right, extension of the axonal MT bundle forms a loop), splayed (lower left, MTs spread out in GC but not looped), spread (lower right, non-coalescent criss-crossed MT).* Cells were *stained with tubulin.* ***B)*** *Classification of MT networks in axons: bundled/organised MTs (left) and disorganized MTs (right, split axonal bundle or areas of non-coalescent criss-crossed MTs*

2.5.2. Live imaging and analysis

For live imaging, time lapse images of culture neurons or NIH/3T3 cells were acquired on a Delta Vision RT (Applied Precision) restoration microscope with a 100×/1.3 Ph3 Uplan Fl phase objective, the Sedat filter set (Chroma 89000) and temperature control incubator (26°C), using a Coolsnap HQ (Photometrics) camera. The Time lapse images for all experiments were taken every 4 s for 2~3 mins with exposure times of 0.5-1 s, and were constructed to movies automatically.

To observe EB1 dynamics upon loss of different proteins, cells were cultured on ConA-coated cover slips. MT plus end comets were labeled by overexpression of *UAS-EB1-GFP* driven by *sca-GAL4 or elav-GAL4* in mutant primary neuron either in wildtype or in different mutant primary neurons. To observe the impact of CytoD treatment on axon retraction primary neurons were cultured in glass-bottom 35mm MatTek dishes. Cells were first marked and imaged one by one to record EB1 dynamics before treatment. Then 0.8 µg/ml CytoD were carefully applied to the cells. After 0.5 hrs, 1 hr and 1.5 hrs, 3 mins movies were collected one by one from all the cells which were recorded before.

For analysis of EB1 dynamics (speed and movement measurements), EB1 comets were tracked manually using the “manual tracking” plugin for ImageJ.

2.6. PALM/STORM or SIM sample preparation, transport, imaging and analysis

2.6.1. PALM/STORM imaging for Singapore

The standard primary *Drosophila* cell culture protocol was followed (Chapter 2.3.1). In order to image, coverslips with fiducial markers (from now on referred to as STORM cover slips) were kindly provided by Dr. Kanchanawong Pakorn. The STORM cover slips were washed with acetone and sterilized with UV light. Cells were incubated at 26°C for at least 6 days.

The cultures were pre-fixed for 1.5 mins using a solution of 0.3% glutaraldehyde (Sigma) and 0.25% Triton X-100 in cytoskeleton buffer (CB, 10 mM MES, pH 6.1, 5 mM glucose, 5 mM EGTA, 5 mM $MgCl_2$ and 150 mM NaCl, all materials from Sigma) as described previously (Xu et al., 2013). To maintain a better ultrastructure of F-actin, cells were post-fixed for 15 mins in 2% glutaraldehyde in CB. To reduce background fluorescence caused by glutaraldehyde fixation, samples were treated with freshly prepared 0.1% sodium borohydride (Sigma) for 7 mins (Xu et al., 2013).

Samples were shipped to Pakorn’s lab in Singapore for imaging. To preserve the samples during shipment, each coverslip was sandwiched between two holders and stored in a 3 cm cell culture dish filled with PBS buffer. The culture dishes were sealed with parafilm. Samples were shipped with cooling pads. The images were taken and analysed by Zhen Zhang in K. Pakorn’s lab.

2.6.2. SIM protocol for imaging Didcot facility

The standard primary *Drosophila* cell culture protocol was followed (Chapter 2.3.1). Cells were cultured on glass-bottom 35mm MatTek dishes (P35G-0.170-14-C), which were coated with poly-L-lysine, and were incubated at 26°C for 10 ds.

Cells were fixed with 4% PFA, and then washed in PBT 3 times. Then, culture dishes were filled with PBS buffer, and sealed by parafilm. The culture dishes were carried to the Central Laser Facility (CLF) of the Science and Technology Facilities Council (STFC) in Didcot. At CLF, cells were incubated with 2 µM SiR-actin (diluted in PBS; Spirochrome) (Lukinavicius et al., 2014) for 1hr, then washed once with PBS. Before imaging, PBS was replaced by imaging buffer (provided by Stephen Webb at Didcot). The images were taken by structured illumination microscopy (SIM).

Chapter 3

Result

3.1. Changing the properties of Shot's interaction with F-actin impacts on MT organisation

Actin-MT linkage is widely accepted to be a key cellular mechanism through which MT networks can be regulated in space and time. Understanding the underpinning molecular mechanisms remains a key challenge in the field of cell biology and the various disciplines building on it. As explained in Chapter 1.4.2 as well as our review (Prokop et al., 2013), Shot links to both actin and MTs during axonal growth and provides an opportunity to advance our understanding of this phenomenon.

3.1.1. Generating constructs

Shot binds to MTs and EB1 through its C-terminus and to actin through its N-terminus. Interfering with any of these three links abolishes the function of Shot-LA (Shot full length isoform) in MT regulation, and MTs become non-coalescent and form criss-crossed areas of disorganisation in axons and growth cones (Sanchez-Soriano et al., 2009, Prokop et al., 2013, Alves-Silva et al., 2012). The underlying molecular mechanisms of the C-terminus have previously been investigated in great detail (Alves-Silva et al., 2012). Here I focus on F-actin interaction of the N-terminus. Binding of Shot to F-actin is achieved by a tandem calponin-homology domain (CH1 and CH2). CH1 and CH2 together form a classical actin-binding domain, also referred to as ABD (Korenbaum and Rivero, 2002). *In vitro*, the ABD of Shot binds to F-actin with a dissociation constant (Kd) of ~0.022μM. However, the CH2 domain alone shows very weak binding to F-actin (Lee and Kolodziej, 2002). Therefore, experiments addressing F-actin binding have made use of the natural isoform Shot-LC which lacks the first CH domain and displays an N-terminal domain distinct from Shot-LA (Fig. 3.1B) (Bottenberg et al., 2009, Lee and Kolodziej, 2002). This isoform is expected to display very little or no F-actin interaction. Accordingly, Shot-LC cannot rescue any phenotype in the nervous system of shot mutant embryos (Bottenberg et al., 2009, Lee and Kolodziej, 2002), including the MT disorganization in neuronal (Sanchez-Soriano et al., 2009). This suggests that linking to actin is important for the Shot MT regulatory function, and I hypothesize that Shot regulates MTs downstream of F-actin through its ABD. However, the Shot-LC isoform also contains an N-terminal domain distinct from the Shot-LA isoform (Fig. 3.1B), it cannot be excluded that this domain may have some dominant impact on Shot function.

In order to investigate the function of Shot ABD in MT regulation further, a number of C-terminally GFP-tagged UAS-constructs based on the Shot-LA isoform were generated (Fig. 3.1B). Shot-LA is the standard isoform which has been used for previous functional and localisation studies in neurons (Bottenberg et al., 2009, Alves-Silva et al.,

2012, Sanchez-Soriano et al., 2009, Sanchez-Soriano et al., 2010, Lee and Kolodziej, 2002) (Fig. 3.1A).

First, we generated a Shot-LA-ΔABD construct, in which the ABD was specifically deleted. The construct was inserted in the *M-6-attB-UAS-1-3-4*-vector and PhiC31-mediated site-specific insertion was used to bring it into a specific attB landing site on the third chromosome (*PBac{y*$^{+}$*-attP-3B} CG13800*^{VK00031}; Bloomington line #9748;)(Alves-Silva et al., 2012). This same landing site was used for all constructs to avoid position effects and achieve equal expression levels of all constructs (Bischof et al., 2007)(see Methods 2.2.1).

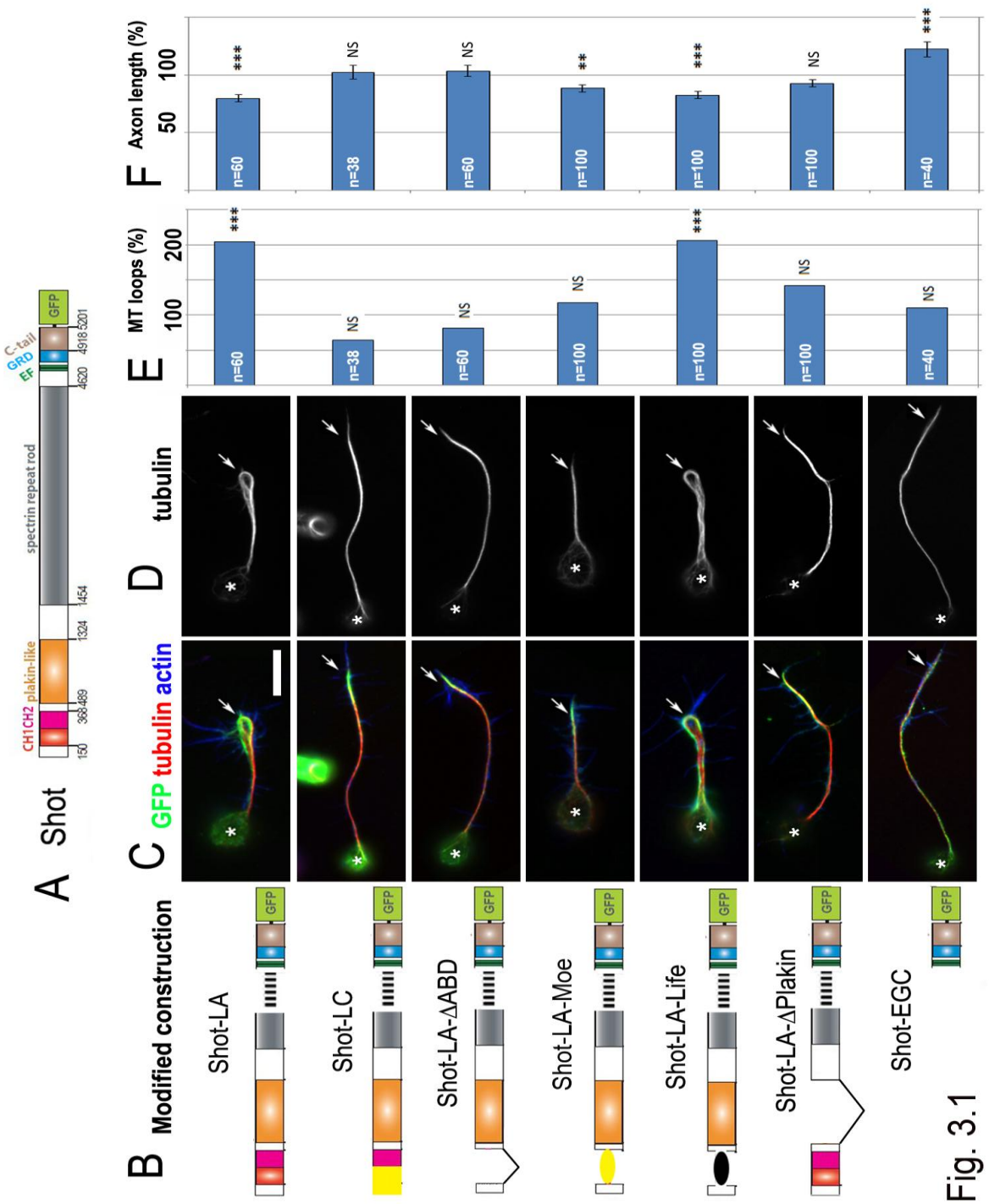
A
Shot
CH1CH2
plakin-like
spectrin repeat rod
GRD
EF
C-tail
GFP
150
368
489
1324
1454
4620
4918
5201
B
Modified construction
Shot-LA
Shot-LC
Shot-LA-ΔABD
Shot-LA-Moe
Shot-LA-Life
Shot-LA-ΔPlakin
Shot-EGC
C
GFP tubulin actin
D
tubulin
E
MT loops (%)
100
200
n=60
n=38
n=60
n=100
n=100
n=100
n=40
***
NS
NS
NS
**
***
NS
***
F
Axon length (%)
50
100
n=60
n=38
n=60
n=100
n=100
n=100
n=40
***
NS
NS
**
***
NS
***

Fig. 3.1

Figure 3.1. *Shot constructs regulate Shot localisation and MT behaviors differently.*

A) *The Shot-LA reference construct containing an actin binding domain composed of two calponin homology domains (CH1+2; red and magenta), a plakin-like domain (orange), a spectrin-repeat rod (green), two EF-hand motifs (blackgreen), a Gas2-related domain (blue), a Ctail (brown) containing two SxIP motifs, and a C-terminal GFP tag; amino acid positions demarcating domains are indicated below.* ***B)*** *Illustration of the modified Shot-LA constructs; stippled line represents the central protein part, the yellow rectangle in Shot-LC an alternative N-terminal domain (due to alternative start site), the yellow ellipse the actin binding domain of Moesin, and the black ellipse is lifeact.* ***C, D)*** *Localisation and axon structure of the different constructs in primary neurons cultured at 6HIV and triple-labelled for actin, tubulin and GFP (C; tubulin channel shown alone in D; asterisk, cell body; arrow, growth cone); scale bar represents 5µm in C, D.* ***E,F)*** *Quantifications of phenotypes caused by overexpression of the constructs in wildtype neurons shown on the left, respectively (all normalised and compared to wild type); numbers in the bars indicate the numbers of neurons analysed in each experiment; for quantifications of neurons showing MTs loops in their GCs (E), P values were calculated using the Chi-square test (NS: P>0.050, *: P<0.050, **: P<0.010,***: P<0.001); for axon length (F), P values were calculated using the Mann-Whitney Rank Sum test (NS: P>0.050, *: P<0.050, **: P<0.010,***: P<0.001).*

3.1.2. The ABD domain is not alone responsible for distal subcellular localization of Shot

To assess the effect of ABD deletion on Shot-LA function, I first expressed the Shot-LA, Shot-LC and Shot-ΔABD constructs in wildtype neurons and analysed their localisation and potential gain-of-function (GOF) phenotypes, as previously done with Shot-LA and Shot-LC (Sanchez-Soriano et al., 2010, Alves-Silva et al., 2012, Sanchez-Soriano et al., 2009).

First, I found that Shot-LA has a strong tendency to enrich on distal MTs at GCs (Fig. 3.1C), as is in agreement with previous descriptions (Sanchez-Soriano et al., 2010, Sanchez-Soriano et al., 2009). When removing actin by applying the actin depolymerising drug latrunculin A (LatA), I found that Shot-LA loses this distal localization (Fig. 3.3) indicating a strong dependence on F-actin (see Discussion 4.2.1). I therefore hypothesised that Shot's ABD is likely to play a role in GC localisation of Shot-LA and, in turn, its role in MT regulation.

I then tested the localization of Shot-LC. Because of its low actin-binding ability, I expected it to fail to enrich distally. Surprisingly, I found that Shot-LC strongly localises to MTs at GCs just like Shot-LA (Fig. 3.1C). However, the unexpected localisation of Shot-LC could be because of the remaining second CH domain or the alternative N-terminal sequence contained in this isoform (Fig. 3.1B). Therefore, I examined my new Shot-LA-ΔABD variant, which lacks both CH domains and contains the N-terminal sequence of Shot-LA (Fig. 3.1B). Surprisingly, also Shot-LA-ΔABD still enriches in the GC area, just like Shot-LA and Shot-LC (Fig. 3.1C). These results suggested that direct actin-binding through Shot's ABD might not be the mediator of distal Shot-LA localisation, and other domains of Shot seem to be required. As the comparison between Shot-LC and Shot-ΔABD suggests, the very N-terminal domain of Shot which differs between these two constructs has no major impact.

Instead, a good candidate is the plakin-like domain, since absence of this domain was previously shown to impact on axonal Shot localisation *in vivo* (Bottenberg et al., 2009). I therefore tested the localisation of the same Shot-LA-Δplakin construct used for the previous *in vivo* studies, in primary *Drosophila* neurons at 6HIV (Fig. 3.1B). Surprisingly, Shot-LA-Δplakin also shows a localisation to distal MTs similar to Shot-LA (Fig. 3.1C).

I therefore speculated that the distal Shot accumulation at GCs might depend on the C-terminus containing the two MT-binding domains, the Gas2-related domain (GRD) and the Ctail (Alves-Silva et al., 2012). To test this, I analysed the neuronal localisation of the Shot-EGC construct which consists of the two EF-hand motifs, GRD and Ctail (Fig. 3.1B). I found that, unlike other Shot constructs, Shot-EGC was homogeneously

distributed along MTs throughout the neurons (Fig. 3.1C), clearly confirming previous descriptions (Alves-Silva et al., 2012). This previous work also describes the localisation of Shot-LA-ΔGRD and Shot-LA-ΔCtail constructs, both of which are detached from MTs but accumulate in actin-rich areas of GCs (Alves-Silva et al., 2012). Therefore, my and previously published results indicate that the enrichment of Shot in GCs is not caused by binding to MTs.

Obviously, actin is essential for the GC localization of Shot as suggested by LatA-induced dispersion of Shot-LA from GCs. But this seems not or only partly be mediated through the ABD (see Discussion 4.2.1 for more detail). Therefore, mere localisation studies are insufficient to clarify how the ABD might contribute to MT regulatory functions of Shot.

3.1.3. The Shot ABD and plakin-like domain are important for MT regulatory functions of Shot

Next I assessed gain-of-function (GOF) phenotypes of the various Shot constructs (Fig. 3.1E, F). Thus, previous work had shown that targeted expression of Shot-LA in primary neurons (using *sca-Gal4* driver) induced statistically highly significant GOF phenotypes which included an increase in the frequency of prominently bundled MT loops in their growth cones as well as axon shortening (Sanchez-Soriano et al., 2010) (and own data, Fig. 3.1D).

I repeated these experiments with Shot-LA and found a similar increase in bundled loops (all normalised to wildtype neurons, 204%, P_{Chi2}=0.001, n=60; Fig. 3.1E) and a reduction in axon length (80±3%, $P_{Mann\text{-}Whitney}$<0.001; Fig. 3.1F). Although Shot-LC and Shot-LA-ΔABD did not display a localisation phenotype, both of them failed to produce GOF phenotypes (Fig. 3.1D): they did not decrease axon length (Shot-LC, 102±6%, $P_{Mann\text{-}Whitney}$=0.688, n=38; Shot-LA-ΔABD, 104±5%, $P_{Mann\text{-}Whitney}$=0.656, n=60; Fig. 3.1F), and they showed no induction of bundled MT loops, but rather a non-significant tendency to suppress them (Shot-LC, 65%, P_{Chi2}= 0.382, n=38; Shot-LA-ΔABD, 82%, P_{Chi2}=0.591, n=60; Fig. 3.1E)

Notably, also Shot-LA-Δplakin failed to produce a robust Shot-LA GOF phenotype (MT loops: 142%, P_{Chi2}=0.095; axon length: 93±3%, $P_{Mann\text{-}Whitney}$=0.120, n=100; Fig. 3.1D-F), as did the Shot C-terminus (EGC; MT loops: 110%, P_{Chi2}=0.883, n=40; Fig. 3.1D, E). However, EGC caused significant axon elongation (122±7%, $P_{Mann\text{-}Whitney}$=0.001, n=40; Fig. 3.1D, F) which might be an effect of its MT-stabilising functions.

From these results, I concluded that both the ABD and plakin-like domains of Shot are important for roles of Shot in MT regulation. This is not reflected in their impact on

Shot localisation, but is consistent with their total (Shot-LC) or partial (Shot-LA-ΔPlakin) requirement during axon growth *in vivo* (Bottenberg et al., 2009).

3.1.4. Rationale for the generation of Shot-LA-Moe and Shot-LA-Life constructs

My studies with the Shot-LC isoform and the Shot-LA-ΔABD construct provided a first indication for a functional dependency of Shot on direct F-actin interaction. To investigate this further, I exchanged the ABD of Shot for other actin binding domains, based on the rationale that they might impose different properties on the ways in which Shot interacts with actin. Such domains would likely display different F-actin affinities, detect different actin-network structures and be influenced through different co-factors.

As good candidate domains for substitution, I chose Lifeact and the actin-binding domain of Moesin which come from two distinct protein families and have different structures and actin-binding properties. Lifeact is the N-terminal 17-amino-acid long conserved actin binding motif of Abp140, which is an actin binding protein from *Saccharomyces cerevisiae* (Riedl et al., 2008). It has been reported that Lifeact labels F-actin accurately and consistently (Lemieux et al., 2014), although it shows certain specificities in its binding, such as low binding affinity to the long actin filaments which is bound by cofilin (Munsie et al., 2009). I am not aware of any reports that Lifeact has dominant effects on actin polymerization and depolymerization, or that it competes with major actin-binding proteins. Lifeact is used frequently for live imaging of F-actin, this also suggests it is no harm for cells (Riedl et al., 2008, Lemieux et al., 2014).

The best indication that Lifeact is substantially different from Shot's ABD is provided by comparative studies with α-actinin. Thus, actinins are members of the spectrin superfamily and contain a tandem ABD similar to that of spectrin or Shot (Broderick and Winder, 2005, Sjoblom et al., 2008). Comparative studies showed that in cells, Lifeact consistently labeled F-actin throughout, whereas the ABD of α-actinin did not bind to all F-actin structures and that the spatial distribution of actin interaction was even changed when the ABD was tagged differently, thus indicating weak actin binding (Lemieux et al., 2014). Also, *in vitro*, Lifeact binds to F-actin with a dissociation constant (Kd) of 2.2 ± 0.3 μM (Riedl et al., 2008). This indicates Lifeact has weaker actin binding affinity than the ABD of Shot (0.022 ± 0.3 μM). Therefore, from these studies I would predict that Lifeact binds to F-actin with higher specificity and lower binding affinity than the Shot ABD.

Ezrin–Radixin–Moesin (ERM) proteins are widely distributed proteins that tend to localise to the cellular cortex, microvilli and adherens junctions where they regulate signalling and the interaction between membrane and cortex (Neisch and Fehon, 2011, Niggli and Rossy, 2008). ERM family members are evolutionary highly conserved

proteins (Fievet et al., 2007, Arpin et al.) which bind actin through their C-terminal ERM association domain (C-ERMAD). Actin-binding of the C-ERMAD can be inhibited through binding of the N-terminal 4.1 protein-Ezrin–Radixin–Moesin (FERM) domain in a “head to tail” folding conformation (Hao et al., 2009). But it has been reported that the isolated C-ERMAD domain of *Drosophila* Moesin is sufficient to bind to actin reliably (Kiehart et al., 2000, Millard and Martin, 2008). Also the Moesin actin binding domain is likely to be different from Shot's ABD. Thus, it has been shown that phosphorylated, purified moesin has a high interaction affinity with F-actin (Kd, ~1.5 nM), however the dissociation time of Ezrin's ABD from F-actin was shown to be much shorter than the dissociation time of α-actinin's ABD, likely reflecting the fact that both actin binding domains have different F-actin binding dynamic in cells (Fritzsche et al., 2013, Fritzsche et al., 2014, Nakamura et al., 1999).

In summary, since different actin binding domains have different actin binding ability, I predicted that replacing Shot ABD with other actin binding domains will affect Shot function. In order to test this hypothesis, UAS-versions of Shot-LA-Life and Shot-LA-Moe were generated in which ABD was replaced by Lifeact or the moesin actin binding domain (Fig. 3.1B). The long constructs (Shot-LA-ΔABD, Shot-LA-Life and Shot-LA-Moe) were inserted into the same specific attB landing site used already for the Shot-LA-ΔABD construct (see Methods 2.2.1).

3.1.5. N-terminal control constructs reveal distinct localisations

I first asked whether these three ABDs do have different actin binding ability and/or potential dominant effects on MT behaviours. For this, N-terminal control constructs were generated containing the N-terminal sequence of Shot-LA followed by either ABD, Lifeact or Moesin actin binding domain (Shot-N-ABD, Shot-N-Life, Shot-N-Moe; Fig. 3.2A). These short constructs were directly transfected into neurons and compared to each other and to an eGFP control. To be able to perform these experiments, new transfection methods were developed for the *Drosophila* primary neuron system, and I contributed to this development (Methods 2.3.2.).

I found that the eGFP control was distributed throughout the neuron, and blebs of GFP enrichment showed no obvious correlation with F-actin accumulations (Fig. 3.2B-D). In contrast, the three hybrid constructs showed different patterns, of which the Shot-N-Life construct showed the most prominent pattern.

Thus, Shot-N-ABD showed a rather homogeneous distribution throughout the entire neurons axons, and there were only occasional accumulations in phalloidin-stained F-actin-rich areas (Fig. 3.2B-D). This staining can be interpreted in two ways: either Shot-N-ABD associates primarily with cortical F-actin rather than networks of long

actin filaments, or these proteins have a high abundance in the cytoplasm, potentially due to the relatively low affinity for F-actin. Unfortunately, these findings came too late during my project, and there was no time anymore to establish cell extraction assays to distinguish between the two possibilities.

Shot-N-Moe showed a localisation pattern very similar to that of Shot-N-ABD (Fig. 3.2B- D), but more frequently showed a patchy localisation in the GC filopodia. Moesin is a protein that specifically localises to the cell cortex (Fehon et al., 2010). In embryonic chick neurons, full length Moesin shows a similar localisation pattern as Shot-N-Moe in *Drosophila* GCs (Amieva and Furthmayr, 1995). Also in PC12 cells, it was shown that Moesin does not strongly co-localise with actin (Marsick et al., 2012). Our observation of Shot-N-Moe is consistent with all those findings. However, like for Shot-N-ABD, Shot-N-Moe may either bind to cortical actin networks specifically and/or bind to actin in a high dynamic state and localises to the cytoplasm instead. Further investigation would be necessary to address this point (see Discussion 4.2.2).

In stark difference to these two constructs, Shot-N-Life did not show any homogeneous distribution in the cytoplasm (Fig. 3.2B-D). Instead, it displayed an almost perfect co-localization with phalloidin-stained F-actin including any labelled regions in cell bodies, axons and GCs. Unlike Shot-N-ABD or Shot-N-Moe, it was not patchy in filopodia but reliably accumulated in all areas of F-actin concentration which were highlighted by phalloidin staining.

Apart from analysing the localisation, I also assessed any potential changes to MT organisation or axon length. However, none of the three N-terminal hybrid domains caused any obvious MT phenotypes (all normalised to eGFP-control; MT loops: Shot-N-ABD, 69%, P_{Chi2}=0.626, n=61; Shot-N-Moe, 95%, P_{Chi2}=1.000, n=142; Shot-N-Life, 86%, P_{Chi2}=0.717, n=158; Fig. 3.2E) or changes in axon length (all normalised to eGFP-control; Shot-N-ABD, 92±6%, $P_{Mann\text{-}Whitney}$=0.145, n=61; Shot-N-Moe, 100±4%, $P_{Mann\text{-}Whitney}$=0.938, n=142; Shot-N-Life, 93±4%, $P_{Mann\text{-}Whitney}$=0.081, n=158; Fig. 3.2F).

Therefore, mere presence of these domains does not cause GOF phenotypes, providing an important control and reference for the following experiments where I analysed the Shot-FL hybrid constructs containing the different actin binding domains in the Shot full length context. It also shows that these actin binding domains behaves very different in relation to actin localisation, which consistent with our pervious hypothesis that these three actin binding domains has distinctive actin binding properties.

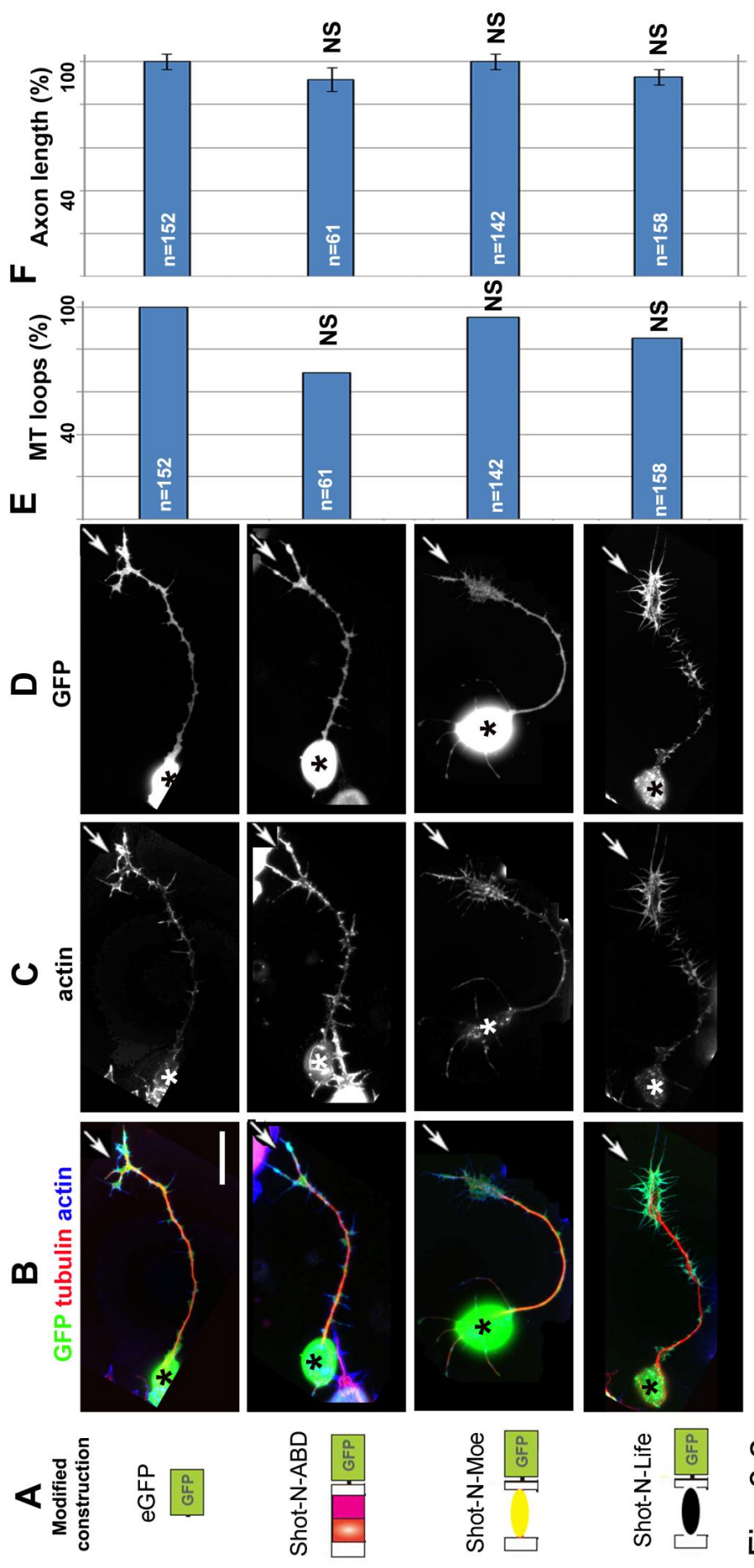
A
Modified construction
eGFP
GFP
Shot-N-ABD
GFP
Shot-N-Moe
GFP
Shot-N-Life
GFP
B
GFP tubulin actin
C
actin
D
GFP
E
MT loops (%)
100
40
n=152
n=61
n=142
n=158
NS
F
Axon length (%)
100
40
n=152
n=61
n=142
n=158
NS

Fig. 3.2

Figure 3.2. *Shot N-terminal control constructs localise differently in axons but have no impact on axon length and MT organization.*

A) *Illustration of the modified Shot N-terminal control constructs (green rectangle, GFP; the red and magenta rectangle, CH1+2 domains; yellow ellipse, actin binding domain of Moesin; black ellipse, Lifeact).* ***B-D)*** *Localisation and axon structure of primary neurons cultured overnight, grown on ConA and transfected with the different constructs and triple-labelled for actin, tubulin and GFP (B; actin channel shown alone in C; GFP channel shown alone in D; asterisk, cell body; arrow, growth cone); scale bar represents 5μm in B, C, D.* ***E,F)*** *Quantifications of phenotypes caused by overexpression of the constructs shown on the left, respectively (all normalised and compared to eGFP control); numbers in the bars indicate the numbers of neurons analysed in each experiment; for quantifications of neurons showing MT loops in their GCs (E), P values were calculated using the Chi-square test (NS: P>0.050, *: P<0.050, **: P<0.010,***: P<0.001); for axon length (F), P values were calculated using the Mann-Whitney Rank Sum test (NS: P>0.050, *: P<0.050, **: P<0.010,***: P<0.001).*

3.1.6. Shot-LA-Moe can partially induce Shot GOF phenotypes in neurons

In order to test whether the different actin binding domains influence behaviours and functions of full length Shot, I first analysed the localisation of Shot-LA hybrid constructs. As describe before, Shot-LA has a strong tendency to enrich on MTs at GCs (Sanchez-Soriano et al., 2009) (Fig. 3.1C). Comparable to this, also Shot-LA-Moe was clearly enriched on MTs at GCs (Fig. 3.1C), suggesting that the Moe domain does not impose any dominant localisation phenotype. This was expected from the very similar localisations of N-Shot-ABD and N-Shot-Moe.

Next I analysed the effect of Shot-LA-Moe on MT organisation and axon length. As described above, expression of Shot-LA causes a significant increase of bundled loops to 204% and a significant shortening of axons to 80%, whereas in Shot-LC and Shot-LA-ΔABD did not show these effects (Fig. 3.1C-F) (Sanchez-Soriano et al., 2010).

In spite of Shot-LA-Moe's close resemblance in localisation to Shot-LA, my analyses failed to reveal any significant increases in bundled loops (normalised to wildtype: 118%, P_{Chi2}=0.474, n=100; Fig. 3.1D, E), which is reminiscent of the behaviour of Shot-LA-ΔABD. This finding is in agreement with the predicted different F-actin affinities between Moe and ABD mentioned in Chapter 3.1.4. Therefore, the typical GC localisation of this construct is likely due to other functional domains of Shot (e.g. the plakin-like domain), as is similarly the case in Shot-ΔABD which lacks its dedicated actin binding domain (Chapter 3.1.2).

Surprisingly, Shot-LA-Moe induces the second Shot GOF phenotype, namely axon shortening (89±3%; $P_{Mann\text{-}Whitney}$=0.008; Fig. 3.1D, F), although it was more moderate than the 80% observed with Shot-LA. This suggests that modified F-actin interaction in Shot-LA-Moe seems to convey some Shot-like properties, whereas other functional abilities seem abolished.

These findings also challenge a hypothesis raised in the past, i.e. that shorter axons upon Shot-LA overexpression are the consequence of MT loop formation in GCs (Dent et al., 1999, Sanchez-Soriano et al., 2010). The findings with Shot-LA-Moe do no longer support this statement but suggest that other MT-regulatory processes downstream of Shot might be involved.

3.1.7. Shot-LA-life displays a very different localisation and MT regulatory pattern in neurons

I next analysed the localisation of Shot-LA-Life. In contrast to Shot-LA and Shot-LA-Moe, Shot-LA-Life displayed a completely new localisation pattern, overriding any endogenous preference for the GC area. In addition to prominent binding to bundled MTs

in GCs, it was also strongly localised all along axons, often as two parallel lines. Such a split localisation in axons was rarely observed with Shot-LA (3%, n=60), but was very frequent for Shot-LA-Life (59%, n=100; P_{Chi2}<0.001 between Shot-LA and Shot-LA-Life; Fig. 3.3A, C-C'', E). All areas of Shot-LA-Life localisation were usually also stained by phalloidin, suggesting a strong correlation of Shot-LA-Life with F-actin (Fig. 3.1C, 3.3A-C'''). This is consistent with our previous finding that the Shot-N-Life construct was the only construct showing strong specifility for F-actin throughout entire neurons. However, in contrast to Shot-N-Life, Shot-LA-Life fully co-localised neither with filopodia nor lamelipodia, it only localised to the proximal part of filopodia, which may be due to the fact that the construct remains anchored on MTs, suggesting that its altered distribution in cells will impact on its MT regulatory role. Therefore, at least one actin binding domain, namely Lifeact, can change the localisation behaviour of Shot, providing an experimental approach to assess the influence of F-actin interaction on MT regulatory roles of Shot.

In agreement with these expectations, Shot-LA-Life has a much more striking functional impact in primary neurons. Very similar to Shot-LA, it causes a significant increase in bundled MT loops to 206% (P_{Chi2}<0.001, n=100; Fig. 3.1D, E) and a reduction in axon length to 83±3% ($P_{Mann-Whitney}$<0.001; Fig. 3.1D, F). However, other changes in MT organisation induced by Shot-LA-Life are very different from all other phenotypes described so far. First, axonal MT bundles are split longitudinally, often along their entire length, thus matching observations from my localisation studies (split MT bundles: Shot-LA, 3%, n=60; Shot-LA-Life, 30%, n=100; P_{Chi2}<0.001 between Shot-LA and Shot-LA-Life; Fig. 3.3A, C-D). In extreme cases, it appears as if the bundled loops in GCs continue back into the axon, thus forming an organisation similar to a stem-loop confirmation in RNA molecules (Fig. 3.1C). As mentioned before, Shot-LA-Life frequently localises on both sides of axons. In these cases, also phalloidin staining can be seen to line axons on both sides, suggesting that Shot-LA-Life might bridge between these actin and MT fractions on either side. Also in the cell bodies, a split is apparent, and both MT cables seem to have individual roots reaching half way into the soma, thus giving it a funnel-shaped appearance (funnel-shaped axon roots: Shot-LA, 13%, n=60; Shot-LA-Life, 40%, n=100; P_{Chi2}<0.001 between Shot-LA and Shot-LA-Life; Fig. 3.3A, B-B''', F).

In conclusion, the different F-actin binding domains clearly have distinct impacts on Shot-mediated MT organisation in neurons. Shot-LA and Shot-LA-Moe show very similar localisation patterns, as do their N-terminal control constructs, and both cause shorter axons, but only Shot-LA induces a strong MT GOF phenotype, as if the mechanisms leading to slowed axon growth require a different actin binding propertiy compare to the mechanisms leading to the formation of bundled loops. Shot-LA-Life resembles Shot-LA with respect to bundled loop formation and axon length phenotypes, but it is very different with respect to its localisation and the axonal bundle split phenotype. These

phenotypes are rarely seen with Shot-LA and correlate with the strong actin-localisation of the Shot-N-Life control construct, suggesting that higher binding specifility to F-actin changes the localisation of Shot and, as a consequence, the output of its MT regulatory roles.

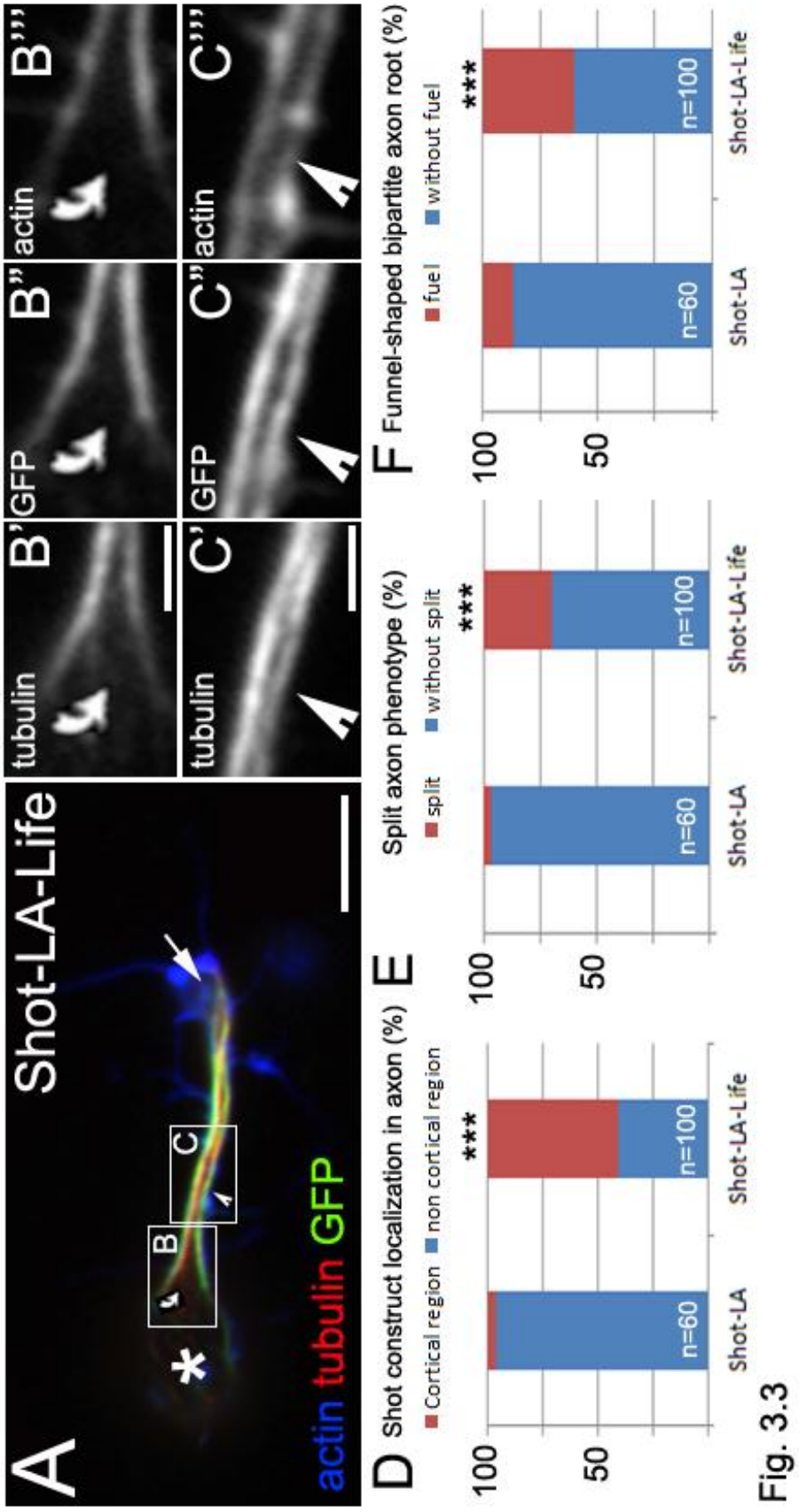
A
Shot-LA-Life
actin tubulin GFP
B
C
tubulin
B'
GFP
B''
actin
B'''
tubulin
C'
GFP
C''
actin
C'''
D Shot construct localization in axon (%)
Cortical region
non cortical region
***
n=60
n=100
Shot-LA
Shot-LA-Life
E Split axon phenotype (%)
split
without split
***
n=60
n=100
Shot-LA
Shot-LA-Life
F Funnel-shaped bipartite axon root (%)
fuel
without fuel
***
n=60
n=100
Shot-LA
Shot-LA-Life
100
50

Fig. 3.3

Figure 3.3. *Details of the phenotypes induced by Shot-LA-Life.*

A) *Primary Drosophila neurons expressing Shot-LA-Life at 6HIV, triple-labelled for actin, tubulin and GFP (asterisks, cell bodies; arrows, growth cones). Boxed areas show magnifications in B' – C'''.* ***B)*** *Funnel-shaped bipartite axon root (curved arrow). B' (tubulin), B'' (GFP) and B''' (actin).* ***C)*** *Shot-LA-Life induced phenotype in axon (white arrow head). Split axon (C', labelled for tubulin) and Shot-LA-Life localise at both side of axon (C'', labelled for GFP, C''', labelled for actin) Scale bar represents 5µm in A, and 1.25µm in B' –C'''.* ***D-F)*** *Quantifications of phenotypes caused by overexpression of Shot-LA or Shot-LA-Life, respectively (all compared to Shot-LA); numbers in the bars indicate the numbers of neurons analysed in each experiment; For all phenotypes, P values were calculated using the* Chi^2 *test (NS: P>0.050, *: P<0.050, **: P<0.010,***: P<0.001).*

3.1.8. Manipulations of neuronal F-actin networks impact on Shot wildtype construct functions

To further assess whether changes of MT organisation induced by hybrid constructs depend on F-actin, I manipulated F-actin networks and assessed the respective impact on GOF phenotypes. As mentioned before, removal of F-actin with the actin depolymerising drug LatA (Fig. 3.4A-D) abolishes the GC localisation of Shot-LA which acquires homogeneous distribution along MTs throughout entire axons instead. Furthermore, it was shown that LatA suppresses the MT loops induced by Shot-LA (from 204% to 21%, compared to Shot-LA, $P_{Chi2}<0.001$, n=73; Fig. 3.4E) (Sanchez-Soriano et al., 2010). I also found that the shorter axon phenotype of Shot-LA is reverted from 89% to 102% (compared to Shot-LA, $P_{Mann\text{-}Whitney}=0.010$, n=73; Fig. 3.4F). This strongly suggests that Shot function in MT loop formation and axon length regulation depends on the presence of and direct interaction with a properly organized F-actin network.

Similar to effects observed with LatA, applying the Arp2/3 complex inhibitor CK666 to neurons expressing Shot-LA suppresses the MT loops from 204% to 120% (compared to Shot-LA, $P_{Chi2}<0.001$, n=100; Fig. 3.4). However, Shot-LA does not lose its GC localisation and only occasionally shows a more homogeneous localisation along axons. Also the shorter axon phenotype of Shot-LA is not rescued by CK666 (83±3%, compared to Shot-LA, $P_{Mann\text{-}Whitney}=0.138$; Fig. 3.4). Obviously the effect resembles those of LatA only partly and a number of explanations can be given. First, Arp2/3 is only one available nucleator and formins, such as DAAM can maintain actin networks to a substantial degree (Gonçalves-Pimentel et al., 2011). As argued in Chapter 3.1.7, MT loop formation seems to require special actin binding in GCs and the effect of CK666 seems to be strong enough to reduce F-actin content to eliminate actin binding. Second, LatA primarily affects F-actin networks in GCs but not in axons (see Chapter 3.2.3), whereas CK666 affects F-actin networks in all areas of the neuron (see Chapter 3.2.5.1). Since other results from my work suggest that axonal actin promotes axon growth (Chapter 3.2.6), the effects observed here with CK666 treatment are difficult to interpret. It would be important to repeat experiments using the F-actin depolymerising drug cytochalasin D (CytoD) of which we know that it affects all F-actin networks of neurons (Chapter 3.2.4), and I would predict that this treatment will abolish all differences between the various Shot hybrid structures.

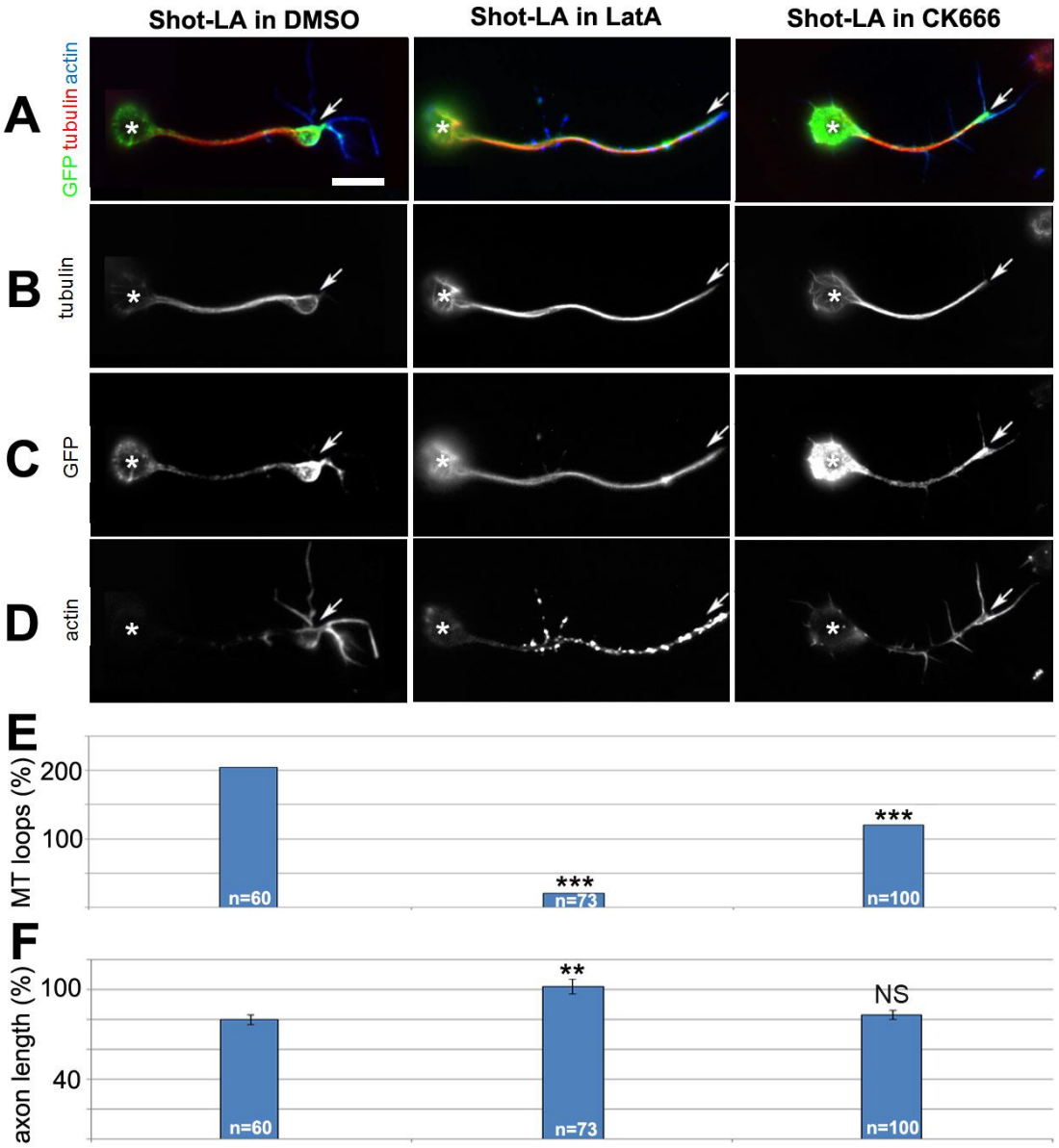
Shot-LA in DMSO
Shot-LA in LatA
Shot-LA in CK666
A
GFP tubulin actin
B
tubulin
C
GFP
D
actin
E
MT loops (%)
200
100
n=60
***
n=73
***
n=100
F
axon length (%)
100
40
n=60
**
n=73
NS
n=100

Figure 3.4. *Impact of the actin-destabilising drug latA and the Arp2/3 inhibitor CK666 on Shot-LA GOF phenotypes.*

A- D) *Axonal localisation and phenotypes in Shot-LA expressing primary neurons at 6HIV, 1 or 2hrs in vehicle (DMSO) or treated with LatA or CK666; cells are triple-labelled for actin, tubulin and GFP (A; tubulin channel shown alone in B; GFP channel shown alone in C; actin channel shown alone in D; asterisk, cell body; arrow, growth cone); scale bar represents 5µm in A, B, C, D.* ***E,F)*** *Quantifications of phenotypes for the above treatments, respectively (all normalised and compared to Shot-LA in DMSO); numbers in the bars indicate the numbers of neurons analysed in each experiment; for quantifications of neurons showing MTs loops in their GCs(E), P values were calculated using the Chi-square test (NS: P>0.050, *: P<0.050, **: P<0.010,***: P<0.001); for axon length (F) P values were calculated using the Mann-Whitney Rank Sum test (NS: P>0.050, *: P<0.050, **: P<0.010,***: P<0.001).*

3.1.9. Conclusions for Chapter 3.1

I found that Shot localisation correlates very little with its MT regulatory functions, and that Shot's ABD is not the only mediator of Shot-LA enrichment in GCs. Instead, further domains of Shot seem required, in particular the plakin-like domain. But other domains, such as the spectrin repeat rod domain, might also contribute (Bottenberg et al., 2009) (see Discussion 4.2.1). Instead, the phenotypic GOF studies of Shot provided a much clearer path to address MT regulatory functions of Shot, and replacement of Shot's ABD clearly changed its MT regulatory functions. These findings suggest that Shot's ABD has unique properties which are crucial for cellular roles of Shot. It seems that only the ABD of Shot has the right binding ability for F-actin or specific actin networks appropriate for MT-regulatory function downstream of actin (see Discussion 4.2.2).

Unfortunately, my attempts to use these lines to rescue phenotypes of Shot deficient neurons were hampered by the fact that the required green balancer chromosomes (which carry a combination of Gal4- and UAS-constructs) (Casso et al., 2000) caused lethality when crossed over chromosomes carrying *UAS-shot-LA-Life* or *UAS-shot-LA-Moe*. Therefore, this experiment will require the generation of new fluorescent balancer chromosomes which are currently being constructed in the Prokop laboratory.

3.2. The roles of F-actin in axon growth and maintenance

In *shot* mutant neurons, MTs are de-stabilised and severely disorganised. On the one hand, these phenotypes can be explained through actin-indepencent MT stabilisation as a primary function of the MT-binding C-terminus of Shot (Sanchez-Soriano et al., 2009). On the other hand, Shot organises MTs through mechanisms acting downstream of F-actin, as described in detail in Chapter 3.1. This actin-dependent MT organisation depends on three parallel interactions of Shot: binding to F-actin, to EB1 at MT plus ends, and association with MTs (Sanchez-Soriano et al., 2009, Alves-Silva et al., 2012). If MT organising functions of Shot depend on F-actin, I would have predicted that depletion of F-actin would lead to MT disorganisation. In order to test my prediction, I used the actin-destabilising drug CytoD to treat wildtype neurons. I found that my prediction was wrong. When treating cultured wildtype neurons with CytoD, the MTs did not become disorganised, but I observed frequent fragmentation in form of gaps within the axonal MT bundles (5% neuron with gaps in wildtype, n=116; 31% neuron with gaps in wildtype with CytoD, n=80, $P_{Chi2}<0.001$; Fig. 3.5.A.II and 3.9), suggesting F-actin roles upstream of MT bundle stability rather than MT bundle organisation.

From these data, I deduced two hypotheses. MT bundles are disorganised in the absence of Shot but maintain their organisation upon removal of F-actin (CytoD treatment). I therefore hypothesise that **(1)** Shot does not only act downstream of F-actin in MT bundle formation and/or maintenance, but F-actin independent functions of Shot seem to be involved. Previous experiments have shown that nocodazole (an MT destabilising drug) also causes MT gaps in *shot* mutant but not in wildtype neurons, suggesting that MT gaps reflect destabilisation of MTs and that Shot has protective function. It was shown that the C-terminus of Shot (EGC; which cannot interact with actin but binds MTs and stabilises them) was sufficient to rescue this phenotype (Alves-Silva et al., 2012). However, these actin-independent MT-protecting functions of Shot are not sufficient to protect MT bundles of wildtype neurons from effects caused by treatment with CytoD (Fig. 3.5.A.II). I therefore hypothesise that **(2)** F-actin has a Shot-independent role in MT bundle maintenance. In consequence, these two hypotheses would mean that MT-stabilising roles of F-actin (Shot-independent) and of Shot (actin-independent) complement each other during the formation and/or maintenance of axonal MT bundles. In the following, I tested these two hypotheses.

3.2.1. Shot has F-actin-independent roles in MT stabilisation

As explained above, abolishing F-actin from wildtype neurons leads to gaps in MT bundles, but there is no obvious increase in curled, non-coalescent MTs, leading to the

above formulated hypothesis that not all MT-organising functions of Shot are dependent on F-actin, and that Shot maintains axonal MT bundles through additional mechanisms.

To test this possibility, I analysed in greater depth the actin-independent roles of Shot in MT bundle protection. When cultured on glass, 66% of *shot*$^{3/sf20}$ mutant neurons contained axons, which was slightly less than the 76% of wildtype neurons (P_{Chi2}=0.041, n=200; Fig. 3.5). When wildtype neurons were treated with CytoD, 69% of neurons grow axons, which is only slightly less than untreated wildtype (P_{Chi2}=0.010, n=566, Fig. 3.5). In contrast, when *shot* mutant neurons are treated with CytoD, MTs seemed to disappear and the percentage of neurons with axons was significantly decreased to 31% (P_{Chi2}<0.001, n=300; Fig. 3.5). This clearly indicates that Shot has F-actin independent roles in MT bundle maintenance, and further supports my hypothesis that F-actin has additional complementary functions in maintaining axonal MTs. As explained in the previous Chapter, the C-terminal EGC domain of Shot binds and stabilises MTs (Alves-Silva et al., 2012). To test whether EGC is sufficient, I expressed the Shot-LA isoform in *shot*^{3} mutant neurons. This generates a situation in which all Shot domains required for the MT guidance function are present, which is enough to rescue the *shot* mutant MT disorganisation phenotype and includes the EGC. These *shot* mutant neurons expresing the Shot-LA rescue construct will from now on be referred to as Shot-LA^{only} neurons.

When culturing Shot-LA^{only} neurons on glass, they displayed axons in 71% of cases (P_{Chi2}=0.396, n=200) very similar to wildtype (76%). MT disorganization in Shot-LA^{only} neurons (145% normalised to wildtype; P_{Chi2}=0.100, n=110; Fig. 3.5.A.V) was far better than in *shot*$^{3/sf20}$ mutant neurons (275% disorganization, P_{Chi2}<0.001, n=155; Fig. 3.5.A.III), indicating a strong rescue of the phenotype. However, this rescue effect disappeared entirely when treating Shot-LA^{only} neurons with 0.4µg/ml CytoD for 4hrs, after which they displayed a phenotype very similar to that of CytoD-treated *shot* mutant neurons (39% of Shot-LA^{only} neurons with axons *vs.* 31% in *shot*^{3} when compared to wildtype; P_{Chi2}<0.001, n=300; Fig. 3.5). Those axons persisting in *shot* mutant and Shot-LA^{only} neurons seemed to contain less MTs (i.e. they were thinner) and they both contained very low amounts of disorganised MTs (MT disorganization normalised to untreated wildtype; 14% in Shot-LA^{only}, P_{Chi2}<0.001, n=71 *versus* 4% in *shot* mutant neurons, P_{Chi2}<0.001, n=132; Fig. 3.5.A.IV and VI). This result suggests that MT-stabilising functions of the Shot EGC domain are not sufficient and that there are other actin-independent roles of Shot in MT bundle maintenance.

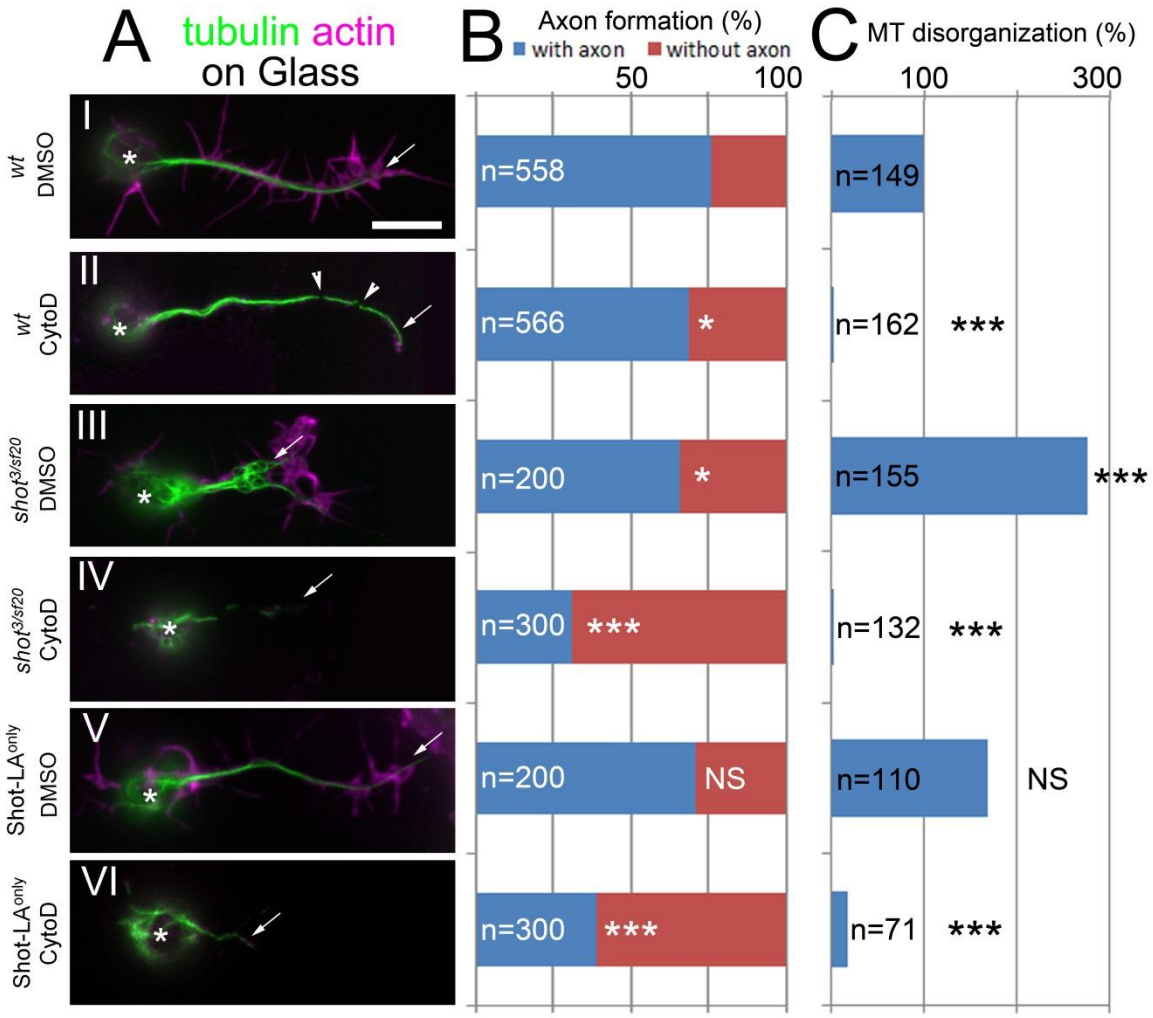
A
tubulin actin
on Glass
B
Axon formation (%)
with axon
without axon
50
100
C
MT disorganization (%)
100
300
I
II
III
IV
V
VI
wt DMSO
wt CytoD
shot3/sf20 DMSO
shot3/sf20 CytoD
Shot-LAonly DMSO
Shot-LAonly CytoD
n=558
n=566
*
n=200
*
n=300
***
n=200
NS
n=300
***
n=149
n=162
***
n=155
***
n=132
***
n=110
NS
n=71
***

Figure 3.5. *F-actin and Shot have distinct and overlapping functions in axonal MT organisation and stabilisation.*

A) *Axonal phenotypes in wildtype primary neurons and shot mutant primary neurons cultured on uncoated glass, expressing or not expressing Shot-LA, at 8HIV, 4hrs in vehicle (DMSO) or treated with CytoD; cells are double-labelled for tubulin and actin (asterisk, cell body; arrow, growth cone; arrowhead, MT gaps); scale bar represents 5µm in A.* ***B,C)*** *Quantifications of phenotypes for the drug treatments given on the left, respectively; numbers in the bars indicate the numbers of neurons analysed in each experiment; for quantifications of axon formation (B, all compared to wild type in DMSO), P values were calculated using the* Chi^2 *test (NS: P>0.050, *: P<0.050, **: P<0.010,***: P<0.001); for MT disorganisation (C, all normalised and compared to wild type in DMSO), P values were calculated using the* Chi^2 *test (NS: P>0.050, *: P<0.050, **: P<0.010,***: P<0.001).*

My results indicate actin-independent roles of Shot in MT bundle maintenance, which cannot be rescued by Shot-LA and go therefore beyond the two known roles of N- and C-terminal Shot domains in MT guidance and stabilisation. Additional functional domains of Shot which are not contained in the Shot-LA isoform seem required. A good candidate is a 3000 aa plakin-repeat region (PRR) which is only contained in the Shot-LH isoform (Fig. 3.6), and for which members of our group have shown that it can associate with axonal MTs (N. Sánchez-Soriano, unpublished data; Fig. 4.5 in Discussion 4.3). Shot-LA-mediated roles in MT guidance and stabilisation could be complemented by functions of the PRR in Shot-LH, and a working hypothesis for its function will be discussed in Chapter 4.3.

Figure 3.6. *Graphic of different Shot isoforms.*

The predicted structures of Shot isoforms.Shot-LA, Shot-LC and Shot-LH were marked in red boxes. Functional domains are described in the box below. Image taken from Centrosome: DB.

3.2.2. Shot displays F-actin-independent roles also in MT bundle organisation

When neurons are cultured on concanavalin A (ConA)-treated cover slips, axonal membranes tend to adhere strongly to the glass surface. I expected therefore that axon loss upon CytoD treatment of Shot-LA^{only} neurons on glass might be delayed on ConA, and this might provide additional opportunities to understand the Shot-LA^{only} phenotype. When I cultured Shot-LA^{only} neurons on ConA-coated cover slips without CytoD treatment, I observed that Shot-LA^{only} neurons formed stable axons in which MT disorganisation was enhanced over wildtype neurons, but clearly far lower than in *shot* mutant neurons (196% disorganisation in Shot-LA^{only} normalised to wildtype, P_{Chi2}=0.044, n=40, Fig. 3.7.A.V; *shot*$^{3/sf20}$: 381% disorganisation, n=40, P_{Chi2}<0.001, Fig. 3.7.A.III). These data were similar to those on uncoated glass and reflected a substantial but incomplete rescue (Fig. 3.5). In contrast, when neurons were treated with CytoD, more axons seems remained on the sticky surface than observed on glass (not measured), although MTs appeared reduced in number in both experimental settings. On ConA, these remaining MTs had a stronger tendency to be disorganised in Shot-LA^{only} neurons with CytoD (MT disorganization: 256%, P_{Chi2}<0.001, n=54; Fig. 3.7.A.VI) whereas disorganised MTs were virtually absent in the parallel CytoD treated *shot*^{3} mutant neurons (MT disorganization: 144%, P_{Chi2}=0.273, n=45; Fig. 3.7.A.IV). Therefore, unlike the experiment on glass, the ConA condition clearly highlights a phenotypic difference between *shot* mutant and *Shot-LA*^{only} neurons. This difference is likely to have its mechanistic explanation in the fact that Shot-LA contains the MT stabilising Gas2-related domain (Alves-Silva et al., 2012) which can protect off-track MTs even if they lose their bundled organisation upon CytoD treatment. However, this stabilisation of individual MTs through the GRD (in contrast to potential bundle stabilisation through the PRR) seems not to be potent enough to prevent axon loss when membranes retract unhindered on uncoated glass surfaces.

However, the even more important difference of CytoD-treated neurons on ConA is that remaining MTs become disorganised in Shot-LA^{only} neurons, whereas MT bundles in wildtype neurons display only gaps but no disorganisation (Fig. 3.7). These data suggest that functional Shot domains not contained in Shot-LA (likely also the PRR) (Roper and Brown, 2003) mediate F-actin-independent roles of Shot not only in MT stabilisation but also in MT bundle organisation (see Discussion 4.3).

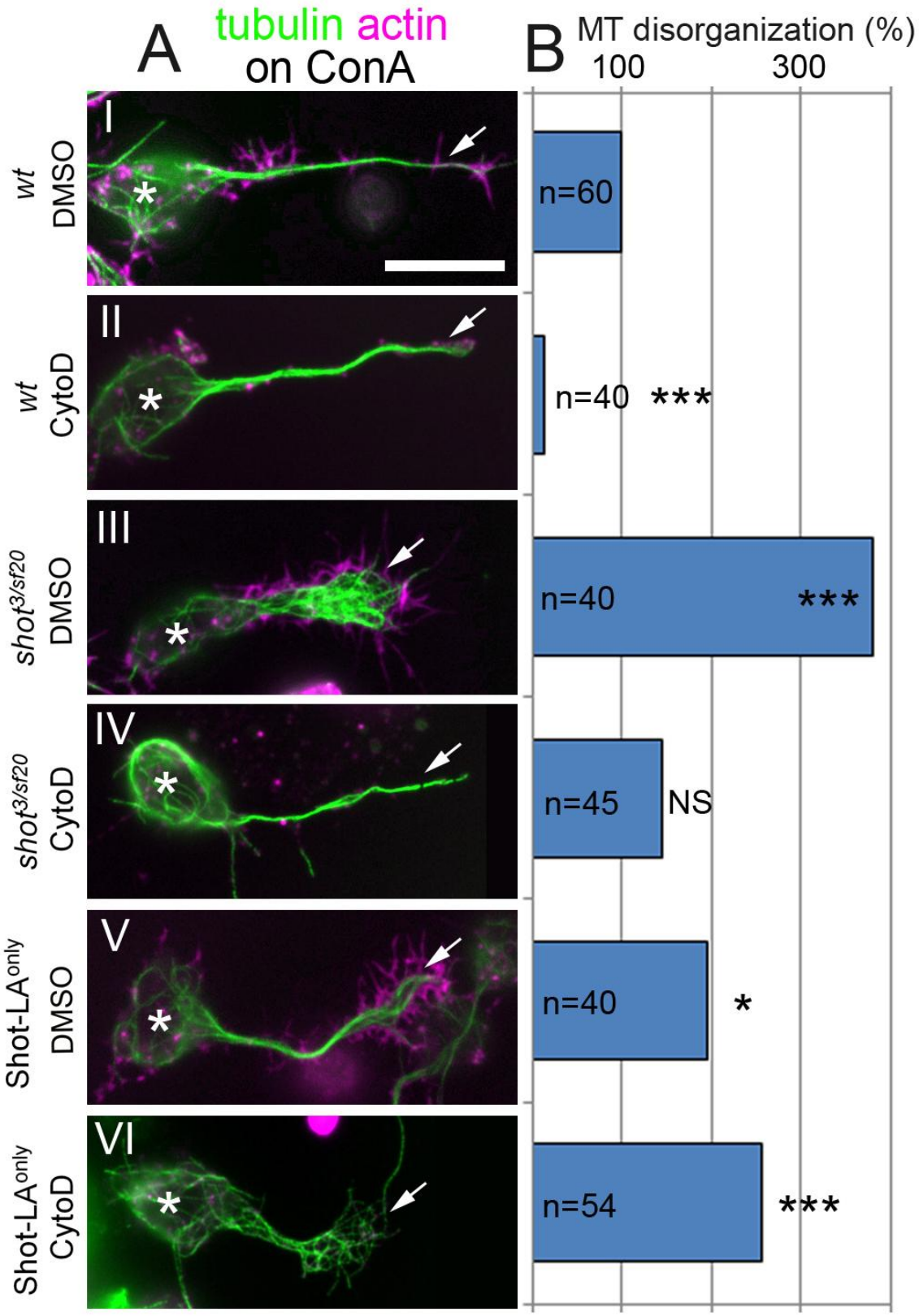
A
tubulin actin
on ConA
B
MT disorganization (%)
100
300
I
wt
DMSO
n=60
II
wt
CytoD
n=40
***
III
shot3/sf20
DMSO
n=40
***
IV
shot3/sf20
CytoD
n=45
NS
V
Shot-LAonly
DMSO
n=40
*
VI
Shot-LAonly
CytoD
n=54
***

Figure 3.7. *Shot has F-actin-independent roles in MT organisation.*

A) *Axonal phenotypes in wildtype primary neurons and shot mutant primary neurons at 8HIV on ConA-treated coverslips, expressing or not expressing Shot-LA, in vehicle (DMSO) or treated with CytoD; cells are double-labelled for tubulin and actin (asterisk, cell body; arrow, growth cone); scale bar represents 10µm in A.* ***B)*** *Quantifications of MT disorganisation for the drug treatments given on the left; numbers in the bars indicate the numbers of neurons analysed in each experiment; all normalised and compared to wild type in DMSO, P values were calculated using the* Chi^2 *test (NS: P>0.050, **: P<0.050, ***: P<0.001).*

3.2.3. F-actin maintains axonal MTs

My experiments clearly support the existence of my first hypothesis, i.e. that Shot has actin-independent roles in MT maintenance. Next, I addressed the second hypothesis, i.e. that there is a complementary Shot-independent role of F-actin in MT bundle maintenance. This hypothesis was originally derived from the MT gaps and axon shortening observed upon treatment of wildtype neurons with CytoD (Chapter 3.2.1), and it became even more obvious when treating *shot* mutant neurons (where MT bundle protecting roles of Shot are absent) with CytoD: in these experiments MTs were lost suggesting that F-actin is required for MT maintenance in the absence of Shot (Chapter 3.2.1).

To further complement these findings, I performed experiments where I affected MT stability through independent, pharmacological means by using the MT-destabilising drug nocodazole. When treating wildtype neurons with nocodazole, 72% of neurons contain axons (P_{Chi2}=0.137, n=478; Fig. 3.8), which is very similar to the 76% of vehicle-treated control neurons (n=558; Fig. 3.8). In agreement with previous descriptions (Alves-Silva et al., 2012), these axons looked surprisingly normal, and no obvious MT gaps were observed. In contrast, wildtype neurons treated with CytoD showed MT gaps (as described already in Chapter 3.2.1), but there was no obvious axon loss (69% of neurons with axons; P_{Chi2}=0.010, n=566; Fig. 3.8). However, when treating neurons jointly with CytoD and nocodazole, MTs appeared severely damaged and only 49% of neurons had axons (P_{Chi2}<0.001, n=595; Fig. 3.8). This provides strong further support for my hypothesis that actin- and MT-dependent mechanisms co-exist in axons and complement each other in axonal MT maintenance.

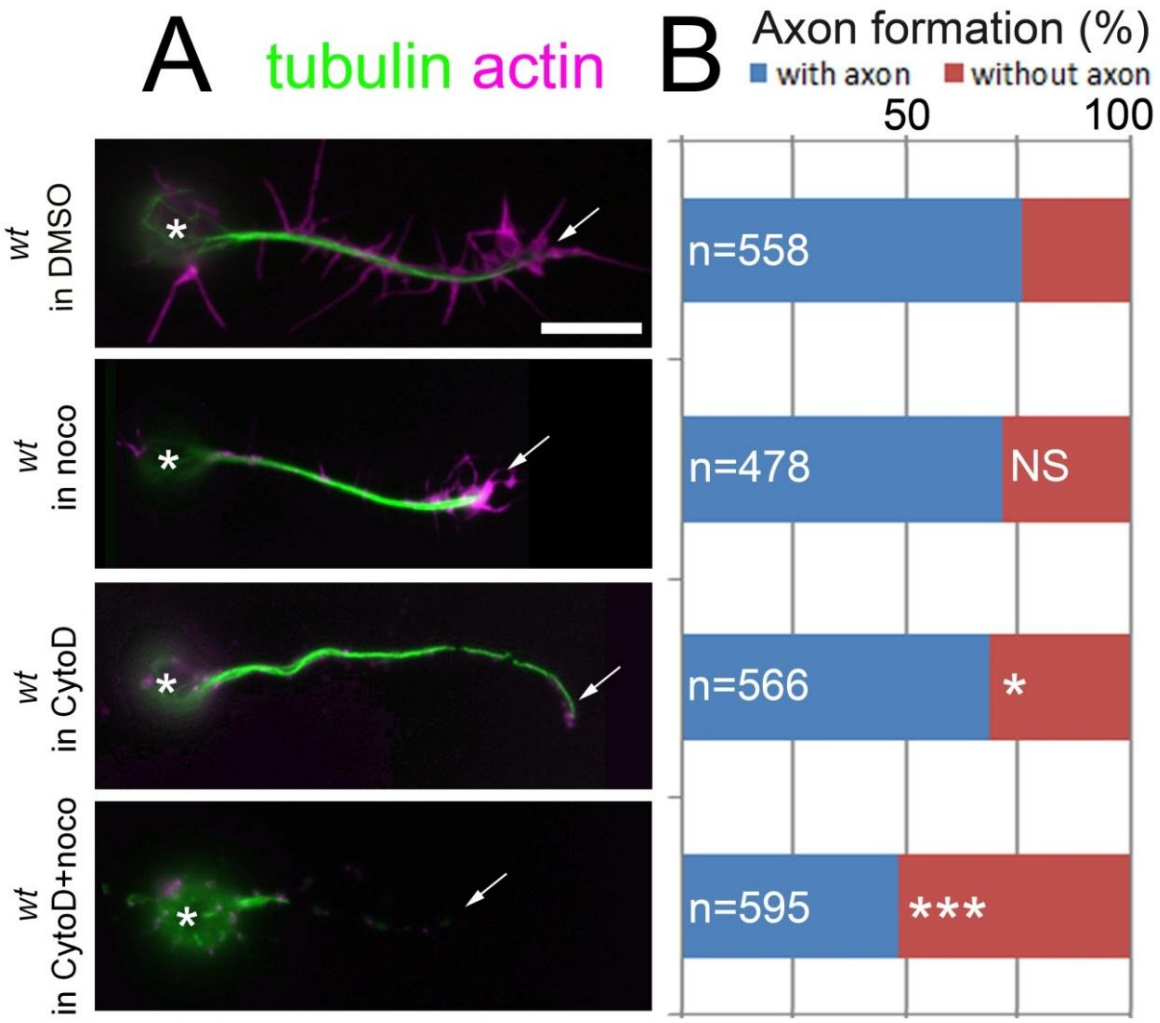
A
tubulin actin
wt in DMSO
wt in noco
wt in CytoD
wt in CytoD+noco
B
Axon formation (%)
with axon
without axon
50
100
n=558
n=478
NS
n=566
*
n=595
***

Figure 3.8. *F-actin has independent roles in MT organisation.*

A) *Axonal phenotypes in primary neurons at 8HIV, 4hrs in vehicle (DMSO) or treated with nocodazole (noco) and/or CytoD as indicated on the left; cells are double-labelled for tubulin and actin (asterisks, cell bodies; arrows, growth cones); scale bar represents 5µm in A.* ***B)*** *Quantifications of neurons displaying axons (all normalised to DMSO-treated wild type); numbers in the bars indicate the numbers of neurons analysed in each experiment, P values were calculated using the Chi^2 test (NS: P>0.050, *: P<0.050, **: P<0.010,***: P<0.001).*

Furthermore, I used an independent genetic condition to test for F-actin roles in MT maintenance. Thus, we found that *efa6*$^{KO\#1}$ mutant neurons lacking the cortical collapse factor Efa6, have a significant increase in MT disorganisation (normalised to wildtype: 170%, P_{Chi2}<0.001, n=100; Fig. 3.9). As will be explained in Chapter 3.3, MT disorganisation in the absence of Efa6 is caused through a very different mechanism as in *shot* mutant neurons. When treating *efa6*$^{KO\#1}$ mutant neurons with CytoD, disorganised MTs are virtually absent and disorganisation of axonal MTs is decreased to 6% (normalised to wildtype; compare to *efa6*$^{KO\#1}$, P_{Chi2}<0.001, n=99; Fig. 3.9), which is clearly less than untreated wildtype. In contrast to *shot* mutant neurons, axons are not eliminated when treating Efa6 deficient neurons with CytoD, and this is likely due to the fact that Shot-protected bundles persist in these neurons. As observed in wildtype neurons where 31% show gaps in their axonal MT bundles after CytoD treatment (compared to *efa6*$^{KO\#1}$ in CytoD, P_{Chi2}<0.001; Fig. 3.9), even more such gaps are observed in treated *efa6*$^{KO\#1}$ mutant neurons (57% normalised to wildtype, n=99, P_{Chi2}<0.001), and this is a dramatic increase over untreated *efa6*$^{KO\#1}$ mutant neurons (4% of neurons with gaps, P_{Chi2}=0.683, n=100; Fig. 3.9).

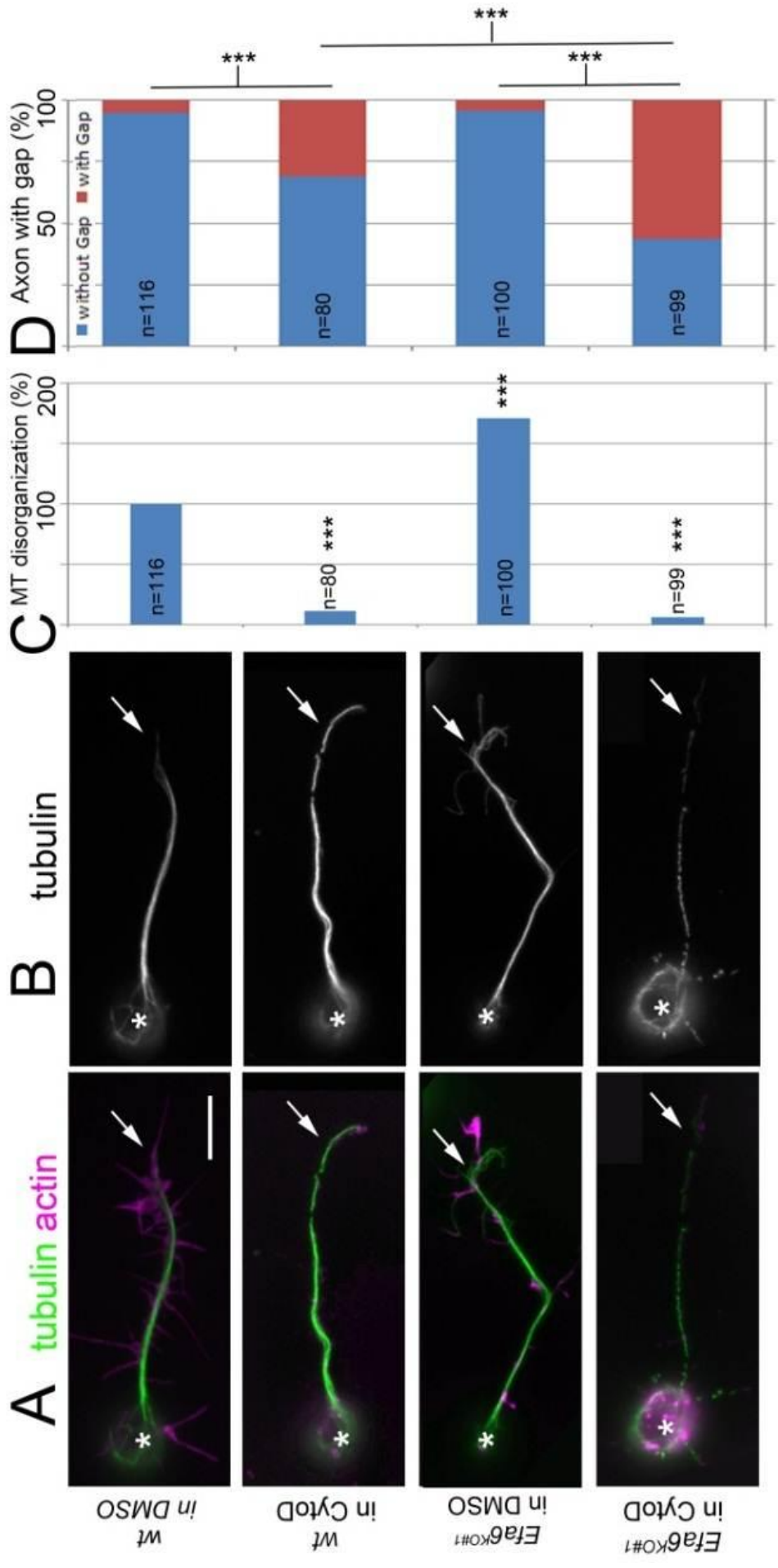
A
tubulin actin
B
tubulin
C
MT disorganization (%)
100
200
n=116
n=80
***
n=100
***
n=99
***
D
Axon with gap (%)
50
100
without Gap
with Gap
n=116
n=80
n=100
n=99
***
***
***
wt
in DMSO
wt
in CytoD
Efa6KO#1
in DMSO
Efa6KO#1
in CytoD

Figure 3.9. *F-actin stabilise the disorganization MT in Efa6 mutant.*

A, B) *Axonal phenotypes in wild type or efa6$^{KO\#1}$primary neurons at 8HIV, 4hrs in vehicle (DMSO) or treated with CytoD; cells are double-labelled for actin, tubulin (A; tubulin channel shown alone in B; asterisk, cell body; arrow, growth cone); scale bar represents 5µm in A, B.* ***C,D)*** *Quantifications of phenotypes for the drug treatments given on the left, respectively; numbers in the bars indicate the numbers of neurons analysed in each experiment; for MT disorganisation (C, all normalised and compared to wild type in DMSO), P values were calculated using the Chi^2 test (NS: P>0.050, *: P<0.050, **: P<0.010,***: P<0.001); for quantifications of neurons showing gaps in their axons (D, comparisons were indicated in figure), P values were calculated using the Chi^2 test (NS: P>0.050, *: P<0.050, **: P<0.010,***: P<0.001).*

Finally, I used another actin depolymerising drug, LatA, which binds actin monomers, but not actin filaments as CytoD does (Morton et al., 2000, Yarmola et al., 2000, Coue et al., 1987). I predicted that LatA would have similar effects on MT stability as CytoD. To test this prediction, I treated wildtype and *shot*^{3} mutant neurons with either DMSO (the drug vehicle), CytoD (0.4ug/ml) for 4hrs or LatA (200nM) for 1hr. Notably, the treatment with LatA and CytoD both caused severe loss of F-actin from GCs in wildtype and *shot*^{3} mutant neurons (Fig. 3.10). These findings are consistent with previous studies (Sanchez-Soriano et al., 2010), and they are plausible since F-actin networks in GCs are highly dynamic and highly dependent on polymerisation (Prokop et al., 2013). In spite of these comparably drastic effects of both drugs on F-actin in GCs, I observed a differential effect on MTs. Thus, *shot*^{3} mutant neurons treated with CytoD displayed loss of disorganised MTs and axons (all normalised to wildtype; MT disorganization: 0%, $P_{Chi2}<0.001$, n=74, Fig. 3.10). Surprisingly, when applying LatA, the axons of *shot*^{3} mutant neurons still contained disorganised MTs (MT disorganization: 163%, $P_{Chi2}<0.001$, n=96; Fig. 3.10), and it did not cause gaps in axonal MT bundles of wildtype neurons and *shot*^{3} mutant neurons (12% neuron with gaps in wildtype with LatA, n=100, $P_{Chi2}=0.228$; 13% neuron with gaps in *shot*^{3} with LatA, n=96, $P_{Chi2}=0.193$). These results suggested that either my hypothesis about actin roles in MT maintenance was to be reconsidered, or that LatA might affect axonal actin in different ways. Recent super-resolution microscopy has shown for the first time that axonal actin displays a very characteristic structure (Xu et al., 2013, Lukinavicius et al., 2014) which, if similarly present in *Drosophila* axons, would provide us with a powerful readout to investigate whether CytoD and LatA might have differential effects on F-actin organisation. These studies are described in the following chapter.

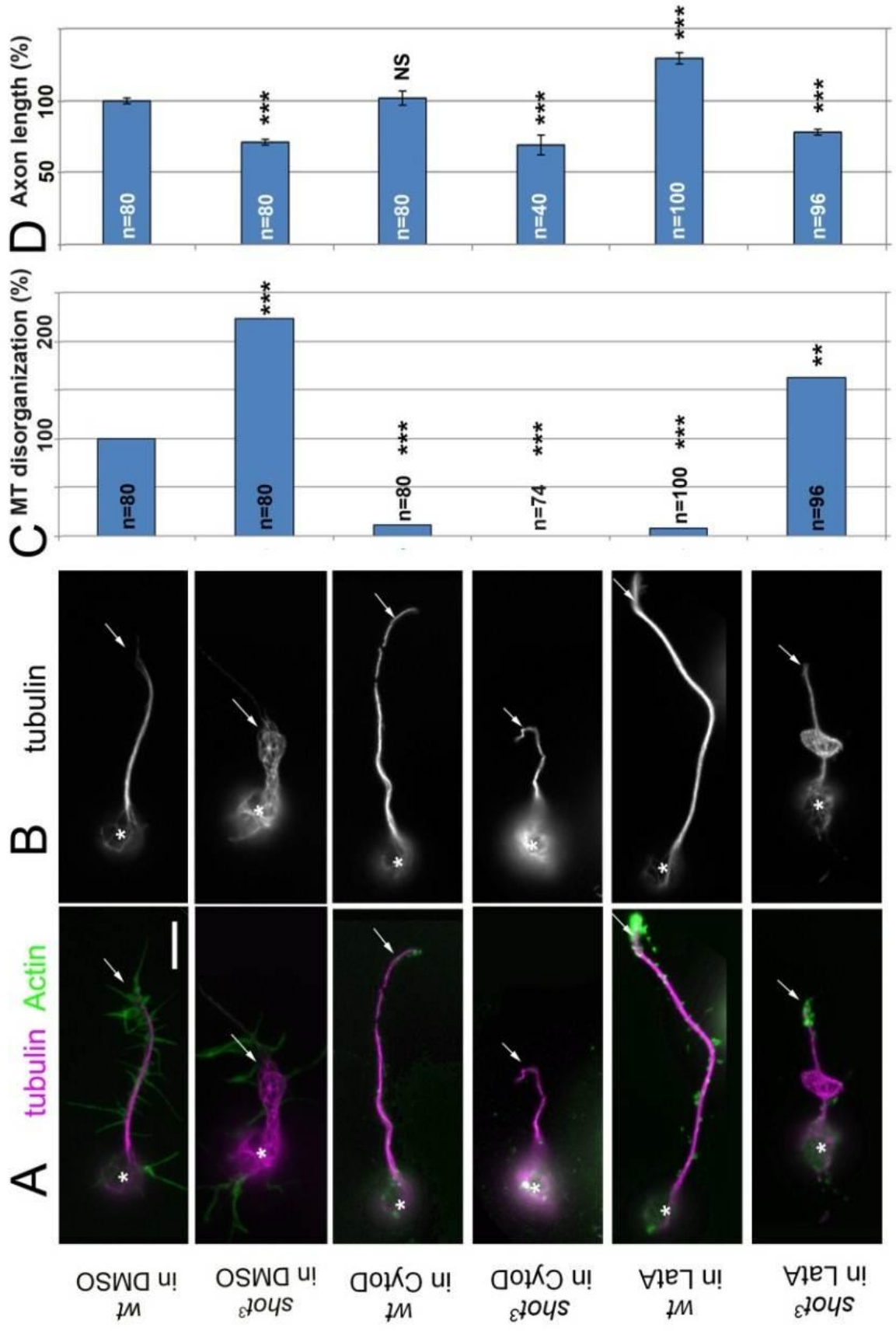
A
tubulin Actin
B
tubulin
C
MT disorganization (%)
100
200
n=80
n=80
***
n=80
***
n=74
***
n=100
***
n=96
**
D
Axon length (%)
50
100
n=80
n=80
***
n=80
NS
n=40
***
n=100
***
n=96
***
wt in DMSO
shot3 in DMSO
wt in CytoD
shot3 in CytoD
wt in LatA
shot3 in LatA

Figure 3.10. *The impact of different pharmacological treatments on MT disorganization.*

A,B) *Axonal phenotypes in wild type or shot^{3} mutants primary neurons at 8HIV, 4hrs in vehicle (DMSO) or treated with CytoD or 2hrs treated with LatA as indicated; cells are double-labelled for tubulin and actin (A; tubulin channel shown alone in B; asterisk, cell body; arrow, growth cone); scale bar represents 5µm.* ***C,D)*** *Quantifications of phenotypes for the drug treatments given on the left, respectively (all normalised and compared to wild type in vehicle); numbers in the bars indicate the numbers of neurons analysed in each experiment; for MT disorganisation (C) P values were calculated using the Chi^{2} test (NS: P>0.050, *: P<0.050, **: P<0.010,***: P<0.001); for axon length (D) P values were calculated using the Mann-Whitney Rank Sum test (NS: P>0.050, *: P<0.050, **: P<0.010,***: P<0.001).*

3.2.4. *Drosophila* axons contain patterned cortical F-actin

As mentioned at the end of Chapter 3.2.3, recent PALM-STORM analyses of mature mouse axons at ~7DIV revealed that F-actin in axons is arranged into periodic ring-like patterns which are evenly spaced into a periodic pattern by spectrin, which are composed of bundled, short, adducin-capped filaments (Fig. 3.11) (Xu et al., 2013). Recently, this periodic ring-like pattern of axonal actin has been confirmed using STED microscopy and new SiR-actin probes (Lukinavicius et al., 2014). These descriptions highlight a number of specific features which could be used as readouts in pharmaco-genetic studies to functionally dissect the regulation and roles of this cortical actin. In order to find out whether such a strategy is feasible in my cellular model, I first addressed whether *Drosophila* axons might display a similar cortical organisation as described for mouse.

To test this, we collaborated with the Pakorn Kanchanawong's group in Singapore. I prepared wildtype neurons at 6DIV, applying the same glutaraldehyde-based fixation protocols as used for mouse neurons (Xu et al., 2013), and they were sent to Singapore using procedures and specific containers described in the methods part (Chapter 2.6.1). In Singapore, the samples were stained using Alexa Fluor 647 (Alexa647) conjugated phalloidin (Invitrogen A22287), and imaged using PALM-STORM. These experiments revealed repetitive actin structures also in axons of *Drosophila* neurons. Thus, the cortical actin is arranged into periodic patterns with uniform spacing of ~180 nm (Fig. 3.11), and these data are consistent with the previous findings in mouse axons (Xu et al., 2013, Lukinavicius et al., 2014). However, axons did not show this pattern continuously along their entire length, but rather in short scattered stretches only (not shown).

Since then, I carried out my own studies at the Science & Technology Facilities Council's (STFC) Central Laser Facility (CLF) at Didcot (UK), using the procedure which is similar to the one used for the work in Singapore, but the outcome was again not good enough for systematic genetic investigation. However, during the write-up of this thesis, my colleague Ines Hahn continued this work in Didcot, now using the SiR-actin probes (Lukinavicius et al., 2014) which have very recently become commercially available (see method Chapter 2.6.2.). These probes are not compatible with STORM microscopy, therefore SIM was used instead. This approach gave impressively reliable results, showing periodic cortical actin patterns all along axons of *Drosophila* neurons (Fig. 3.11), providing a readout that can be used for systematic pharmaco-genetic investigation. We conclude that essential features of cortical actin are conserved in *Drosophila* neurons, providing new means to study the regulation and function of axonal actin, complementing our functional readouts such as MT organisation or axon length.

When Ines Hahn treated wildtype neurons (10DIV) with LatA (@200nM for 6hrs), she found that the cortical actin pattern appeared mainly unaffected whereas it was completely abolished upon treatment with CytoD (@0.4µg/ml for 6hrs) (Fig. 3.11). This result clearly indicates that different actin depolymerisation drugs have differential effects on cortical actin, and these differences make sense when considering the nature of the two drugs and the proposed organisation of axonal actin rings (see Discussion 4.2.5). Importantly, these results correlate with my findings that LatA does not affect MT maintenance in the axon of *shot* mutant neurons, since this treatment leaves axonal actin unaffected.

A

Cortical cytoskeleton model in axons

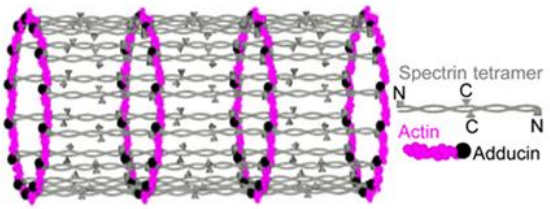

Xu et al., 2013, Science 339, 452ff

B

Mouse hippocampal neuron
7 DIV; Two-color STORM

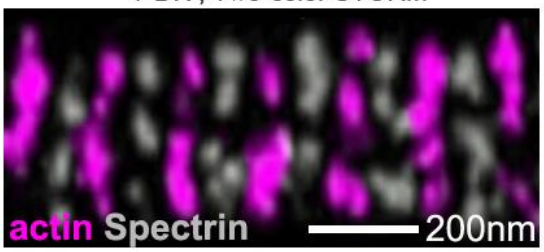

Xu et al., 2013, Science 339, 452ff

C

Drosophila wt
6 DIV; PALM/STORM

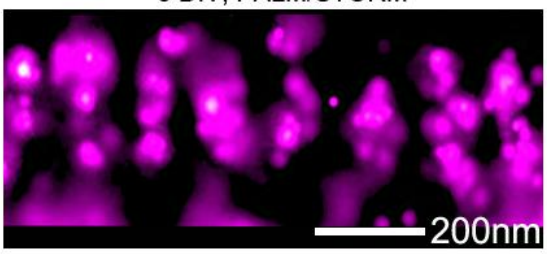

collab. Dr. Kanchanawong (Singapore)

D

Drosophila wt @DMSO for 6hr
10 DIV; SIM

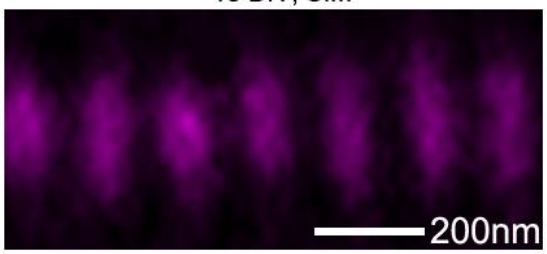

Images were taken at STFC's CLF

E

Drosophila wt @0.4ug/ml CytoD for 6hr
10 DIV; SIM

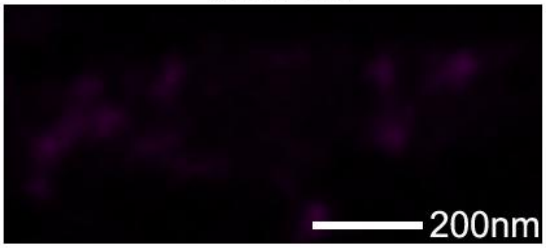

Images were taken at STFC's CLF

F

Drosophila wt @200nM LatA for 6hr
10 DIV; SIM

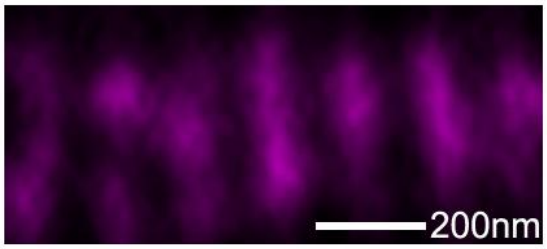

Images were taken at STFC's CLF

Figure 3.11. *Advanced microscopy reveals a periodic ring-like pattern of axonal actin in Drosophila neurons.*

A) *A cortical cytoskeleton model in axons has been proposed (Xu et al., 2013). Short actin filaments (magenta) form periodic ring-like patterns in axon. Spectrin tetramers (gray) connect between two actin ring structures ("C" indicates the C terminus of Spectrin, "N", the N terminus); adducin (black) caps actin filament plus ends.* ***B)*** *Two-colour STORM image of the axonal actin structure of a mouse hippocampal neuron at 7 DIV (Xu et al., 2013).* ***C)*** *PALM/STORM image of axonal actin structures of a Drosophila wildtype primary neuron at 6 DIV (collaboration with Dr. Kanchanawong, Singapore).* ***D-F)*** *SIM images of axonal actin in Drosophila wildtype primary neurons at 10 DIV, treated 6hrs with vehicle (DMSO), CytoD or LatA as indicated; images were taken at STFC's CLF. Scale bar represents 200nm in B-F; actin in magenta and spectrin in gray.*

3.2.5. Manipulations of actin regulating proteins support roles of cortical actin in MT maintenance

The cortical axonal actin model, predicts that actin filaments are short and, hence, numerous (Fig. 3.11) (Xu et al., 2013). I therefore reasoned that these actin structures should be less dependent on actin filament elongators, such as profilin, but be highly dependent on actin filament-seeding nucleators, such as Arp2/3. From my experiments with *shot* mutant neurons where non-coalescent ("off-track") MTs become severely depleted when adding CytoD but not LatA, I hypothesised that genetic or pharmacological conditions affecting actin elongators or nucleators should likewise show differential MT depletion phenotypes when combined with *shot* LOF during axon development. I predicted that loss of the actin nucleators could have a similar impact on MT stability as CytoD, whereas loss of actin filament elongators might show mild or no effects like LatA.

3.2.5.1. Manipulations of Arp2/3 cause loss of MTs

First, I tested requirements of the nucleator Arp2/3, using two independent approaches: LOF of its neuronal activator SCAR, known to be crucial in the *Drosophila* nervous system (Schenck et al., 2004), and application of the specific Arp2/3 inhibitor CK666 (Hetrick et al., 2013). Since, both tools had not been used in primary fly neurons before, I first analysed their phenotypes alone. I found that both caused a significantly reduction in filopodia number (all normalised to wildtype; $SCAR^{\Delta 37}$: 51±3%, $P_{Mann-Whitney}$<0.001, n=120; CK666 @100nM for 2hrs: 72±5%, $P_{Mann-Whitney}$<0.001, n=80; Fig. 3.12) but did not obviously affect filopodial length (not measured). These findings are consistent with previous studies using deficiency of the Arp2/3 component Sop2/Arpc1 (Gonçalves-Pimentel et al., 2011), and my own data with the $Sop2^{1}$ mutant neurons clearly confirmed those findings (Appendix 6.1). To further demonstrate specificity of CK666, I performed a number of studies which combine CK666 with genetic manipulation of different actin nucleators. Those studies strongly suggested specificity of CK666 (Appendix 6.1). I also discovered additional, unknown roles of the SCAR complex in the regulation of MT organisation, which will not be further considered here (Appendix 6.2).

Having convinced myself that lack of SCAR and applying CK666 inhibit Arp2/3 function, I used them in *shot* mutant neurons to find out whether they would affect MT stability, as observed upon CytoD treatment. As mentioned before, in $shot^{3}$ mutant neurons, axonal MTs tend to be misguided and become significantly disorganised (all normalised to wildtype; MT disorganisation: 223%, P_{Chi2}<0.001, n=60; Fig. 3.12) and axons are shorter (71±2%, $P_{Mann-Whitney}$<0.001; Fig. 3.12) (Sanchez-Soriano et al., 2009,

Alves-Silva et al., 2012). Also, the number of filopodia is decreased to 65±3% ($P_{Mann-Whitney}$<0.001, n=120; Fig. 3.12), which is also consistent with previous founding (Sanchez-Soriano et al., 2009).

When combining *shot*^{3} with the *SCAR*$^{\Delta 37}$mutant allele, filopodia numbers are similar to *shot*^{3} or *SCAR*$^{\Delta 37}$ alone (62±3%, $P_{Mann-Whitney}$<0.001, n=160; Fig. 3.12), suggesting that Shot and Arp2/3 act in the same pathway of filopodia regulation. However, although the axons are still short (71±2%, $P_{Mann-Whitney}$<0.001; Fig. 3.12), the disorganised MTs vanish and axons appear much thinner and are consistently bundled (MT disorganisation: 135%, P_{Chi2}=0.071, Fig. 3.12).

When *shot*^{3} mutant neurons were treated with CK666, the filopodia number is significantly lower than seen in *shot*^{3} mutant or CK666-treated neurons, respectively (47±3%, $P_{Mann-Whitney}$<0.001, n=100; Fig. 3.12), suggesting that the statement of Shot and Arp2/3 acting in the same filopodia-regulating pathway may be only partially true. However, since filopodia regulation was not within the remit of my work, I refrained from investigating this further. Instead, I focussed on the MT phenotypes. As observed for *shot*^{3} *SCAR*$^{\Delta 37}$ double mutant neurons, the disorganised MTs vanished in CK666-treated *shot*^{3} mutant neurons, and their axons became more bundled (MT disorganisation:116%, P_{Chi2}=0.546), whilst axons remained short as typical of *shot* LOF (70±3%, $P_{Mann-Whitney}$<0.001; Fig. 3.12).

From these data, I conclude that, in *shot* mutant neurons where MTs are less stable (Alves-Silva et al., 2012), additional loss of Arp2/3 function (SCAR, CK666) causes non-colescent MTs to vanish. Therefore, these data indicated that during development, nucleator function is crucial for MT maintenance in axons, likely because it affects cortical F-actin required to maintain MTs.

Since neurons lacking both Shot and Arp2/3 function maintain a fraction of seemingly bundled MTs, and since their axon length is unchanged, us tempts to speculate that only straight MTs in *shot* mutant neurons actively contribute to axonal growth, but not the disorganised "off-track" MTs (Discussion 4.2.3).

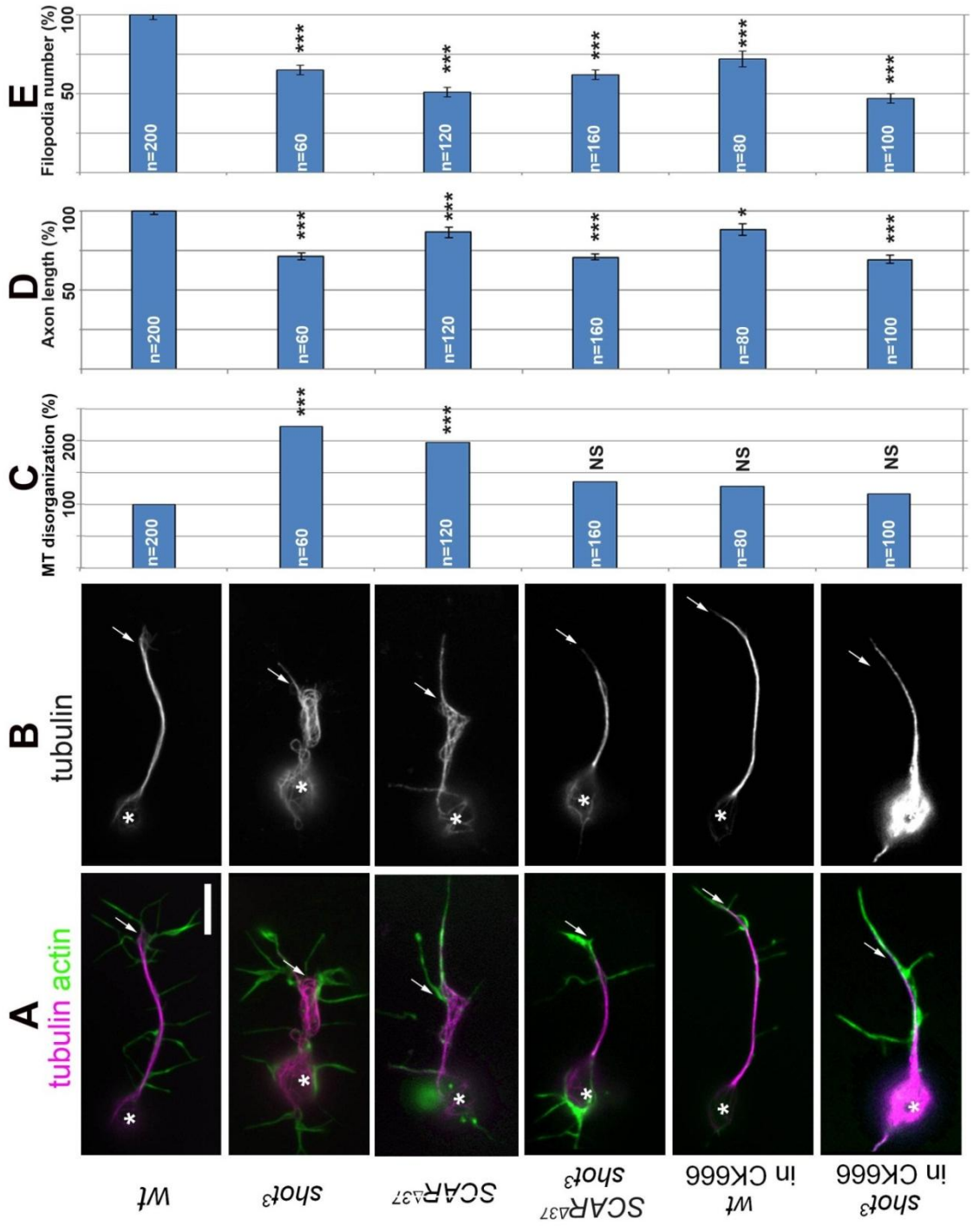
A
tubulin actin
B
tubulin
C
MT disorganization (%)
D
Axon length (%)
E
Filopodia number (%)
n=200
n=60
n=120
n=160
n=80
n=100
***
*
NS
wt
shot3
SCAREA37
SCAREA37 shot3
wt in CK666
shot3 in CK666

Figure 3.12. *Manipulations of Arp2/3 support roles of cortical actin in maintaining disorganised axonal MTs.*

A,B) *Axonal phenotypes in wild type, shot^{3}, SCAR$^{\Delta 37}$ mutant, SCAR$^{\Delta 37}$ shot^{3} double-mutants primary neurons at 6HIV, and wild type or shot^{3} mutant primary neurons, treated with CK666 for 2hrs, total cultured 6HIV; cells are double-labelled for tubulin and actin (A; tubulin channel shown alone in B; asterisk, cell body; arrow, growth cone); scale bar represents 5µm.* ***C-E)*** *Quantifications of phenotypes caused by the mutants and drug treatments given on the left, respectively (all normalised and compared to wild type or in vehicle); numbers in the bars indicate the numbers of neurons analysed in each experiment; for MT disorganisation (C), P values were calculated using the Chi^{2} test (NS: P>0.050, *: P<0.050, **: P<0.010,***: P<0.001); for axon length (D) or filopodia number (E) P values were calculated using the Mann-Whitney Rank Sum test (NS: P>0.050, *: P<0.050, **: P<0.010,***: P<0.001). Note that the SCAR mutant neurons display an MT disorganisation phenotype which is not suppressed by its own impact on actin, and which seems a function of the SCAR complex rather than SCAR alone (see Appendix 6.2).*

3.2.5.2. Loss of profilin function does not affect MT maintenance

Next, I tested neurons deficient for the actin elongator Chickadee/Chic, the fly homologue of profilin (Verheyen and Cooley, 1994). All my data were consistent with previous reports (Sanchez-Soriano et al., 2010, Gonçalves-Pimentel et al., 2011). Thus, in *chic*^{221} mutant neurons, filopodia are severely shortened (72±2%, $P_{Mann\text{-}Whitney}$<0.001, n=462; Fig. 3.13), GCs are predominantly narrow, axons are longer (126±5%, $P_{Mann\text{-}Whitney}$<0.001, n=120; Fig. 3.13) and axonal MTs are less disorganised than wildtype (60%, P_{Chi2}=0.032, n=120; Fig. 3.13).

I then tested double-mutant neurons simultaneously lacking Chic and Shot. My hypothesis predicted that loss of Chic, although having a severe effect on GCs, should not suppress the *shot* mutant MT disorganisation phenotype. In *chic*^{221} *shot*^{3} double mutant neurons, three parallel phenotypes can be observed: First, axons are short (70±3%, $P_{Mann\text{-}Whitney}$<0.001, n=80; Fig. 3.13) and this is reminiscent of *shot*^{3} mutant neurons. Second, they display short filopodia (69±2%; $P_{Mann\text{-}Whitney}$<0.001, n=398; Fig. 3.13) as observed in *chic* mutant neurons alone, and filopodia numbers are reduced to 75±4% ($P_{Mann\text{-}Whitney}$<0.001, n=80; Fig. 3.13) which is a typical *shot* mutant phenotype (Sanchez-Soriano et al., 2009). Finally, neurons display 233% MT disorganisation (P_{Chi2}<0.001, n=80) similar to the 223% observed in *shot*^{3} alone (Fig. 3.13), so the *shot* mutant phenotype prevails. GCs tend to be broad and contain disorganised MTs as is typical of *shot* mutant neurons (Sanchez-Soriano et al., 2009).

These results are consistent with my hypothesis that Chic is less relevant for cortical F-actin and therefore not a potent suppressor of F-actin dependent MT maintenance. They support the idea that F-actin in axons is short and stable (and very recent SIM analyses by Ines Hahn confirm that periodic actin structures are maintained in *chic* mutant axons; unpublished data). However, there are certain differences between profilin-deficient and LatA-treated axons. Thus, as explained in Chapter 3.2.3., in *shot* mutant neurons treated with LatA, disorganised MTs persist in axons but not in GCs (MT disorganisation: in GCs, 52%, P_{Chi2}=0.029; in axon, 547%, P_{Chi2}<0.001; n=74; all normalised and compared to wildtype). In contrast, disorganized MTs remained in both GCs and axons in *chic*^{221} *shot*^{3} (MT disorganisation: in GCs, 193%, P_{Chi2}<0.001; in axon, 523%, P_{Chi2}<0.001; n=80, all normalised and compared to wildtype). This might mean that MT disorganisation phenotypes are qualitatively different in axons and GCs, and that disorganised MTs in GCs are more dependent on their prominent actin networks. These networks are virtually abolished upon LatA treatment, but only partially affected by Chic deficiency (Discussion 4.2.3).

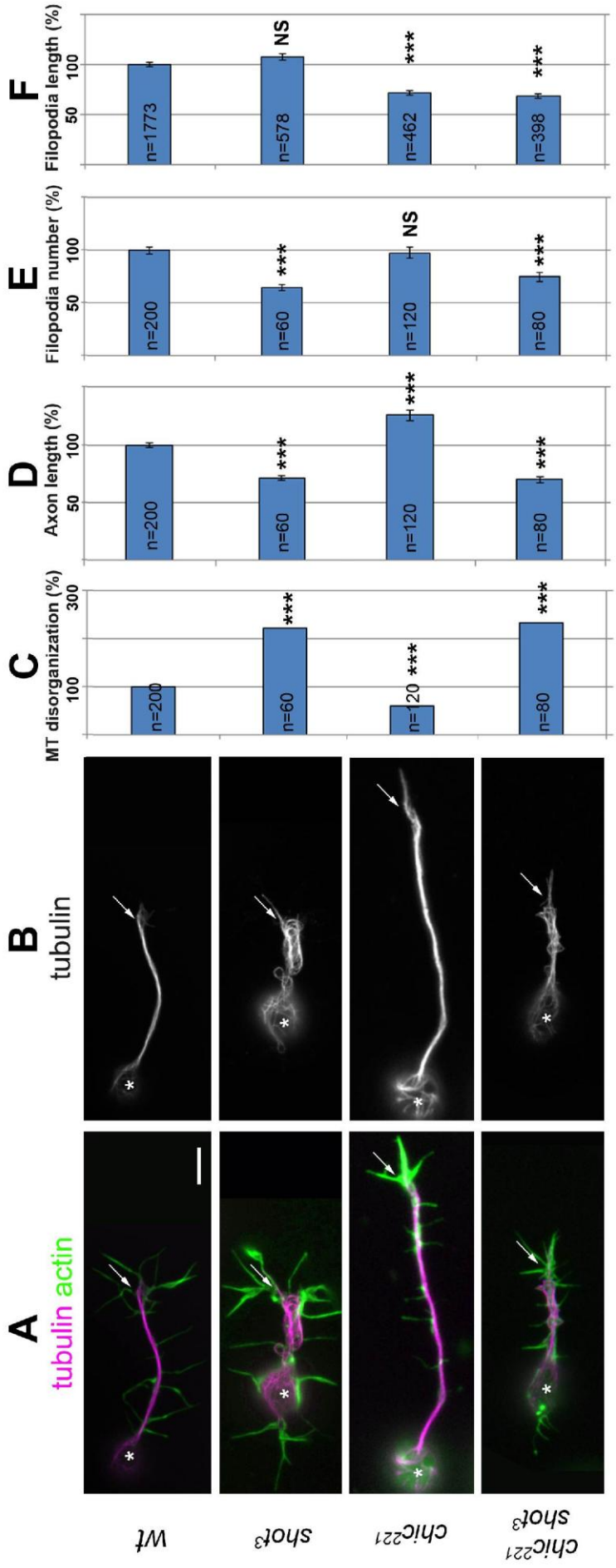
A
tubulin actin
B
tubulin
C
MT disorganization (%)
D
Axon length (%)
E
Filopodia number (%)
F
Filopodia length (%)
n=200
n=60
n=120
n=80
n=1773
n=578
n=462
n=398
***
NS
wt
shot3
chic221
chic221 shot3

Figure 3.13. *Loss of profilin function does not suppress MT disorganization.*

A,B) *Axonal phenotypes in wild type, shot^{3}, chic^{221} or chic^{221} shot^{3} mutant primary neurons at 6HIV; cells are double-labelled for actin and tubulin (A; tubulin channel shown alone in B; asterisk, cell body; arrow, growth cone); scale bar represents 5µm.* ***C-F)*** *Quantifications of phenotypes caused by the mutant given on the left, respectively (all normalised and compared to wild type); numbers in the bars indicate the numbers of neurons (C-E) or filopodia (F) analysed in each experiment; for MT disorganisation (C), P values were calculated using the Chi^{2} test (NS: P>0.050, *: P<0.050, **: P<0.010,***: P<0.001); for axon length (D), filopodia number (E) or filopodia length (F) P values were calculated using the Mann-Whitney Rank Sum test (NS: P>0.050, *: P<0.050, **: P<0.010,***: P<0.001).*

3.2.6. Unravelling potential mechanisms for MT-stabilising roles of cortical F-actin

3.2.6.1. Candidate approach: investigating potential roles of Myosin VI and Spectrins

The potential mechanisms which might mediate between cortical F-actin and MT maintenance are completely unknown, but I tested a few players which could potentially be involved: for example, MyosinVI (Jaguar/Jag in *Drosophila*) is an F-actin binding motor protein which has established links to the MT regulator CLIP-190 (Lantz and Miller, 1998). Jag takes on a characteristic patchy localisation in the centre of GCs, and Jag deficiency has recently been found to affect MT organisation in primary neurons (Beaven, 2012). As a first indicator of potential differential behaviour of Jag downstream of distinct F-actin network manipulations, I monitored Jag localisation in $chic^{221}$ and $SCAR^{\Delta 37}$ mutant neurons by staining with Jag antibody, but found that its localisation was completely unchanged in the mutant neurons (Fig. 3.14). I therefore did not carry Jag into further functional studies.

Another good candidate mediator between F-actin and MTs is Spectrin, which is known to bind to cortical F-actin and mediate the regular periodicity of the ring pattern (Xu et al., 2013). F-actin and Spectrin are therefore expected to show mutual dependency, and the various functional domains of Spectrins (Broderick and Winder, 2005) would provide ideal means to interact with other proteins to mediate MT stabilisation. I carried out some initial immuno-staining with anti-α-Spectrin antibody (Garbe et al., 2007) which suggested slightly stronger staining in axons of $chic^{221}$ compared to $SCAR^{\Delta 37}$ mutant neurons (Fig. 3.14). However, these data were hard to quantify. Ideally, they would have to be carried out via supra-resolution microscopy, but this was not possible within the time frame of this project. The obvious next step would be to generate *shot ß-spectrin* double mutant, however, time of my PhD is not long enough to permit this most important experiment.

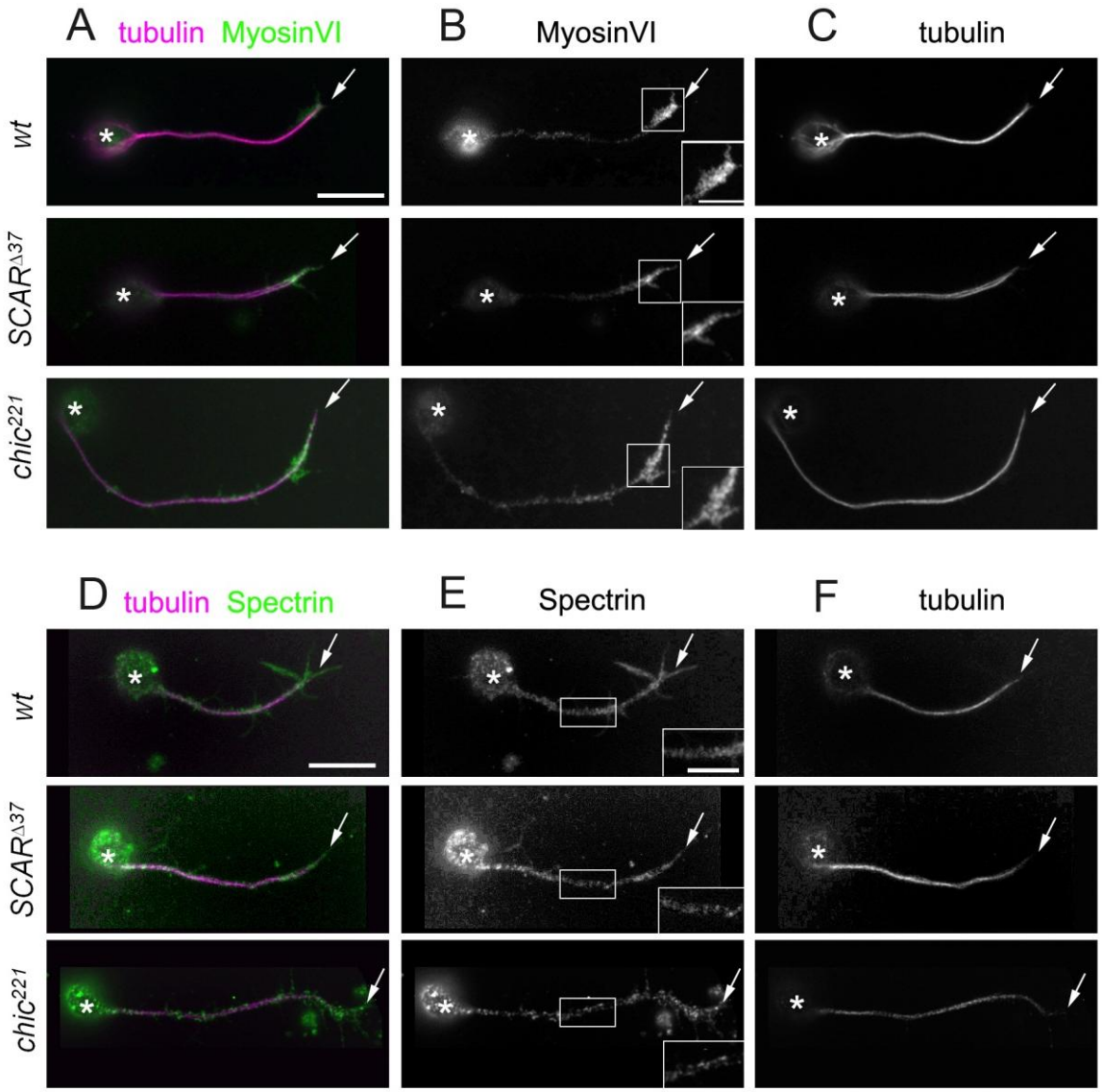
A tubulin MyosinVI
B MyosinVI
C tubulin
wt
SCAR^Δ37
chic^221
D tubulin Spectrin
E Spectrin
F tubulin
wt
SCAR^Δ37
chic^221

Figure 3.14. *Genetic actin manipulations do not affect Myosin VI and α-spectrin localisation.*

A-C) *Localisation of Myosin VI in wildtype, SCAR$^{\Delta 37}$, chic^{221} primary neurons at 6HIV; cell were double-labelled for Myosin VI and tubulin as indicated (A; Myosin VI channel shown alone in B, boxed areas in B show 1.5 times magnifications of the Myosin VI staining in GCs; tubulin channel shown alone in C);* ***D-F)*** *localisation of α-spectrin in wildtype, SCAR$^{\Delta 37}$ and chic^{221} primary neurons at 6HIV; cells were double-labelled for α-spectrin and tubulin as indicated (D; α-spectrin channel shown alone in E, boxed areas in B show 1.5 times magnifications of the α-spectrin staining in axons; tubulin channel shown alone in F); asterisks, cell bodies; arrows, growth cones; scale bar represents 10μm in A-F, and 5μm in the boxed areas of C and E.*

3.2.6.2. Live imaging reveals MT polymerisation as a target mechanism in actin-dependent MT maintenance

The most insightful data came from live cell analyses performed on EB1::GFP expressing wildtype or *shot* mutant neurons, which clearly suggest that MT polymerisation is an essential target mechanism in actin-dependent MT maintenance.

Using live imaging, I observed the different behaviours of EB1 comets in wildtype and *shot*^{3} mutant neurons after treating with CytoD (@0.8µg/ml; only did once; Fig. 3.15). EB1 comets in each neuron are tracked one round before applying CytoD and then every 30mins after treating with CytoD. In wildtype neurons, upon application of CytoD, the amount of EB1 comets is unchanged (normalised and compared to wildtype without CytoD treatment; 0.5hrs, 107±6%, $P_{Mann\text{-}Whitney}$=0.486; 1hr, 92±6%, $P_{Mann\text{-}Whitney}$=0.476; 1.5hrs, 96±7%, $P_{Mann\text{-}Whitney}$=0.516; n=6, n=cell number; Fig. 3.15). However, the velocity of EB1 comets decreased gradually (normalised and compared to wildtype without CytoD treatment; 0.5hrs, 97±5%, $P_{Mann\text{-}Whitney}$=0.364, n=6/70; 1hr, 91±8%, $P_{Mann\text{-}Whitney}$=0.052, n=6/53; 1.5hrs, 76±6%, $P_{Mann\text{-}Whitney}$<0.001, n=6/57; n=cell number/EB1 comets; Fig. 3.15).

In contrast, in *shot* mutant neurons, comet dynamics changed drastically after drug application (Fig. 3.15). Within 30mins, only 64±5% EB1 comets were still visible (number of EB1 comets normalised and compared to untreated wildtype: 0.5hrs, $P_{Mann\text{-}Whitney}$=0.002, n=9, Fig. 3.15). At this time, the EB1 comets which are still visible have slowed down in their movement and have stopped to progress, showing instead pulse-like forward-backward movements (EB1 comet velocity normalised and compared to untreated wildtype: 58±5%, $P_{Mann\text{-}Whitney}$<0.001, n=9/60, Fig. 3.15). Over time, these comets become even smaller and most of them vanish (the number of EB1 comets: 1hr, 26±6%, $P_{Mann\text{-}Whitney}$<0.001; 1.5hrs, 20±6%, $P_{Mann\text{-}Whitney}$<0.001, n=9, Fig. 3.15). This loss of EB1::GFP is not observed in CytoD-treated wildtype neurons (Fig. 3.15), hence, is not a fluorescence bleaching effect but rather represents true loss of EB1 from MT plus ends. In parallel, the speed of remaining EB1 comets continuously decrease overtime (the velocity of EB1 comets: 1hr, 46±5%, $P_{Mann\text{-}Whitney}$<0.001, n=9/27; 1.5hrs, 29±7%, $P_{Mann\text{-}Whitney}$<0.001, n=9/19, Fig. 3.15), which was much more severe than in wildtype. Since EB1 is known to localise primarily to MT plus ends which actively polymerise (Mimori-Kiyosue et al., 2000, Honnappa et al., 2009, Alves-Silva et al., 2012), loss of the speed and localisation in CytoD-treated *shot* mutant neurons is therefore more likely the consequence of halted polymerisation, as is consistent with the pulse-like movements observed immediately after CytoD application.

Therefore, although the actual mechanisms of actin-mediated MT stabilisation remains unknown, I was able to pinpoint MT polymerisation as one essential target

process, thus narrowing down the search. Genetic screens might have to be used to identify key molecular players, and visualisation of EB1 could be an important readout to this end (see Discussion 4.2.3). However, carrying out such a screen was not possible within the time frame of my project.

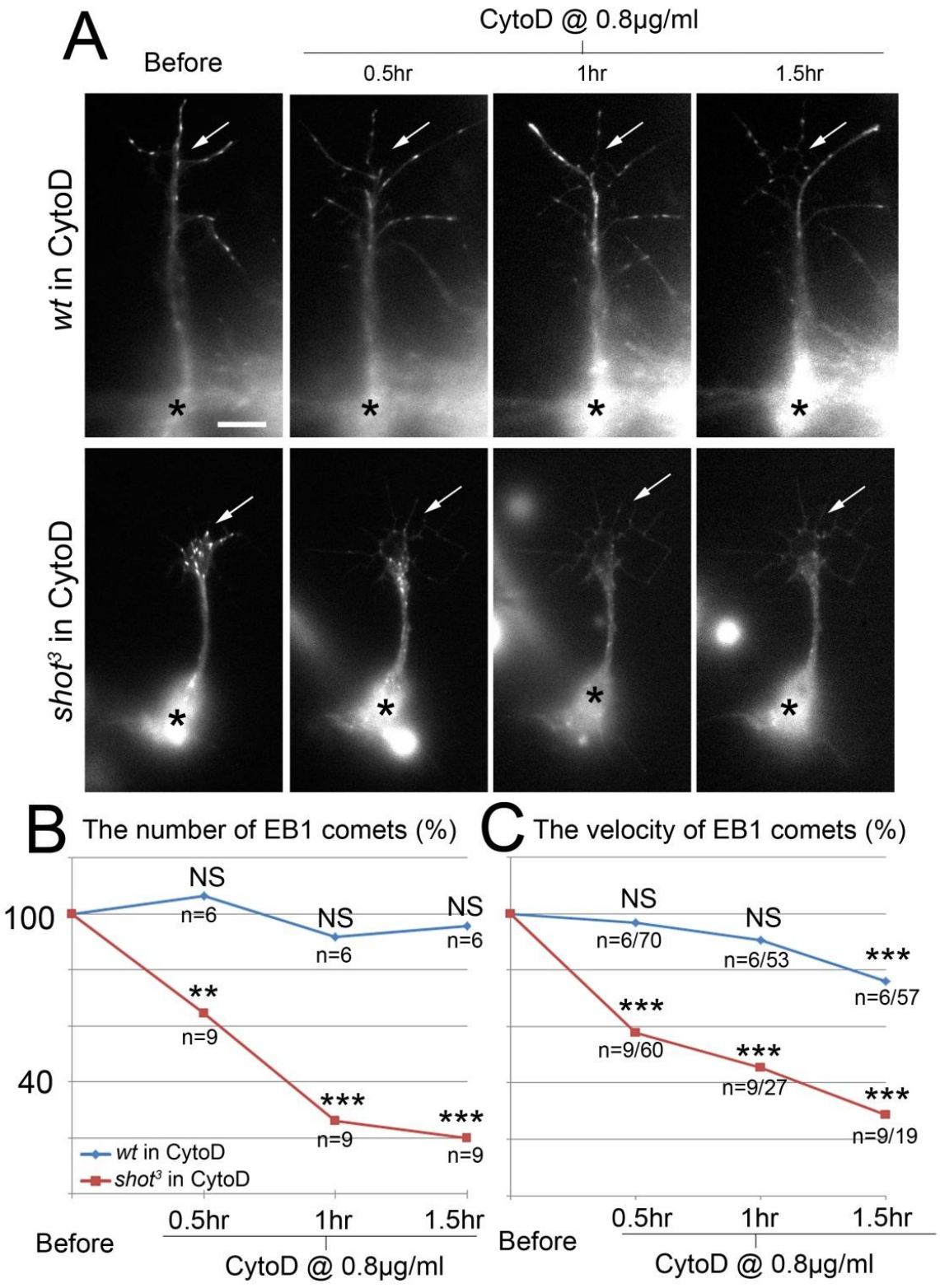
A
Before
CytoD @ 0.8μg/ml
0.5hr
1hr
1.5hr
wt in CytoD
shot3 in CytoD
B
The number of EB1 comets (%)
100
40
NS
n=6
NS
n=6
NS
n=6
**
n=9
***
n=9
***
n=9
wt in CytoD
shot3 in CytoD
Before
0.5hr
1hr
1.5hr
CytoD @ 0.8μg/ml
C
The velocity of EB1 comets (%)
NS
n=6/70
NS
n=6/53
***
n=6/57
***
n=9/60
***
n=9/27
***
n=9/19
Before
0.5hr
1hr
1.5hr
CytoD @ 0.8μg/ml

Figure 3.15. *Studying MT polymerisation upon actin manipulations.*

A) *Still images taken from live movies of wildtype and shot^{3} mutant neurons at 6HIV in culture, both expressing EB1::GFP and treated with CytoD @0.8µg/ml as indicated at the top. Different time points have been recorded. White dots indicate EB1 comets (asterisks, cell bodies; arrows, GCs); scale bar represents 5µm.* ***B, C)*** *Quantifications of the number (B) and velocity (C) of EB1 comets. Normalised and compared to wiltdtype or shot^{3} before treating with CytoD; numbers under the bars indicate the numbers of neurons or neurons/EB1 comets analysed in each experiment; P values were calculated using the Mann-Whitney Rank Sum test (NS: P>0.050, *: P<0.050, **: P<0.010,***: P<0.001).*

3.2.7. Different actin manipulations have differential effects on axon growth

3.2.7.1. Systematic analyses of genetic and pharmacological actin manipulation

My analyses with *chic* mutant neurons had revealed a significant elongation of axons (Chapter 3.2.5.2), and this phenomenon had been reported previously (Sanchez-Soriano et al., 2010). In addition, the live analyses with CytoD treated wildtype neurons revealed a decrease in comet velocity, suggesting a net loss in MT polymerisation within neurons as a function of F-actin loss. Since net polymerisation of MTs is likely to impact on axon growth dynamics, I wondered therefore whether different actin manipulations might affect axonal growth behaviours in predictable ways. To test this, I performed systematic analyses of axon lengths upon a whole range of actin manipulations. I divided the manipulations of actin into two classes. The class 1 conditions include those treatments which were shown or speculated to affect actin in the axon shafts and were found to abolish maintenance of disorganised MTs in *shot* mutant neurons (CytoD; Arp2/3 LOF: *Sop2*, *SCAR*, CK666; from now on referred to as class 1 conditions). In contrast, class 2 conditions include those conditions which were found to have no strong effect on the periodic actin pattern in axons and did not affect MT maintenance (LatA; *chic*; from now on referred to as class 2 conditions). It needs to be pointed out that both classes of actin manipulations have comparably strong negative effects on the more dynamic F-actin networks of GCs (Fig. 3.16).

To our surprise at first sight, the class 1 condition had a surprisingly mild effect on axon extension. Thus, when treating wildtype neurons with CytoD, axon length is similar to vehicle (DMSO) treated controls (96±4%, $P_{Mann\text{-}Whitney}$=0.980, n=100; Fig. 3.16). Similarly, also Arp2/3 LOF did not produce an axon elongation phenotype: Neurons lacking *Sop2/Arpc1* (*Sop2*^{1}) displayed axon lengths in the range of 109±6%, not statistically different from wildtype (normalised to wildtype; $P_{Mann\text{-}Whitney}$=0.657, n=80; Fig. 3.16). Neurons treated with the Arp2/3 inhibitor CK666 displayed axon lengths in the range of 105±5%, not statistically different from wildtype (normalised to wildtype; $P_{Mann\text{-}Whitney}$=0.948, n=80; Fig. 3.16). As detailed in the Appendix, *SCAR*$^{\Delta 37}$ mutant neurons displayed an axon length of 87±3% (Chapter 6.2). However, since these axons display a MT disorganisation phenotype (Appendix 6.2), results may be skewed due to defects in other mechanisms relevant for axon length regulation.

In contrast to class 1 conditions, class 2 conditions revealed a consistent elongation phenotype. When treating wildtype neurons with LatA, axons displayed 130±5% axon length ($P_{Mann\text{-}Whitney}$<0.001, n=100). Similarly, we found that axons of *chic*^{221} mutant neurons were significantly elongated to 141±5% ($P_{Mann\text{-}Whitney}$<0.001, n=100; Fig. 3.16), an effect that was even slightly larger in this set of experiments than observed in my other experiments with *chic* mutant neurons (Chapter 3.2.5.2). Furthermore, when

combining two class 2 conditions by treating *chic*^{221} mutant neurons with LatA, all filopodia and lamellipodia were removed from GCs, as expected of LatA treatment, but axons were similarly elongated as observed for neurons with only one of the conditions alone (*chic*^{221} with LatA: 140±5%, $P_{Mann\text{-}Whitney}$ <0.001, n=100; normalised and compared to wildtype neurons; Fig. 3.16).

All these findings are consistent with a model in which (axonal) cortical actin is more likely to be growth promoting whereas actin in GCs is inhibitory (Discussion 4.2.4). Considering that GCs contain prominent actin networks which undergo constant backflow (as an obstacle to MT advance) and that GCs undergo frequent pausing (Prokop et al., 2013), a growth inhibiting role of GCs would make sense. In this scenario, class 1 conditions affect both axonal promotion and GC inhibition, and resulting effects cancel each other out, whereas class 2 conditions affect only GC inhibition, but maintain growth promoting properties of (axonal) cortical F-actin (Fig. 3.16). If this interpretation is correct, I would expect that class 1 conditions should be epistatic over class 2 conditions. To test this, I treated *chic*^{221} mutant neurons (class 2) with CytoD (class 1) and found that axons were reduced to wildtype-like length, as is typical of the class 2 treatments (*chic*^{221} with CytoD: 100±4%, $P_{Mann\text{-}Whitney}$=0.706, n=100; normalised and compared to wildtype neurons; Fig. 3.16). In my model this result suggests that CytoD removed the growth promoting actin fraction in the axon shaft which allows *chic* mutant axons to grow longer since it specifically removes the growth-inhibiting actin networks of GCs.

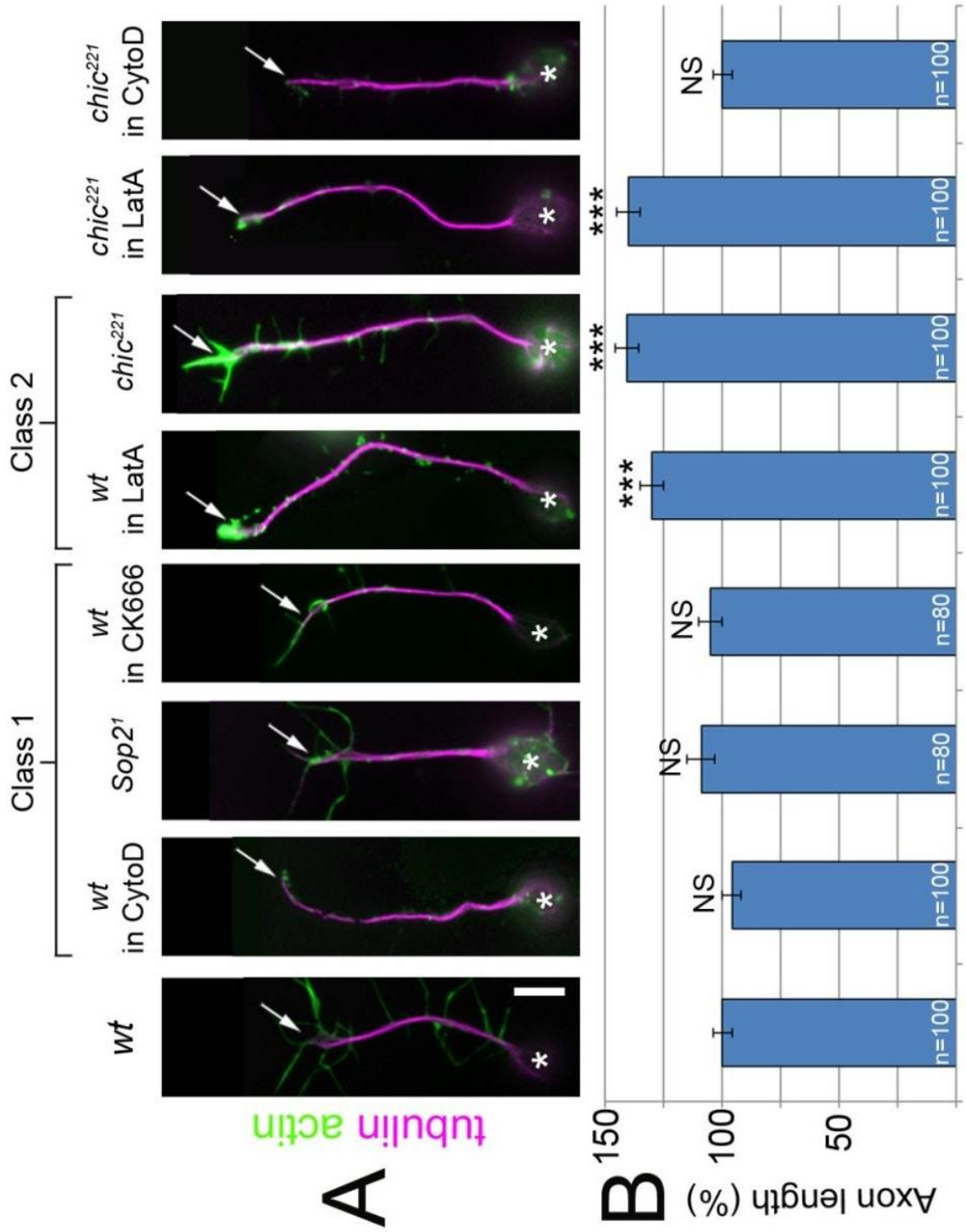
A
tubulin actin
wt
wt in CytoD
Sop2¹
wt in CK666
wt in LatA
chic²²¹
chic²²¹ in LatA
chic²²¹ in CytoD
Class 1
Class 2
B
Axon length (%)
150
100
50
NS
***
n=100
n=80

Figure 3.16. *Treatments expected to affect or not affect cortical actin have differential effects on axon growth.*

A) *Axonal phenotypes in different mutant or drug treatment primary neurons at 6 or 8HIV, cells are double-labelled for tubulin and actin (A; tubulin channel shown alone in B; asterisk, cell body; arrow, growth cone); scale bar represents 5μm.* ***B)*** *Quantifications of axon length caused by mutants or for the drug treatments given above, respectively (all normalised and compared to wild type in vehicle); numbers in the bars indicate the numbers of neurons analysed in each experiment; P values were calculated using the Mann-Whitney Rank Sum test (NS: P>0.050, *: P<0.050, **: P<0.010,***: P<0.001).*

3.2.7.2. Further experimental approaches to gain roles of (axonal) cortical actin in axon growth

Another approach to test this hypothesis, is to study other factors involved in more specific aspects of actin regulation, such as adducin who were proposed as essential regulators of axonal cortical actin (Xu et al., 2013), whereas next to nothing is known about their potential roles in GCs. If their contributions to GCs are minor, Spectrin LOF and adducin LOF could represent class 3 conditions, in which axonal promotion but not GC inhibition is affected. Unfortunately, these rather important studies took place towards the end of my project and stayed preliminary. The outcome is briefly described here.

Drosophila's adducin-encoding gene is called *hu li tai shao / hts* for which a suitable null mutant allele (*hts*^{1}) has been described (Yue and Spradling, 1992, Lin et al., 1994). I therefore studied *hts*^{1} homozygous mutant neurons and found that filopodia numbers were slightly decreased (88±5%, $P_{Mann\text{-}Whitney}$ =0.034, n=125; Fig. 3.17), suggesting mild regulatory contributions of Hts to actin filament networks in GCs. I also observed that axons are slightly shorter, although these data were of low significance (92±3%, $P_{Mann\text{-}Whitney}$ =0.019, n=125; Fig. 3.17). In principle, these data would be in agreement with our model, since *hts* LOF is expected to affect primarily growth promoting roles of (axonal) cortical actin, but to leave inhibitory roles of GC actin mostly untouched.

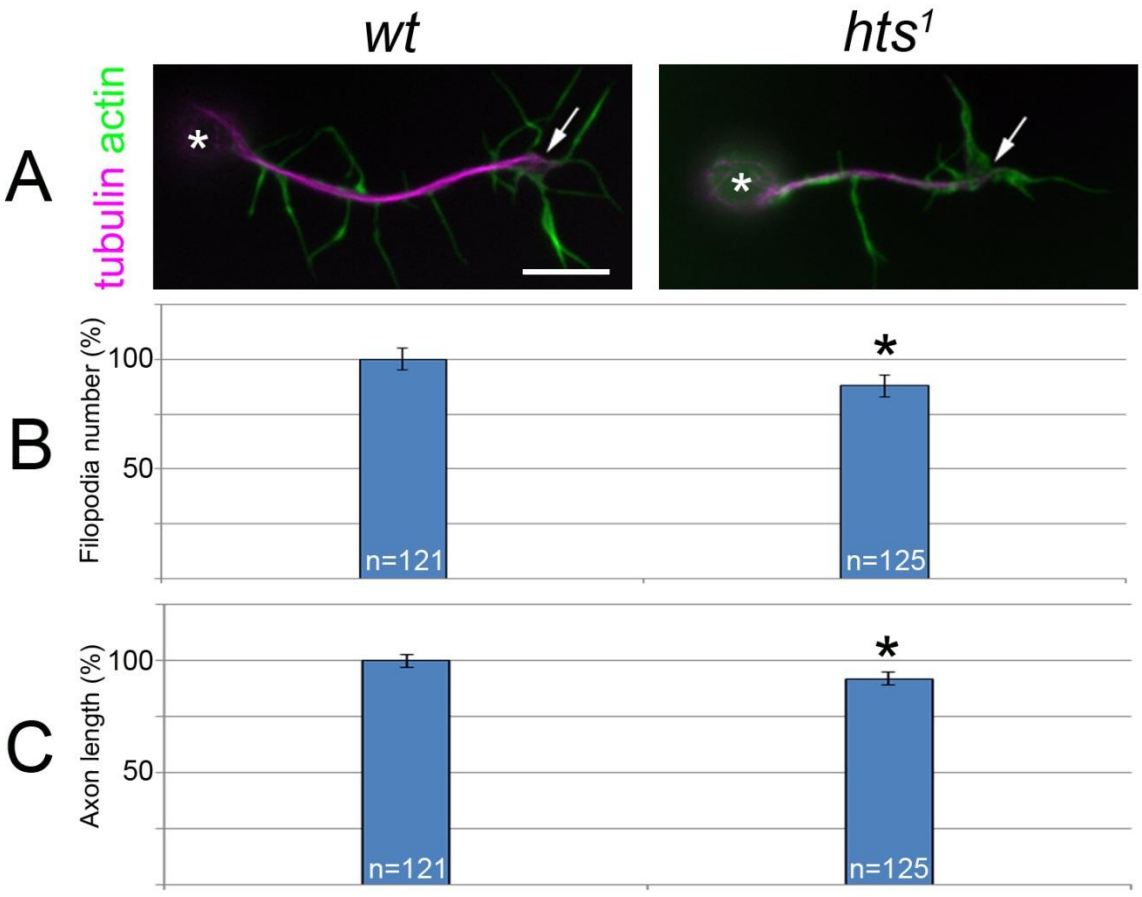
wt
hts1
A
tubulin actin
*
*
B
Filopodia number (%)
100
50
n=121
n=125
*
C
Axon length (%)
100
50
n=121
n=125
*

Figure 3.17. *Adducin has mild effects on axon growth.*

A) *Axonal phenotypes in wildtype or hts^{1} mutant primary neurons at 6HIV, cells are double-labelled for tubulin and actin (asterisk, cell body; arrow, growth cone); scale bar represents 5μm.* ***B, C)*** *Quantifications of phenotypes caused by mutants given above, respectively (all normalised and compared to wild type in vehicle); numbers in the bars indicate the numbers of neurons analysed in each experiment; for filopodia number (B) or axon length (C) P values were calculated using the Mann-Whitney Rank Sum test (NS: P>0.050, *: P<0.050, **: P<0.010,***: P<0.001).*

Another way to directly assess potential growth-promoting roles of cortical actin in axons is to measure axon lengths of primary cultured neurons at post-GC stages. Thus, it was reported previously that *Drosophila* primary neurons undergo synaptic differentiation after 1DIV in culture (Kuppers-Munther et al., 2004), and actin staining in cultures after this stage does not reveal the presence of obvious GCs anymore (Fig. 3.18). To be absolutely certain that GCs had vanished, neurons at 3DIV in culture were analysed and compared them to neurons at 7DIV. These measurements showed that the axon length is almost doubled from 3DIV to 7DIV (181±7%, $P_{Mann\text{-}Whitney}$ <0.001, n=58; normalised and compared to 3DIV; data were generated by Ines Hahn; only did once; Fig. 3.18). Having established that axons keep growing days after GCs were lost and synapses have formed, we wanted to examine if MTs are still dynamic during ageing. Since hardly any data are available, I tested this possibility myself. Analogous to experiments in Chapter 3.2.6.2, I used neurons expressing EB1::GFP under the control of the *elav-Gal4* driver and performed live imaging at 10DIV. These analyses clearly revealed that axonal MTs remain dynamic even at very mature stages. It shows a typical pattern of anterogradely and retrogradely moving comets (not measured), and moves with an even faster speed compared to cultured neurons at 19HIV (normalised and compared to 19HIV; 126±4%, $P_{Mann\text{-}Whitney}$ <0.001, n=11/121, cell number/EB1 comets; Fig. 3.18). Therefore, these data demonstrate that MT bundles remain in a dynamic state at post-GC stages which can be expected to be important for their maintenance (steady-state turnover rate), but would also to allow neurons to continue growing through gearing the machinery towards net plus polymerisation. Such machinery can explain the long known phenomenon that pulling axons either experimentally or through tissue growth during body growth at late embryonic and postnatal stages leads to significant axon elongation (Bray, 1984, Heidemann et al., 1995).

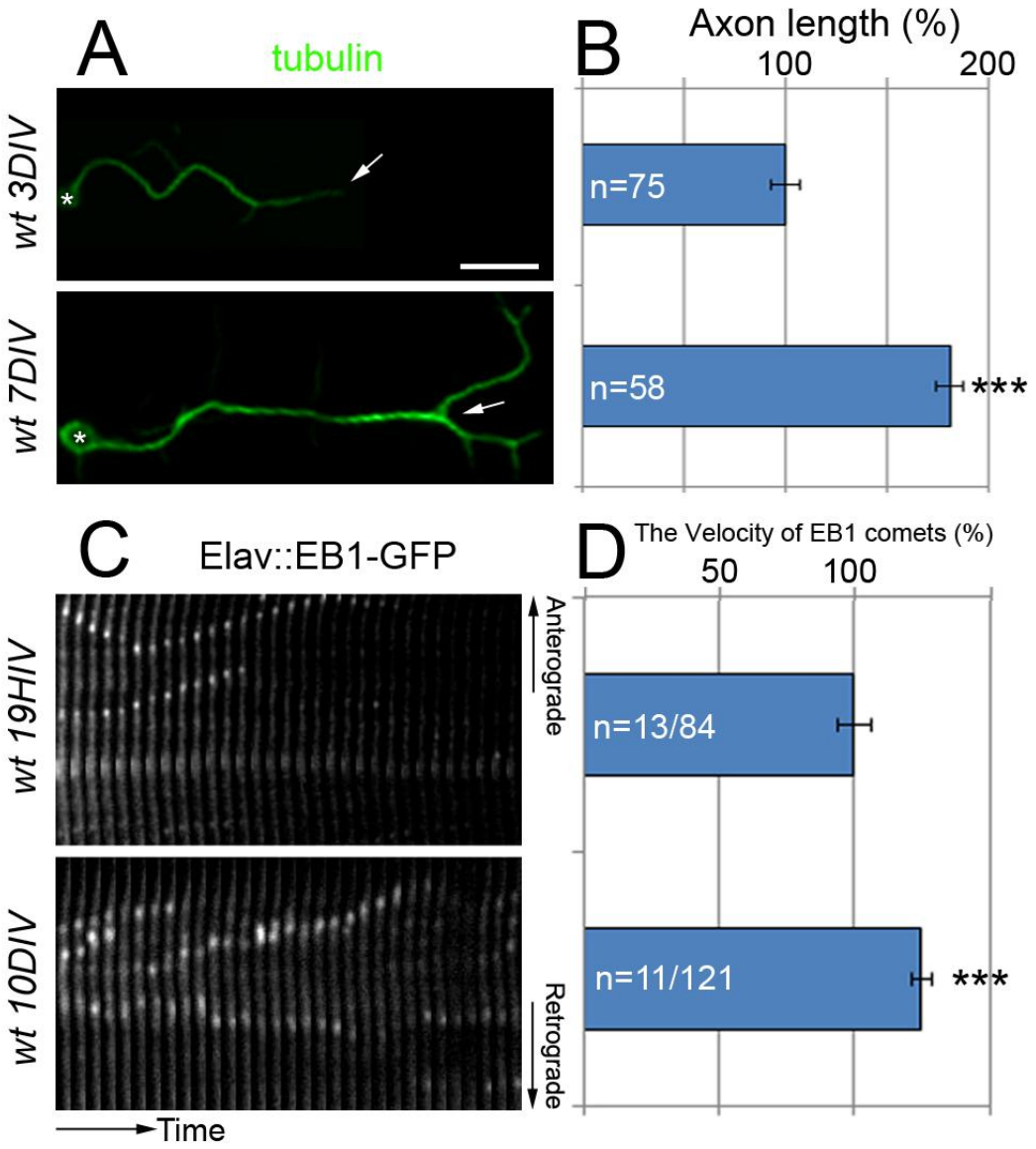
A
tubulin
wt 3DIV
wt 7DIV
B
Axon length (%)
100
200
n=75
n=58
***
C
Elav::EB1-GFP
wt 19HIV
wt 10DIV
Anterograde
Retrograde
Time
D
The Velocity of EB1 comets (%)
50
100
n=13/84
n=11/121
***

Figure 3.18. *Further studies addressing roles of cortical actin during Post-GC stages.*

A) *Axon length in wildtype primary neurons at 3DIV or 7DIV, cells are labelled for tubulin (asterisk, cell body; arrow, distal region); scale bar represents 10μm.* ***B)*** *Quantifications of axon length. All normalised and compared to wild type at 3DIV; numbers in the bars indicate the numbers of neurons analysed in each experiment; P values were calculated using the Mann-Whitney Rank Sum test (NS: P>0.050, *: P<0.050, **: P<0.010,***: P<0.001).* ***C)*** *Kymographs of the time series of the EB1 comets have been taken in wildtype at 19HIV or 10DIV. In order to track the EB1 comets, Elav-GAL4::EB1-GFP has been overexpressed in wildtype primary neuron. The length of time series is 2mins.* ***D)*** *Quantifications of the velocity of EB1 comets. All normalized and compared to wild type at 19HIV; numbers in the bars indicate the numbers of neurons/the numbers of EB1 comets analysed in each experiment; P values were calculated using the Mann-Whitney Rank Sum test (NS: P>0.050, *: P<0.050, **: P<0.010,***: P<0.001).*

3.2.8. Conclusions for Chapter 3.2

Taken together, my data suggest that Shot and F-actin display common and independent functions in MT maintenance and growth: Shot and F-actin co-operate in MT bundle formation, Shot mainly maintains MT bundles independent of F-actin likely requiring domains not contained in Shot-LA, and F-actin has Shot-independent roles in MT maintenance including stabilisation of non-coalescent MTs, and promote axon growth during axon development. The stabilisation of non-coalescent MTs occurs through maintaining their proliferative ability. These mechanisms might likewise be contributing to the axonal growth promoting roles at pre- and post-GC stages, which will be easy to assess through live imaging with EB1::GFP.

3.3. The cortical collapse factor Efa6 maintains MT organisation in axons

When MTs reach the cellular cortex, they tend to either undergo catastrophes or become stabilised (Kaverina et al., 1998). The underlying mechanisms are poorly understood. Interestingly, MTs in narrow axons grow over considerable distances although they are in constant close proximity to the cell cortex. The model developed in the Prokop laboratory proposes that spectraplakins prevent cortical collapse by guiding polymerising and extending MTs along cortical actin (Alves-Silva et al., 2012, Prokop, 2013). In the absence of Shot, the lifetime of MT polymerisation is reduced to 50% (Alves-Silva et al., 2012), and this may be due to cortical collapse. In this scenario, cortical collapse would be a powerful control mechanism to ensure that MTs escaping Shot-mediated guidance get eliminated.

To explore the existence of potential cortical collapse mechanisms in axons, I focussed my attention on Efa6. In *C. elegans*, Efa6 has been reported to limit MT growth at the cell cortex of non-neuronal cells (O'Rourke et al., 2010). Importantly, Efa6 was also shown to negatively regulate regenerative axon growth in *C. elegans* (Chen et al., 2011), indicating that Efa6 is relevant in the nervous system in the context of axon biology. I therefore investigated the role of *Drosophila* Efa6.

3.3.1. Molecular composition of *Drosophila* Efa6

As mentioned before (Chapter 1.5.2), Efa6 contains a conserved Sec7 domain which promotes ARF6 activation through guanine nucleotide exchange, a pleckstrin homology (PH) domain which can target Efa6 to the plasma membrane via binding to PI(4,5)P2 (Macia et al., 2008, Franco et al., 1999), and a coiled-coil domain. These functional domains of Efa6 are highly conserved through evolution (a comparison to *C. elegans* and mammalian homologues are shown in Appendix 6.4). The N-terminus of Efa6 was shown in *C. elegans* to be responsible for MT collapse functions (O'Rourke et al., 2010). Interestingly, the sequence of the N-terminus is very little conserved. The length of the N-terminus (complete region before the Sec7 domain) is very different between *C. elegans* (353aa), *Drosophila* (897aa) and mammalian Efa6A (542aa). However, there are some similarities between different species. Thus, the first half of the N-terminus (1-410aa) of *Drosophila* Efa6 is rich in serines (13%) and carries a positive charge (pI=9.77) (analysis by the Protein Calculator programe), and also the very beginning of the *C. elegans* and mouse Efa6 N-terminus have positive charge (analysis by PEPSTATS; Fig. 3.19). Furthermore, the *Drosophila* Efa6 N-terminus contains two SxIP motifs surrounded by arginines, which indicate potential EB1 binding (Honnappa et al., 2009). The *C. elegans* and mouse Efa6A N-terminus do not contain SxIP motifs, however, they both contain the SxLP motif which might have potential EB1 binding ability

(Fig. 3.19). Finally, it has been reported that there is an 18aa (25-42aa) long motif in the *C. elegans* Efa6 N-terminus with MT binding capacity, and this is conserved in the *Drosophila* Efa6 N-terminus (18aa, 323-340aa; Fig. 3.19) (O'Rourke et al., 2010). Given these structural similarities, Efa6 may perform a potentially conserved function in cortical collapse across the animal kingdom.

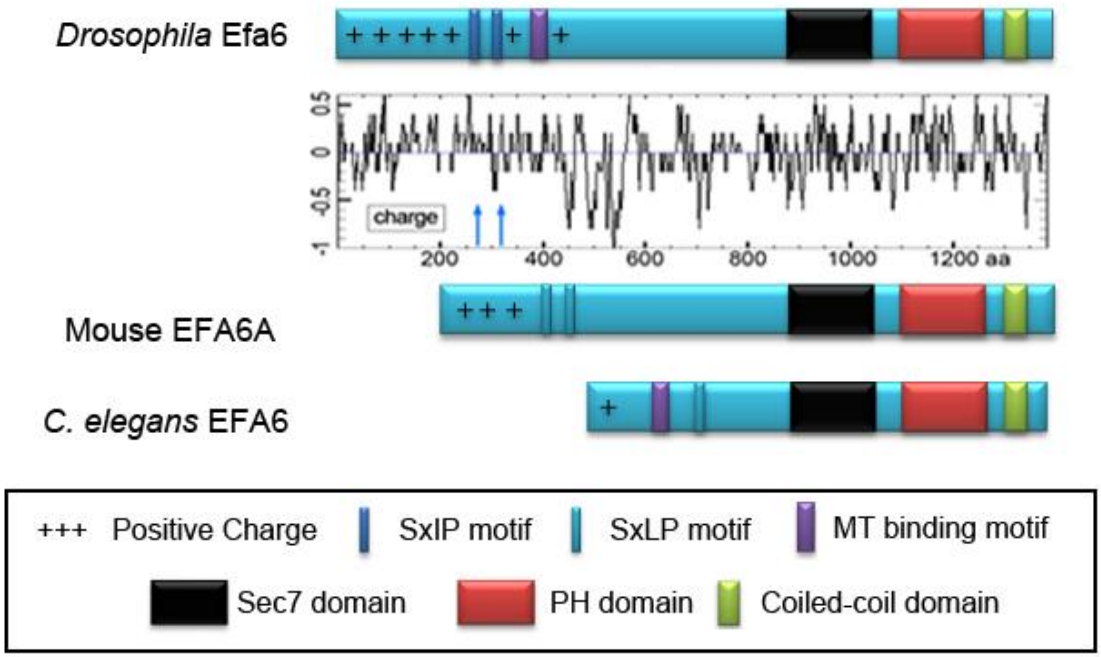

Figure 3.19. *The model of Efa6 constructs in different species.*

The model of Efa6 constructs in different species, as indicated on the left. Functional domains and motifs are described in the box below. The charge plot of Drosophila Efa6 was generated using the Protein Calculator program and the positions of the two SxIP motifs are indicated by blue arrows.

3.3.2. Efa6 is expressed in the CNS and localises to axons

In embryonic epithelial cells, *Drosophila* Efa6 is predominantly cortical (Huang et al., 2009), and for *C.elegans* Efa6 it was shown that its PH domain mediates membrane localisation (Chen et al., 2011). Drosophila Efa6 is expressed in the CNS at least at late embryonic stages (Fig. 3.20) (Huang et al., 2009). I therefore assessed, whether fly Efa6 potentially localises to axonal membranes.

In order to study its localisation, I made use of a previously published fly line in which genomic engineering was used to tag Efa6 with GFP in its genomic location (Huang et al., 2009). Expression patterns are therefore expected to reflect the endogenous protein levels and distributions. In primary neurons obtained from

Efa6::GFP embryos and cultured for 6HIV on glass, either uncoated or coated with ConA, GFP clearly localised all along axons, in somata and in GCs. The localisation appeared dotted and seemed enriched at membranes (Fig. 3.20). To assess whether this localisation was potentially actin-dependent, I treated these neurons with CytoD. However, even under these conditions, Efa6 remained strongly localised all along axons (Fig. 3.20).

I next analysed whether Efa6 expression persisted beyond developmental stages. For this, brains of Efa6::GFP animals were analysed at adult stages and compared to non-fluorescent control brains. These analyses clearly revealed that Efa6::GFP remained expressed in the adult brain at reasonable levels (data generated together with Thomas Shallcross; Fig. 3.20). To complement this finding, I carried out analyses in primary neurons of Efa6::GFP neurons after 6DIV. As explained before (Chapter 3.2.7.2), primary neurons in culture have undergone synaptic differentiation within less than a day and GCs have vanished from neurons at this stage (Kuppers-Munther et al., 2004). Therefore, neurons at 6DIV can be considered to be equivalent to adult stage. In these neurons, Efa6::GFP is still evenly localised all along axons (Fig. 3.20).

Therefore, my analyses indicate that endogenous Efa6 is expressed in neurons at all life stages and that it is localised all along axons, likely at the cell cortex.

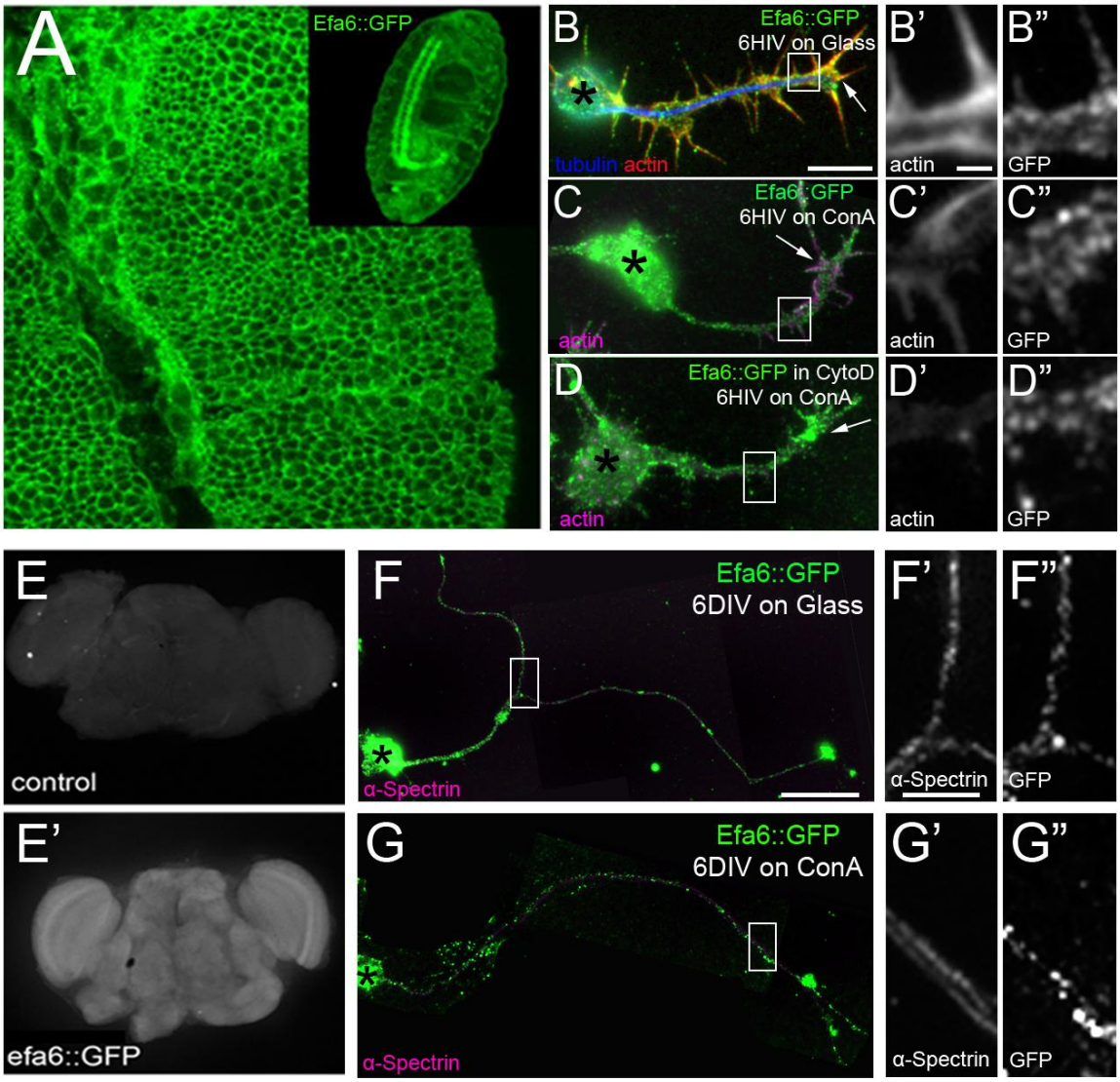
A
Efa6::GFP
B
Efa6::GFP
6HIV on Glass
tubulin actin
B'
actin
B"
GFP
C
Efa6::GFP
6HIV on ConA
actin
C'
actin
C"
GFP
D
Efa6::GFP in CytoD
6HIV on ConA
actin
D'
actin
D"
GFP
E
control
E'
efa6::GFP
F
Efa6::GFP
6DIV on Glass
α-Spectrin
F'
α-Spectrin
F"
GFP
G
Efa6::GFP
6DIV on ConA
α-Spectrin
G'
α-Spectrin
G"
GFP

Figure 3.20. *Efa6 is expressed in the CNS and localises to axons.*

A) *The expression pattern of Efa6::GFP in the Drosophila CNS at late embryonic stages (Huang et al., 2009).* ***B-D")*** *The expression pattern of Efa6::GFP in Drosophila primary neurons at 6HIV, cultured on glass (B), ConA and treated with DMSO (C) or ConA treated with CytoD (@0.4µg/ml) for 4hrs (D); cells are triple-labelled for actin, tubulin and GFP as indicated; boxes in main images are shown as single channel blow-ups on the right. Asterisks, cell bodies; arrows, growth cones; scale bar in B represents 5µm, in B' represents 0.6µm.* ***E-E')*** *The expression pattern of Efa6::GFP in Drosophila adult brain (image taken by Thomas Shallcross).* ***F-G")*** *The expression pattern of Efa6::GFP in Drosophila primary neurons at 6DIV, cultured on glass or ConA. Cells are double-labelled for α-Spectrin and GFP as indicated (F and G); boxes in F and G are shown as single channel blow-ups on the right. Scale bar in F represents 10µm and in F' represents 2.5µm.*

3.3.3. Efa6 is required to maintain axonal MT bundles

Having established the presence of Efa6 in axons, I next assessed its functional contributions in *Drosophila* neurons, using three parallel genetic *efa6* LOF conditions (targeted gene knock-down, chromosomal deficiency and genomically engineered mutant alleles) in primary neurons, of which all consistently caused a dramatic increase in MT disorganisation.

First I analysed filopodia, since mammalian homologues of Efa6 had been shown to influence F-actin networks at the peripheral membrane in non-neuronal cells (Franco et al., 1999, Sironi et al., 2009), inducing accumulation of F-actin and ectopic or supernumerous filopodia in peripheral membrane ruffles (Klein et al., 2008). For *Drosophila* Efa6 in neurons, this situation is far less clear. Thus, filopodia numbers were significantly increased in *efa6*^{RNAi} expressing (128±7%, $P_{Mann\text{-}Whitney}$=0.002, n=120) and *efa6*$^{KO\#1}$ mutant neurons (123±7%, $P_{Mann\text{-}Whitney}$ =0.025, n=100), but it was unchanged in *efa6*^{Def}, *efa6*$^{GX6[w-]}$ and *efa6*$^{GX6[w+]}$ mutant neurons (92±5%%, $P_{Mann\text{-}Whitney}$=0.161, n=80, 93±4%, $P_{Mann\text{-}Whitney}$=0.253, n=120 and 115±5%, $P_{Mann\text{-}Whitney}$=0.085, n=120, respectively; Fig. 3.21). Therefore, potential actin phenotypes point in the right direction (more filopodia) but are not certain at this point.

Next I analysed MT phenotypes, based on the findings in *C. elegans* that Efa6 can act as a MT collapse factor. Firstly, I used targeted gene knock-down by expressing *UAS-Efa6-RNAi* (*efa6*^{RNAi}, VDRC# 42321) (Johnson et al., 2011, Bina et al., 2010) with the pan-neuronal *sca/elav-Gal4* driver line (see methods). Compared to wildtype controls, these neurons showed an increase in MT disorganisation to 154% (P_{Chi2}=0.013, n=120; Fig. 3.21).

Secondly, I used the chromosomal deficiency *Df(3R)Exel6273* and *Df(3R)ED6091i* which, when crossed over one another, uncover the entire *efa6* locus and 9 further genes (flybase.com; Fig. 6.5. in the Appedix). In *Df(3R)Exel6273*/*Df(3R)ED6091i* mutant neurons (referred to as *efa6*^{Def}), MT disorganisation was increased to 252% as compared to wildtype controls (P_{Chi2}<0.001, n=80; Fig. 3.21).

Thirdly, I used the mutant alleles *efa6*$^{KO\#1}$, *efa6*$^{GX6[w-]}$ and *efa6*$^{GX6[w+]}$, three genomically engineered precise deletions of the *efa6* gene (Huang et al., 2009). All three alleles showed a severe increase in MT disorganisation (*efa6*$^{GX6[w-]}$: 178%, P_{Chi2}<0.001, n=120; *efa6*$^{GX6[w+]}$: 192% P_{Chi2}<0.001, n=120; *efa6*$^{KO\#1}$:247%, P_{Chi2}<0.001, n=100; Fig. 3.21).

Ideally, I would have liked to rescue the MT disorganisation of *efa6* deficient neurons, but the required *efa6* full length constructs were not available to me at that stage of the project. However, the very consistent phenotype of MT disorganisation in three independent genetic LOF approachs appears proof enough for a role of Efa6

during the organisation of axonal MTs. Notably, all three conditions caused an increase in axon length ranging from 116-120% ($P_{Mann\text{-}Whitney}$ <0.001, n=80~120; Fig. 3.21), but the molecular mechanism explaining this phenotype are not clear.

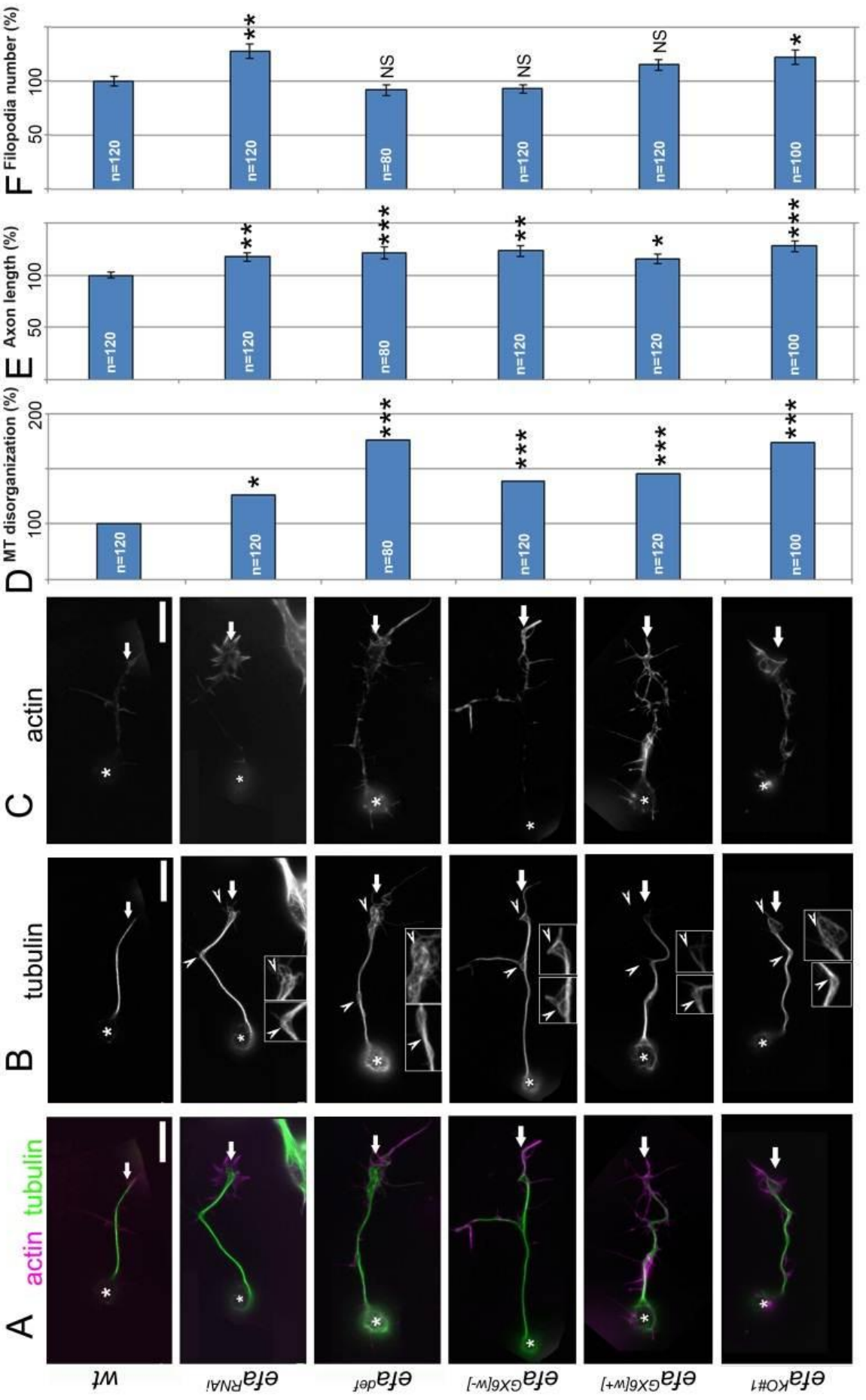
A
actin
tubulin
B
tubulin
C
actin
D
MT disorganization (%)
E
Axon length (%)
F
Filopodia number (%)
wt
efaRNAi
efadef
efaGX6[w-]
efaGX6[w+]
efaKO#1
n=120
n=80
n=100
NS

Figure 3.21. *Efa6 is required to maintain axonal MT bundles.*

A-C) *Axonal phenotypes in wild type, efa6^{RNAi} (sca-Gal4:: efa6^{GD14945}), efa6 deficiency and different efa6 null mutant primary neurons at 6HIV; cells are double-labelled for actin and tubulin as indicated (A; tubulin channel shown alone in B; actin channel shown alone in C; asterisks, cell bodies; arrows, GCs; arrowheads, MT disorganization in GCs and axons; box in B, 2 times magnification of MT disorganization); scale bar represents 5µm.* ***D-F)*** *Quantifications of phenotypes caused by the mutants given on the left, respectively (all normalized and compared to wild type); numbers in the bars indicate the numbers of neurons analysed in each experiment; for MT disorganisation (C) P values were calculated using the Chi^2 test (NS: P>0.050, **: P<0.050, ***: P<0.001); for axon length (D) and filopodia number (E), P values were calculated using the Mann-Whitney Rank Sum test (NS: P>0.050, **: P<0.050, ***: P<0.001).*

3.3.4. The function of Efa6 in axonal MT regulation seems not to depend on Arf6

In mammals, Efa6 was shown to be a GEF of the Arf6 GTPase (Franco et al., 1999, Sironi et al., 2009). However, work in *C. elegans* suggested that roles in MT collapse and axon regeneration are independent of the Sec7 domain required for the GEF function (Chen et al., 2011, O'Rourke et al., 2010). In agreement with this view, the gene product of genomically GFP-tagged *arf6* gene did not reveal any strong expression in the developing CNS of *Drosophila* (Huang et al., 2009).

In primary neurons derived from these *arf6-GFP* flies, I found that the expression of Arf6 is discontinuous in axons. The expression levels are much lower than Efa6::GFP, whereas expression levels in the soma are comparable (Fig. 3.22). This localisation seemed unaffected when treating Arf6::GFP neurons with CytoD (Fig. 3.22).

Next the $arf6^{GX16[w-]}$ null mutant allele, a genomically engineered precise deletion of the Arf6 locus, was used to studied whether this condition would reproduce the Efa6 deficient MT disorganisation (data generated by Ines Hahn) (Huang et al., 2009). Unlike in *efa6* mutants, there was no significant change in MT disorganization of $arf6^{GX16[w-]}$ mutant neurons (normalised and compared with wildtype; 139%, P_{Chi2}=0.128, n=138; Fig. 3.22). However, the axon length was shorter in $arf6^{GX16[w-]}$ mutant neurons (normalised and compared with wildtype; 90±7%, $P_{Mann\text{-}Whitney}$=0.016, n=138; Fig. 3.22), contrasting with longer axons of *efa6* mutant neurons. These results suggest that the function of Efa6 in axonal MT regulation does not depend on Arf6.

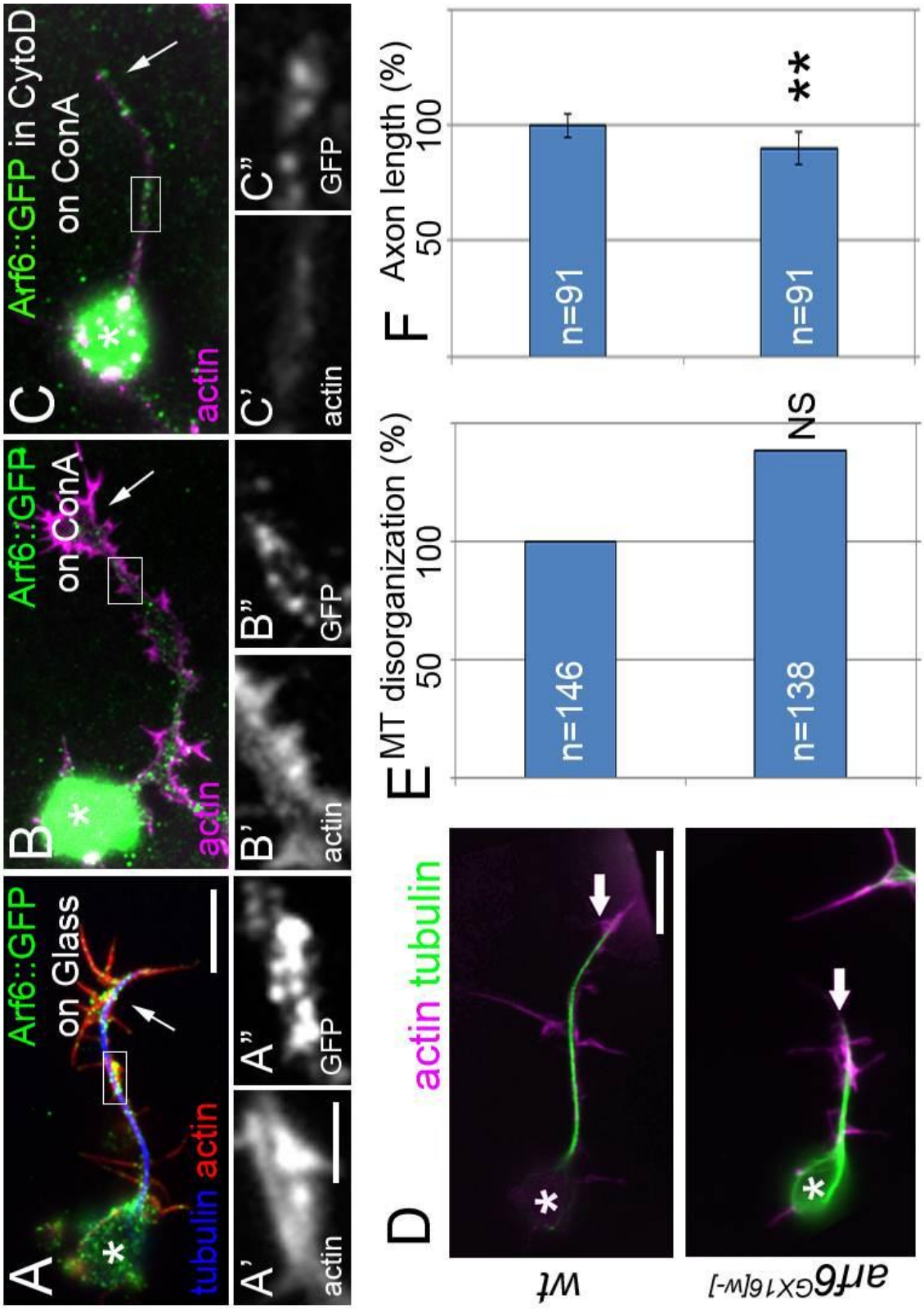
A
Arf6::GFP
on Glass
tubulin actin
A'
actin
A"
GFP
B
Arf6::GFP
on ConA
actin
B'
actin
B"
GFP
C
Arf6::GFP in CytoD
on ConA
actin
C'
actin
C"
GFP
D
actin tubulin
wt
arf6GX16[w-]
E
MT disorganization (%)
50
100
n=146
n=138
NS
F
Axon length (%)
50
100
n=91
n=91
**

Figure 3.22. *Arf6 has different expression pattern and impact on axon in neuron.*

A-C") *The expression pattern of Arf6::GFP in Drosophila primary neurons at 6HIV, cultured on glass (A), ConA and treated with DMSO (B) or ConA treated with CytoD (@0.4µg/ml) for 4hrs (C); cells are double or triple-labelled for actin, tubulin and GFP as indicated; boxes in main images are shown as single channel blow-ups under. Asterisks, cell bodies; arrows, growth cones; scale bar in A-C represents 5µm, in A'-C" represents 1.25µm.* ***D)*** *Axonal phenotypes in wild type and* $arf6^{GX16[w-]}$ *mutant neurons at 6HIV; cells are double-labelled for actin and tubulin as indicated (D; asterisk, cell body; arrow, growth cone); scale bar represents 5µm.* ***E,F)*** *Quantifications of phenotypes caused by the mutant conditions presented on the left (normalized and compared to wild type); numbers in the bars indicate the numbers of neurons analysed in each experiment; for MT disorganisation (E), P values were calculated using the* Chi^2 *test (NS: P>0.050, **: P<0.050, ***: P<0.001); for axon length (F), P values were calculated using the Mann-Whitney Rank Sum test (NS: P>0.050, **: P<0.050, ***: P<0.001).*

3.3.5. Efa6 appears to act as a MT collapse factor in *Drosophila* neurons

The best way to study cortical MT collapse is to use MT plus end markers in combination with live imaging. As described before (Chapter 3.2.6.2), a good marker to trace MT polymerisation events is EB1::GFP. Therefore, I targeted expression of *UAS-EB1-GFP* to *efa6*$^{GX6[w-]}$ mutant neurons and analysed their MT dynamics.

As argued in the introduction of Chapter 3.1, MTs are likely guided by Shot and thus protected from cortical collapse, especially in axons. Since filming sequences during live imaging are in the range of 4mins rather than cumulative over longer time periods, I did not expect any obvious phenotypes in axons. Indeed, there were no measurable effects on a number of parameters of MT dynamics in axons when assessed in kymographs (Fig. 3.23) or via careful picture-by-picture analysis of movies (Fig. 3.23). Thus, when comparing control to *efa6*$^{GX6[w-]}$ mutant neurons, the number of EB1::GFP comets per µm axon length was 88±8% ($P_{Mann-Whitney}$ =0.474, n=19; Fig. 3.23). These data were confirmed when staining fixed neurons (without EB1::GFP expression) for endogenous EB1. In these experiments, the *efa6*$^{KO\#1}$ mutant neurons showed comet number per axon length that were unchanged (110±17%, $P_{Mann-Whitney}$ =0.675, n=20; Fig. 3.23), and there was no difference in percentages of anterograde versus retrograde events (control: anterograde 71%, retrograde 29%, n=19/296; *efa6*$^{GX6[w-]}$: anterograde 75%, retrograde 25%, n=19/302; P_{Chi2}=0.359; Fig. 3.23).

In contrast, in GCs, there were clear differences between wildtype and *efa6*$^{GX6[w-]}$ mutant neurons (Fig. 3.23). In wildtype neurons, EB1::GFP comets tend to vanish when reaching the GC periphery and only a fraction of MTs continues extending into filopodia. However, when counting EB1::GFP dots in live movies (the average of 3 time points per filmed GC), the number in *efa6*$^{GX6[w-]}$ mutant neurons was increased to 166±19%, when compared and normalised to wildtype ($P_{Mann-Whitney}$ <0.001, n=19; Fig. 3.23). This finding was confirmed when staining fixed preparations of neurons not expressing EB1::GFP for endogenous EB1: *efa6*$^{KO\#1}$ mutant neuron displayed 159±18% EB1 dots per GC when compared and normalised to control neurons ($P_{Mann-Whitney}$=0.022, n=20; Fig. 3.23).

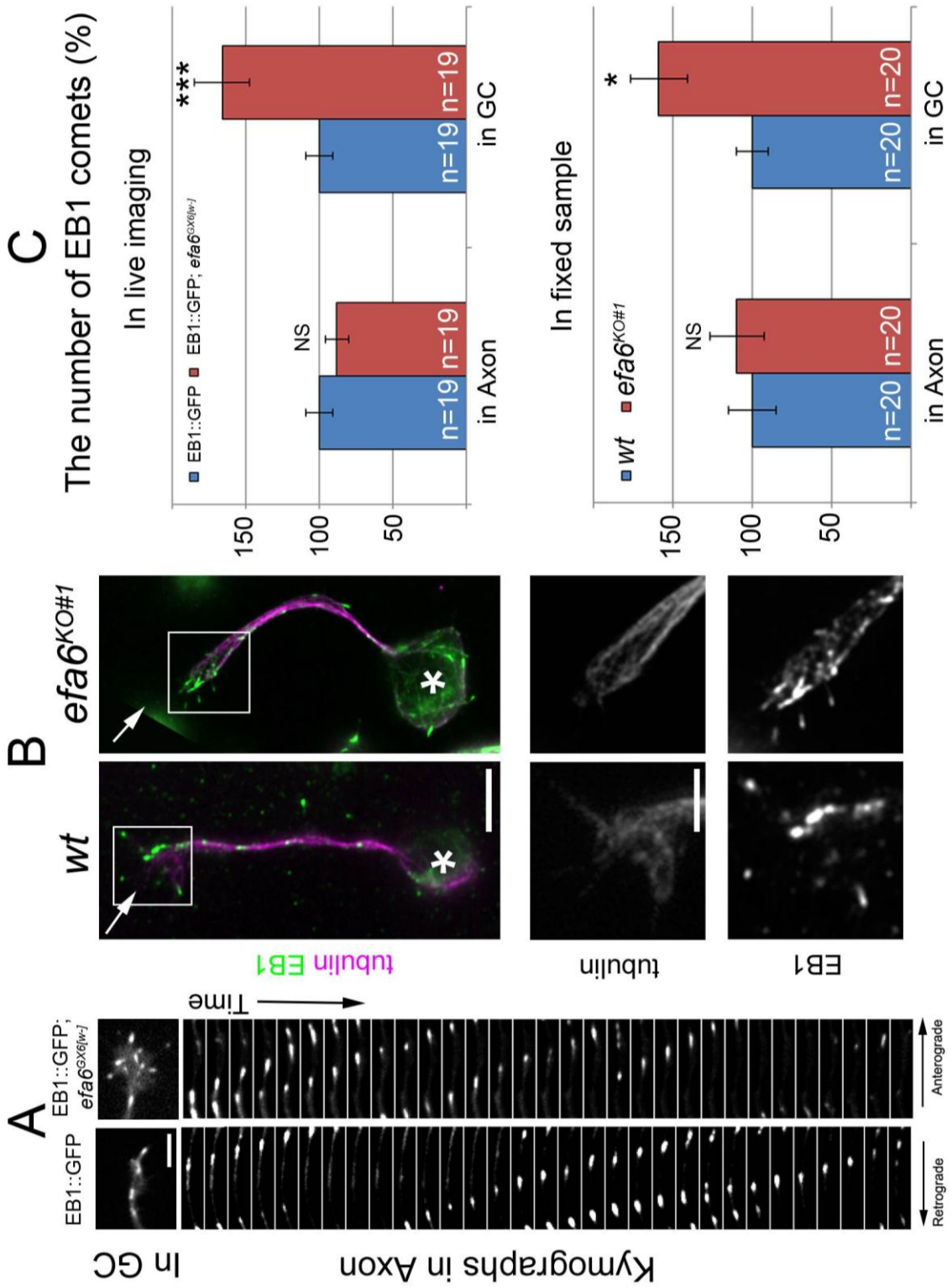
A
EB1::GFP
EB1::GFP; efa6GX6[w-]
Kymographs in Axon
In GC
Time
Anterograde
Retrograde
B
wt
efa6KO#1
tubulin EB1
tubulin
EB1
C
The number of EB1 comets (%)
In live imaging
EB1::GFP
EB1::GFP; efa6GX6[w-]
***
NS
n=19
in Axon
in GC
In fixed sample
wt
efa6KO#1
*
n=20
150
100
50

Figure 3.23. *Efa6 acts as a MT collapse factor in Drosophila neurons.*

A) *Still image of GCs (top) and kymographs (120 seconds are shown) are shown of axonal regions, both from live movies of control and efa6$^{GX6[w-]}$ mutant neurons at 6HIV and expressing EB1::GFP.* ***B)*** *Endogenous EB1 in fixed wild type and efa6$^{GX16[w-]}$ mutant primary neurons at 6HIV; cells are double-labeled for EB1 and tubulin as indicated (boxes in main images are shown as single channel close-ups below; asterisks, cell bodies; arrows, GCs). Scale bar in upper image represents 5µm and 2.5µm close-ups.* ***C)*** *Quantifications of the number of EB1 comets in efa6 mutant neurons obtained from movie stills or images of fixed neurons, in axon and in GC, respectively (normalised and compared to control or wild type); numbers in the bars indicate the numbers of neurons analysed in each experiment; P values were calculated using the Chi^2 test (NS: P>0.050, **: P<0.050, ***: P<0.001).*

In agreement with the increased number of EB1 comets in the GC, also the number of MTs which were successful in entering filopodia was increased. Thus, in GCs of wildtype neurons ~25% of filopodia were reported to contain MTs (Sanchez-Soriano et al., 2010), and this number is consistent with my findings (20±2%). In contrast, in *efa6* mutant neurons this number was doubled when compared to wildtype (*efa6*$^{GX6[w-]}$:185±9%, $P_{Mann\text{-}Whitney}$<0.001, n=120; *efa6*$^{GX6[w+]}$, 205±10%, $P_{Mann\text{-}Whitney}$ <0.001, n=120; Fig. 3.24). These data suggest that Efa6 eliminates MTs in GCs, consistent with a role as cortical collapse factor and potentially explaining why *efa6* mutant neurons in *C. elegans* were found to regenerate better (see Discussion 4.4) (Chen et al., 2011).

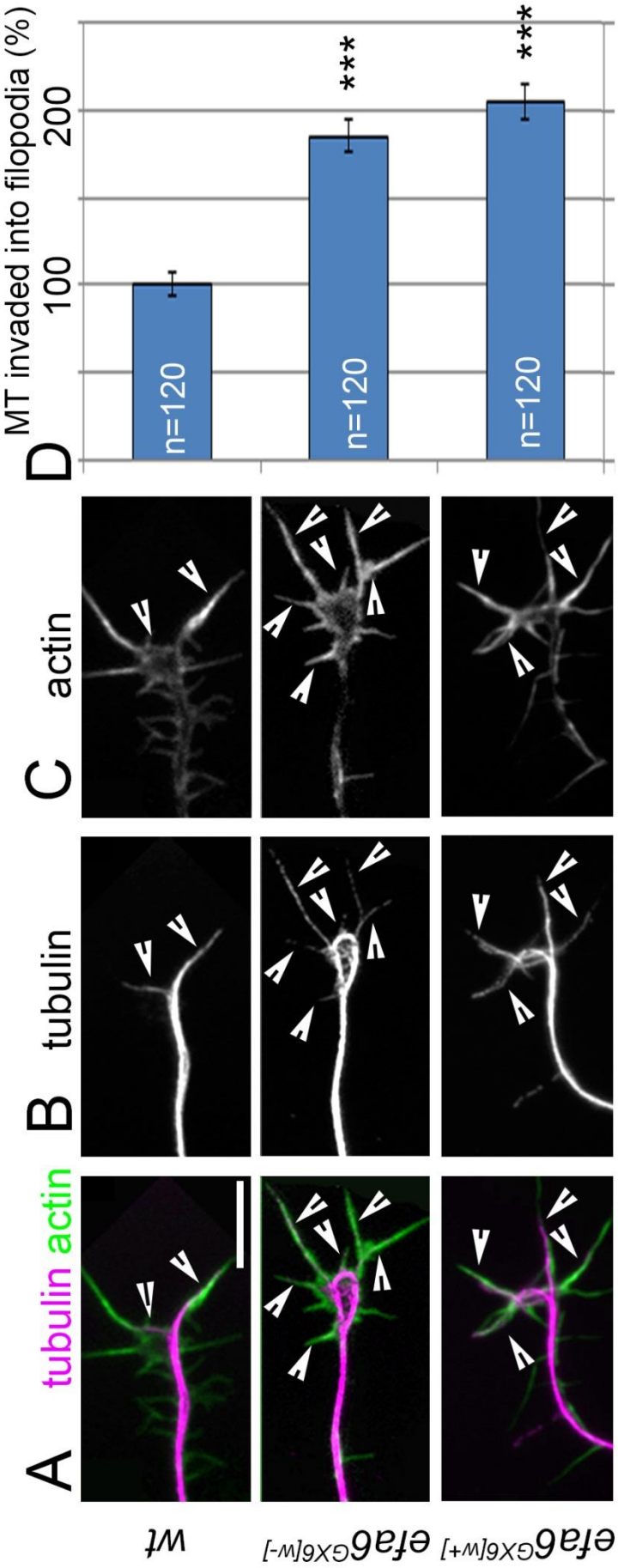
D
MT invaded into filopodia (%)
100
200
n=120
n=120
n=120
***
***
C
actin
B
tubulin
A
tubulin actin
wt
efa6GX6[w-]
efa6GX6[w+]

Figure 3.24. *More MT invade into filopodia in Efa6 mutant.*

A-C) *GCs showing MT invasion of filopodia (arrow heads) in wildtype and efa6 mutant primary neurons at 6HIV; cells are double-labeled for tubulin and actin (D, tubulin channel shown alone in E; actin channel shown alone in F); scale bar represents 5µm.* ***D)*** *Quantifications of phenotypes of the genotypes given on the left, respectively (all normalised and compared to wild type); numbers in the bars indicate the numbers of neurons analysed in each experiment; P values were calculated using the Mann-Whitney Rank Sum test (NS: P>0.050, *: P<0.050, **: P<0.010,***: P<0.001).*

3.3.6. Efa6 is required to maintain axonal MT bundles in differentiated neurons

As speculated elsewhere, axon maintenance likely involves continued MT polymerisation to renew and repair MTs (Prokop, 2013). My own data with neurons at 10DIV further support this statement (Fig. 3.17). Like in developing axons where MT polymerisation is guided by spectraplakins, MT extension during axon maintenance could be dependent on the same mechanisms, and postnatal neurodegeneration in mice and humans mutant for the spectraplakin dystonin supports this notion (Prokop, 2013). Similarly, cortical collapse as a control mechanism to eliminate off-track MTs leaving the axon bundle could be further required. The continued presence of Efa6 in the mature nervous system (Chapter 3.3.2) would be in agreement with this hypothesis.

I therefore analysed *efa6*$^{KO\#1}$ mutant primary neurons at 5 and 10DIV. I observed that the number of neurons containing disorganised axonal MTs increased with age (normalised to wildtype; 5DIV, 148%, P_{Chi2}=0.007, n=79; 10DIV, 161%, P_{Chi2}<0.001, n=96; only did once Fig. 3.25). However, these data reflect only the number of neurons with disorganisation, but not the severity of the disorganisation phenotype. Suitable assays for this were recently established by Ines Hahn in our group who used the area of disorganisation divided by axon length as a parameter. Using this measure she could show that there is a steady increase in the degree of MT disorganisation over time (Ines Hahn, unpublished results).

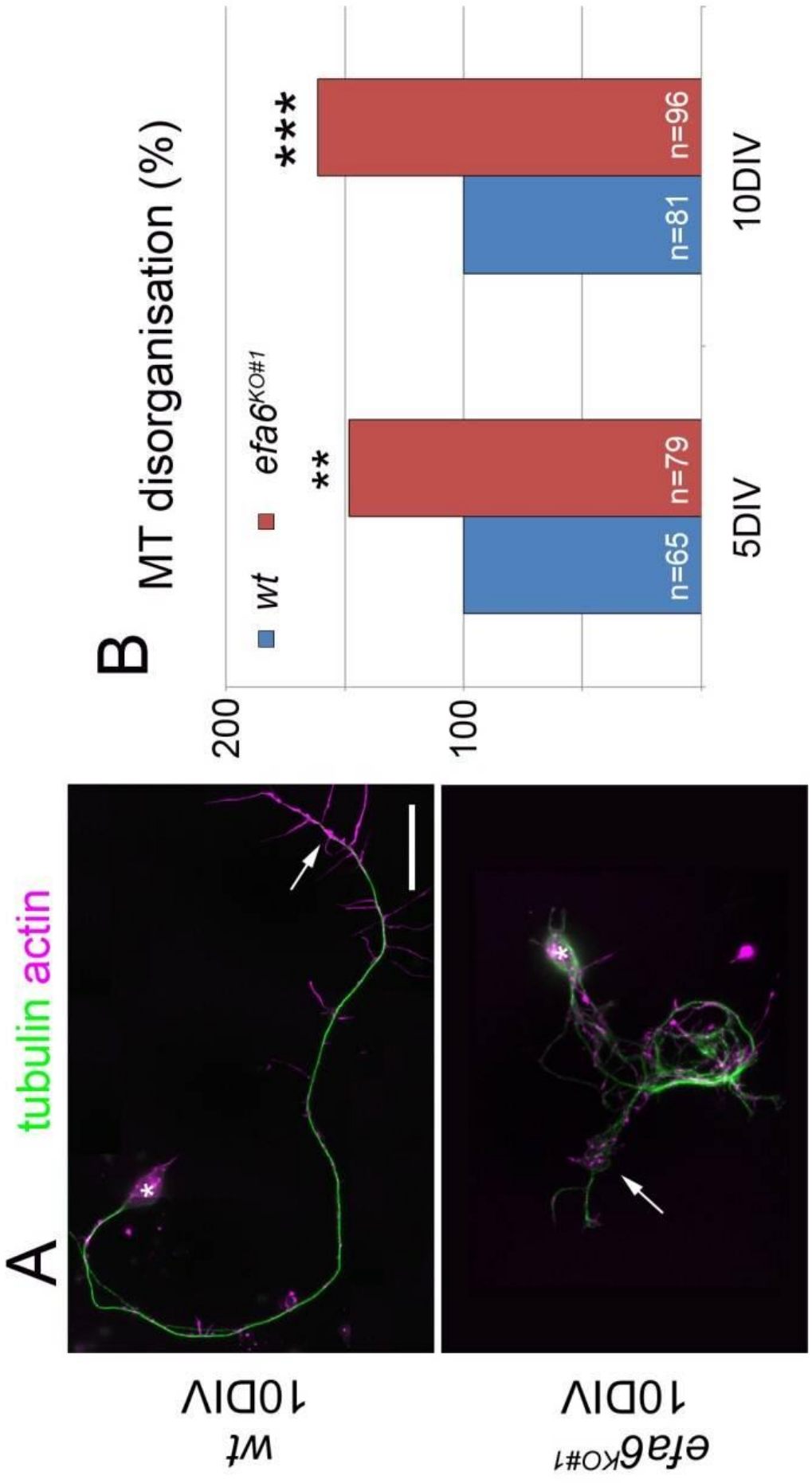
A
tubulin actin
wt
10DIV
efa6KO#1
10DIV
B
MT disorganisation (%)
wt
efa6KO#1
200
100
**
***
n=65
n=79
n=81
n=96
5DIV
10DIV

Figure 3.25. *Efa6 is required to maintain axonal MT bundles in differentiated neurons.*

A) *The MT disorganization phenotypes in wildtype or efa6$^{KO\#1}$ mutant primary neurons at 10DIV; cells are double-labeled for tubulin and actin (asterisks, cell bodies; arrows, growth cones); scale bar represents 10µm.* ***B)*** *Quantifications showing the number of neurons with MT disorganization at 5DIV and 10DIV (all normalised and compared to wild type); numbers in the bars indicate the numbers of neurons analysed in each experiment; P values were calculated using the Chi^2 test (NS: P>0.050, *: P<0.050, **: P<0.010,***: P<0.001).*

3.3.7. Structure-function analysis of Efa6

Building on existing data for *C. elegans* (O'Rourke et al., 2010, Chen et al., 2011), I hypothesised that also the MT collapse function of *Drosophila* Efa6 might depend on its N-terminus. If this were true, I would expect that releasing the Efa6 N-terminus from the membrane might generate a dominant negative construct able to collapse MTs even within the cytoplasm. To test this hypothesis two constructs were generated (in collaboration with Meredith Lees in our group). We generated a partial N-terminal construct which only contains the positively charged part (0-410aa; termed Efa6-Nterm) and a construct containing the entire N-terminus excluding the Sec7, PH and coil-coiled domains (0-897aa; Efa6-ΔCtail; Fig. 3.26).

I first tested the effect of these constructs in *Drosophila* primary neurons, using our newly established transfection methods (Methods 2.3.2; Compare Chapter 3.1.5). When transfecting eGFP-encoding control constructs into primary *Drosophila* neurons, roughly 20% of neurons became fluorescent and, of these, around 75% neurons displayed axons with normally bundled MTs (Fig. 3.26), and this number was similarly observed in untreated wildtype neuron cultures (Chapter 3.2.3; Fig. 3.5) suggesting that the transfection procedure has no negative impact on axonal development. However, when transfecting Efa6-Nterm or Efa6-ΔCtail construct into primary *Drosophila* neurons, MTs became severely damaged and sparse, and only 40% or 36% of transfected neuron showed axons which tended to show degenerating MT networks (Efa6-Nterm, $P_{Chi2}<0.001$, n=600; Efa6-ΔCtail, $P_{Chi2}<0.001$, n=383; Fig. 3.26).

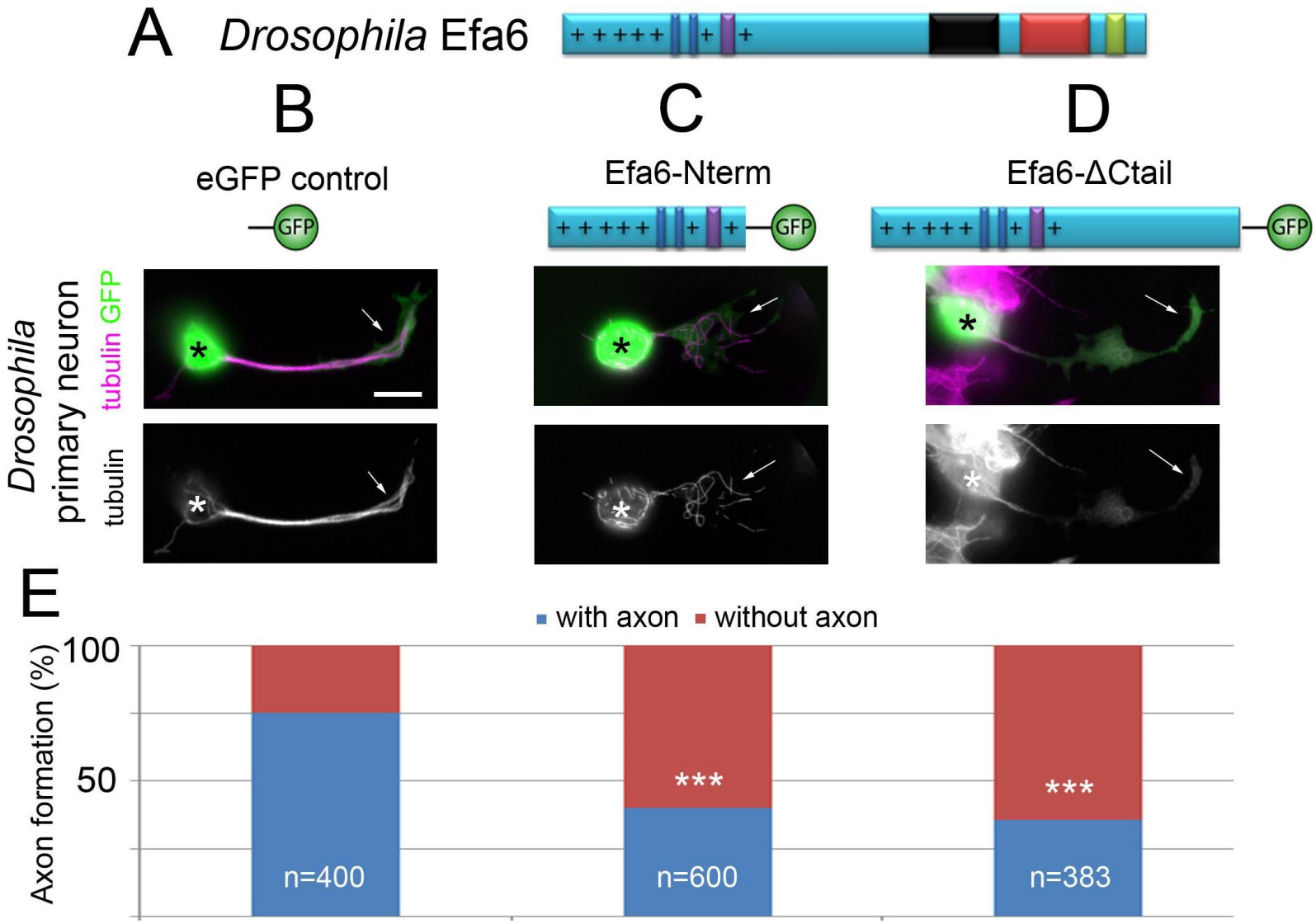
A
Drosophila Efa6
B
C
D
eGFP control
Efa6-Nterm
Efa6-ΔCtail
GFP
Drosophila primary neuron
tubulin GFP
tubulin
E
with axon
without axon
Axon formation (%)
100
50
***
***
n=400
n=600
n=383

Figure 3.26. *The effect of N-terminal Efa6 in Drosophila neurons.*

A) *Schematic of the full length Efa6 protein.* ***B-D)*** *Drosophila primary neurons at 16HIV, grown on ConA and transfected with control or different Efa6 modified constructs, double-labeled for tubulin and GFP (tubulin channel alone shown below; asterisks, cell bodies; arrows, growth cones); scale bar represents 5μm in B, C.* ***E)*** *Quantifications of the axon formation in control or Efa6 constructs transfected neuron, respectively (all compared to control); numbers in the bars indicate the numbers of neurons analysed in each experiment; P values were calculated using the* Chi^2 *test (NS: P>0.050, *: P<0.050, **: P<0.010,***: P<0.001).*

To obtain independent support for these data, I used the mouse NIH/3T3 fibroblast cell line which was previously used very successfully for work on Shot in our group and was found to mirror a number of effects observed in *Drosophila* primary neurons (Alves-Silva et al., 2012). When I transfected the Efa6-Nterm or Efa6-ΔCtail constructs into NIH/3T3 fibroblasts and analysed cells 24hrs later, almost all transfected cells showed a complete absence of MTs or, at least, severe reduction in MT network densities (Fig. 3.27).

In order to better understand this phenotype, I analysed different time points after transfection. It seemed that the expression of Efa6-Nterm did not set in before 5HIV. At 7HIV, the loss of MTs was already correlated with the construct expression level. In a number of weakly expressing cells, MTs appeared reduced in numbers but were still visible, and I could observe clear plus end tracking behaviours (Fig. 3.27). In contrast, in cells with strong expression levels, MTs were already eliminated. These data strongly indicate that MT collapse sets in within a relatively short time frame of 2-3hrs after expression of the transfected constructs sets in.

3.3.8. Conclusion for Chapter 3.3

Efa6 is a cortical collapse factor that is expressed in the CNS and localises all along the axons where it is likely to perform a check point function eliminating off-track MTs accidentally leaving the axonal MT bundles. This function is independent of Arf6. The check point function of Efa6 is not only required during development, but also needed during axonal maintenance in differentiated neurons, and this may play an important role in axon ageing (see Discussion 4.4.2). The essential MT eliminating function clearly resides in the N-terminus of Efa6.

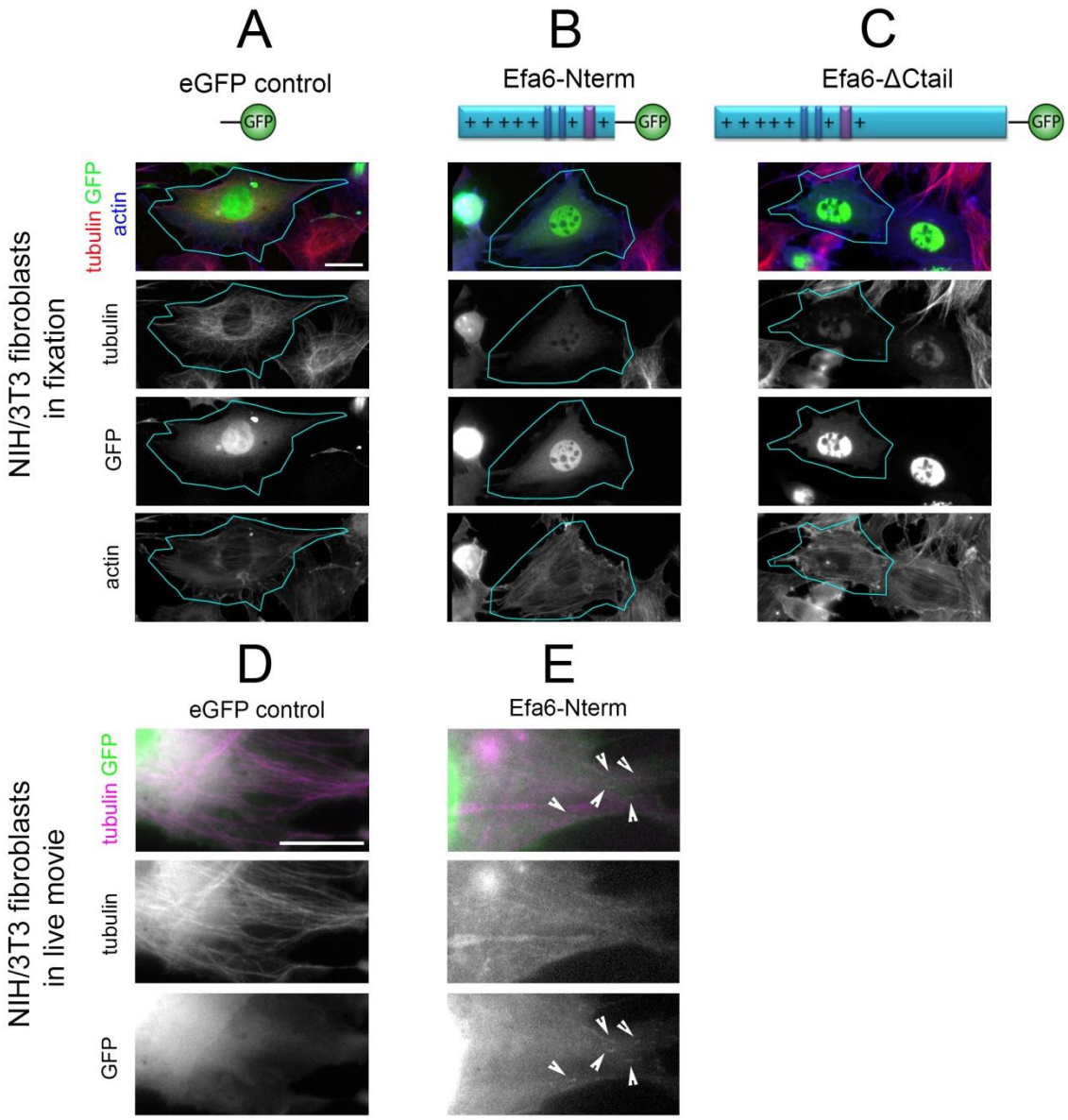
A
eGFP control
GFP
B
Efa6-Nterm
GFP
C
Efa6-ΔCtail
GFP
NIH/3T3 fibroblasts in fixation
tubulin GFP actin
tubulin
GFP
actin
D
eGFP control
E
Efa6-Nterm
NIH/3T3 fibroblasts in live movie
tubulin GFP
tubulin
GFP

Fig. 3.27

Figure 3.27. *The effect of N-terminal Efa6 in mouse fibroblasts.*

A-C) *NIH/3T3 fibroblasts at 24HIV transfected with control or N-terminal Efa6 constructs, fixed and triple-labeled for tubulin, GFP and actin (tubulin, GFP and actin channel shown below respectively as indicated). Scale bar represents 20µm.* ***D,E)*** *Still image from the live movie of NIH/3T3 fibroblasts at 7HIV, co-transfected with tubulin and control or Efa6-Nterm, revealing MT plus end tracking of Efa6-Nterm (tubulin and GFP channel shown below respectively as indicated; arrowhead, the Efa6-Nterm localisation). Scale bar represents 10µm.*

Chapter 4

Discussion

4.1. New understanding of actin and cortical factors in MT regulation during axon growth and maintenance

Axons are slender neuronal protrusions, which are up to meters long in human. Axons act as the cables that provide the essential information highways in the nervous system by electrically wiring the brain and body (Jessell et al., 2000). The proper function of nervous systems requires that axons grow and wire up correctly during development or regeneration. Once axons are correctly formed, their uniquely challenging architecture has to be maintained for organism's lifetime. About 50% of axons are usually lost at high age in the healthy brain (Adalbert and Coleman, 2012, Marner et al., 2003). Notably, axon degeneration is considered as the cause rather than consequence for neuron decay in the context of various neurodegenerative diseases. However, the mechanisms that regulate the formation and maintenance of axons are still little understood.

To gain such insights, my PhD project has focussed on mechanisms which regulate the MT bundles that form the structural backbones of axons as well as the highways for life sustaining transport between cell bodies and the growth cones or synaptic endings. These mechanisms are important since these MT bundles are essential mediators of axon growth during development or regeneration and axon maintenance during ageing (Prokop, 2013, Prokop et al., 2013).

Here, I have used systematic combinatorial genetics and pharmacology to unravel mechanisms and roles of actin and the cortical collapse factor Efa6 in MT regulation during axon formation and maintenance. Capitalising on fast and genetically and experimentally amenable research possible in *Drosophila* neurons, both in primary culture and *in vivo*, I was able to gain a number of novel mechanisms contributing to the *de novo* alignment and maintenance of ordered MT bundles.

Previous work clearly demonstrated that the actin-MT linker Shot, the homologue of mammalian dystonin, guides polymerising MTs along actin structures to arrange them into parallel bundles. This involves binding to actin via the N-terminal ABD and to MTs via the C-terminal GRD and C-tail (Alves-Silva et al., 2012, Sanchez-Soriano et al., 2009). Here, I have studied the role of Shot ABD during axon growth, and my data strongly suggest that Shot ABD domain has unique properties that can sense specific properties of F-actin networks, and this is important for its ability to appropriately regulate MT behaviours (see Discussion 4.2.2).

These results clearly support a model in which changes in actin networks will have impact on MT behaviours. This model was further supported by my studies with pharamco-genetic actin manipulations which confirmed and complemented previous findings (Gonçalves-Pimentel et al., 2011), i.e. that changes in actin networks affect MT bundling and axon growth behaviours. Furthermore, I found that functions of F-actin in

MT organisation do not restrict to the guidance and bundling behaviours of extending MTs, but I discovered that actin has Shot-independent roles in MT maintenance. Whilst the molecular mechanisms underpinning this function are still unclear, I have shown that a likely target of actin is the polymerisation of MTs which was clearly affected when destabilising actin in *shot* mutant neurons, as shown in live imaging experiments.

Another major step forward was to develop a more refined understanding of actin networks in neurons and to consider them in functional models. Thus, it had been proposed that the axonal actin in mouse neurons is arranged into periodic pattern of 180 nm intervals, involving the typical cortical actin regulators Spectrin and adducin (Xu et al., 2013, Lukinavicius et al., 2014). Using STORM/PALM and SIM, we found a very similar periodic pattern of axonal actin in *Drosophila* neurons. Building on the predicted nature of these actin structures as bundles of short and adducin-capped, stable actin filaments typical of cortical actin (Xu et al., 2013), I started to apply pharmaco-genetic manipulations which, so far, are in agreement with the structural model as well as with the effects on the functional readouts I developed here (i.e. axon growth behaviours and MT maintenance in *shot* mutant neurons). As will be discussed (in Chapter 4.2.3&4.2.4), this suggests to me that actin in the axon shaft has a growth-promoting role consistent also with the positive impact of actin on MT polymerisation observed in my live imaging experiments. To my knowledge, these are the first data providing insight into the roles of actin in axon shafts.

In sum, my work provides a number of complementary data and novel means to understand how axonal actin influences MT bundle organisation and axon growth, mediated by the regulators which govern F-actin network organisation in different axonal compartments, the actin-MT crosslinking functions through Shot, as well as other mechanisms downstream of actin influencing MT polymerisation behaviours.

However, I did not only gain new insights into cross-talk between actin and MTs, but also into actin-independent mechanisms of MT regulation. Thus, it has long been known that structural MAPs, such as MAP1B, MAP2 and tau, associate with MTs to stabilise them against depolymerisation or crosslink them into bundles (Halpain and Dehmelt, 2006). Such functions can be expected to contribute to the proper organisation of MT bundles. Previous studies had shown that also Shot acts like a structural MAP in that it associates with MTs and, through its GRD domain, stabilises them against effects of the MT depolymerising drug nocodazole (Alves-Silva et al., 2012). My experiments with Shot-LA^{only} neurons treated with CytoD suggested that these functions of Shot might indeed play a role during MT maintenance in axons. However, this Shot-mediated protection of MTs only worked on ConA substrate and not on uncoated glass, suggesting that it does not play a major role in developing axons. Instead, my experiments revealed a further actin-dependent function of Shot relating to MT bundle stabilisation. This

function, either alone or in conjunction with GRD-mediated stabilisation, efficiently protects axonal MTs when actin networks are depleted. I did not address the molecular mechanisms of this actin-independent bundle-maintaining role of Shot, but the work from previous group members suggests that the plakin repeat region in the Shot-LH isoform may be important, as will be discussed (see 4.3).

Not all mechanisms I discovered are involved in actively organising and maintaining MT bundles, but there are also mechanisms which act as check-points to repair and clean up accidental disorganisation. Thus, I found that the cortical MT collapse factor Efa6 localises to axons, likely the axonal cortex, and is able to eliminate MTs which leave the bundled organisation and go off-track. It was shown for the Efa6 homologue in *C. elegans* that the MT eliminating function requires its N-terminal (O'Rourke et al., 2010). My results suggest that this is similarly the case for *Drosophila* Efa6, although its N-terminus is not at all conserved. The molecular mechanisms remains unknown, but I could show that the Efa6 N-terminus displays MT plus end tracking behaviours consistent with the presence of two SxIP motifs known to be required for EB1 binding (Honnappa et al., 2009). The working model I propose is that Efa6 localises to axonal membranes via its PH domain, ready to bind to EB1 to capture the plus ends of off-track MTs which can then be destabilised (further discussed in 4.4).

In conclusion, my work has revealed a whole range of new insights and mechanisms that help to refine our model view of axon biology. These new mechanisms strongly suggest that different MT-regulatory mechanisms act in parallel in axons and complement each other in one common mechanism of MT bundle formation and maintenance. As will be discussed below (4.5), we propose a local homeostasis model for axons which provides new ways to think about problems of ageing as well as a range of different neurodegenerative diseases.

4.2. Actin regulates axon growth and maintenance by several different mechanisms

Actin-MT cross-talk is a long known phenomenon. As described in Chapter 1.4., actin networks can cross-talk with MTs in many different ways: (1) through direct physical interaction in that actin network contraction can push MTs sideways or hinder its advance through antagonising backflow (Forscher and Smith, 1988, Schaefer et al., 2008, Lee and Suter, 2008); (2) through mono-molecular actin-MT cross-linkage via linker molecules such as Shot, MAP1B or tau to guide or capture MTs (Alves-Silva et al., 2008, Sanchez-Soriano et al., 2009, Alves-Silva et al., 2012); (3) through oligo-molecular cross-linkage where MTBPs bind to ABPs (e.g. the ABP IQGAP1 interacting with MT-associating CLIP-170 to mediate cortical MT capture, or interaction of EB3 with the ABP

drebrin) (Geraldo et al., 2008, Briggs and Sacks, 2003); (4) through signalling, in particular clutch-dependent signalling at adhesion or receptor sites which can then instruct MT behaviours (Suter and Forscher, 2000). In my project, I have gained new insights into actin-MT crosstalk.

4.2.1. Actin is crucial in Shot localisation

Shot association with F-actin is required to guide MT polymerisation in the direction of axon growth (Alves-Silva et al., 2012, Sanchez-Soriano et al., 2009). My experiments have shown that the previously described enriched Shot-LA localisation at GCs (Sanchez-Soriano et al., 2009) seems to depend on the prominent F-actin networks at this site, because it is abolished upon LatA treatment (Chapter 3.1.8). Since the experiments with super-resolution or analysing MT maintenance in *shot* mutant neurons, have revealed that LatA seems to have no or minor effects on cortical actin, this suggests that especially networks composed of longer actin filaments seem required for Shot enrichment at GCs (Chapter 3.2.3). I also found that GC localisation of Shot-LA is not abolished upon CK666 treatment expected to reduce the number but not principal presence of actin filaments, suggesting that this specific Shot localisation is more dependent on the type than the quantity of actin networks in GCs. MTs seem to play no role in the GC accumulation of Shot, since localisation of the C-terminal EGC construct (composed of EF-hand motif, GRD and Ctail; Fig. 3.1) is homogeneous all along MTs,. This notion is also supported by the localisation of Shot-ΔGRD and Shot-ΔCtail constructs, both of which are detached from MTs but still localise to actin-rich zones of GCs (Alves-Silva et al., 2012). From these data, I conclude that the networks of long actin filaments in GCs are crucial for concentrating Shot in this area.

However, my experiments revealed some surprises concerning the domains required for the GC localisation of Shot. Thus, neither removing ABD nor the plakin-like domain abolished the GC localisation of Shot-LA, suggesting that they might have redundant functions in Shot localisation downstream of F-actin. Even more, the N-terminal ABD-containing Shot construct did not concentrate at GCs (Fig. 3.2) suggesting that the ABD might not even contribute to this localisation. Of the two domains tested by me, the ABD is likely to interact directly with F-actin (Lee and Kolodziej, 2002) whereas the plakin-like domain could bind to proteins which themselves are actin-dependent in their localisation. Accordingly, it has been shown that the plakin-like domain of the mammalian epidermal spectraplakin BPAG1e interacts with integrins and transmembrane collagens, the localisation of which is likely dependent on F-actin (Aumailley et al., 2006). In agreement with this interpretation, Shot-Δplakin is unable to compartmentalise Fasciclin II to their appropriate axon segments (Bottenberg et al.,

2009), suggesting direct or indirect links of the plakin-like domain to that transmembrane adhesion factor. To test this hypothesis, Shot-LA-ΔABD-Δplakin double-deletion constructs would be required, but were not generated in the context of my project. Alternatively, further Shot domains could be involved in Shot-LA localisation to GCs. For example, the Spectrin repeat-containing rod of Shot has been shown to be required for localisation *in vivo* (Bottenberg et al., 2009), but was unfortunately never tested in primary neurons.

Therefore, a scenario for the localisation of Shot-LA emerges which seems as complex as localisation in tendon cells where Shot-LC, Shot-Δplakin and even EGC constructs show an almost indistinguishable pattern, with some potential variations displayed only by Shot-Δrod (Bottenberg et al., 2009, Alves-Silva et al., 2012). This robustness of Shot localisation seems to reflect its manifold interactions with different classes of binding partners in cells, in agreement with its enormous length and the very different functional domains it contains. However, as has become clear, localisation is not a good indicator for Shot functions.

4.2.2. The unique properties of Shot ABD is important for Shot MT regulatory function

Using GOF analysis, I found that the function of Shot is affected when substituting the Shot ABD by Lifeact or the actin-binding domain of Moesin (Moe). This strongly indicates that Shot ABD domains provide a specific property required for proper Shot function in MT regulation. However, in order to further prove this statement, it will be important to use the Shot-LA-Life and Shot-LA-Moe constructs to perform rescue experiments in *shot* mutant neurons and embryos. I predict that Shot-LA-Life is more likely to display a dominant phenotype whereas Shot-LA-Moe might perform a mild rescue.

But what might be the properties of Shot ABD which are so crucial for MT regulatory functions of Shot-LA? I can think of several hypothesises. First, *in vitro*, the F-actin affinities of Shot ABD are likely to be set to a defined level between Moe or Lifeact, This level could be important to allow specific association/dissociation dynamics required for Shot to guide proper MT extension. However, the mere actin affinity may be not enough to explain how Shot ABD regulates its MT regulation function since actin networks in cells are much complex and play important roles in many aspacts of cell biology. For example, my experiments showing that CK666 had no impact on Shot-LA localisation at GCs suggest that organisational properties are more important than F-actin abundance. The impact of the more complex F-actin network properties in neurons can be address with FRAP (fluorescent recovery after photobleaching) studies. It would

now be helpful to also test Shot-∆plakin or conditions where actin is removed with CytoD (removing all F-actin) or LatA (removing F-actin but not cortical networks). This would directly address potential links between F-actin and the plakin-like domain and address the importance of qualitatively distinct F-actin networks.

Notably, the importance of qualitative network requirements is not only suggested by localisation studied but also by some of my functional analyses. Thus, the phenotype of bundled loop formation in GCs upon overexpression of Shot-LA is both diminished by applying LatA and CK666. Howerer, the shorter axon phenotype caused by overexpression of Shot-LA is rescued by applying LatA, but not by applying CK666. This suggests that the number of actin filament in GCs is essential for Shot function. To test this further, loss of actin elongator function (*profilin* or *ena*) in Shot-LA overexpressing neurons could be used, and I would predict that Shot-LA will no longer accumulate in GCs under these conditions. Moreover, the analysis of Shot-LA-Life upon LatA or CK666 treatments or in *chic* mutant neurons might reveal significant differences from Shot-LA, thus demonstrating that the correct actin interaction through the ABD is functionally important for Shot roles in MT regulation.

Finally, the ABD of Shot may differ from Moe and Lifeact through a specific ability to interact intra-molecularly with other functional Shot domains. For example, the ABD of Shot is closely related to the ABD of spectrins (Roper et al., 2002). Spectrins forms antiparallel dimers in which the N-terminal ABD becomes aligned with the C-terminal EF-hand motifs; it has been proposed that, in this case, calcium-binding to the EF-hand motifs influences actin-binding properties of the ABD (Broderick and Winder, 2005). To test this possibility, a number of experiments could be done. On the one hand, the tandem EF hand domains of Shot show the typical features required for calcium binding (R. Kammerer, personal communication), but functionally they have so far only been shown to interact with Krasavietz/eIF5C (Kra) important for axonal pathfinding and filopodia formation (Lee et al., 2007, Sanchez-Soriano et al., 2009). It would therefore be necessary to directly test the calcium-binding capabilities of the Shot EF-hand domains. To test potential anti-parallel dimer formation, Shot could be tagged with CFP on one end and YFP on the other, to be able to assess antiparallel dimer formation using Fluorescence resonance energy transfer (FRET) analysis.

4.2.3. Actin can stabilise MTs by maintaining their polymerisation

During my project, I have found a novel mechanism of MT regulation in axons which involves F-actin dependent stabilisation of MTs potentially through promoting their polymerisation. In wildtype neurons treated with CytoD gaps occur in axonal MT bundles, but not when treated with LatA (which affects F-actin in GCs but hardly in the axon shaft). Accordingly, in *shot* mutant neurons (where MTs are not directly protected), treatment with LatA caused disorganised MTs of GCs to disappear, but not in axon shafts. However, when *shot* mutant neurons were treated with CytoD, MTs disappeared both in GCs and axon shafts (Fig. 4.1). These data suggest that LatA-resistant cortical actin can maintain MTs in axon. In *shot* deficient neurons double-mutant for $SCAR^{\Delta 37}$ or treated with CK666, disorganised MTs disappeared both in GC and axons, and this is consistent with our prediction that abolishing Arp2/3 nucleator function should affect cortical actin which has short but therefore more numerous actin filaments. In contrast, in $chic^{221}$ $shot^{3}$ double-mutant neurons, disorganised MTs remained in both GCs and axons (Fig. 4.1). This is consistent with the fact that cortical actin has short actin filaments and should therefore be little dependent on elongator functions. In all, a case can be made for the role of cortical F-actin in MT maintenance, but obviously this is currently not more than a working hypothesis.

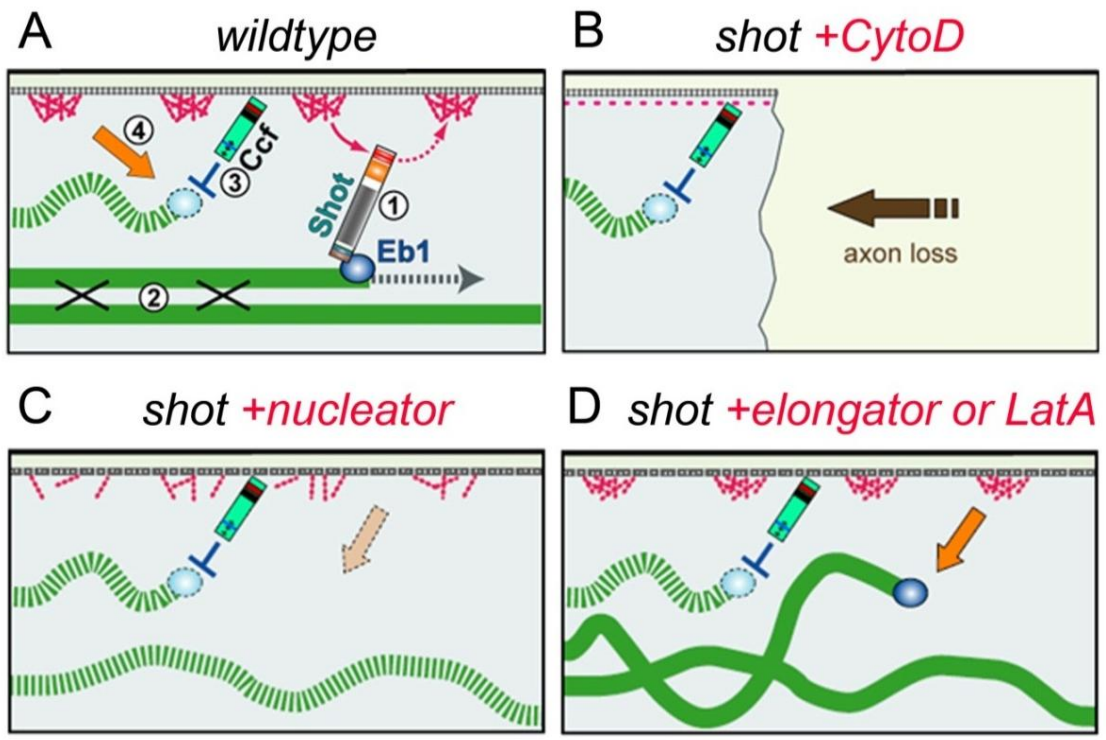

Figure 4.1. *A model describing the effect of different F-actin manipulation on MT maintenance.*

A) *Different MT regulatory mechanisms work together to maintain MT bundles: (1) MT guidance of extending MTs through Shot, (2) MT bundling function involving Shot, (3) cortical collapse factors (Ccf) such as Efa6 eliminate off-track MTs, (4) functions downstream of cortical F-actin counteract Efa6 function by maintaining non-coalescent MTs.* ***B-D)*** *different actin manipulation in shot mutant neuron cause different degrees of damage to MT bundles.*

But how does actin maintain MTs? A first clue about the mechanisms underlying roles of F-actin in MT maintenance come from live analyses of *shot* mutant neurons treated with CytoD, in which the speed and number of EB1 becomes rapidly decreased, suggesting that F-actin maintains MT polymerisation in the absence of Shot. Whilst this phenotype is very robust, the molecular mechanisms remain unclear. They could either be downstream of F-actin directly or downstream of other cortical components, such as Spectrin, ankyrins or adducin, which would also explain why particularly cortical actin networks seem to have this MT-maintaining function. The localisation of these proteins can be expected to be influenced by the manipulations of F-actin networks affecting for example the amount of actin filaments, and dislocalisation of these proteins may impact on their MT regulatory functions, thus establishing an indirect effect from F-actin to MT regulation. Whilst I have started analyses with spectrin and adducin mutant neurons, I have not yet considered Ankyrin as another potential candidate for MT regulation. Thus,

a well-known function of Ankyrin is linking Spectrins to the membrane (Bennett and Baines, 2001, Baines, 2010). Furthermore, Ankyrin protein can cap MT plus ends thus causing the disassembly of MTs (Pecqueur et al., 2012). The C-terminal part of Ankyrin isoform (Ank2L) has been suggested to bind to, stabilise and organise presynaptic MTs in *Drosophila* (Pielage et al., 2008). Ankyrin can also directly bind Go protein (a heterotrimeric G protein) which is known to promote neurite outgrowth. This function is conserved between *Drosophila* and mammals (Luchtenborg et al., 2014). Therefore, I hypothesise that reduced actin at the cortex may affect the localisation of Spectrin and Ankyrin which can then have functional impact on MT stabilisation. To further investigate this aspect, live imaging can be used in neurons lacking these various components to test whether they reveal changes in MT polymerisation.

4.2.4. How different actin networks contribute to axon growth regulation

There is an argument in the field of axon growth that GCs are promoting axon growth through pulling the axon, and this argument goes back several decades (Bray, 1984, Heidemann et al., 1995, Franze et al., 2013). However, another view is that F-actin produces friction that opposes MT extension and therefore slows down axon growth (Pak et al., 2008), suggesting that GCs are rather inhibitory. For example, thick cortical actin networks are a barrier to initial axon outgrowth (Brandt, 1998, Flynn et al., 2012), GCs are frequently pausing during pathfinding *in vivo* and culture thus slowing down growth (Lowery and Van Vactor, 2009), and actin backflow opposes MT advance in GCs (Pak et al., 2008, Prokop, 2013). In addition, F-actin networks of GCs enlarge the leading edge thus generating more plasma membrane perpendicular to advancing MTs, and these membranes are likely to collapse these MTs as I observed in my live analyses (Fig. 3.23). Such collapse of MTs mediated by Efa6 might explain why *efa6* mutant neurons in *C. elegans* have a better rate of regeneration (Chen et al., 2011). Therefore, I propose that GCs and the F-actin within is more likely to be inhibitory than favorable for axon growth. Local forces produced within GCs (Giannone et al., 2009) are more likely to contribute to signaling events important for guidance than to pull the axon forward.

My data so far support this hypothesis. As mentioned in Chapter 3.2.7.1, I found that the Class 2 treatments (profilin, LatA) which have no effect on the short and stabilised cortical actin in axon, but reduces the long and vulnerable actin filaments of GCs, increase axon length significantly when compared to wild type (Fig. 4.2). In contrast, the Class 1 treatments (Arp2/3, CK666, CytoD), which impair actin in both GCs and axons, result in similar axon length to wildtype (Fig. 4.2). These findings are best explained by proposing that axonal actin is growth promoting (green arrow in Fig. 4.2), whereas GCs and the actin within are growth inhibiting (red T). In this scenario, when

simultaneously removing growth-slowing GCs and the growth-promoting actin of axons, both effects cancel each other out and result in wildtype-like extension. This is further supported by establishing potential Class 3 treatments (e.g. Spectrin or adducin) expected to primarily affect axonal actin but less so the GCs (see Chapter 3.2.7.2). In agreement with this, I found that axons are shorter in *adducin* mutant neurons (Fig. 4.2). If this finding can be confirmed in future studies, this would further confirm my hypothesis.

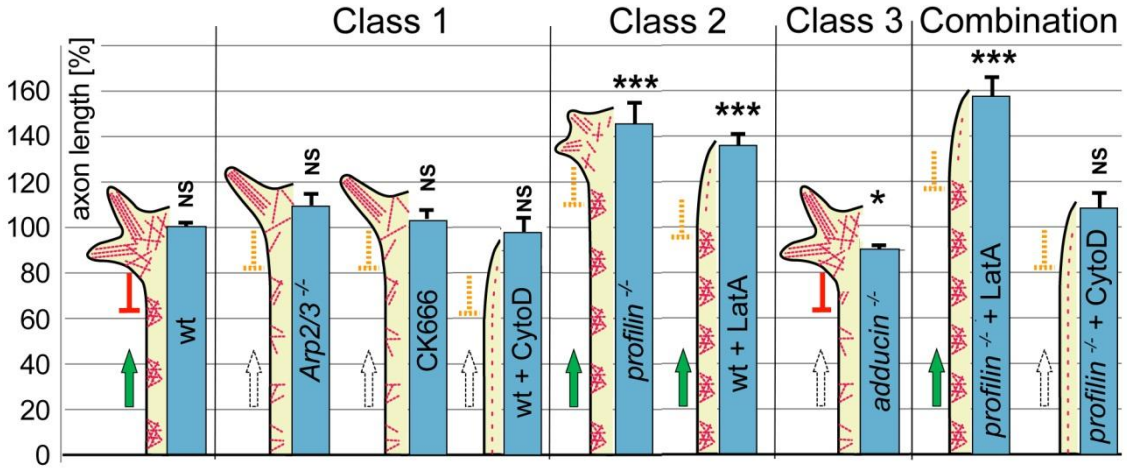

Figure 4.2. *Different class of actin manipulation impact on axon growth differently.*

I propose that Arp2/3 deficiency (Arp2/3$^{-/-}$), Arp2/3 inhibition (CK666 drug) and the drug CytoD affect all F-actin (magenta), whereas profilin loss and LatA application leave axonal actin structures intact, in contrast, lack of adducin causes loss of actin in axon but not in GC ; their effects on axon length (blue bars) are consistent with a model where axonal actin promotes growth (green arrow), antagonised by growth-slowing properties of GCs (red T).

A number of further strategies can be used to investigate the proposed growth-promoting roles of axonal actin. First, since axons keep growing after neurons have undergone synaptogenesis (i.e. have lost their GCs; Fig. 3.18), one could use pharmaco-genetic manipulations and ask whether class 1 and 2 treatments have differential effects. The prediction would be that class 2 treatments have little impact whereas class 1 treatments should negatively impact. To restrict genetic approaches to post-GC stages of neurons, transgenic knock-down constructs can be used in combination with the mifepristone-inducible *ELAV-GeneSwitch* system (Osterwalder et al., 2001). Second, the analysis of axon length can also be carried out in mouse cortical neuron (Sanchez-Soriano et al., 2009), and these neurons are long enough to use them in conjunction with

micro-fluid chambers (Dajas-Bailador et al., 2012). Using such chambers would allow applying actin-destabilising drugs selectively to GCs or axons (Fig. 4.3). Through this, my theory could be directly tested and it could be tested whether this mechanism is evolutionarily conserved.

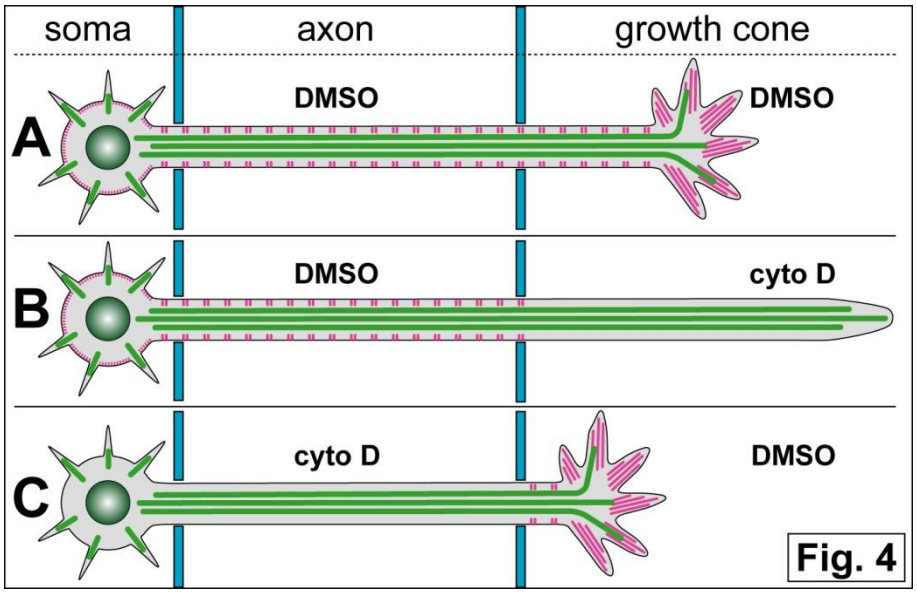

Figure 4.3. *Using micro-fluid chambers in mouse cortical neuron to investigate axon growth.*

I predict that selectively abolish actin by applying CytoD in GC or in axon will impact on axon growth differently.

If the promotion of axon growth through actin in the axon shaft can be established as a valid concept, it will then be important to unravel the underlying mechanisms. One mechanism that clearly seems to be relevant is the promotion of MT polymerisation downstream of F-actin. As my results have shown, this mechanism is not only relevant in *shot* mutant neurons but also in wildtype neurons treated with CytoD there was a decline in polymerisation speed. Such decline would naturally be expected to reduce net polymerisation of MT mass in axons, hence reduce growth capacity. A second mechanism that could be at play is MT sliding. Thus, kinesins as well as dynein have been implicated in MT sliding in the axon, and this could be a mechanism that contributes to growth promoting forces (Lu et al., 2013, del Castillo et al., 2015, Myers et al., 2006a). Interestingly, physical links of dynein/Dynactin were proposed to contribute in this context suggesting another mechanisms through which actin could contribute (Myers et al., 2006b). Finally, the guidance function of F-actin during MT extension could play a role. For example, axons of *chic* mutant neurons are strongly elongated whereas, upon additional loss of Shot in double-mutant neurons, axon length is reduced to the *shot*

mutant length. Therefore, *shot* is over *chic* function in this context. This could even mean that Shot is an active promoter of axon length downstream of *chic* mutant changes in actin networks. For example, it could be speculated that Shot disengages from cortical actin when reaching GCs of wildtype neurons where long actin filaments prevail, but not so in the absence of Chic.

To address this possibility, I performed genetic interaction studies analysing *chic* LOF in *shot* heterozygous mutant background (*chic*$^{221/05205}$ *shot*$^{3/+}$), hypothesising that changes in F-actin networks induced by Chic deficiency might have less effect on MT bundling and axon elongation if one copy of Shot is removed. However, all phenotypes I observed were comparable to those of *chic*^{221} mutant neurons, thus failing to indicate an active role of Shot: the *chic*$^{221/05205}$ *shot*$^{3/+}$ mutant neurons have longer axons (135±5%, $P_{Mann\text{-}Whitney}$<0.001, n=105) comparable to *chic* alone, more and shorter filopodia (117±6%, $P_{Mann\text{-}Whitney}$=0.007, n=105; 65±1%, $P_{Mann\text{-}Whitney}$<0.001, n=1194) also comparable to *chic* alone (Gonçalves-Pimentel et al., 2011), and the disorganisation of MT networks is similar to wildtype (129%, P_{Chi2}=0.190, n=105). This could either mean that Shot performs its role with high affinity (i.e. is little vulnerable to dosage variations), or that my hypothesis about the role of Shot is not correct. Further experiments will have to clarify the actual mechanisms which act downstream of axonal actin during axon elongation.

4.2.5. The role of cortical actin rings

The recently proposed model of cortical rings of adducin-capped, short, bundled actin filaments, arranged by Spectrin into a periodic pattern of 180nm intervals in axons of mouse neurons (Xu et al., 2013) seems to hold true also in *Drosophila* neurons. Thus, we could reproduce the periodic pattern of 180 nm using STORM and SIM, and our pharmaco-genetic analysis I performed so far meet all our predictions base on the above model. For example, LatA has little effect in all assays used, and this is in agreement with the known fact that LatA only binds actin monomers but not actin filaments and is therefore less likely to affect cortical actin which is plus end-capped by Adducin (Morton et al., 2000, Yarmola et al., 2000, Coue et al., 1987). In contrast, CytoD binds and destabilises actin filament plus ends (Casella et al., 1981, Wakatsuki et al., 2001), hence, potentially competes with Adducin and can actively destabilise cortical F-actin. Genetically, I saw little impact of profilin consistent with the fact that actin filaments are short in those networks, whereas loss of Arp2/3 had severe impact suggesting that these networks require high numbers of filaments to execute their proper cellular functions.

Currently, the function of the axonal actin rings is unknown, but it has been speculated to be involved in maintaining the elasticity and stability of axons and regulating the organisation of proteins (e.g. voltage-gated channels) in the plasma

membrane (Xu et al., 2013). As I have discussed above (Chapter 4.2.1, 4.2.3 and 4.2.4), my data suggest that it plays important roles in the regulation of axonal MT bundles including spectraplakin-mediated guidance of extending MTs (Prokop et al., 2013, Alves-Silva et al., 2012), maintaining axonal MTs through promoting their polymerisation, or potentially assisting in MT sliding mechanisms and therefore force production. Such functions seem to be important for axon growth (see Chapter 4.2.4), axon maintenance during ageing (see chapter 4.2.3), but also deliver important explanations for processes of axon degeneration/regeneration as well as plasticity, as will be explained in the following.

When an axon is injured, the early phase of axon regeneration involves axon degeneration of the proximal axon stump, and this seems to be triggered by the destruction of axonal actin networks through calcium-induced calpain activation (Bradke et al., 2012). If my findings apply in this context, the loss of F-actin would trigger the subsequent loss of MTs in this segment and thus mediate axon retraction. Notably, MT loss was particularly prominent in the absence of Shot which contains EF hand domains as potential calcium sensors.

Cortical axonal actin seems also to be important for the formation of axon branches (Kalil and Dent, 2014). Thus, it has been reported that the MT severing protein Spastin positively regulates axon branching through severing axonal MT bundles, thus producing MT fragments which can reorient and initiate transverse MT bundles which, in turn, establish a collateral branch (Yu et al., 2008, Qiang et al., 2010). These off-track MTs and MT fragments are likely to be dependent on and regulated through axonal actin (Gallo, 2011). Accordingly, actin regulators were shown to play roles in axon branching, and inhibition of the actin nucleator Arp2/3 or the actin elongator Ena/VASP both lead to a decrease of axon branching (Strasser et al., 2004, Dwivedy et al., 2007). Since collateral branches are often initiated by filopodial protrusions forming on the axon shaft, axonal actin rings could be an important platform for rapid modification. For example, axonal actin could be targeted by upstream actin regulators to reorganise their short actin filaments for instantaneous polymerisation processes to form the local accumulation of actins which are considered to be the precursors of axonal filopodia (Gallo, 2011).

Apart from unraveling the various functions of cortical actin rings of axons, it is important to further explore their genetic regulation. As explained above (Chapter 4.2.4), pharmaco-genetic analyses are so far consistent with the proposed model derived from mouse axons (Xu et al., 2013), but important further players need to be thoroughly investigated, including Spectrin, adducin and ankyrin. Additional factors that will need consideration are Enabled which is a multi-functional player in actin regulation and very likely to play a role (Bear and Gertler, 2009). Furthermore, Arp2/3 function goes

alongside formins, in particular DAAM in *Drosophila* neurons (Gonçalves-Pimentel et al., 2011), and DAAM would be a promising candidate for further investigations. Whilst providing further insights into the regulation of actin rings, analysing these other candidate genes will provide further genetic means also to investigate the role of cortical actin in axons.

4.3. Actin-independent roles of Shot in MT bundle maintenance

It was already known that MT stabilising functions (nocodazole resistance) of Shot through its GRD domain are mostly actin-independent (Alves-Silva et al., 2012), and my experiments with CytoD-treated Shot-LA^{only} and *shot* mutant neurons cultured on ConA seem to have generated a condition in which this function can be further analysed (explained in Chapter 3.2.2).

Furthermore, I now found that there are other, more important actin-independent functions of Shot. From my results, I hypothesise that Shot plays roles in MT bundle maintenance through one of its internal domains, the plakin repeat region (PRR) which is found only in one predicted Shot isoform (Fig. 3.6) (Roper and Brown, 2003). In my experiments, I made several findings in support this hypothesis.

First, when Shot-LA^{only} neurons are treated with CytoD, their axons collapse when grown on glass and show a high degree of MT disorganisation when grown on ConA where membranes seems to display a tendency to retract with less rigour (see Chapter 3.2.1 and 3.2.2). Together, these results clearly show that Shot-LA only represents part of the full repertoire of Shot functions. My live imaging experiments with CytoD-treated *shot* mutant and wildtype neurons had shown that Shot can sustain MT polymerisation in the absence of F-actin. Since axons are still lost in Shot-LA^{only} mutant neurons cultured on glass (analogous to Fig. 4.4F), this suggests that GRD-mediated functions of Shot-LA cannot explain the robust maintenance of MT polymerisation observed in CytoD-treated wildtype neurons over long time periods (Fig. 4.2)

Second, Shot-LA^{only} neurons are not fully rescued when cultured on ConA-treated cover slips. A reasonable explanation is that when neurons are cultured on ConA-treated cover slips, axons are strongly adhered and become wider, providing more space for MTs to expand. If bundle-formation and maintenance mainly depends on MT guidance into parallel bundles through Shot-LA (Fig. 4.4D), axons growing on ConA provide a far more challenging situation where MTs can become disorganised. This condition can be improved, if this role of Shot is complemented by its PRR-mediated bundle maintaining functions, holding MTs together and stabilising bundles from within (black cross in Fig. 4.4A).

A further support comes from previous experiments in the Prokop laboratory with a C-terminal truncated version of Shot-LA (Shot-ΔCtail) which was unable to rescue MT disorganisation in *shot* mutant neurons. In contrast, an identical truncation of the endogenous protein in the *shot*^{V104} mutant allele has no obvious phenotype (Figs. 4.4B; Juliana Alves-Silva and Natalia Sánchez-Soriano, unpublished results). However, *shot*^{V104} shows a mild MT disorganisation phenotype when neurons are plated on ConA, suggesting that it displays only partial function: it displays the MT bundle maintenance function, whereas it lacks the guidance function which requires Ctail.

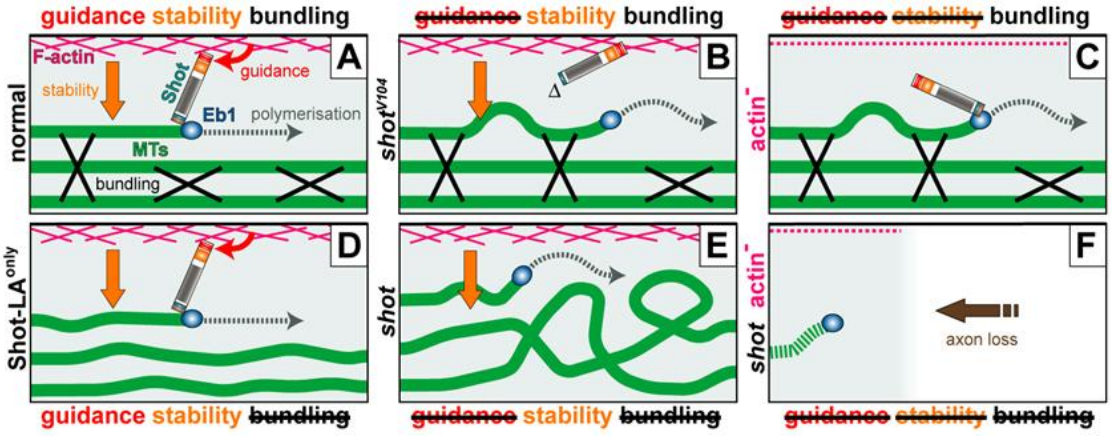

Figure 4.4. *The model of Shot actin-independent function in MT bundling.*

This figure illustrates the hypothesised impact that different pharmacological treatments or genetic manipulations have on axonal MT bundles. Shot has at least three important functions in axons: guidance of extending MTs (red curved arrow); stabilisation of MT polymerisation in the absence of actin (orange arrow); MT bundling (black cross).

The PRR is a good candidate domain of Shot mediating its actin-independent MT bundle maintenance. The PRR of the mammalian Shot homologue dystonin can potential bind to intermediate filaments (Leung et al., 2002). However, intermediate filaments are virtually absent in *Drosophila* (Adams et al., 2000). Interestingly, the *Drosophila* Futsch is the homologue of mammalian MAP1B which can cross-link MTs through its N- and C-terminal MT-binding domains; however, in deviation from MAP1B, Futsch contains a large domain composed of IF-like repeat domains (IFD) (Halpain and Dehmelt, 2006, Hummel et al., 2000, Bettencourt da Cruz et al., 2005, Gogel et al., 2006). One possibility is therefore that the PRR of Shot binds the IFD of Futsch (Fig. 4.5). In support of this view, the isolated PRR localises along axons (Fig. 4.5B), suggesting that it might bind to Futsch, thus potentially establishing a link from Shot to Futsch through the central PRR. A rapid first test would be to test the expression of PRR in the absence of Futsch using futsch null mutant neurons. Next, one could use genetic interaction studies to

further support functional links between Shot and Futsch. For example, one could use trans-heterozygous constellations (*futsch*$^{P158/+}$ *shot*$^{3/+}$) and treat these neurons with CytoD to see whether both genes contribute to the same actin-independent pathway in maintaining MT bundles. Another approach would be to use *shot*^{V104} mutant embryos and test whether these are more dependent on Futsch function (*futsch*$^{P158/+}$; *shot*^{V104}/ *shot*^{V104}). Finally, one could perform standard pull-down assays of PRR and IFB to assay the direct interaction between these two domains.

Through the experiment mentioned above, it would be possible to test the working hypothesis and thus, hopefully, gain a better understanding of Shot actin-independent functions. At the same time, this would provide explanation for the function of the IFD of Futsch which is not present in mammalian MAP1B, thus presenting exciting evolutionary explanations for how *Drosophila* compensates for the absence for intermediate filament genes. Since also the Shot homologue dystonin displays PRR-containing isoforms, confirming the proposed Shot-Futsch links would suggest that there might also be intermediate filament-dystonin links in mammalian neurons for which first functional concepts could then be provided.

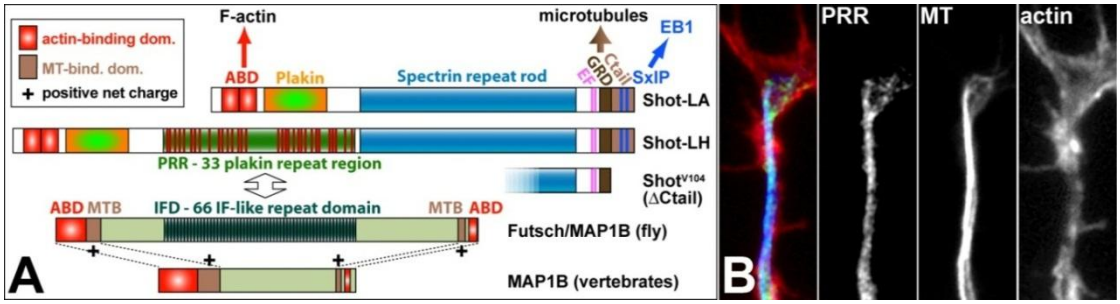

Figure 4.5. *Shot PRR is a potential domain in actin-impendent roles of Shot in MT bundle maintenance.*

A) *Illustration of the functional domains of different Shot isoforms, shot*^{V104} *mutants, fly Futsch/MAP1B and vertebrate MAP1B. Functional domains are shown as indicated.* ***B)*** *The isolated PRR localises to MTs in Drosophila neurons. Figure kindly provided by Andreas Prokop.*

4.4. The cortical collapse factor Efa6 eliminates MTs and performs check point functions in axons

Human EFA6 was first identified as an Arf6 GEF which performs its function via its Sec7 domain (Franco et al., 1999). Later on, the PH domain and coiled-coil domain of Efa6 also have been found to regulate actin cytoskeleton organisation at the plasma membrane (Franco et al., 1999, Derrien et al., 2002). These functional domains are

highly conserved over species. Recently, it has been found that in *C. elegans,* Efa6 limits MT growth at the cell cortex and inhibits axon regeneration, and this requires the PH domain and N-terminus (Chen et al., 2011). Although, the N-terminus of Efa6 is evolutionarily not well conserved at the sequence level, its MT collapse function is clearly well conserved in *Drosophila* suggesting that the functional mechanisms required are encoded in this region through features not obviously reflected in the sequence. To give an example explaining this, the sequence of the Ctail region of Shot is not at all conserved with that of mammalian spectraplakins but clearly functionally conserved, which is due to defined short SxIP motifs and the generally high content of positively charged amino acids (Alves-Silva et al., 2012). Interestingly, also the Efa6 N-term is positively charges and contains SxIP motifs, and these features seem to be partially conserved in *C. elegans* and mouse (Fig. 3.19).

My data have clearly shown that the N-terminus of *Drosophila* Efa6 has MT collapse function acting as an axon-destabilising dominant negative factor when expressed in neurons in the absence of this membrane-anchoring PH domain (Fig. 3.26). Accordingly, in the absence of Efa6, axon length is increased to ~120%, there are more EB1 comets in GCs, and more MTs protrude into the filopodia (Fig. 3.21, 3.23 and 3.24). These findings are consistent with the model I mentioned before in which occasional MTs going off-track can be eliminated by Efa6 function at the plasma membrane, whereas persisting off-track MTs in axons contribute to MT disorganisation over time and failure to eliminate them in GCs contributes to extra growth, likely explaining improved axon regeneration in *efa6* mutant neurons of *C. elegans* (Chen et al., 2011).

4.4.1. What are the mechanisms through which Efa6 removes MTs?

MT can be removed in different ways, for example through plus end depolymerisation by specific mitotic centromere-associated kinesin (MCAK) (Howard and Hyman, 2007, Kinoshita et al., 2006), or through ATP-dependent severing protein, such as Katanin, Spastin and Fidgetin (Mukherjee et al., 2012, Sharp et al., 2012, Sharp and Ross, 2012). Of the latter class, Katanin mainly affects MTs in neuronal cell bodies, and axonal MTs which are less protected by Tau (Sharp and Ross, 2012, Yu et al., 2008). One hypothesis is that Katanin cuts MTs at the centrosomes into small fragments, and then these MT segments are transported to axons acting as nuclei which can polymerise into new MTs (Sharp and Ross, 2012, Yu et al., 2008). In contrast, Spastin can sever MTs in both cell bodies and axons (Yu et al., 2008), and in axons this is important for axonal branching (Sharp and Ross, 2012, Yu et al., 2008).

A number of observations provide potential hints about the molecular mechanisms of Efa6. First, I have observed a plus end tracking behaviour when overexpressing Efa6-

Nterm and this might suggest that it operates in a mode similar to MCAK which binds MT plus ends through EB1 to then actively depolymerise them (Lee et al., 2008). However, it still needs to be confirmed whether the SxIP motifs of Efa6 and binding to EB1 are required. One strategy to address this is to perform CoIPs or pull downs to assess binding of EB1 to Efa6 and test whether SxIP mutations interfere with this interaction. Using N-terminal Efa6 constructs in which the SxIP motifs are mutated would also allow to test whether MT plus end binding is required for MT collapse.

Alternatively, binding along the shaft of MTs via the positive net charge of the N-terminus could be a major functional requirement. In *C.elegans*, another MT-binding motif in form of a short stretch of 18 amino acids in the N-terminus has been shown to be important (O'Rourke et al., 2010). This motif is conserved in *Drosophila* (Fig. 3.19) and its functional relevance can be similarly tested using constructs carrying a deletion of this motif. If this direct interaction with MT shafts is required, the function might be more similar to severing proteins.

A major step would also be to assess the role of Efa6 N-terminus in MT collapse using *in vitro* systems of MT polymerisation, thus testing whether Efa6 acts directly as a collapse factor or whether additional proteins are required for its function. Furthermore, it needs to be further confirmed that the Efa6 N-terminus needs to be tethered to the plasma membrane, likely through the PH domain, so that Efa6 is properly compartmentalised and can function as a check-point rather than act as a dominant negative element. To test this, one can replace the PH domain with other membrane binding motifs, such as CAAX box which has been used in *C.elegans* to demonstrate membrane tethering requirements for Efa6 function (O'Rourke et al., 2010).

Through these various experiments, further molecular understanding of the roles that Efa6 plays in axon growth, maintenance and regeneration will be gained, thus consolidating its role as an important regulator of axon biology.

4.4.2. Efa6 may play an important role during axonal aging

One hypothesis explaining a number of neurodegenerative diseases or normal axon decay during ageing is based on the observation that axons can form patches of disorganised MTs, so called diverticula, which trap mitochondria leading to oxidative stress and eventually axonal and neuronal decay (Fiala et al., 2007, Adalbert and Coleman, 2012). I found that MTs became disorganised in *efa6* mutant neurons, and observed abundant Efa6 expression in the adult *Drosophila* brain, and the same is true for the Efa6A gene in the mammalian nervous system (Sakagami et al., 2004, Chen et al., 2011, Huang et al., 2009). Therefore, if Efa6 acts as a check point preventing MT disorganisation through removal of accidental off-track MTs, the loss of Efa6 might be

more important during nervous system maintenance than development, since it can be expected that MT polymerisation continues in the ageing nervous system to prevent senescence of MT bundles (Prokop, 2013). One prediction from this hypothesis would be that MT disorganisation increases over time, since Shot-dependent mechanisms of MT bundle formation are not affected in these neurons.

During my project work, I used a readout that was insufficient to properly address this point. Thus, I used a binary readout determining whether there is any MT disorganisation in axons or not. This readout showed a high degree of disorganisation, almost comparable to *shot* mutant neurons (Fig. 3.21). Since then, Ines Hahn developed a new readout determining the area of disorganisation divided by axon length, and this readout shows a very mild phenotype in developing axons but an increase in severity over the next days (unpublished). Taken together, my and Ines' results would mean that first crystallisation points of disorganisation are being formed already in developing axons which then develop into prominent diverticula over time. On-going experiments by Ines also show that knock-down of Efa6 in the nervous system leads to decreased performance in climbing assays (assessing motor fitness) over time (unpublished). These findings are in agreement with a model in which Efa6 plays an important role during axonal ageing by eliminating disorganised MTs and thus preventing the formation of diverticula.

However, further experiments need to be done. First, we need to determine whether neurons or their axons decay upon *efa6* deficiency, and for this cell death markers can be used (Sarkissian et al., 2014) and many Gal4 lines for the simultaneous knock-down of *efa6* whilst analysing their anatomy with suitable reporter genes (Milyaev et al., 2012). Second, fly models of neurodegeneration, such as Alzheimer's disease (Nussbaum et al., 2013), can be used to ask whether absence of Efa6 enhances their phenotypes, or whether targeted expression of Efa6 can ameliorate the condition. As one promising data set, Ines Hahn already established that double mutant constellations of *shot* with *efa6* lead to a vastly enhanced MT disorganisation phenotype, indicative of the fact that their roles are complementary and in agreement with our model.

4.5. How applicable are these insights from Drosophila to mammalian axon biology?

Drosophila has been widely used to study the roles and regulation of the cytoskeleton in neurons and neuronal disease (Sanchez-Soriano et al., 2007, Prokop et al., 2013). The axon biology is highly conserved between *Drosophila* and mammals in many aspects. First, cytoskeletal dynamics and network organisation in neurons is comparable between *Drosophila* and mammals, such as the anterograde and retrograde

tracking of EB1 (indicating similar MT dynamics), the number, length, protrusion and retraction of filopodia (actin dynamics) or the axon growth rate (Sanchez-Soriano et al., 2010). Furthermore, I could show that the axonal actin rings first found in mouse (Xu et al., 2013) are likewise existing in *Drosophila* mature neuron.

Second, known key regulators of the cytoskeleton, in particular the actin-binding (e.g. Enabled/VASP, Myosin II, formins, Fascin) and MT-binding proteins (CLASP, Lis1, MAPs/Futsch, dystonin/BPAG1, MACF1/ACF7/Shot, CLIP-170/190), are evolutionarily highly conserved between mammals *and Drosophila* (Lantz and Miller, 1998, Swan et al., 1999, Lemos et al., 2000, Halpain and Dehmelt, 2006, Dehmelt and Halpain, 2005, Roper et al., 2002, Carl et al., 1999, Prokop et al., 2013).

Furthermore, also the functions of proteins which regulate axon biology tend to be conserved between *Drosophila* and mammals. For example, functional deficiency of the human Spectraplakin dystonin causes Hereditary Sensory Autonomic Neuropathy (Edvardson et al., 2012) and in mouse models (Ferrier et al., 2014, Horie et al., 2014). It has been shown in mouse and *Drosophila* alike that loss of spectraplakins causes MT bundle disorganisation and makes axonal MTs vulnerable to MT-destabilising drugs (Dalpe et al., 1998, Yang et al., 1999, Sanchez-Soriano et al., 2009), and the underlying molecular mechanisms were studied and understood in flies (Alves-Silva et al., 2012). Another example is Tau, a MAP which plays an important role in stabilising MTs in axon (Morris et al., 2011). Hyperphosphorylated Tau is considered as a hallmark for Alzheimer's disease (Iqbal et al., 2009, Wang and Liu, 2008, Zempel and Mandelkow, 2014, Buee et al., 2000, Iqbal et al., 2010, Matus, 1991). Although Tau is not highly conserved in *Drosophila* at the sequence level except for its MT-binding domains, there is a clear functional correlation upon loss of Tau (Gistelinck et al., 2012, Bolkan and Kretzschmar, 2014). Other examples of functional conservation concern roles of actin binding proteins, such as Ena/VASP and Arp2/3 in filopodia formation (Korobova and Svitkina, 2008, Gonçalves-Pimentel et al., 2011, Lebrand et al., 2004, Prokop et al., 2013).

Taken together, the axon biology from *Drosophila* to mammals displays great similarities in many aspects, such as cytoskeleton regulation, conservation of protein sequence and function. Therefore, novel mechanisms found through research in *Drosophila* neurons are likely to also apply to mammalian neurons and help to focus research in higher animals.

4.6. Key conclusions and future prospects

My project has address timely problems within the field of cell biology, i.e. the quest for understanding actin-linkage and cortical capture/collapse - two aspects that have long

been acknowledged to be pivotal for the regulation of axon growth and maintenance. For this, I have used experimentally and genetically amenable neurons of Drosophila, which provide fantastic cellular and subcellular readouts. Through capitalising on these advantages, I have unravelled several novel molecules and mechanisms involved in the linkage/capture/collapse phenomenon and provided a better understanding of the regulation of MTs during axon growth and maintenance.

My work has revealed a number of new mechanisms involved in MT bundle formation and maintenance complementing the already proposed roles of Shot in the guidance of extending MTs. It could be speculated that these various mechanisms complement each other to form a common machinery of MTs bundle formation and maintenance in axons leading to a model of "local axonal homeostasis" (Fig. 4.6). This model proposes that MTs undergo steady turn-over requiring machinery that maintains this process in order. To achieve this, a number of MT-regulating mechanisms operate locally in the axon, i.e. there is no requirement for central orchestration from the cell body.

Interestingly, three of the proposed mechanisms (1, 2 and 3 in Fig. 4.6) lead to MT disorganisation when abolished, whereas the actin-dependent maintenance of disorganised MTs (4 in Fig. 4.6) has the opposite effect, suggesting that the system is in a fine balance. More mechanisms are clearly contributing to this regulation, such as regulators of MT polymerisation, MT severing or mechanisms of MT sliding. Aberration of any of these could lead to MT disorganisation and thus the formation of axon swellings or diverticula, which are considered detrimental for axons (Adalbert and Coleman, 2012). This working hypothesis can now be directly tested, building on the ease of experimentation in the fly system, to be then translated into mammalian biology. The “local homoeostasis” model describes mechanisms which prevent MT disorganisation, thus helping to maintain the nervous system during healthy ageing. Many of the factors proposed to be involved (dystonin, spastin, stathmin, kinesin-1, MAP1B, tau) already have close links to neurodegeneration, but for none of them the pathomechanism are clear. The model of local homeostasis provides a promising new framework for work on these factors and the causes of neurodegeneration in the context of one common axonal cell biology.

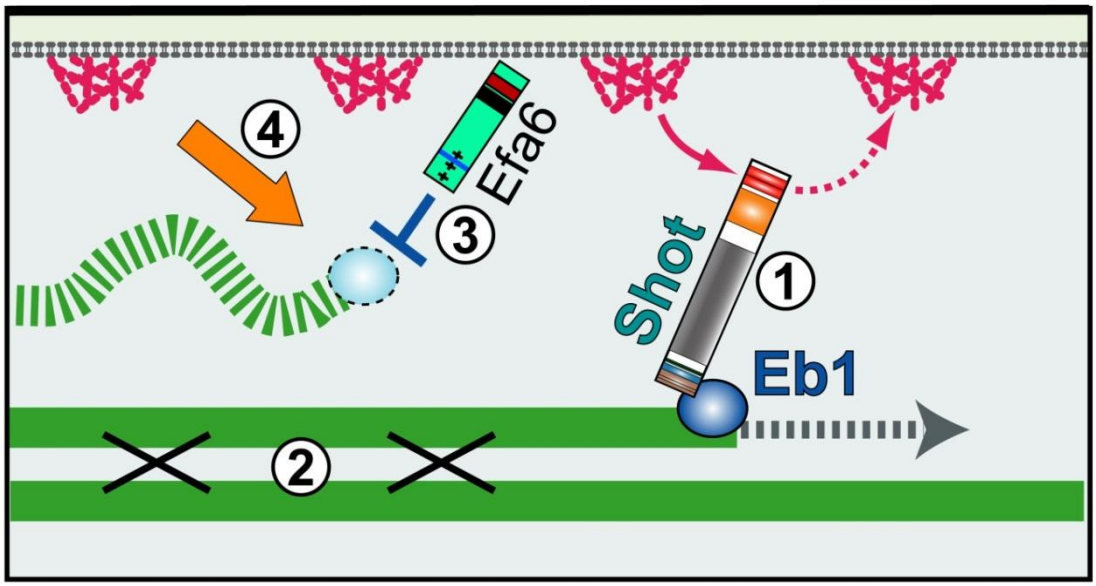

Figure 4.6. *Cartoon description of local homeostasis.*

1) *Guidance function: Shot guides polymerising MTs along F-actin to lay them into parallel bundles.* ***2)*** *Bundling function: MT binding protein, such as MAP1B and tau, cross-links MTs.* ***3)*** *Check point function: Efa6 localise at the cortex to eliminate "lost" MTs.* ***4)*** *Stabilising function: cortical actin selectively stabilises MTs.*

References

Adalbert, R. & Coleman, M. P. 2012. Axon pathology in age-related neurodegenerative disorders. *Neuropathol Appl Neurobiol*.

Adams, M. D., Celniker, S. E., Holt, R. A., Evans, C. A., Gocayne, J. D., Amanatides, P. G., Scherer, S. E., Li, P. W., Hoskins, R. A., Galle, R. F., George, R. A., Lewis, S. E., Richards, S., Ashburner, M., Henderson, S. N., Sutton, G. G., Wortman, J. R., Yandell, M. D., Zhang, Q., Chen, L. X., Brandon, R. C., Rogers, Y. H., Blazej, R. G., Champe, M., Pfeiffer, B. D., Wan, K. H., Doyle, C., Baxter, E. G., Helt, G., Nelson, C. R., Gabor, G. L., Abril, J. F., Agbayani, A., An, H. J., Andrews-Pfannkoch, C., Baldwin, D., Ballew, R. M., Basu, A., Baxendale, J., Bayraktaroglu, L., Beasley, E. M., Beeson, K. Y., Benos, P. V., Berman, B. P., Bhandari, D., Bolshakov, S., Borkova, D., Botchan, M. R., Bouck, J., Brokstein, P., Brottier, P., Burtis, K. C., Busam, D. A., Butler, H., Cadieu, E., Center, A., Chandra, I., Cherry, J. M., Cawley, S., Dahlke, C., Davenport, L. B., Davies, P., de Pablos, B., Delcher, A., Deng, Z., Mays, A. D., Dew, I., Dietz, S. M., Dodson, K., Doup, L. E., Downes, M., Dugan-Rocha, S., Dunkov, B. C., Dunn, P., Durbin, K. J., Evangelista, C. C., Ferraz, C., Ferriera, S., Fleischmann, W., Fosler, C., Gabrielian, A. E., Garg, N. S., Gelbart, W. M., Glasser, K., Glodek, A., Gong, F., Gorrell, J. H., Gu, Z., Guan, P., Harris, M., Harris, N. L., Harvey, D., Heiman, T. J., Hernandez, J. R., Houck, J., Hostin, D., Houston, K. A., Howland, T. J., Wei, M. H., Ibegwam, C., et al. 2000. The genome sequence of Drosophila melanogaster. *Science,* 287**,** 2185-95.

Ahmad, F. J., Echeverri, C. J., Vallee, R. B. & Baas, P. W. 1998. Cytoplasmic dynein and dynactin are required for the transport of microtubules into the axon. *J Cell Biol,* 140**,** 391-401.

Ahmad, F. J., He, Y., Myers, K. A., Hasaka, T. P., Francis, F., Black, M. M. & Baas, P. W. 2006. Effects of dynactin disruption and dynein depletion on axonal microtubules. *Traffic,* 7**,** 524-37.

Akhmanova, A. & Steinmetz, M. O. 2008. Tracking the ends: a dynamic protein network controls the fate of microtubule tips. *Nat Rev Mol Cell Biol,* 9**,** 309-22.

Akhmanova, A. & Steinmetz, M. O. 2010. Microtubule +TIPs at a glance. *J Cell Sci,* 123**,** 3415-9.

Alves-Silva, J., Hahn, I., Huber, O., Mende, M., Reissaus, A. & Prokop, A. 2008. Prominent actin fiber arrays in Drosophila tendon cells represent architectural elements different from stress fibers. *Mol Biol Cell,* 19**,** 4287-97.

Alves-Silva, J., Sánchez-Soriano, N., Beaven, R., Klein, M., Parkin, J., Millard, T., Bellen, H., Venken, K. J. T., Ballestrem, C., Kammerer, R. A. & Prokop, A. 2012. Spectraplakins promote microtubule-mediated axonal growth by functioning as structural microtubule-associated proteins and EB1-dependent +TIPs (Tip Interacting Proteins). *J. Neurosci,* 32**,** 9143-58.

Amieva, M. R. & Furthmayr, H. 1995. Subcellular localization of moesin in dynamic filopodia, retraction fibers, and other structures involved in substrate exploration, attachment, and cell-cell contacts. *Exp Cell Res,* 219**,** 180-96.

Aratyn, Y. S., Schaus, T. E., Taylor, E. W. & Borisy, G. G. 2007. Intrinsic dynamic behavior of fascin in filopodia. *Mol Biol Cell,* 18**,** 3928-40.

Araujo, H., Machado, L. C., Octacilio-Silva, S., Mizutani, C. M., Silva, M. J. & Ramos, R. G. 2003. Requirement of the roughest gene for differentiation and time of death of interommatidial cells during pupal stages of Drosophila compound eye development. *Mech Dev,* 120**,** 537-47.

Araujo, S. J. & Tear, G. 2003. Axon guidance mechanisms and molecules: lessons from invertebrates. *Nat Rev Neurosci,* 4**,** 910-22.

Arpin, M., Chirivino, D., Naba, A. & Zwaenepoel, I. Emerging role for ERM proteins in cell adhesion and migration. *Cell Adh Migr,* 5**,** 199-206.

Ashburner, M. 1993. Epilogue. *In:* Bate, M. & Martínez Arias, A. (eds.) *The development of Drosophila melanogaster.* Cold Spring Harbor: CSH Laboratory Press.

Aumailley, M., Has, C., Tunggal, L. & Bruckner-Tuderman, L. 2006. Molecular basis of inherited skin-blistering disorders, and therapeutic implications. *Expert reviews in molecular medicine,* 8**,** 1-21.

Baas, P. W., Vidya Nadar, C. & Myers, K. A. 2006. Axonal transport of microtubules: the long and short of it. *Traffic,* 7**,** 490-8.

Baines, A. J. 2010. The spectrin-ankyrin-4.1-adducin membrane skeleton: adapting eukaryotic cells to the demands of animal life. *Protoplasma,* 244**,** 99-131.

Bamburg, J. R. & Bloom, G. S. 2009. Cytoskeletal pathologies of Alzheimer disease. *Cell motility and the cytoskeleton,* 66**,** 635-49.

Bashaw, G. J., Kidd, T., Murray, D., Pawson, T. & Goodman, C. S. 2000. Repulsive axon guidance: Abelson and Enabled play opposing roles downstream of the roundabout receptor. *Cell,* 101**,** 703-15.

Bashaw, G. J. & Klein, R. 2010. Signaling from axon guidance receptors. *Cold Spring Harb Perspect Biol,* 2**,** a001941.

Basto, R., Lau, J., Vinogradova, T., Gardiol, A., Woods, C. G., Khodjakov, A. & Raff, J. W. 2006. Flies without centrioles. *Cell,* 125**,** 1375-86.

Bear, J. E. & Gertler, F. B. 2009. Ena/VASP: towards resolving a pointed controversy at the barbed end. *J Cell Sci,* 122**,** 1947-53.

Beaven, R. 2012. *Molecular mechanisms of +TIPs in axonal extension.* PhD, The University of Manchester.

Bellen, H. J., Tong, C. & Tsuda, H. 2010. 100 years of Drosophila research and its impact on vertebrate neuroscience: a history lesson for the future. *Nat Rev Neurosci,* 11**,** 514-22.

Bennett, V. & Baines, A. J. 2001. Spectrin and ankyrin-based pathways: metazoan inventions for integrating cells into tissues. *Physiol Rev,* 81**,** 1353-92.

Bettencourt da Cruz, A., Schwarzel, M., Schulze, S., Niyyati, M., Heisenberg, M. & Kretzschmar, D. 2005. Disruption of the MAP1B-related protein FUTSCH leads to changes in the neuronal cytoskeleton, axonal transport defects, and progressive neurodegeneration in Drosophila. *Molecular biology of the cell,* 16**,** 2433-42.

Bichenback, J. (ed.) 2013. *International Perspectives on Spinal Cord Injury,* Switzerland: WHO, ISCOS.

Bielas, S. L., Serneo, F. F., Chechlacz, M., Deerinck, T. J., Perkins, G. A., Allen, P. B., Ellisman, M. H. & Gleeson, J. G. 2007. Spinophilin facilitates dephosphorylation of doublecortin by PP1 to mediate microtubule bundling at the axonal wrist. *Cell,* 129**,** 579-91.

Bina, S., Wright, V. M., Fisher, K. H., Milo, M. & Zeidler, M. P. 2010. Transcriptional targets of Drosophila JAK/STAT pathway signalling as effectors of haematopoietic tumour formation. *EMBO Rep,* 11**,** 201-7.

Bischof, J., Maeda, R. K., Hediger, M., Karch, F. & Basler, K. 2007. An optimized transgenesis system for Drosophila using germ-line-specific phiC31 integrases. *Proceedings of the National Academy of Sciences of the United States of America,* 104**,** 3312-7.

Blanchoin, L., Boujemaa-Paterski, R., Sykes, C. & Plastino, J. 2014. Actin dynamics, architecture, and mechanics in cell motility. *Physiol Rev,* 94**,** 235-63.

Bolkan, B. J. & Kretzschmar, D. 2014. Loss of Tau results in defects in photoreceptor development and progressive neuronal degeneration in Drosophila. *Developmental neurobiology,* 74**,** 1210-25.

Bottenberg, W., Sanchez-Soriano, N., Alves-Silva, J., Hahn, I., Mende, M. & Prokop, A. 2009. Context-specific requirements of functional domains of the Spectraplakin Short stop in vivo. *Mech Dev,* 126**,** 489-502.

Boulakirba, S., Macia, E., Partisani, M., Lacas-Gervais, S., Brau, F., Luton, F. & Franco, M. 2014. Arf6 exchange factor EFA6 and endophilin directly interact at the plasma membrane to control clathrin-mediated endocytosis. *Proc Natl Acad Sci U S A,* 111**,** 9473-8.

Bouquet, C. & Nothias, F. 2007. Molecular mechanisms of axonal growth. *Adv Exp Med Biol,* 621**,** 1-16.

Bradke, F., Fawcett, J. W. & Spira, M. E. 2012. Assembly of a new growth cone after axotomy: the precursor to axon regeneration. *Nature reviews. Neuroscience,* 13**,** 183-93.

Brancolini, C., Benedetti, M. & Schneider, C. 1995. Microfilament reorganization during apoptosis: the role of Gas2, a possible substrate for ICE-like proteases. *EMBO J,* 14**,** 5179-90.

Brandt, R. 1998. Cytoskeletal mechanisms of axon outgrowth and pathfinding. *Cell and tissue research,* 292**,** 181-9.

Bray, D. 1984. Axonal growth in response to experimentally applied mechanical tension. *Dev Biol,* 102**,** 379-89.

Briggs, M. W. & Sacks, D. B. 2003. IQGAP proteins are integral components of cytoskeletal regulation. *EMBO Rep,* 4**,** 571-4.

Broadie, K., Baumgartner, S. & Prokop, A. 2011. Extracellular matrix and its receptors in Drosophila neural development. *Dev Neurobiol,* 71**,** 1102-30.

Broderick, M. J. & Winder, S. J. 2005. Spectrin, alpha-actinin, and dystrophin. *Adv Protein Chem,* 70**,** 203-46.

Buck, K. B. & Zheng, J. Q. 2002. Growth cone turning induced by direct local modification of microtubule dynamics. *J Neurosci,* 22**,** 9358-67.

Budnik, V., Koh, Y. H., Guan, B., Hartmann, B., Hough, C., Woods, D. & Gorczyca, M. 1996. Regulation of synapse structure and function by the Drosophila tumor suppressor gene dlg. *Neuron,* 17**,** 627-40.

Buee, L., Bussiere, T., Buee-Scherrer, V., Delacourte, A. & Hof, P. R. 2000. Tau protein isoforms, phosphorylation and role in neurodegenerative disorders. *Brain Res Brain Res Rev,* 33**,** 95-130.

Cagan, R. 2009. Principles of Drosophila eye differentiation. *Current topics in developmental biology,* 89**,** 115-35.

Carl, U. D., Pollmann, M., Orr, E., Gertlere, F. B., Chakraborty, T. & Wehland, J. 1999. Aromatic and basic residues within the EVH1 domain of VASP specify its interaction with proline-rich ligands. *Curr Biol,* 9**,** 715-8.

Carlier, M. F., Laurent, V., Santolini, J., Melki, R., Didry, D., Xia, G. X., Hong, Y., Chua, N. H. & Pantaloni, D. 1997. Actin depolymerizing factor (ADF/cofilin) enhances the rate of filament turnover: implication in actin-based motility. *J Cell Biol,* 136**,** 1307-22.

Casella, J. F., Flanagan, M. D. & Lin, S. 1981. Cytochalasin D inhibits actin polymerization and induces depolymerization of actin filaments formed during platelet shape change. *Nature,* 293**,** 302-5.

Casso, D., Ramirez-Weber, F. & Kornberg, T. B. 2000. GFP-tagged balancer chromosomes for Drosophila melanogaster. *Mechanisms of development,* 91**,** 451-4.

Challacombe, J. F., Snow, D. M. & Letourneau, P. C. 1996. Actin filament bundles are required for microtubule reorientation during growth cone turning to avoid an inhibitory guidance cue. *J Cell Sci,* 109 (Pt 8)**,** 2031-40.

Challacombe, J. F., Snow, D. M. & Letourneau, P. C. 1997. Dynamic microtubule ends are required for growth cone turning to avoid an inhibitory guidance cue. *J. Neurosci.,* 17**,** 3085-3095.

Chedotal, A. 2007. Slits and their receptors. *Adv Exp Med Biol,* 621**,** 65-80.

Chen, L., Wang, Z., Ghosh-Roy, A., Hubert, T., Yan, D., O'Rourke, S., Bowerman, B., Wu, Z., Jin, Y. & Chisholm, A. D. 2011. Axon regeneration pathways identified by systematic genetic screening in C. elegans. *Neuron,* 71**,** 1043-57.

Chesarone, M. A. & Goode, B. L. 2009. Actin nucleation and elongation factors: mechanisms and interplay. *Curr Opin Cell Biol,* 21**,** 28-37.

Chilton, J. K. 2006. Molecular mechanisms of axon guidance. *Dev Biol,* 292**,** 13-24.

Choi, S., Ko, J., Lee, J. R., Lee, H. W., Kim, K., Chung, H. S., Kim, H. & Kim, E. 2006. ARF6 and EFA6A regulate the development and maintenance of dendritic spines. *J Neurosci,* 26**,** 4811-9.

Clohisey, S. M., Dzhindzhev, N. S. & Ohkura, H. 2014. Kank Is an EB1 interacting protein that localises to muscle-tendon attachment sites in Drosophila. *PLoS One,* 9**,** e106112.

Cohan, C. S., Welnhofer, E. A., Zhao, L., Matsumura, F. & Yamashiro, S. 2001. Role of the actin bundling protein fascin in growth cone morphogenesis: localization in filopodia and lamellipodia. *Cell Motil Cytoskeleton,* 48**,** 109-20.

Conde, C. & Caceres, A. 2009. Microtubule assembly, organization and dynamics in axons and dendrites. *Nat Rev Neurosci,* 10**,** 319-32.

Coue, M., Brenner, S. L., Spector, I. & Korn, E. D. 1987. Inhibition of actin polymerization by latrunculin A. *FEBS Lett,* 213**,** 316-8.

Dajas-Bailador, F., Bonev, B., Garcez, P., Stanley, P., Guillemot, F. & Papalopulu, N. 2012. microRNA-9 regulates axon extension and branching by targeting Map1b in mouse cortical neurons. *Nature neuroscience*.

Dalpe, G., Leclerc, N., Vallee, A., Messer, A., Mathieu, M., De Repentigny, Y. & Kothary, R. 1998. Dystonin is essential for maintaining neuronal cytoskeleton organization. *Molecular and cellular neurosciences,* 10**,** 243-57.

Davenport, R. W., Dou, P., Rehder, V. & Kater, S. B. 1993. A sensory role for neuronal growth cone filopodia. *Nature,* 361**,** 721-724.

De Arcangelis, A., Georges-Labouesse, E. & Adams, J. C. 2004. Expression of fascin-1, the gene encoding the actin-bundling protein fascin-1, during mouse embryogenesis. *Gene Expr Patterns,* 4**,** 637-43.

Dehmelt, L. & Halpain, S. 2005. The MAP2/Tau family of microtubule-associated proteins. *Genome biology,* 6**,** 204.

del Castillo, U., Lu, W., Winding, M., Lakonishok, M. & Gelfand, V. I. 2015. Pavarotti/MKLP1 regulates microtubule sliding and neurite outgrowth in Drosophila neurons. *Current biology : CB,* 25**,** 200-5.

Dent, E. W., Callaway, J. L., Szebenyi, G., Baas, P. W. & Kalil, K. 1999. Reorganization and movement of microtubules in axonal growth cones and developing interstitial branches. *The Journal of neuroscience : the official journal of the Society for Neuroscience,* 19**,** 8894-908.

Dent, E. W. & Gertler, F. B. 2003. Cytoskeletal dynamics and transport in growth cone motility and axon guidance. *Neuron,* 40**,** 209-27.

Dent, E. W., Gupton, S. L. & Gertler, F. B. 2011. The growth cone cytoskeleton in axon outgrowth and guidance. *Cold Spring Harb Perspect Biol,* 3.

Dent, E. W. & Kalil, K. 2001. Axon branching requires interactions between dynamic microtubules and actin filaments. *J Neurosci,* 21**,** 9757-69.

Derrien, V., Couillault, C., Franco, M., Martineau, S., Montcourrier, P., Houlgatte, R. & Chavrier, P. 2002. A conserved C-terminal domain of EFA6-family ARF6-guanine nucleotide exchange factors induces lengthening of microvilli-like membrane protrusions. *J Cell Sci,* 115**,** 2867-79.

Dickinson, R. E. & Duncan, W. C. 2010. The SLIT-ROBO pathway: a regulator of cell function with implications for the reproductive system. *Reproduction,* 139**,** 697-704.

Domeniconi, M. & Filbin, M. T. 2005. Overcoming inhibitors in myelin to promote axonal regeneration. *J Neurol Sci,* 233**,** 43-7.

Dominguez, R. 2009. Actin filament nucleation and elongation factors--structure-function relationships. *Crit Rev Biochem Mol Biol,* 44**,** 351-66.

Dübendorfer, A. & Eichenberger-Glinz, S. 1980. Development and metamorphosis of larval and adult tissues of *Drosophila in vitro*. *In:* Kurstak, E., Maramorosch, K. & Dübendorfer, A. (eds.) *Invertebrate systems in vitro.* Amsterdam: Elsevier North Holland.

Dwivedy, A., Gertler, F. B., Miller, J., Holt, C. E. & Lebrand, C. 2007. Ena/VASP function in retinal axons is required for terminal arborization but not pathway navigation. *Development,* 134**,** 2137-46.

Edvardson, S., Cinnamon, Y., Jalas, C., Shaag, A., Maayan, C., Axelrod, F. B. & Elpeleg, O. 2012. Hereditary sensory autonomic neuropathy caused by a mutation in dystonin. *Ann Neurol,* 71**,** 569-72.

Efimov, A., Schiefermeier, N., Grigoriev, I., Ohi, R., Brown, M. C., Turner, C. E., Small, J. V. & Kaverina, I. 2008. Paxillin-dependent stimulation of microtubule catastrophes at focal adhesion sites. *J Cell Sci,* 121**,** 196-204.

Etienne-Manneville, S. 2010. From signaling pathways to microtubule dynamics: the key players. *Curr Opin Cell Biol,* 22**,** 104-11.

Eva, R., Crisp, S., Marland, J. R., Norman, J. C., Kanamarlapudi, V., ffrench-Constant, C. & Fawcett, J. W. 2012. ARF6 directs axon transport and traffic of integrins and regulates axon growth in adult DRG neurons. *J Neurosci,* 32**,** 10352-64.

Fan, X., Labrador, J. P., Hing, H. & Bashaw, G. J. 2003. Slit stimulation recruits Dock and Pak to the roundabout receptor and increases Rac activity to regulate axon repulsion at the CNS midline. *Neuron,* 40**,** 113-27.

Fehon, R. G., McClatchey, A. I. & Bretscher, A. 2010. Organizing the cell cortex: the role of ERM proteins. *Nat Rev Mol Cell Biol,* 11**,** 276-87.

Ferrier, A., Sato, T., De Repentigny, Y., Gibeault, S., Bhanot, K., O'Meara, R. W., Lynch-Godrei, A., Kornfeld, S. F., Young, K. G. & Kothary, R. 2014. Transgenic expression of neuronal dystonin isoform 2 partially rescues the disease phenotype of the dystonia musculorum mouse model of hereditary sensory autonomic neuropathy VI. *Hum Mol Genet,* 23**,** 2694-710.

Fiala, J. C., Feinberg, M., Peters, A. & Barbas, H. 2007. Mitochondrial degeneration in dystrophic neurites of senile plaques may lead to extracellular deposition of fine filaments. *Brain Struct Funct,* 212**,** 195-207.

Fievet, B., Louvard, D. & Arpin, M. 2007. ERM proteins in epithelial cell organization and functions. *Biochim Biophys Acta,* 1773**,** 653-60.

Fletcher, D. A. & Mullins, R. D. 2010. Cell mechanics and the cytoskeleton. *Nature,* 463**,** 485-92.

Flynn, K. C., Hellal, F., Neukirchen, D., Jacob, S., Tahirovic, S., Dupraz, S., Stern, S., Garvalov, B. K., Gurniak, C., Shaw, A. E., Meyn, L., Wedlich-Soldner, R., Bamburg, J. R., Small, J. V., Witke, W. & Bradke, F. 2012. ADF/cofilin-mediated actin retrograde flow directs neurite formation in the developing brain. *Neuron,* 76**,** 1091-107.

Forscher, P. & Smith, S. J. 1988. Actions of cytochalasins on the organization of actin filaments and microtubules in a neuronal growth cone. *J. Cell Biol.,* 107**,** 1505-1516.

Franco, M., Peters, P. J., Boretto, J., van Donselaar, E., Neri, A., D'Souza-Schorey, C. & Chavrier, P. 1999. EFA6, a sec7 domain-containing exchange factor for ARF6, coordinates membrane recycling and actin cytoskeleton organization. *EMBO J,* 18**,** 1480-91.

Franze, K., Janmey, P. A. & Guck, J. 2013. Mechanics in neuronal development and repair. *Annu Rev Biomed Eng,* 15**,** 227-51.

Fritzsche, M., Lewalle, A., Duke, T., Kruse, K. & Charras, G. 2013. Analysis of turnover dynamics of the submembranous actin cortex. *Mol Biol Cell,* 24**,** 757-67.

Fritzsche, M., Thorogate, R. & Charras, G. 2014. Quantitative analysis of ezrin turnover dynamics in the actin cortex. *Biophys J,* 106**,** 343-53.

Fukata, M., Watanabe, T., Noritake, J., Nakagawa, M., Yamaga, M., Kuroda, S., Matsuura, Y., Iwamatsu, A., Perez, F. & Kaibuchi, K. 2002. Rac1 and Cdc42 capture microtubules through IQGAP1 and CLIP-170. *Cell,* 109**,** 873-85.

Gallo, G. 2011. The cytoskeletal and signaling mechanisms of axon collateral branching. *Dev Neurobiol,* 71**,** 201-20.

Garbe, D. S., Das, A., Dubreuil, R. R. & Bashaw, G. J. 2007. beta-Spectrin functions independently of Ankyrin to regulate the establishment and maintenance of axon connections in the Drosophila embryonic CNS. *Development,* 134**,** 273-84.

Geraldo, S. & Gordon-Weeks, P. R. 2009. Cytoskeletal dynamics in growth-cone steering. *J Cell Sci,* 122**,** 3595-604.

Geraldo, S., Khanzada, U. K., Parsons, M., Chilton, J. K. & Gordon-Weeks, P. R. 2008. Targeting of the F-actin-binding protein drebrin by the microtubule plus-tip protein EB3 is required for neuritogenesis. *Nat Cell Biol,* 10**,** 1181-9.

Giannone, G., Mege, R. M. & Thoumine, O. 2009. Multi-level molecular clutches in motile cell processes. *Trends Cell Biol,* 19**,** 475-86.

Gistelinck, M., Lambert, J. C., Callaerts, P., Dermaut, B. & Dourlen, P. 2012. Drosophila models of tauopathies: what have we learned? *Int J Alzheimers Dis,* 2012**,** 970980.

Gogel, S., Wakefield, S., Tear, G., Klambt, C. & Gordon-Weeks, P. R. 2006. The Drosophila microtubule associated protein Futsch is phosphorylated by Shaggy/Zeste-white 3 at an homologous GSK3beta phosphorylation site in MAP1B. *Molecular and cellular neurosciences,* 33**,** 188-99.

Gonçalves-Pimentel, C., Gombos, R., Mihály, J., Sánchez-Soriano, N. & Prokop, A. 2011. Dissecting regulatory networks of filopodia formation in a *Drosophila* growth cone model. *PLoS ONE,* 6**,** e18340.

Goodwin, S. S. & Vale, R. D. 2010. Patronin regulates the microtubule network by protecting microtubule minus ends. *Cell,* 143**,** 263-74.

Gouveia, S. M. & Akhmanova, A. 2010. Cell and molecular biology of microtubule plus end tracking proteins: end binding proteins and their partners. *Int Rev Cell Mol Biol,* 285**,** 1-74.

Grubb, M. S. & Burrone, J. 2010. Building and maintaining the axon initial segment. *Curr Opin Neurobiol,* 20**,** 481-8.

Hall, A. & Lalli, G. 2010. Rho and Ras GTPases in axon growth, guidance, and branching. *Cold Spring Harb Perspect Biol,* 2**,** a001818.

Halpain, S. & Dehmelt, L. 2006. The MAP1 family of microtubule-associated proteins. *Genome Biol,* 7**,** 224.

Hao, J. J., Liu, Y., Kruhlak, M., Debell, K. E., Rellahan, B. L. & Shaw, S. 2009. Phospholipase C-mediated hydrolysis of PIP2 releases ERM proteins from lymphocyte membrane. *The Journal of cell biology,* 184**,** 451-62.

Hartman, M. A., Finan, D., Sivaramakrishnan, S. & Spudich, J. A. 2011. Principles of unconventional myosin function and targeting. *Annu Rev Cell Dev Biol,* 27**,** 133-55.

Heidemann, S. R., Lamoureux, P. & Buxbaum, R. E. 1995. Cytomechanics of axonal development. *Cell biochemistry and biophysics,* 27**,** 135-55.

Herrmann, H. & Strelkov, S. V. 2011. History and phylogeny of intermediate filaments: now in insects. *BMC Biol,* 9**,** 16.

Hetrick, B., Han, M. S., Helgeson, L. A. & Nolen, B. J. 2013. Small molecules CK-666 and CK-869 inhibit actin-related protein 2/3 complex by blocking an activating conformational change. *Chemistry & biology,* 20**,** 701-12.

Hirokawa, N., Niwa, S. & Tanaka, Y. 2010. Molecular motors in neurons: transport mechanisms and roles in brain function, development, and disease. *Neuron,* 68**,** 610-38.

Hong, K., Hinck, L., Nishiyama, M., Poo, M. M., Tessier-Lavigne, M. & Stein, E. 1999. A ligand-gated association between cytoplasmic domains of UNC5 and DCC family receptors converts netrin-induced growth cone attraction to repulsion. *Cell,* 97**,** 927-41.

Honnappa, S., Gouveia, S. M., Weisbrich, A., Damberger, F. F., Bhavesh, N. S., Jawhari, H., Grigoriev, I., van Rijssel, F. J., Buey, R. M., Lawera, A., Jelesarov, I., Winkler, F. K., Wuthrich, K., Akhmanova, A. & Steinmetz, M. O. 2009. An EB1-binding motif acts as a microtubule tip localization signal. *Cell,* 138**,** 366-76.

Horie, M., Watanabe, K., Bepari, A. K., Nashimoto, J., Araki, K., Sano, H., Chiken, S., Nambu, A., Ono, K., Ikenaka, K., Kakita, A., Yamamura, K. & Takebayashi, H. 2014. Disruption of actin-binding domain-containing Dystonin protein causes dystonia musculorum in mice. *Eur J Neurosci,* 40**,** 3458-71.

Howard, J. & Hyman, A. A. 2007. Microtubule polymerases and depolymerases. *Curr Opin Cell Biol,* 19**,** 31-5.

Huang, J., Zhou, W., Dong, W., Watson, A. M. & Hong, Y. 2009. From the Cover: Directed, efficient, and versatile modifications of the *Drosophila* genome by genomic engineering. *Proc Natl Acad Sci U S A,* 106**,** 8284-9.

Huang, X., Cheng, H. J., Tessier-Lavigne, M. & Jin, Y. 2002. MAX-1, a novel PH/MyTH4/FERM domain cytoplasmic protein implicated in netrin-mediated axon repulsion. *Neuron,* 34**,** 563-76.

Huber, A. B., Kolodkin, A. L., Ginty, D. D. & Cloutier, J. F. 2003. Signaling at the growth cone: ligand-receptor complexes and the control of axon growth and guidance. *Annu Rev Neurosci,* 26**,** 509-63.

Hudson, A. M. & Cooley, L. 2002. A subset of dynamic actin rearrangements in Drosophila requires the Arp2/3 complex. *J Cell Biol,* 156**,** 677-87.

Hummel, T., Krukkert, K., Roos, J., Davis, G. & Klambt, C. 2000. Drosophila Futsch/22C10 is a MAP1B-like protein required for dendritic and axonal development. *Neuron,* 26**,** 357-70.

Huot, J. 2004. Ephrin signaling in axon guidance. *Prog Neuropsychopharmacol Biol Psychiatry,* 28**,** 813-8.

Iqbal, K., Liu, F., Gong, C. X., Alonso Adel, C. & Grundke-Iqbal, I. 2009. Mechanisms of tau-induced neurodegeneration. *Acta Neuropathol,* 118**,** 53-69.

Iqbal, K., Liu, F., Gong, C. X. & Grundke-Iqbal, I. 2010. Tau in Alzheimer disease and related tauopathies. *Current Alzheimer research,* 7**,** 656-64.

Janke, C. & Bulinski, J. C. 2011. Post-translational regulation of the microtubule cytoskeleton: mechanisms and functions. *Nat Rev Mol Cell Biol,* 12**,** 773-86.

Janke, C. & Kneussel, M. 2010. Tubulin post-translational modifications: encoding functions on the neuronal microtubule cytoskeleton. *Trends Neurosci,* 33**,** 362-72.

Jessell, T., Schwartz, J. & Kandel, E. 2000. Principles of neural science. McGraw-Hill Medical.

Johnson, R. I., Sedgwick, A., D'Souza-Schorey, C. & Cagan, R. L. 2011. Role for a Cindr-Arf6 axis in patterning emerging epithelia. *Mol Biol Cell,* 22**,** 4513-26.

Johnston, S. A., Talaat, A. M. & McGuire, M. J. 2002. Genetic immunization: what's in a name? *Arch Med Res,* 33**,** 325-9.

Kalil, K. & Dent, E. W. 2014. Branch management: mechanisms of axon branching in the developing vertebrate CNS. *Nat Rev Neurosci,* 15**,** 7-18.

Kapitein, L. C. & Hoogenraad, C. C. 2011. Which way to go? Cytoskeletal organization and polarized transport in neurons. *Mol Cell Neurosci,* 46**,** 9-20.

Kaverina, I., Rottner, K. & Small, J. V. 1998. Targeting, capture, and stabilization of microtubules at early focal adhesions. *J Cell Biol,* 142**,** 181-90.

Keleman, K. & Dickson, B. J. 2001. Short- and long-range repulsion by the Drosophila Unc5 netrin receptor. *Neuron,* 32**,** 605-17.

Kellerman, K. A. & Miller, K. G. 1992. An unconventional myosin heavy chain gene from Drosophila melanogaster. *J Cell Biol,* 119**,** 823-34.

Kiehart, D. P., Galbraith, C. G., Edwards, K. A., Rickoll, W. L. & Montague, R. A. 2000. Multiple forces contribute to cell sheet morphogenesis for dorsal closure in Drosophila. *J Cell Biol,* 149**,** 471-90.

Kim, T., Cooper, J. A. & Sept, D. 2010. The interaction of capping protein with the barbed end of the actin filament. *J Mol Biol,* 404**,** 794-802.

Kinoshita, K., Noetzel, T. L., Arnal, I., Drechsel, D. N. & Hyman, A. A. 2006. Global and local control of microtubule destabilization promoted by a catastrophe kinesin MCAK/XKCM1. *J Muscle Res Cell Motil,* 27**,** 107-14.

Klein, S., Partisani, M., Franco, M. & Luton, F. 2008. EFA6 facilitates the assembly of the tight junction by coordinating an Arf6-dependent and -independent pathway. *J Biol Chem,* 283**,** 30129-38.

Kodama, A., Karakesisoglou, I., Wong, E., Vaezi, A. & Fuchs, E. 2003. ACF7. An essential integrator of microtubule dynamics. *Cell,* 115**,** 343-354.

Kodama, A., Lechler, T. & Fuchs, E. 2004. Coordinating cytoskeletal tracks to polarize cellular movements. *J Cell Biol,* 167**,** 203-7.

Kohler, R. E. 1994. *Lords of the fly. Drosophila genetics and the experimental life,* Chicago, London, The University of Chicago Press.

Korenbaum, E. & Rivero, F. 2002. Calponin homology domains at a glance. *J Cell Sci,* 115**,** 3543-5.

Korobova, F. & Svitkina, T. 2008. Arp2/3 complex is important for filopodia formation, growth cone motility, and neuritogenesis in neuronal cells. *Mol Biol Cell,* 19**,** 1561-74.

Krause, M. & Gautreau, A. 2014. Steering cell migration: lamellipodium dynamics and the regulation of directional persistence. *Nat Rev Mol Cell Biol,* 15**,** 577-90.

Kuppers-Munther, B., Letzkus, J. J., Luer, K., Technau, G., Schmidt, H. & Prokop, A. 2004. A new culturing strategy optimises Drosophila primary cell cultures for structural and functional analyses. *Developmental biology,* 269**,** 459-78.

Lantz, V. A. & Miller, K. G. 1998. A class VI unconventional myosin is associated with a homologue of a microtubule-binding protein, cytoplasmic linker protein-170, in neurons and at the posterior pole of *Drosophila* embryos. *J. Cell Biol.,* 140**,** 897-910.

Lebrand, C., Dent, E. W., Strasser, G. A., Lanier, L. M., Krause, M., Svitkina, T. M., Borisy, G. G. & Gertler, F. B. 2004. Critical role of Ena/VASP proteins for filopodia formation in neurons and in function downstream of netrin-1. *Neuron,* 42**,** 37-49.

Lee, A. C. & Suter, D. M. 2008. Quantitative analysis of microtubule dynamics during adhesion-mediated growth cone guidance. *Dev Neurobiol,* 68**,** 1363-77.

Lee, S. & Kolodziej, P. A. 2002. Short stop provides an essential link between F-actin and microtubules during axon extension. *Development,* 129**,** 1195-1204.

Lee, S., Nahm, M., Lee, M., Kwon, M., Kim, E., Zadeh, A. D., Cao, H., Kim, H. J., Lee, Z. H., Oh, S. B., Yim, J. & Kolodziej, P. A. 2007. The F-actin-microtubule crosslinker Shot is a platform for Krasavietz-mediated translational regulation of midline axon repulsion. *Development,* 134**,** 1767-77.

Lee, T., Langford, K. J., Askham, J. M., Bruning-Richardson, A. & Morrison, E. E. 2008. MCAK associates with EB1. *Oncogene,* 27**,** 2494-500.

Lemieux, M. G., Janzen, D., Hwang, R., Roldan, J., Jarchum, I. & Knecht, D. A. 2014. Visualization of the actin cytoskeleton: different F-actin-binding probes tell different stories. *Cytoskeleton (Hoboken),* 71**,** 157-69.

Lemos, C. L., Sampaio, P., Maiato, H., Costa, M., Omel'yanchuk, L. V., Liberal, V. & Sunkel, C. E. 2000. Mast, a conserved microtubule-associated protein required for bipolar mitotic spindle organization. *EMBO J,* 19**,** 3668-82.

Lepinoux-Chambaud, C. & Eyer, J. 2013. Review on intermediate filaments of the nervous system and their pathological alterations. *Histochem Cell Biol,* 140**,** 13-22.

Letourneau, P. C. 2009. Actin in axons: stable scaffolds and dynamic filaments. *Results Probl Cell Differ,* 48**,** 65-90.

Leung, C. L., Green, K. J. & Liem, R. K. 2002. Plakins: a family of versatile cytolinker proteins. *Trends Cell Biol,* 12**,** 37-45.

Li, M., Ng, S. S., Wang, J., Lai, L., Leung, S. Y., Franco, M., Peng, Y., He, M. L., Kung, H. F. & Lin, M. C. 2006. EFA6A enhances glioma cell invasion through ADP ribosylation factor 6/extracellular signal-regulated kinase signaling. *Cancer Res,* 66**,** 1583-90.

Li, X., Matsuoka, Y. & Bennett, V. 1998. Adducin preferentially recruits spectrin to the fast growing ends of actin filaments in a complex requiring the MARCKS-related domain and a newly defined oligomerization domain. *J Biol Chem,* 273**,** 19329-19338.

Li, X., Saint-Cyr-Proulx, E., Aktories, K. & Lamarche-Vane, N. 2002. Rac1 and Cdc42 but not RhoA or Rho kinase activities are required for neurite outgrowth induced by the Netrin-1 receptor DCC (deleted in colorectal cancer) in N1E-115 neuroblastoma cells. *J Biol Chem,* 277**,** 15207-14.

Liao, T. S., Call, G. B., Guptan, P., Cespedes, A., Marshall, J., Yackle, K., Owusu-Ansah, E., Mandal, S., Fang, Q. A., Goodstein, G. L., Kim, W. & Banerjee, U. 2006. An efficient genetic screen in Drosophila to identify nuclear-encoded genes with mitochondrial function. *Genetics,* 174**,** 525-33.

Lin, H., Yue, L. & Spradling, A. C. 1994. The Drosophila fusome, a germline-specific organelle, contains membrane skeletal proteins and functions in cyst formation. *Development,* 120**,** 947-56.

Lowery, L. A. & Van Vactor, D. 2009. The trip of the tip: understanding the growth cone machinery. *Nat Rev Mol Cell Biol,* 10**,** 332-43.

Lu, W., Fox, P., Lakonishok, M., Davidson, M. W. & Gelfand, V. I. 2013. Initial neurite outgrowth in Drosophila neurons is driven by kinesin-powered microtubule sliding. *Current biology : CB,* 23**,** 1018-23.

Luchtenborg, A. M., Solis, G. P., Egger-Adam, D., Koval, A., Lin, C., Blanchard, M. G., Kellenberger, S. & Katanaev, V. L. 2014. Heterotrimeric Go protein links Wnt-Frizzled signaling with ankyrins to regulate the neuronal microtubule cytoskeleton. *Development,* 141**,** 3399-409.

Lukinavicius, G., Reymond, L., D'Este, E., Masharina, A., Gottfert, F., Ta, H., Guther, A., Fournier, M., Rizzo, S., Waldmann, H., Blaukopf, C., Sommer, C., Gerlich, D. W., Arndt, H. D., Hell, S. W. & Johnsson, K. 2014. Fluorogenic probes for live-cell imaging of the cytoskeleton. *Nat Methods,* 11**,** 731-3.

Luo, L., Liao, Y. J., Jan, L. Y. & Jan, Y. N. 1994. Distinct morphogenetic functions of similar small GTPases: Drosophila Drac1 is involved in axonal outgrowth and myoblast fusion. *Genes Dev,* 8**,** 1787-802.

Machesky, L. M. & Insall, R. H. 1998. Scar1 and the related Wiskott-Aldrich syndrome protein, WASP, regulate the actin cytoskeleton through the Arp2/3 complex. *Curr Biol,* 8**,** 1347-56.

Machesky, L. M., Mullins, R. D., Higgs, H. N., Kaiser, D. A., Blanchoin, L., May, R. C., Hall, M. E. & Pollard, T. D. 1999. Scar, a WASp-related protein, activates nucleation of actin filaments by the Arp2/3 complex. *Proc Natl Acad Sci U S A,* 96**,** 3739-44.

Macia, E., Partisani, M., Favard, C., Mortier, E., Zimmermann, P., Carlier, M. F., Gounon, P., Luton, F. & Franco, M. 2008. The pleckstrin homology domain of the Arf6-specific exchange factor EFA6 localizes to the plasma membrane by interacting with phosphatidylinositol 4,5-bisphosphate and F-actin. *J Biol Chem,* 283**,** 19836-44.

Mack, T. G., Koester, M. P. & Pollerberg, G. E. 2000. The microtubule-associated protein MAP1B is involved in local stabilization of turning growth cones. *Mol Cell Neurosci,* 15**,** 51-65.

Manns, R. P., Cook, G. M., Holt, C. E. & Keynes, R. J. 2012. Differing Semaphorin 3A Concentrations Trigger Distinct Signaling Mechanisms in Growth Cone Collapse. *J Neurosci,* 32**,** 8554-9.

Marner, L., Nyengaard, J. R., Tang, Y. & Pakkenberg, B. 2003. Marked loss of myelinated nerve fibers in the human brain with age. *J Comp Neurol,* 462**,** 144-52.

Marsick, B. M., San Miguel-Ruiz, J. E. & Letourneau, P. C. 2012. Activation of ezrin/radixin/moesin mediates attractive growth cone guidance through

regulation of growth cone actin and adhesion receptors. *J Neurosci,* 32**,** 282-96.

Matthews, K. A., Kaufman, T. C. & Gelbart, W. M. 2005. Research resources for Drosophila: the expanding universe. *Nat Rev Genet,* 6**,** 179-93.

Matus, A. 1991. Microtubule-associated proteins and neuronal morphogenesis. *J Cell Sci Suppl,* 15**,** 61-7.

McGough, A., Pope, B., Chiu, W. & Weeds, A. 1997. Cofilin changes the twist of F-actin: implications for actin filament dynamics and cellular function. *J Cell Biol,* 138**,** 771-81.

Millard, T. H. & Martin, P. 2008. Dynamic analysis of filopodial interactions during the zippering phase of Drosophila dorsal closure. *Development,* 135**,** 621-6.

Millecamps, S. & Julien, J. P. 2013. Axonal transport deficits and neurodegenerative diseases. *Nat Rev Neurosci,* 14**,** 161-76.

Milyaev, N., Osumi-Sutherland, D., Reeve, S., Burton, N., Baldock, R. A. & Armstrong, J. D. 2012. The Virtual Fly Brain browser and query interface. *Bioinformatics,* 28**,** 411-5.

Mimori-Kiyosue, Y., Shiina, N. & Tsukita, S. 2000. The dynamic behavior of the APC-binding protein EB1 on the distal ends of microtubules. *Curr Biol,* 10**,** 865-8.

Mlodzik, M., Baker, N. E. & Rubin, G. M. 1990. Isolation and expression of scabrous, a gene regulating neurogenesis in Drosophila. *Genes Dev,* 4**,** 1848-61.

Moore, S. W., Tessier-Lavigne, M. & Kennedy, T. E. 2007. Netrins and their receptors. *Adv Exp Med Biol,* 621**,** 17-31.

Morris, M., Maeda, S., Vossel, K. & Mucke, L. 2011. The many faces of tau. *Neuron,* 70**,** 410-26.

Morton, W. M., Ayscough, K. R. & McLaughlin, P. J. 2000. Latrunculin alters the actin-monomer subunit interface to prevent polymerization. *Nat Cell Biol,* 2**,** 376-8.

Mukherjee, S., Diaz Valencia, J. D., Stewman, S., Metz, J., Monnier, S., Rath, U., Asenjo, A. B., Charafeddine, R. A., Sosa, H. J., Ross, J. L., Ma, A. & Sharp, D. J. 2012. Human Fidgetin is a microtubule severing the enzyme and minus-end depolymerase that regulates mitosis. *Cell Cycle,* 11**,** 2359-66.

Munsie, L. N., Caron, N., Desmond, C. R. & Truant, R. 2009. Lifeact cannot visualize some forms of stress-induced twisted F-actin. *Nat Methods,* 6**,** 317.

Myers, E. W., Sutton, G. G., Delcher, A. L., Dew, I. M., Fasulo, D. P., Flanigan, M. J., Kravitz, S. A., Mobarry, C. M., Reinert, K. H., Remington, K. A., Anson, E. L., Bolanos, R. A., Chou, H. H., Jordan, C. M., Halpern, A. L., Lonardi, S., Beasley, E. M., Brandon, R. C., Chen, L., Dunn, P. J., Lai, Z., Liang, Y., Nusskern, D. R., Zhan, M., Zhang, Q., Zheng, X., Rubin, G. M., Adams, M. D. & Venter, J. C. 2000. A whole-genome assembly of Drosophila. *Science,* 287**,** 2196-204.

Myers, J. P. & Gomez, T. M. 2011. Focal adhesion kinase promotes integrin adhesion dynamics necessary for chemotropic turning of nerve growth cones. *The Journal of neuroscience : the official journal of the Society for Neuroscience,* 31**,** 13585-95.

Myers, K. A., He, Y., Hasaka, T. P. & Baas, P. W. 2006a. Microtubule transport in the axon: Re-thinking a potential role for the actin cytoskeleton. *The Neuroscientist : a review journal bringing neurobiology, neurology and psychiatry,* 12**,** 107-18.

Myers, K. A., Tint, I., Nadar, C. V., He, Y., Black, M. M. & Baas, P. W. 2006b. Antagonistic forces generated by cytoplasmic dynein and myosin-II during growth cone turning and axonal retraction. *Traffic,* 7**,** 1333-51.

Nakamura, F., Huang, L., Pestonjamasp, K., Luna, E. J. & Furthmayr, H. 1999. Regulation of F-actin binding to platelet moesin in vitro by both phosphorylation of threonine 558 and polyphosphatidylinositides. *Molecular biology of the cell,* 10**,** 2669-85.

Nakamura, F., Stossel, T. P. & Hartwig, J. H. 2011. The filamins: organizers of cell structure and function. *Cell Adh Migr,* 5**,** 160-9.

Nakano, K. & Mabuchi, I. 2006. Actin-capping protein is involved in controlling organization of actin cytoskeleton together with ADF/cofilin, profilin and F-actin crosslinking proteins in fission yeast. *Genes Cells,* 11**,** 893-905.

Nambiar, R., McConnell, R. E. & Tyska, M. J. 2010. Myosin motor function: the ins and outs of actin-based membrane protrusions. *Cell Mol Life Sci,* 67**,** 1239-54.

Neisch, A. L. & Fehon, R. G. 2011. Ezrin, Radixin and Moesin: key regulators of membrane-cortex interactions and signaling. *Curr Opin Cell Biol,* 23**,** 377-82.

Ng, J. & Luo, L. 2004. Rho GTPases regulate axon growth through convergent and divergent signaling pathways. *Neuron,* 44**,** 779-93.

Niggli, V. & Rossy, J. 2008. Ezrin/radixin/moesin: versatile controllers of signaling molecules and of the cortical cytoskeleton. *Int J Biochem Cell Biol,* 40**,** 344-9.

Nkyimbeng-Takwi, E. & Chapoval, S. P. 2011. Biology and function of neuroimmune semaphorins 4A and 4D. *Immunol Res,* 50**,** 10-21.

Nolen, B. J., Tomasevic, N., Russell, A., Pierce, D. W., Jia, Z., McCormick, C. D., Hartman, J., Sakowicz, R. & Pollard, T. D. 2009. Characterization of two classes of small molecule inhibitors of Arp2/3 complex. *Nature,* 460**,** 1031-4.

Nugent, A. A., Kolpak, A. L. & Engle, E. C. 2012. Human disorders of axon guidance. *Curr Opin Neurobiol,* 22**,** 837-43.

Nussbaum, J. M., Seward, M. E. & Bloom, G. S. 2013. Alzheimer disease: a tale of two prions. *Prion,* 7**,** 14-9.

O'Rourke, S. M., Christensen, S. N. & Bowerman, B. 2010. Caenorhabditis elegans EFA-6 limits microtubule growth at the cell cortex. *Nat Cell Biol,* 12**,** 1235-41.

Okada, K., Bartolini, F., Deaconescu, A. M., Moseley, J. B., Dogic, Z., Grigorieff, N., Gundersen, G. G. & Goode, B. L. 2010. Adenomatous polyposis coli protein nucleates actin assembly and synergizes with the formin mDia1. *J Cell Biol,* 189**,** 1087-96.

Osterwalder, T., Yoon, K. S., White, B. H. & Keshishian, H. 2001. A conditional tissue-specific transgene expression system using inducible GAL4. *Proc Natl Acad Sci U S A,* 98**,** 12596-601.

Padovani, D., Folly-Klan, M., Labarde, A., Boulakirba, S., Campanacci, V., Franco, M., Zeghouf, M. & Cherfils, J. 2014. EFA6 controls Arf1 and Arf6

activation through a negative feedback loop. *Proc Natl Acad Sci U S A,* 111**,** 12378-83.

Pak, C. W., Flynn, K. C. & Bamburg, J. R. 2008. Actin-binding proteins take the reins in growth cones. *Nat Rev Neurosci,* 9**,** 136-47.

Paul, A. S. & Pollard, T. D. 2009. Review of the mechanism of processive actin filament elongation by formins. *Cell Motil Cytoskeleton,* 66**,** 606-17.

Pecqueur, L., Duellberg, C., Dreier, B., Jiang, Q., Wang, C., Pluckthun, A., Surrey, T., Gigant, B. & Knossow, M. 2012. A designed ankyrin repeat protein selected to bind to tubulin caps the microtubule plus end. *Proc Natl Acad Sci U S A,* 109**,** 12011-6.

Perletti, L., Talarico, D., Trecca, D., Ronchetti, D., Fracchiolla, N. S., Maiolo, A. T. & Neri, A. 1997. Identification of a novel gene, PSD, adjacent to NFKB2/lyt-10, which contains Sec7 and pleckstrin-homology domains. *Genomics,* 46**,** 251-9.

Perlson, E., Hendricks, A. G., Lazarus, J. E., Ben-Yaakov, K., Gradus, T., Tokito, M. & Holzbaur, E. L. 2013. Dynein interacts with the neural cell adhesion molecule (NCAM180) to tether dynamic microtubules and maintain synaptic density in cortical neurons. *J Biol Chem,* 288**,** 27812-24.

Pielage, J., Cheng, L., Fetter, R. D., Carlton, P. M., Sedat, J. W. & Davis, G. W. 2008. A presynaptic giant ankyrin stabilizes the NMJ through regulation of presynaptic microtubules and transsynaptic cell adhesion. *Neuron,* 58**,** 195-209.

Prokop, A. 2013. The intricate relationship between microtubules and their associated motor proteins during axon growth and maintenance. *Neur Dev,* 8**,** 17.

Prokop, A., Beaven, R., Qu, Y. & Sánchez-Soriano, N. 2013. Using fly genetics to dissect the cytoskeletal machinery of neurons during axonal growth and maintenance. *J. Cell Sci.,* 126**,** 2331-41.

Prokop, A., Küppers-Munther, B. & Sánchez-Soriano, N. 2012. Using primary neuron cultures of *Drosophila* to analyse neuronal circuit formation and function. *In:* Hassan, B. A. (ed.) *The making and un-making of neuronal circuits in Drosophila.* New York: Springer Science + Business Media, LLC.

Pulver, S. R., Cognigni, P., Denholm, B., Fabre, C., Gu, W. X., Linneweber, G., Prieto-Godino, L., Urbancic, V., Zwart, M. & Miguel-Aliaga, I. 2011. Why flies? Inexpensive public engagement exercises to explain the value of basic biomedical research on Drosophila melanogaster. *Adv Physiol Educ,* 35**,** 384-92.

Qiang, L., Yu, W., Andreadis, A., Luo, M. & Baas, P. W. 2006. Tau protects microtubules in the axon from severing by katanin. *J Neurosci,* 26**,** 3120-9.

Qiang, L., Yu, W., Liu, M., Solowska, J. M. & Baas, P. W. 2010. Basic fibroblast growth factor elicits formation of interstitial axonal branches via enhanced severing of microtubules. *Mol Biol Cell,* 21**,** 334-44.

Qualmann, B. & Kessels, M. M. 2008. Actin nucleation: putting the brakes on Arp2/3. *Curr Biol,* 18**,** R420-3.

Qurashi, A., Sahin, H. B., Carrera, P., Gautreau, A., Schenck, A. & Giangrande, A. 2007. HSPC300 and its role in neuronal connectivity. *Neural Dev,* 2**,** 18.

Rasband, M. N. 2010. The axon initial segment and the maintenance of neuronal polarity. *Nat Rev Neurosci,* 11**,** 552-62.

Reeve, E. C. R. 2001. Encyclopedia of genetics. Fitzroy Dearborn Publishers.

Riedl, J., Crevenna, A. H., Kessenbrock, K., Yu, J. H., Neukirchen, D., Bista, M., Bradke, F., Jenne, D., Holak, T. A., Werb, Z., Sixt, M. & Wedlich-Söldner, R. 2008. Lifeact: a versatile marker to visualize F-actin. *Nat Methods,* 5**,** 605-7.

Rogers, S. L., Rogers, G. C., Sharp, D. J. & Vale, R. D. 2002. Drosophila EB1 is important for proper assembly, dynamics, and positioning of the mitotic spindle. *J Cell Biol,* 158**,** 873-84.

Roote, J. & Prokop, A. 2013. How to design a genetic mating scheme: a basic training package for Drosophila genetics. *G3,* 3**,** 353-8.

Roper, K. 2007. Rtnl1 is enriched in a specialized germline ER that associates with ribonucleoprotein granule components. *J Cell Sci,* 120**,** 1081-92.

Roper, K. & Brown, N. H. 2003. Maintaining epithelial integrity: a function for gigantic spectraplakin isoforms in adherens junctions. *J Cell Biol,* 162**,** 1305-15.

Roper, K., Gregory, S. L. & Brown, N. H. 2002. The 'spectraplakins': cytoskeletal giants with characteristics of both spectrin and plakin families. *J Cell Sci,* 115**,** 4215-25.

Roth, L., Nasarre, C., Dirrig-Grosch, S., Aunis, D., Cremel, G., Hubert, P. & Bagnard, D. 2008. Transmembrane domain interactions control biological functions of neuropilin-1. *Mol Biol Cell,* 19**,** 646-54.

Round, J. & Stein, E. 2007. Netrin signaling leading to directed growth cone steering. *Curr Opin Neurobiol,* 17**,** 15-21.

Ryder, E., Blows, F., Ashburner, M., Bautista-Llacer, R., Coulson, D., Drummond, J., Webster, J., Gubb, D., Gunton, N., Johnson, G., O'Kane, C. J., Huen, D., Sharma, P., Asztalos, Z., Baisch, H., Schulze, J., Kube, M., Kittlaus, K., Reuter, G., Maroy, P., Szidonya, J., Rasmuson-Lestander, A., Ekstrom, K., Dickson, B., Hugentobler, C., Stocker, H., Hafen, E., Lepesant, J. A., Pflugfelder, G., Heisenberg, M., Mechler, B., Serras, F., Corominas, M., Schneuwly, S., Preat, T., Roote, J. & Russell, S. 2004. The DrosDel collection: a set of P-element insertions for generating custom chromosomal aberrations in Drosophila melanogaster. *Genetics,* 167**,** 797-813.

Sakagami, H., Honma, T., Sukegawa, J., Owada, Y., Yanagisawa, T. & Kondo, H. 2007. Somatodendritic localization of EFA6A, a guanine nucleotide exchange factor for ADP-ribosylation factor 6, and its possible interaction with alpha-actinin in dendritic spines. *Eur J Neurosci,* 25**,** 618-28.

Sakagami, H., Matsuya, S., Nishimura, H., Suzuki, R. & Kondo, H. 2004. Somatodendritic localization of the mRNA for EFA6A, a guanine nucleotide exchange protein for ARF6, in rat hippocampus and its involvement in dendritic formation. *Eur J Neurosci,* 19**,** 863-70.

Sakagami, H., Suzuki, H., Kamata, A., Owada, Y., Fukunaga, K., Mayanagi, H. & Kondo, H. 2006. Distinct spatiotemporal expression of EFA6D, a guanine nucleotide exchange factor for ARF6, among the EFA6 family in mouse brain. *Brain Res,* 1093**,** 1-11.

Sanchez-Soriano, N., Goncalves-Pimentel, C., Beaven, R., Haessler, U., Ofner-Ziegenfuss, L., Ballestrem, C. & Prokop, A. 2010. *Drosophila* growth cones: a

genetically tractable platform for the analysis of axonal growth dynamics. *Dev Neurobiol,* 70**,** 58-71.

Sanchez-Soriano, N. & Prokop, A. 2005. The influence of pioneer neurons on a growing motor nerve in Drosophila requires the neural cell adhesion molecule homolog FasciclinII. *J Neurosci,* 25**,** 78-87.

Sanchez-Soriano, N., Tear, G., Whitington, P. & Prokop, A. 2007. Drosophila as a genetic and cellular model for studies on axonal growth. *Neural Dev,* 2**,** 9.

Sanchez-Soriano, N., Travis, M., Dajas-Bailador, F., Goncalves-Pimentel, C., Whitmarsh, A. J. & Prokop, A. 2009. Mouse ACF7 and drosophila short stop modulate filopodia formation and microtubule organisation during neuronal growth. *J Cell Sci,* 122**,** 2534-42.

Sarkissian, T., Timmons, A., Arya, R., Abdelwahid, E. & White, K. 2014. Detecting apoptosis in Drosophila tissues and cells. *Methods,* 68**,** 89-96.

Schaefer, A. W., Schoonderwoert, V. T., Ji, L., Mederios, N., Danuser, G. & Forscher, P. 2008. Coordination of actin filament and microtubule dynamics during neurite outgrowth. *Dev Cell,* 15**,** 146-62.

Schenck, A., Qurashi, A., Carrera, P., Bardoni, B., Diebold, C., Schejter, E., Mandel, J. L. & Giangrande, A. 2004. WAVE/SCAR, a multifunctional complex coordinating different aspects of neuronal connectivity. *Dev Biol,* 274**,** 260-270.

Schmandke, A. & Schwab, M. E. 2014. Nogo-A: Multiple Roles in CNS Development, Maintenance, and Disease. *Neuroscientist,* 20**,** 372-386.

Schnaar, R. L. & Lopez, P. H. 2009. Myelin-associated glycoprotein and its axonal receptors. *J Neurosci Res,* 87**,** 3267-76.

Schneider, I. 1964. Differentiation of larval *Drosophila* eye-antennal discs *in vitro*. *J. Exp. Zool.,* 156**,** 91-104.

Schwab, M. E. 2010. Functions of Nogo proteins and their receptors in the nervous system. *Nature reviews. Neuroscience,* 11**,** 799-811.

Schwarz, T. L. 2013. Mitochondrial trafficking in neurons. *Cold Spring Harb Perspect Biol,* 5**,** a011304.

Shapiro, L., Love, J. & Colman, D. R. 2007. Adhesion molecules in the nervous system: structural insights into function and diversity. *Annual review of neuroscience,* 30**,** 451-74.

Sharp, D. J., O'Rourke, B. & Zhang, D. 2012. Microtubules cut loose at the cell cortex. *Fly (Austin),* 6**,** 12-5.

Sharp, D. J. & Ross, J. L. 2012. Microtubule-severing enzymes at the cutting edge. *J Cell Sci,* 125**,** 2561-9.

Sironi, C., Teesalu, T., Muggia, A., Fontana, G., Marino, F., Savaresi, S. & Talarico, D. 2009. EFA6A encodes two isoforms with distinct biological activities in neuronal cells. *J Cell Sci,* 122**,** 2108-18.

Sjoblom, B., Salmazo, A. & Djinovic-Carugo, K. 2008. Alpha-actinin structure and regulation. *Cell Mol Life Sci,* 65**,** 2688-701.

Stein, E., Zou, Y., Poo, M. & Tessier-Lavigne, M. 2001. Binding of DCC by netrin-1 to mediate axon guidance independent of adenosine A2B receptor activation. *Science,* 291**,** 1976-82.

Stiess, M., Maghelli, N., Kapitein, L. C., Gomis-Ruth, S., Wilsch-Brauninger, M., Hoogenraad, C. C., Tolic-Norrelykke, I. M. & Bradke, F. 2010. Axon extension occurs independently of centrosomal microtubule nucleation. *Science,* 327**,** 704-7.

Strasser, G. A., Rahim, N. A., VanderWaal, K. E., Gertler, F. B. & Lanier, L. M. 2004. Arp2/3 is a negative regulator of growth cone translocation. *Neuron,* 43**,** 81-94.

Stroud, M. J., Kammerer, R. A. & Ballestrem, C. 2011. Characterization of G2L3 (GAS2-like 3), a new microtubule- and actin-binding protein related to spectraplakins. *J Biol Chem,* 286**,** 24987-95.

Stroud, M. J., Nazgiewicz, A., McKenzie, E. A., Wang, Y., Kammerer, R. A. & Ballestrem, C. 2014. GAS2-like proteins mediate communication between microtubules and actin through interactions with end-binding proteins. *J Cell Sci,* 127**,** 2672-82.

Suter, D. M. & Forscher, P. 2000. Substrate-cytoskeletal coupling as a mechanism for the regulation of growth cone motility and guidance. *J. Neurobiol.,* 44**,** 97-113.

Suter, D. M. & Miller, K. E. 2011. The emerging role of forces in axonal elongation. *Prog Neurobiol,* 94**,** 91-101.

Suter, D. M., Schaefer, A. W. & Forscher, P. 2004. Microtubule dynamics are necessary for Src family kinase-dependent growth cone steering. *Current Biology,* 14**,** 1194-1199.

Swan, A., Nguyen, T. & Suter, B. 1999. Drosophila Lissencephaly-1 functions with Bic-D and dynein in oocyte determination and nuclear positioning. *Nat Cell Biol,* 1**,** 444-9.

Swiech, L., Blazejczyk, M., Urbanska, M., Pietruszka, P., Dortland, B. R., Malik, A. R., Wulf, P. S., Hoogenraad, C. C. & Jaworski, J. 2011. CLIP-170 and IQGAP1 cooperatively regulate dendrite morphology. *J Neurosci,* 31**,** 4555-68.

Terada, S., Kinjo, M., Aihara, M., Takei, Y. & Hirokawa, N. 2010. Kinesin-1/Hsc70-dependent mechanism of slow axonal transport and its relation to fast axonal transport. *EMBO J,* 29**,** 843-54.

Tessier-Lavigne, M. & Goodman, C. S. 1996. The molecular biology of axon guidance. *Science,* 274**,** 1123-33.

Ujfalusi, Z., Vig, A., Hild, G. & Nyitrai, M. 2009. Effect of tropomyosin on formin-bound actin filaments. *Biophys J,* 96**,** 162-8.

Uribe, R. & Jay, D. 2009. A review of actin binding proteins: new perspectives. *Mol Biol Rep,* 36**,** 121-5.

Vallenius, T. 2013. Actin stress fibre subtypes in mesenchymal-migrating cells. *Open Biol,* 3**,** 130001.

Venken, K. J. & Bellen, H. J. 2005. Emerging technologies for gene manipulation in Drosophila melanogaster. *Nat Rev Genet,* 6**,** 167-78.

Verheyen, E. M. & Cooley, L. 1994. Profilin mutations disrupt multiple actin-dependent processes during Drosophila development. *Development,* 120**,** 717-28.

Villarroel-Campos, D. & Gonzalez-Billault, C. 2014. The MAP1B case: an old MAP that is new again. *Dev Neurobiol,* 74**,** 953-71.

Vitaliani, R., Mason, W., Ances, B., Zwerdling, T., Jiang, Z. & Dalmau, J. 2005. Paraneoplastic encephalitis, psychiatric symptoms, and hypoventilation in ovarian teratoma. *Ann Neurol,* 58**,** 594-604.

Wakatsuki, T., Schwab, B., Thompson, N. C. & Elson, E. L. 2001. Effects of cytochalasin D and latrunculin B on mechanical properties of cells. *J Cell Sci,* 114**,** 1025-36.

Wang, J. Z. & Liu, F. 2008. Microtubule-associated protein tau in development, degeneration and protection of neurons. *Prog Neurobiol,* 85**,** 148-75.

Weber, A. 1999. Actin binding proteins that change extent and rate of actin monomer-polymer distribution by different mechanisms. *Mol Cell Biochem,* 190**,** 67-74.

Wills, Z., Marr, L., Zinn, K., Goodman, C. S. & Van Vactor, D. 1999. Profilin and the Abl tyrosine kinase are required for motor axon outgrowth in the Drosophila embryo. *Neuron,* 22**,** 291-9.

Wolter, P., Schmitt, K., Fackler, M., Kremling, H., Probst, L., Hauser, S., Gruss, O. J. & Gaubatz, S. 2012. GAS2L3, a novel target gene of the dream complex, is required for proper cytokinesis and genomic stability. *J Cell Sci*.

Wong, K., Ren, X. R., Huang, Y. Z., Xie, Y., Liu, G., Saito, H., Tang, H., Wen, L., Brady-Kalnay, S. M., Mei, L., Wu, J. Y., Xiong, W. C. & Rao, Y. 2001. Signal transduction in neuronal migration: roles of GTPase activating proteins and the small GTPase Cdc42 in the Slit-Robo pathway. *Cell,* 107**,** 209-21.

Wu, X., Kodama, A. & Fuchs, E. 2008. ACF7 regulates cytoskeletal-focal adhesion dynamics and migration and has ATPase activity. *Cell,* 135**,** 137-48.

Xu, K., Zhong, G. & Zhuang, X. 2013. Actin, spectrin, and associated proteins form a periodic cytoskeletal structure in axons. *Science,* 339**,** 452-6.

Xu, N. J. & Henkemeyer, M. 2012. Ephrin reverse signaling in axon guidance and synaptogenesis. *Semin Cell Dev Biol,* 23**,** 58-64.

Yang, Q., Zhang, X. F., Pollard, T. D. & Forscher, P. 2012. Arp2/3 complex-dependent actin networks constrain myosin II function in driving retrograde actin flow. *J Cell Biol*.

Yang, Y., Bauer, C., Strasser, G., Wollman, R., Julien, J. P. & Fuchs, E. 1999. Integrators of the cytoskeleton that stabilize microtubules. *Cell,* 98**,** 229-38.

Yarmola, E. G. & Bubb, M. R. 2006. Profilin: emerging concepts and lingering misconceptions. *Trends Biochem Sci,* 31**,** 197-205.

Yarmola, E. G., Somasundaram, T., Boring, T. A., Spector, I. & Bubb, M. R. 2000. Actin-latrunculin A structure and function. Differential modulation of actin-binding protein function by latrunculin A. *J Biol Chem,* 275**,** 28120-7.

Yazdani, U. & Terman, J. R. 2006. The semaphorins. *Genome Biol,* 7**,** 211.

Ypsilanti, A. R., Zagar, Y. & Chedotal, A. 2010. Moving away from the midline: new developments for Slit and Robo. *Development,* 137**,** 1939-52.

Yu, J. Z. & Rasenick, M. M. 2006. Tau associates with actin in differentiating PC12 cells. *FASEB J,* 20**,** 1452-61.

Yu, W., Qiang, L., Solowska, J. M., Karabay, A., Korulu, S. & Baas, P. W. 2008. The microtubule-severing proteins spastin and katanin participate differently in the formation of axonal branches. *Mol Biol Cell,* 19**,** 1485-98.

Yue, L. & Spradling, A. C. 1992. hu-li tai shao, a gene required for ring canal formation during Drosophila oogenesis, encodes a homolog of adducin. *Genes Dev,* 6**,** 2443-54.

Zallen, J. A., Cohen, Y., Hudson, A. M., Cooley, L., Wieschaus, E. & Schejter, E. D. 2002. SCAR is a primary regulator of Arp2/3-dependent morphological events in *Drosophila*. *J Cell Biol,* 156**,** 689-701.

Zempel, H. & Mandelkow, E. 2014. Lost after translation: missorting of Tau protein and consequences for Alzheimer disease. *Trends Neurosci,* 37**,** 721-732.

Zhang, T., Dayanandan, B., Rouiller, I., Lawrence, E. J. & Mandato, C. A. 2011. Growth-arrest-specific protein 2 inhibits cell division in *Xenopus* embryos. *PLoS One,* 6**,** e24698.

Ziel, J. W. & Sherwood, D. R. 2010. Roles for netrin signaling outside of axon guidance: a view from the worm. *Dev Dyn,* 239**,** 1296-305.

Chapter 6

Appendices

6.1. Genetically validate the specificity of CK666

To further demonstrate the specificity of CK666, I performed a number of studies in different genetic backgrounds which strongly suggested specificity of the drug.

CK666 binds between Arp2 and Arp3 and blocks their movement into the active conformation (Nolen et al., 2009). Therefore, we predict that treating Arp2/3 mutant with CK666 will not result in filopodia number decreasing more than *sop* mutant or the CK666 treatment alone.

To test this hypothesis, we cultured primary neurons carrying loss-of-function mutations in the Sop2 gene, which encodes the ArpC1/p40 subunit of the Arp2/3 complex. As previously mentioned, the filopodia number of $Sop2^{1}$ mutant neurons and *wildtype* neurons treated with CK666 both significantly decrease. When $Sop2^{1}$ mutant neurons were treated with 100nM CK666 for 2hr, the filopodia number is significantly decreased (all normalised to wildtype; 61±4%, $P_{Mann\text{-}Whitney}<0.001$, n=80; Fig. 6.1). However, it was not significantly different from untreated $sop2^{1}$ mutant neurons (68±5%, $P_{Mann\text{-}Whitney}=0.533$, n=80; Fig. 6.1) or wildtype neurons treated with CK666 (78±6%, $P_{Mann\text{-}Whitney}=0.137$, n=80; Fig. 6.1). This data is consistent with our prediction.

It has been shown that DAAM is strongly required for filopodia formation, and together with Arp2/3, it represents the key actin nucleator in *Drosophila* primary neurons. Any further potential nucleator activity appears insufficient to provide enough F-actin to induce filopodial protrusions (Gonçalves-Pimentel et al., 2011). Therefore, we predicted that treating *daam* mutant neuron with CK666, filopodia number further would decrease compared to *daam* mutant or CK666 treatment alone.

Compare to wildtype, we found that the filopodia number of $daam^{ex68/ex1}$ (77±5%, $P_{Mann\text{-}Whitney}=0.004$, n=60,) or $daam^{ex68/ex1}$ with CK666 (67%, $P_{Mann\text{-}Whitney}<0.001$, n=60) are both significantly decreased (Fig. 6.1). However, when comparing $daam^{ex68/ex1}$ mutant neurons treated with CK666 to $daam^{ex68/ex1}$ mutants or CK666 treatment alone, the filopodia number is slightly decreased, but there is no significantly statistics different between them ($P_{Mann\text{-}Whitney}=0.123$ and $P_{Mann\text{-}Whitney}=0.341$, respectively; Fig. 6.1).

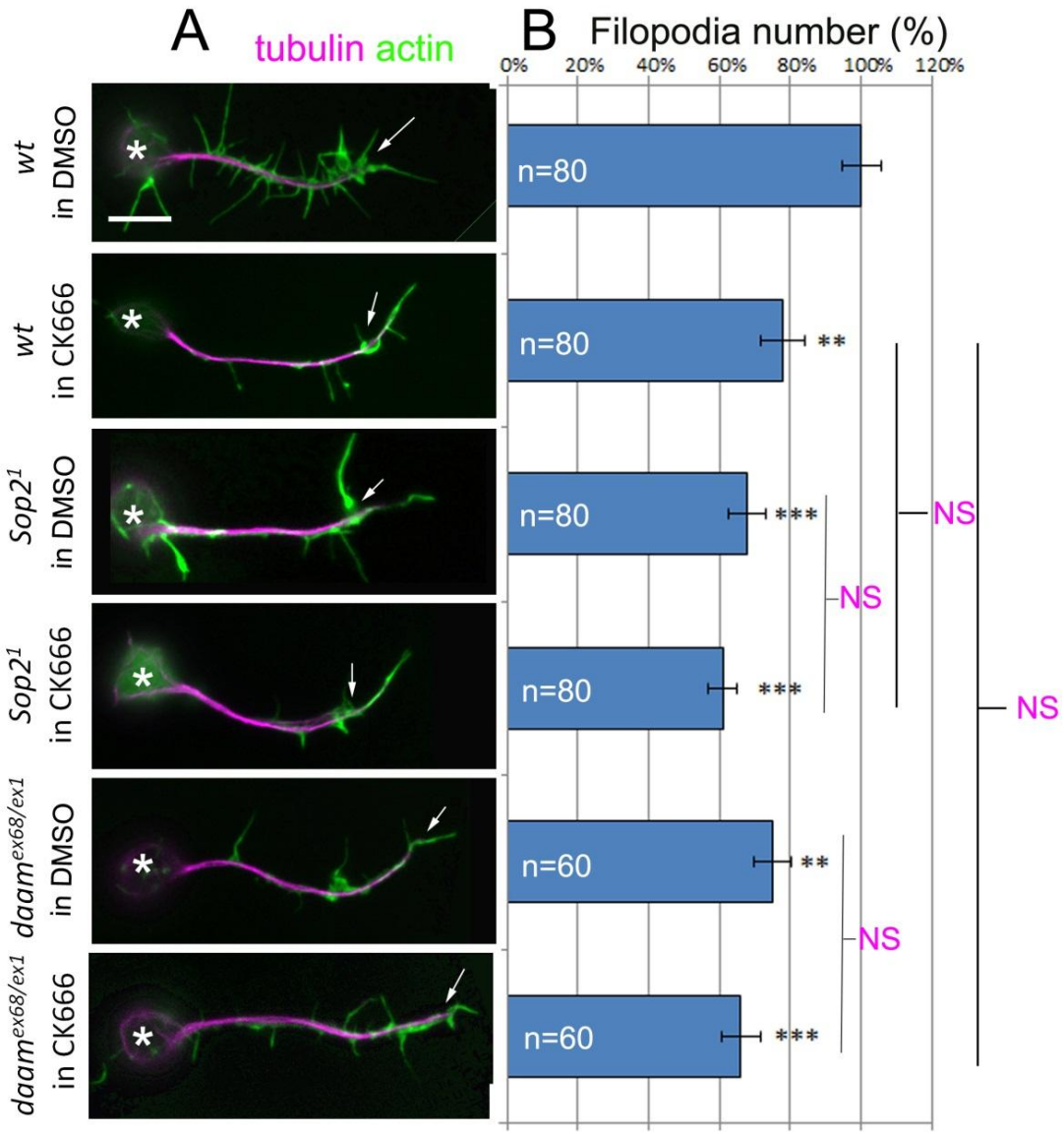
A
tubulin actin
wt in DMSO
wt in CK666
Sop2¹ in DMSO
Sop2¹ in CK666
daam^ex68/ex1 in DMSO
daam^ex68/ex1 in CK666
B
Filopodia number (%)
0%
20%
40%
60%
80%
100%
120%
n=80
n=80
n=80
n=80
n=60
n=60
**
***
***
**
***
NS
NS
NS
NS

Figure 6.1. *Validation of CK666.*

A) *Axonal phenotypes in wild type, Sop2^{1} or daam$^{ex68/ex1}$ mutants primary neurons at 6HIV in vehicle (DMSO) or treated with CK666. Cells are double-labelled for actin and tubulin as indicated; asterisks, cell bodies; arrows, growth cones; scale bar 5μm.* ***B)*** *Quantifications of filopodia number for the treatments. All normalized to wild type in vehicle; P value in black, all compared to wild type in vehicle; P value in magenta, compare mutant with CK666 treatment to their respective DMSO controls or wild type with CK666 as indicated); numbers in the bars indicate the numbers of neurons analysed in each experiment; P values were calculated using the Mann-Whitney Rank Sum test (NS: P>0.050, **: P<0.050, ***: P<0.001).*

6.2. The SCAR complex is required to maintain MT organisation in axons

It has been well demonstrated that the evolutionarily conserved WAVE/SCAR complex is composed of five protein: CYFIP (PIR121 or Sra1), Kette (Nap1), Abi, SCAR (WAVE) and HSPC300 (Qurashi et al., 2007). SCARΔ37 mutant neurons are believed to be depleted of any function of the SCAR/WAVE complex (Schenck et al., 2004), which is the essential activator of Arp2/3 ((Machesky and Insall, 1998, Machesky et al., 1999, Schenck et al., 2004, Zallen et al., 2002)). *SCAR$^{\Delta 37}$* mutant neurons are therefore expected to abolish Arp2/3 complex activity. In accordance with this, *SCAR$^{\Delta 37}$* mutant neurons show similar actin depletion phenotypes (reduced lamellipodia, filopodia numbers reduced to 51%; Fig. 3.12) as *Sop2^{1}* mutant neurons lacking the essential Arp2/3 component ArpC1 (filopodia numbers reduced to 68±5%; Fig. 6.1) (Gonçalves-Pimentel et al., 2011).

However, whereas *Sop2^{1}* mutant neurons show no obvious alterations of axonal MT bundles (82%, P_{Chi2}=0.498, n=80), the *SCAR$^{\Delta 37}$* mutant neurons or *SCAR$^{\Delta 37/def(Df(2L)BSC145)}$* displayed considerable MT disorganisation (197%, P_{Chi2}<0.001, n=120 and 240%, P_{Chi2}<0.001, n=40, respectively; Fig.6.2). Axon length was also affected (87±3%, $P_{Mann\text{-}Whitney}$<0.001, n=120 and 74±4%, $P_{Mann\text{-}Whitney}$<0.001, n=40, respectively; Fig. 6.2). I therefore wondered whether this reflected a SCAR/WAVE complex-dependent function in MT regulation or a complex-independent function of SCAR alone.

To test this hypothesis, I studied another essential component of the SCAR/WAVE complex: Hem-2/NAP1/Kette, the homologue of mammalian NCKAP1. Like SCAR, Kette is strongly expressed in the *Drosophila* nervous system and, upon LOF (*Hem^{03335}* mutant allele), it causes the same mutant phenotypes in embryos as *SCAR$^{\Delta 37}$* (Schenck et al., 2004). I therefore analysed *Hem^{03335}* mutant primary neurons at 6HIV (Fig. 6.2). In these neurons, I found the same reduction in filopodia numbers (52±4%, $P_{Mann\text{-}Whitney}$<0.001, n=60) as well as axon length (83±3%, $P_{Mann\text{-}Whitney}$=0.001, n=60), and the same disorganisation of MTs (207%, P_{Chi2}<0.001, n=60), as observed upon SCAR LOF (Fig. 6.2).

Since MT disorganisation is a key phenotype in *shot* mutant neurons (Sanchez-Soriano et al., 2009, Alves-Silva et al., 2012), I wondered whether SCAR might work in the context of this Shot function. I therefore analysed whether SCAR LOF mutant phenotypes would be enhanced in *shot$^{3/+}$* heterozygous mutant background. As mentioned before, SCAR LOF alone causes filopodial reduction to 51%, axon length is reduced to 87±3%, and MT disorganisation is increased to 197%. When combined with *shot* heterozygous background, I found that *SCAR$^{\Delta 37/\Delta 37}$ shot$^{3/+}$* as well as *SCAR$^{\Delta 37/k13811}$ shot$^{3/+}$* mutant neurons displayed lower filopodia numbers (68±3%, $P_{Mann\text{-}Whitney}$<0.001, n=80 and n=120 respectively; Fig. 6.2), axons were mildly elongated (109±4%, n=80 and

n=120 respectively; for *SCAR*$^{\Delta 37/\Delta 37}$ shot$^{3/+}$, it is not significantly different, $P_{Mann-Whitney}$=0.084, however for *SCAR*$^{\Delta 37/k13811}$ shot$^{3/+}$, it is significantly different, $P_{Mann-Whitney}$=0.021; Fig. 6.2), and both *SCAR*$^{\Delta 37/\Delta 37}$ *shot*$^{3/+}$ and *SCAR*$^{\Delta 37/k13811}$ *shot*$^{3/+}$ mutant neurons show an increase in disorganised MT networks (210%, P_{Chi2}<0.001, n=80 and 227%, P_{Chi2}<0.001, n=120, respectively; Fig. 6.2). Overall, these phenotypes match those of *SCAR* LOF and fail to indicate any potential mechanistic relation to Shot.

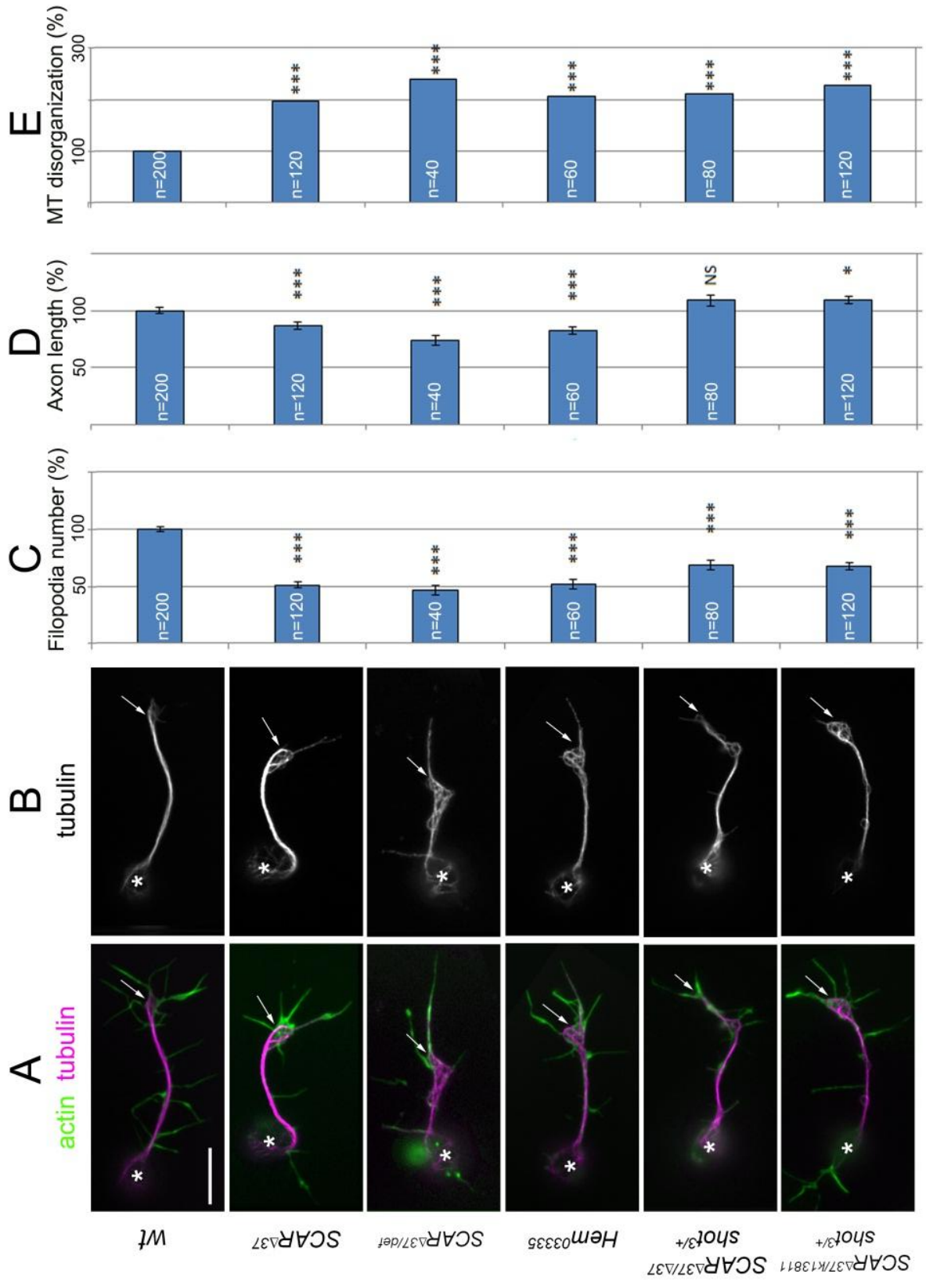
A
actin tubulin
B
tubulin
C
Filopodia number (%)
D
Axon length (%)
E
MT disorganization (%)
n=200
n=120
n=40
n=60
n=80
n=120
***
NS
*
wt
SCARΔ37
SCARΔ37/def
Hem03335
SCARΔ37/Δ37 shot3/+
SCARΔ37/k13811 shot3/+

Figure 6.2. *The SCAR complex plays Arp2/3-independent roles in axonal MT organisation.*

A,B) *Axonal phenotypes in wild type, shot^{3}, SCAR$^{\Delta 37}$, SCAR$^{\Delta 37/def}$, Hem^{03335}, SCAR$^{\Delta 37}$ shot$^{3/+}$ or SCAR$^{\Delta 37/k13811}$ shot$^{3/+}$ mutant primary neurons at 6HIV; cells are double-labelled for actin and tubulin as indicated (A; tubulin channel shown alone in B; asterisks, cell bodies; arrows, growth cones); scale bar represents 5 µm.* ***C-E)*** *Quantifications of phenotypes caused by the mutants on the left, respectively (all normalized and compared to wild type); numbers in the bars indicate the numbers of neurons analysed in each experiment; for filopodia number (C) or axon length (D), P values were calculated using the Mann-Whitney Rank Sum test (NS: P>0.050, **: P<0.050, ***: P<0.001); for MT disorganisation (E) P values were calculated using the Chi-square test (NS: P>0.050, **: P<0.050, ***: P<0.001).*

6.3. Examine the efficiency and lifespan of CK666 in *Drosophila* primary cell culture system

It has been mentioned that that treatment with CK666 dramatically reduced the density of the actin network in veils at the leading edge in a concentration- and time-dependent manner (Yang et al., 2012). Therefore, I want to test the efficiency and lifespan of CK666 in our Drosophila primary cell culture system. I tested a combination between two concentrations (50nM or 100nM) and two time point (2hr and 4hr). I found that neurons, when treated with 50nM CK666 for 2hr, have a reduced filopodia number (61±5%, $P_{Mann\text{-}Whitney}$<0.001, n=40; Fig. 6.3), which is similar to the level of actin nucleator mutant (Fig. 6.1). At the meantime, the culture is healthy and the morphology of neurons looks normal. When neuron were treated with 100nM CK666 for 2hr or 4hr, the filopodia number is also decrease to similar levels of 50nM CK666 for 2hr (2hr: 53±5%, $P_{Mann\text{-}Whitney}$<0.001, n=40, 4hr: 61±4%, $P_{Mann\text{-}Whitney}$<0.001, n=40; Fig. 6.3), and the culture is also healthy and the morphology of neurons looks normal. This data suggest that 50nM CK666 is efficient to inhibit Arp2/3 function in a short time. Since the high concentration of drug will not harm the cells and is reliable overtime, I have set up the CK666 drug treatment procedure as 100nM for 2hr.

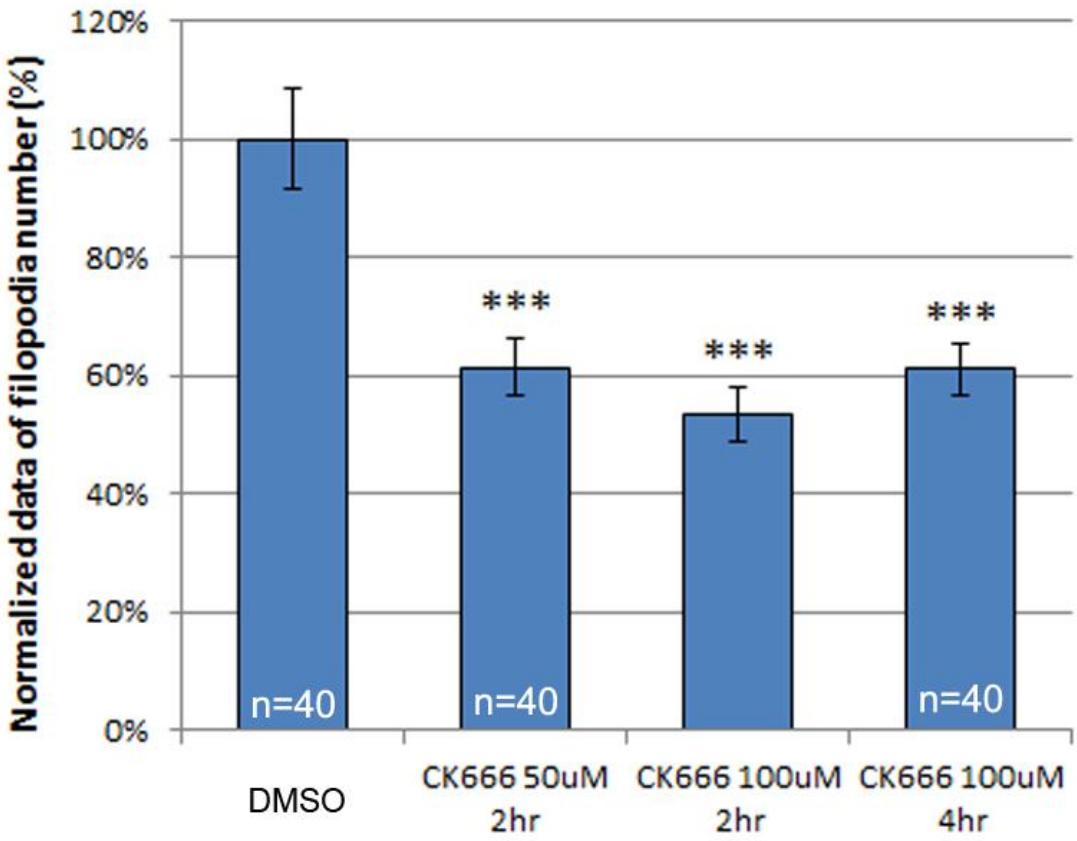

Figure 6.3. *Optimizing CK666 application in Drosophila primary neurons.*

*Quantifications of filopodia number of wild type primary neurons at 6HIV in vehicle (DMSO) or treated with CK666 at different concentrations and time periods (indicated below bar). Data were all normalized and compared to wild type in vehicle; numbers in the bars indicate the numbers of neurons analysed in each experiment. P values were calculated using the Mann-Whitney Rank Sum test (NS: P>0.050, **: P<0.050, ***: P<0.001).*

6.4. The protein sequence of Efa6 in different species

The protein sequences of Efa6 were shown below (include *Drosophila*, *C.elegans*, Human, mouse and Rat). The functional domains are indicated in the protein sequence by different colour.

Dark Blue	EB1 binding motifs (SxIP or SxLP)
Red	MT binding motif
Green	Sec7 region
Magenta	PH domain
Blue	Coiled-coil

1. Drosophila, dEfa6, cDNA IP15395, 1390aa

MSEELKVVLRRSEQHSGFGFSLLGTTGPPHVIYDIVENSPAADCGAVEAGDVILKVNGTDVHRYT
TKEVLKCLRLSEQLVTLELKRDPKLKARIKEQLANTQSPHYVDIESPNIYDYHSSSTNSSPNHRPN
AGGKGAATTPSQTGLRYKSPTHLPSLRQNSSPLLASGSTTTTTTATHTHSHSRNSSASSTKIKVV
ETSITTSTTNVVGLTSPTGSVGCGVGGEATSPTFRPSRIPQALTKCAVPKPVPVLHSPQNKRPRP
SQIPTKAANGNGNGHTAHLPPQSLQHSNSYSGSPVTRQRFADREPEREPEPNSAPPQPAKAPR
FEAYMMTGDLILNLSRTPQTSNPLPAQAKKIDSLRDSPSRLVNPRINGALAPRASGESSPTSSSSV
DSPTNTSSDSVKREAKLLQKQQQQQQQQTYQQQQQRDSINNSYNRKDSLTNDTLLMCEELEPD
EEGEYVLEEDNKQQRQRQQQQRYRQQQNQQRYEYYQNEDELEEQEEVEEEREEDQTHYDITN
IETYQSGVGRGDDDDSDRQCLVDDDDDDDAYDDEENDAGDEDYSTNSLGSGSAKQRLRALKQ
RTATRQQQRNRDAVDCAGRSGSGSSSTTVKSEAGGLGLDETSFSVSTSPISLSTPLIDKETANSV
PTSPEPSSLVPESSSGAGAGAVVVRRHNGHVVRKCDAAGFRTSKSEDHLQQIQREGIAAVIPIDI
DEDVNSSLNTLLDTRQDSEDSQASDRDRIVWTYNAPLQPHQLAALQRQQQQQEQQFQQQQQQ
LHQQHLQQQQQLQQQHQQQQQQQQQQQQQQQQQLYGGMVLSDPSDSDSTILVSDAAAHQRQ
QLKQQLRAQQQQQRERERDRDRDREQSEHKVVIQVRGLDSNSSGGNGTNGRSEEDVVTLTDE
PLGMMTVGMRDASPPVSDDGSDVESLHSYHYSPKAVDMPSAIRLAKRLHSLDGFKKSDVSRHL
SKNNDFSRAVADEYLKHFTFEKKSLDQALREFLQQFSLSGETQERERVLVHFSKRFLDCNPGTF
NSQDAVHTLTCAIMLLNTDLHGQNINRKMSCAEFVDNLADLNDGENFPKDVLKSLYQAIKTKPLE
WALDEEAGDLQQQRANNSALGNVGLNPFLDPPELATAVEYKKGYVMRKCCYDSSFKKTPFGKR
SWKMFYCTLRDLVLYLHKDEHGFRKSQMSDNLHNAIRIHHALATKANDYTKKQHVFRLQTADQA
EYLFQTSDSKELQSWVETINYVCAAISAPPLEGGVGSQKRFQRPLLPSKQSKLMLKEQLDSHEV
QLAQLDQELNEHKKGPIPSKGLALQNYKEKESYLQYELRRYRTYVSILSAKMLADQQQLELQAQQ
PSPASHEEEADTFPVGTTACTPPTPQSINQKDQQKEQQQQQPTNRKEKKKK

2. C. elegans, EFA-6, Y55D9A.1a, 816aa

MAKVASSGAEEALATIDGAPRRNVKKSEAFVMSGDVLISLNRNVSSTYAKLLGDQLPPGTTVASS
IHPHQLSRATASAGVSFPSMNRNGAAAQKLSRLPVSTSQIERRGSLARKTSEESSPTAIRMLKTA
PIERMESTDVEESEEETVMMTTDEKENQKKPNENDDEVMVVDEEQFIVVSNDMKSPNEEIVAKS
LRSAMFTMPTDNHHHSYNSSPQISTLSPHLRSNGDGPSRSPVYDDVDDDLNGSLDAKDMSNNS
HQQSFRSPENYSEKDTPSKHSVVTIDGSGVSNHYDQDGMFSHVYYSTQDTTPKHGSPSLRKQIF
ESRTTPNTAASNSSASASPSLHATSESRGATGGVSLRSAESSNLNQTAVPSTSTNSVGGEREAA
QIARNLYELKNCTSTQVADRLNEQNEFSFLILVKYLELFQFSTTRIDAALREFLSRVELRGESSARE
RLLRVFSARYLECNPAIFDSLDEVHTLTCALLLLNSDLHGPNMGKKMTARDFITNIAHTGCTFKRE
MLKTLFQSIKDNAISLQNSAKNSTANGSVASTSRRQPQQIYEVDPDSVVEYYSGFLMRKYVRETD
GGKTPFGRRSWRMVYARLRGLVLYFDTDEHPKATSRYASLENAVSLHHALAEPAPDYKKKSFVF
RVRIAHGGEILFQTSNQKELQEWCEKINFVAAAFSSPTLPLPVTSKPETAPMPRLPRIPCLAPITKQ
LSTHEARVAELNEMIEIVSQSVSPNQPQQLITDRWVLLSFEKRRYSTYINVLRRSLEARKASSATT
MNIMMTPTRRQQQNQKPVVSEDRLSYTDAVNGAAAH

3. Human, PSD, PSD-004, ENSP00000020673, 1024aa

MAQGAMRFCSEGDCAISPPRCPRRWLPEGPVPQSPPASMYGSTGSLLRRVAGPGPRGRELGR
VTAPCTPLRGPPSPRVAPSPWAPSSPTGQPPPGAQSSVVIFRFVEKASVRPLNGLPAPGGLSRS
WDLGGVSPPRPTPALGPGSNRKLRLEASTSDPLPARGGSALPGSRNLVHGPPAPPQVGADGLY
SSLPNGLGGPPERLATLFGGPADTGFLNQGDTWSSPREVSSHAQRIARAKWEFFYGSLDPPSS
GAKPPEQAPPSPPGVGSRQGSGVAVGRAAKYSETDLDTVPLRCYRETDIDEVLAEREEADSAIE
SQPSSEGPPGTAYPPAPRPGPLPGPHPSLGSGNEDEDDDEAGGEEDVDDEVFEASEGARPGS
RMPLKSPVPFLPGTSPSADGPDSFSCVFEAILESHRAKGTSYTSLASLEALASPGPTQSPFFTFEL
PPQPPAPRPDPPAPAPLAPLEPDSGTSSAADGPWTQRGEEEEAEARAKLAPGREPPSPCHSED
SLGLGAAPLGSEPPLSQLVSDSDSELDSTERLALGSTDTLSNGQKADLEAAQRLAKRLYRLDGFR
KADVARHLGKNNDFSKLVAGEYLKFFVFTGMTLDQALRVFLKELALMGETQERERVLAHFSQRY
FQCNPEALSSEDGAHTLTCALMLLNTDLHGHNIGKRMTCGDFIGNLEGLNDGGDFPRELLKALYS
SIKNEKLQWAIDEEELRRSLSELADPNPKVIKRISGGSGSGSSPFLDLTPEPGAAVYKHGALVRKV
HADPDCRKTPRGKRGWKSFHGILKGMILYLQKEEYKPGKALSETELKNAISIHHALATRASDYSK
RPHVFYLRTADWRVFLFQAPSLEQMQSWITRINVVAAMFSAPPFPAAVSSQKKFSRPLLPSAATR
LSQEEQVRTHEAKLKAMASELREHRAAQLGKKGRGKEAEEQRQKEAYLEFEKSRYSTYAALLRV
KLKAGSEELDAVEAALAQAGSTEDGLPPSHSSPSLQPKPSSQPRAQRHSSEPRPGAGSGRRKP

4. Mouse, Efa6A, Psd-201, ENSMUST00000041391.4, 1024aa

MAQGAMRFCSEGDCAISPPRCPRRWLPEGPVPQSPPASMYGSTGSLIRRVVGPGPRGRDLGR
VTAPCTPLRAPPSPHIAPSPWGPSSPTGQPPPGAQSSVVIFRFVEKASVRPLNGLPASGGLSRS
WDLGGISAPRPTPALGPGCNRKLRLEASTSDPLPAGGGSVLPGSRDPSRGPLVPPQIGADGLYS
SLPNGLGGTPEHLAMHFRGPADTGFLNQGDTWSSPREVSSHAQRIARAKWEFFYGSLDAPSSG
AKPPEQVLPSRGVGSKQGSGVAVGRAAKYSETDLDKVPLRCYRETDIDEVLAEREEADSAIESQ
PSSEGPHGTAQPPASRPSPCPGPSSSLGSGNEDDEAGGEEDVDDEVFEASEGARPGDHMPHS
GLLKSPVPFLLGTSPSADGPDSFSCVFEAILESHRAKGTSYSSLASLEALASPGPTQSPFFTFEMP
PQPPAPRPDPPAPAPLAPLEPDSGTSSAADGPWTQRREVEESDAGATLAPRKELPSPSHSEDS
FGLGAAPLGSEPPLSQLVSDSDSELDSTERLALGSTDTLSNGQKADLEAAQRLAKRLYRLDGFR
KADVARHLGKNNDFSKLVAGEYLKFFVFTGMTLDQALRVFLKELALMGETQERERVLAHFSQRY
FQCNPEALSSEDGAHTLTCALMLLNTDLHGHNIGKRMTCGDFIGNLEGLNDGGDFPRELLKALYS
SIKNEKLQWAIDEEELRRSLSELADPNPKVIKRVSGGSGSSSSPFLDLTPEPGAAVYKHGALVRK
VHADPDCRKTPRGKRGWKSFHGILKGMILYLQKEEYQPGKALSEAELKNAISIHHALATRASDYS
KRPHVFYLRTADWRVFLFQAPSLEQMQSWITRINVVAAMFSAPPFPAAVSSQKKFSRPLLPSAAT
RLSQEEQVRTHEAKLKAMASELREHRAAHLGKKARGKEADEQRQKEAYLEFEKSRYGTYAALLR
VKMKAASEELDTIEAALAQAGSTEDGCPPPHSSPSLRPKPTSQPRAQRPGSETRAGAGSTRPKP

5. Rat, Psd, Psd-201, ENSRNOT00000026378, 1023aa

MAQGAMRFCSEGDCAISPPRCPRRWLPEGPVPQSPPASMYGSTGSLIRRVVGPGPRGRDLGR
VTAPCTPLRAPPSPHIAPSPWGPSSPTGKPPPGAQSSVVIFRFVEKASVRPLNGLPASGGLSRS
WDLGGISPSRPTPALGPGCNRKLRLEASTSDPLPAGGGSVLPGSRDPSRGPLIPPQIGADGLYS
SLPNGLGGTPEHLVMHFRGPADTGFLNQGDTWSSREVSSHAQRIARAKWEFFYGSLDPPSSGA
KPPEQALPSHGVGSKQGSGVAVGRAAKYSETDLDKVPLRCYRETDIDEVLAEREEADSAIESQP
SSEGPPGTTQPPASRPSPCPGPSSSLGSGNGDDEAGGEEDVDDEVFEASEGARPGDHMPHSG
LLKSPVPFLPGTSPSADGPDSFSCMFEAIMESHRAKGTSYSSLASLEALASPGPTQSPFFTFEMP
PQPPAPRPDPPAPAPLAPLEPDSGTSSVADGPWTQRREVEESDAGATLAPRKELPSPSHSEDSL
GLGAAPLGSEPPLSQLVSDSDSELDSTERLALGSTDTLSNGQKADLEAAQRLAKRLYRLDGFRK
ADVARHLGKNNDFSKLVAGEYLKFFVFTGMTLDQALRVFLKELALMGETQERERVLAHFSQRYF
QCNPEALSSEDGAHTLTCALMLLNTDLHGHNIGKRMTCGDFIGNLEGLNDGGDFPRELLKALYSS
IKNEKLQWAIDEEELRRSLSELADPNPKVIKRVSGGSGSSSSPFLDLTPEPGAAVYKHGALVRKV
HADPDCRKTPRGKRGWKSFHGILKGMILYLQKEEYQPGKALSEAELKNAISIHHALATRASDYSK
RPHVFYLRTADWRVFLFQAPSLEQMQSWITRINVVAAMFSAPPFPAAVSSQKKFSRPLLPSAATR
LSQEEQVRTHEAKLKAMASELREHRAAHLGKKARGKEAEEQRQKETYLEFEKSRYGTYAALLRV
KMKAASEELDAIEAALAQAGSTEEGCPPPHSSPSLQPNPTSQPRAQRPGSEARAGAGSTRPKP

6.5. Genomic area uncovered by the overlapping *efa6* deficiencies

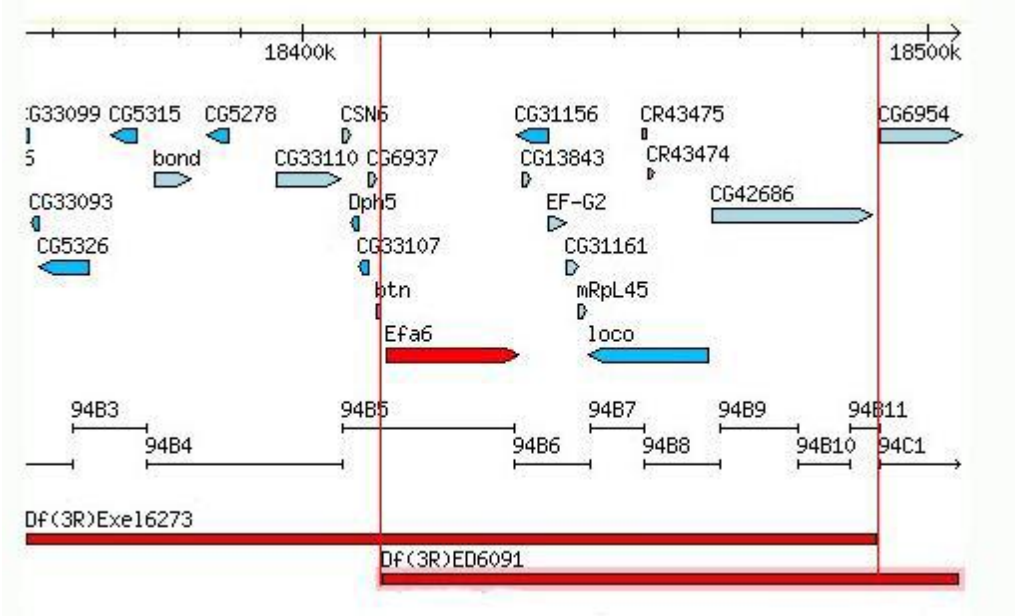

Figure 6.4. *Genomic area uncovered by the overlapping efa6 deficiencies.*

The efa6 gene (in red) is inside the overlapping area of Df(3R)Exel6273 and Df(3R)ED6091, which is indicate by two red lines. Information comes from flybase.org.